

**The NKG2D system as modulator of
host-microbial interactions in the gut**

submitted by

Lic. Ana MONTALBAN-ARQUES

for the Academic Degree of

Doctor of Philosophy (PhD)

at the

Medical University of Graz

Institute of Pathology

under the Supervision of

Univ.Prof. Dr.med.univ. Gregor GORKIEWICZ

2016

Statutory declaration

I hereby declare that this thesis is my own original work and that I have fully acknowledged by name all of those individuals and organizations that have contributed to the research for this thesis. Due acknowledgement has been made in the text to all other material used. Throughout this thesis and in all related publications I followed the “Standards of Good Scientific Practice and Ombuds Committee at the Medical University of Graz“.

September 2016.

*And the wings grew strong,
and let me fly alone*

Acknowledgements

First, I would like to acknowledge my advisor, Gregor for his support along these four years. For always have an optimistic attitude, even when presenting negative results; and for pushing me in the first months of my PhD to think about how our completely new project could evolve to a fancy idea. That freedom to create and perform experiments based on my own hypothesis, even when crazy, has been the most valuable knowledge I take from my PhD.

Thank you to the DK-MOLIN, a brilliant PhD program that gave me the opportunity of being part of a big family. Thank you for all the opportunities offered along these years, which have been essential to grow up as a scientist, but also personally.

I would like to say a big thank you to my ZMF colleagues and my PathoLadies (girlsss). I am very glad to have met you all. For all those moments inside and outside the lab, for all your scientific and personal support, for all the coffee/tea breaks, dinners, cocktail-nights, never-ending conversations and lots of fun. Without you this way would have been tough.

To my Thesis committee members: Christoph, Jorge and Sabine, who gave me lots of feedback and made a great contribution in pushing my project forward. Thank you for the productive discussions that helped to develop my project from beginning to the end.

To our super-technician Silvia, who always gave me support and solved on time our last-minute requests. Thank for your patient and commitment.

I would like to thank Nadia Guerra for the opportunity to perform my stay abroad at her lab, and Jenny Mc. Govern for all I learned from her. I got a really valuable experience during those months in London.

Por último, pero no por ello menos importante, quería agradecerle a toda mi familia y amigos el apoyo que me han dado durante estos años y por haberme hecho sentir que estaban a mi lado, a pesar de la distancia que nos separaba. Gracias por todas las visitas que me habéis hecho, tanto en Graz como en Londres. Habéis sido un soplo de aire fresco y me habéis recargado las pilas a base de risas, mimos y buenos momentos que formarán para siempre parte del recuerdo.

Querría hacer una especial mención a mis tíos Alfonso y Fiona, los cuáles siempre me animaron a salir fuera, a descubrir el mundo y a crecer a base de las experiencias que vivir en un país extranjero me iba a dar. Gracias por haber seguido tan de cerca mis pasos y alegraros sinceramente de cada uno de ellos. Gracias por vuestros consejos de mantener siempre los pies en la tierra, por alto o lejos que se vuele y por recordarme que la humildad es el valor máspreciado.

Gracias mamá y papá por haberme apoyado siempre en mis decisiones y haber creído siempre en mí. Habéis sido el motor que me ha impulsado cada vez que han flaqueado las fuerzas. Gracias por esos kits de supervivencia que tantas veces me habéis hecho llegar y que yo he recibido con tanta ilusión; por todos los consejos que me habéis dado, y por escucharme siempre, aunque a veces no entendiérais una palabra de lo que os estaba diciendo.

A mi hermano Andrés, por haberse convertido en el hermano mayor en mi ausencia. Gracias por todo el cariño que me has mostrado cada vez que volvía a casa, por no importarte cederme el sitio en la mesa y mantenerme al día de todo. Gracias por esas felicitaciones y deseos en los cumpleaños que no hemos podido pasar juntos, y por tener tanta paciencia con tu hermana.

A Edu, por haber aparecido en mi vida en el momento que más lo necesitaba. Gracias por haberte atrevido a aventurarte en un proyecto nada fácil y a pesar de ello, haber hecho que lo pareciese. Gracias por haberme acompañado en el tramo final de esta larga carrera y convertir los meses más difíciles en los más bonitos que podré recordar.

A mi abuela y mis ángeles de la guarda, a los cuales adoro y adoraré siempre, allá donde estén. Gracias por tener siempre las mejores palabras y consejos para vuestra nieta; por haber tenido la sonrisa siempre pintada en la cara, por difícil que haya sido a veces sacarla; por haberme recibido en el aeropuerto ansiosos y con los brazos abiertos; por haberme preparado las comidas que más me gustan cada vez que he vuelto a casa. Gracias por alegraros como nadie de mis logros y por guiar mis pasos, cuidarme y hallanarme el camino desde allí arriba. Me lo habéis hecho muy fácil.

"PhD student Ana Montalban-Arques received funding from the Austrian Science Fund FWF (W1241) and the Medical University Graz through the PhD Program Molecular Fundamentals of Inflammation (DK-MOLIN)."

Table of Contents

STATUTORY DECLARATION.....	II
ACKNOWLEDGEMENTS.....	IV
TABLE OF CONTENTS	VIII
ABBREVIATIONS	1
LIST OF FIGURES	4
LIST OF TABLES.....	10
ABSTRACT (ENGLISH).....	11
ABSTRACT (GERMAN).....	12
I. INTRODUCTION	14
1. THE HUMAN GASTROINTESTINAL TRACT	14
1.1. <i>Anatomy and function of the GIT</i>	14
1.1.1. Stomach.....	14
1.1.2. Small intestine.....	15
1.1.3. Large intestine.....	15
1.2. <i>Gut mucosal barrier</i>	15
1.2.1. Lumen.....	15
1.2.2. Mucous layer.....	16
1.2.3. Epithelium.....	17
1.2.4. Lamina propria.....	17
1.3. <i>Chronic inflammatory diseases of the GIT associated with dysbiosis</i>	18
1.3.2. Celiac Disease.....	19
1.3.3. H. pylori gastritis.....	19
1.3.4. Lymphocytic gastritis.....	20
2. GUT MICROBIOTA.....	22
2.1 <i>Definition</i>	22
2.2. <i>Composition, distribution and abundance</i>	22
2.3. <i>Host-microbial interactions</i>	24
2.3.1. Functions of the microbiota in the GIT	24
2.3.2. Homeostasis vs. dysbiosis.....	25
2.3.2. Association of the microbiota with inflammatory diseases	25
2.3.3. Pathobionts associated with GI inflammatory diseases: H. pylori and P. acnes.....	26
2.3.3.1. <i>Helicobacter pylori</i>	26
2.3.3.2. <i>Propionibacterium acnes</i>	28
2.4. <i>Microbial metabolites: Short-chain fatty acids (SCFAs)</i>	29
2.4.1. Definition, composition and concentration.....	29
2.4.2. Metabolization, transport, absorption and signal transduction of SCFAs.....	30
2.4.3. Role of SCFAs in the GIT	31
3. THE GUT IMMUNE SYSTEM.....	33
3.1. <i>Development of the immune system by the gut microbiota</i>	33
3.2. <i>Microbial recognition by Toll-like receptors (TLRs)</i>	34
3.3. <i>NKG2D system</i>	35
3.3.1. NKG2D receptor.....	35
3.3.2. NKG2D ligands.....	36
3.3.3. Interleukin 15.....	38

3.3.4. Intraepithelial lymphocytes.....	39
3.3.5. The diverse roles of the NKG2D system.....	40
3.3.5.1. Infection.....	41
3.3.5.2. Cell transformation.....	41
3.3.5.3. Inflammatory and autoimmune diseases.....	42
3.3.5.4. Other types of cell stress that activate the NKG2D system.....	42
3.3.5.5. The NKG2D system is also active under a physiological status.....	43
3.3.6. The interplay between the NKG2D system and cytokines.....	43
3.3.7. Association of the NKG2D system with the microbiota.....	45
3.3.8. Phylogenetics of the NKG2D system: A matter of mammals.....	47
II. AIMS.....	48
III. MATERIALS AND METHODS.....	48
1. HUMAN SAMPLES.....	48
2. MOUSE COLONY.....	49
3. CELL LINES AND CULTURE.....	49
4. BACTERIA STRAINS AND CULTURE.....	50
5. HISTOLOGY AND IMMUNOHISTOCHEMISTRY.....	50
6. CYTOSPIN AND IMMUNOCYTOCHEMISTRY.....	51
7. SCFAs STIMULATION.....	51
8. BACTERIAL INFECTION ASSAY.....	51
9. QUANTITATIVE REAL-TIME PCR.....	52
9.1. RNA isolation from human FFPE samples and human cell lines.....	52
9.2. RNA isolation from mouse gut samples.....	53
9.3. DNA isolation from FFPE human samples.....	53
10. LAMINA PROPRIA AND INTRAEPITHELIAL LYMPHOCYTE ISOLATION.....	54
11. FLOW CYTOMETRY.....	55
11.1. Cell lines and staining.....	55
11.2. Mouse lymphocytes.....	56
12. GUT MICROBIOTA ANALYSIS.....	57
13. DSS- INDUCED COLITIS.....	58
14. SCFAs MEASUREMENTS BY GC-MS.....	59
15. STATISTICAL ANALYSIS.....	59
16. ETHICS STATEMENT.....	59
IV. RESULTS.....	60
1. LYG IS NOT ASSOCIATED WITH <i>H. PYLORI</i> INFECTION BUT SHOWS AN OVERABUNDANCE OF <i>P. ACNES</i>	60
2. THE NKG2D/NKG2D LIGAND SYSTEM IS INDUCED IN LYMPHOCYTIC GASTRITIS.....	62
3. THE GIT DISPLAYS UBIQUITOUS EXPRESSION OF THE NKG2D SYSTEM.....	65
4. THE NKG2D SYSTEM EXPRESSION IS ALTERED IN GI DISEASES CHARACTERIZED BY DYSBIOSIS.....	67
5. GASTRIC ECs RESPOND TO DIFFERENT <i>P. ACNES</i> STRAIN STIMULI BY INDUCTION OF THE NKG2D SYSTEM, BUT NOT TO <i>H. PYLORI</i>	70
6. GASTRIC ECs RESPOND TO SCFAs BY INDUCTION OF THE NKG2D SYSTEM.....	75
6. 1. Initial test using different concentrations of SCFAs at different time points.....	75
6. 2. AGS and MKN28 gastric ECs lines challenged with 5mM SCFAs or HCl for 4h (gene and protein expression).....	80
7. NKG2D LIGANDS AND IL15 EXPRESSION IS DIFFERENTIALLY MODIFIED BY MICROBIAL METABOLITES IN THE UPPER AND LOWER GI ECs.....	87
8. NKG2D DEFICIENCY IN MICE IS NOT AFFECTING THE IMMUNE CELL POPULATIONS UNDER HOMEOSTATIC CONDITIONS NEITHER IN THE LAMINA PROPRIA NOR IN THE INTRAEPITHELIAL COMPARTMENT.....	92
9. INDUCTION OF COLITIS BY DSS DOES NOT TRIGGER DIFFERENCES IN IMMUNE CELL POPULATIONS.....	93
10. NKG2D ABSENCE DOES NOT HAVE A STRONG INFLUENCE IN THE ACUTE COLITIS MODEL.....	94

11. REGIONALIZATION OF THE LPLS AND IELS ALONG THE GIT IN MICE.....	96
12. ABSENCE OF THE NKG2D RECEPTOR DOES NOT INFLUENCE THE EXPRESSION OF TLR2, 4 & 5, NKG2D LIGANDS OR IL15.....	100
13. TLR GENE EXPRESSION PRESENT POSITIVE CORRELATIONS WITH THE NKG2D SYSTEM ALONG THE GIT, WHICH CAN BE GENOTYPE-DEPENDENT.....	101
14. NKG2D RECEPTOR DEFICIENCY INFLUENCES GUT MICROBIOTA COMPOSITION.....	103
V. DISCUSSION	109
VI. CONCLUSIONS	116
VII. BIBLIOGRAPHY	119
VIII. APPENDIX.....	147
APPENDIX 1. HUMAN SAMPLES USED IN THIS STUDY.....	147
APPENDIX 2. MICE USED IN THIS STUDY	148
APPENDIX 3 PRIMERS USED IN THIS STUDY	150
<i>A. Human primers.....</i>	<i>150</i>
<i>B. Mice primers.....</i>	<i>151</i>
APPENDIX 4 DSS MICE EXPERIMENT DATA COMPILATION	152
APPENDIX 5. FLOW CYTOMETRY AB COCKTAILS USED IN MICE EXPERIMENTS.....	154
APPENDIX 6. SPEARMEN R-VALUES AND P VALUES CORRESPONDING TO TLRs AND NKG2D SYSTEM CORRELATION ANALYSIS	155
APPENDIX 7. PROTOCOL FOR GUT IELS AND LPLS ISOLATION.....	157

Abbreviations

Ab: Antibody

AMPs: Antimicrobial peptides

APC: Antigen presenting cell

bp: Base pair

BW: Body weight

CagA: Cytotoxin associated gene A

CD: Crohn's disease

CeD: Celiac Disease

CFU: Colony Forming Unit

DC: Dendritic Cell

DSS: Dextran Sodium Sulfate

DTT: 1,4-Dithiothreitol

EC: Epithelial cell

FBS: Fetal Bovine Serum

FFPE: Formalin-fixed paraffin-embedded

GALT: Gut -associated lymphoid tissue

GC-MS: Gas Chromatography Mass Spectrometry

GF: Germ-free

GI: Gastrointestinal

GIT: Gastrointestinal tract

GPCR: G-protein-coupled receptors

GPI: Glycosylphosphatidylinositol

GvHD: Graft-versus-host disease

HCl: Chloridic acid

HCMV: Human cytomegalovirus

HDAC: Histone deacetylase

HpG: *H. pylori*-gastritis

HPF: High Power Field

HPLC: High performance liquid chromatography

IBD: Inflammatory Bowel Disease
IEC: Intestinal epithelial cell
IEL: Intraepithelial lymphocyte
IL: Interleukin
ILFs: Isolated lymphoid follicles
LDA: Linear Discriminant Analysis
LEfSe: Linear Discriminant Analysis Effect Size
LPS: Lipopolysaccharide
LyC: Lymphocytic Colitis
LyG: Lymphocytic Gastritis
mAb: Monoclonal Ab
MALT: Mucosa-associated lymphoid tissue
MAMPs: Microbial-associated molecular pattern
MCT-1: Monocarboxylate-Transporter 1
mDCs: Mononuclear Dendritic Cells
MICA: MHC class I polypeptide-related sequence A
MICB: MHC class I polypeptide-related sequence B
MLN: Mesenteric Lymph Nodes
MLST: Multilocus sequence typing
MOI: Multiplicity of Infection
MTBE: Methyl tert-butyl ether
Mult1: Murine UL16-binding protein-like transcript 1 protein
NEAA: Non-essential aminoacids
NKG2D: Natural Killer Group 2 Member D
NKG2DL: Natural Killer Group 2 Member D Ligand
OD: Optical Density
OTU: Operational Taxonomic Unit
PAMPs: Pathogen-associated molecular pattern
PCR: Polymerase Chain Reaction
PG: Peptidoglycan
PI: Propidium iodide

PRRs: Pattern recognition receptors
PVDF: Polyvinylidene fluoride
Rae1: Retinoic acid early inducible-1 proteins
RAET1: Retinoic acid early transcript 1
RDP: Ribosomal Database Project
RT-qPCR: Real time quantitative PCR
SCFAs: Short-chain fatty acids
sIgA: Soluble Immunoglobulin A
SMCT-1: Sodium-coupled monocarboxylate transporter 1
SNPs: Single-nucleotide polymorphism
SPF: Specific Pathogen Free
TGF β : Transforming growth factor beta
TLRs: Toll-like Receptors
UC: Ulcerative Colitis
ULBP: UL16 binding protein
VacA: Vacuolating cytotoxin A

List of figures

FIGURE 1. REPRESENTATION OF THE MOLECULAR MECHANISMS TRIGGERING LYG.....	22
FIGURE 2. SCHEME REPRESENTING SOME FEATURES OF THE HOST-MICROBE INTERPLAY.....	24
FIGURE 3. GRAPHIC REPRESENTATION OF THE STOMACH MICROBIOTA UNDER HOMEOSTASIS, IN HPG AND LYG. 29	
FIGURE 4. POTENTIAL MICROBIAL STRATEGIES TO IMPROVE GUT MUCOSAL IMMUNITY	32
FIGURE 5. REPRESENTATION OF THE DIFFERENT MOLECULAR STRUCTURES OF THE NKG2D RECEPTOR AND ITS LIGANDS IN HUMAN AND MOUSE.....	38
FIGURE 6. SPATIAL CHARACTERISTICS OF THE GIT.....	40
FIGURE 7. INTERPLAY BETWEEN CYTOKINES AND THE NKG2D SYSTEM IN THE TUMOR MICROENVIRONMENT..	45
FIGURE 8. SCHEME REPRESENTING THE POSSIBLE ACTIVATION OF THE NKG2D SYSTEM DUE TO <i>P. ACNES</i> AND THE SCFAS THROUGH ADHERENCE, INVASION, TLR SIGNALING OR DIRECT CELL STRESS.	47
FIGURE 9. <i>P. ACNES</i> SPECIFIC QPCR IN HEALTHY CONTROLS VS. HPG AND LYG HUMAN FFPE STOMACH BIOPSIES..	61
FIGURE 10. VALIDATION OF NGS RESULTS BY QPCR.	61
FIGURE 11. H&E AND IMMUNOHISTOCHEMICAL STAINING OF CD4 ⁺ AND CD8 ⁺ T-CELLS IN HUMAN GASTRIC CORPUS BIOPSIES OF HEALTHY CONTROLS, HPG AND LYG CASES.....	62
FIGURE 12. BAR CHARTS REPRESENTING THE AVERAGE NUMBER OF CD4 ⁺ AND CD8 ⁺ T CELLS IN 5 HPF AND THE NUMBER OF IELS PER 100 Ecs IN CONTROLS, HPG AND LYG PATIENTS.	63
FIGURE 13. GENE EXPRESSION ANALYSIS OF THE NKG2D/NKG2D LIGAND SYSTEM AND IL15 IN FFPE STOMACH BIOPSIES FROM CONTROLS, HPG AND LYG PATIENTS.	64
FIGURE 14. MICA/B IHC IN HEALTHY CONTROLS, LYG AND HPG STOMACH FFPE SAMPLES.....	65
FIGURE 15. <i>NKG2D</i> , <i>MICA</i> , <i>MICB</i> , AND <i>IL15</i> MRNA EXPRESSION IN HUMAN MUCOSAL BIOPSIES OF HEALTHY INDIVIDUALS DETERMINED BY QRT-PCR ANALYSES.....	67
FIGURE 16. <i>NKG2D</i> , <i>MICA</i> , <i>MICB</i> , AND <i>IL15</i> MRNA EXPRESSION IN HUMAN MUCOSAL FFPE BIOPSIES OF STOMACH (HEALTHY, LYG, HPG), DUODENUM (HEALTHY, CED AND HPG) ILEUM (HEALTHY AND CD) AND COLON (HEALTHY AND UC) BY QRT-PCR ANALYSES.	70
FIGURE 17. SUMMARY HEAT-MAP REPRESENTING THE MRNA OR PROTEIN EXPRESSION OF THE MAIN PLAYERS IN THE NKG2D SYSTEM ACTIVATION, IN THE DIFFERENT GI PATHOLOGIES TESTED IN THIS STUDY.....	70
FIGURE 18. <i>MICA</i> , <i>MICB</i> AND <i>IL15</i> MRNA EXPRESSION IN AGS CELLS CHALLENGED FOR 24H WITH THE ACTIVE FORM, SUPERNATANT OR HEAT- INACTIVATED <i>P. ACNES</i> AND <i>E. COLI</i>	71
FIGURE 19. <i>MICA</i> , <i>MICB</i> AND <i>IL15</i> MRNA EXPRESSION IN AGS AND MKN28 CELLS AFTER 24H OF INFECTION WITH <i>P. ACNES</i> (STRAINS PA-1.1 AND PA-2.2), <i>H. PYLORI</i> (STRAINS PMSS1 AND SS1) AND <i>E. COLI</i> (DSM 30083).	72
FIGURE 20. MICA/B PROTEIN EXPRESSION WAS ASSESSED IN AGS AND MKN28 CELLS BY FLOW-CYTOMETRY AFTER 24H OF INFECTION WITH <i>P. ACNES</i> (PA-1.1 AND PA-2.2 STRAINS), <i>H. PYLORI</i> (PMSS1 AND SS1 STRAINS) OR <i>E. COLI</i> (DSM 30083 STRAIN).	73
FIGURE 21. COLONY FORMING UNITS PER ML (CFU/ML), OF <i>P. ACNES</i> , <i>H. PYLORI</i> , AND <i>E. COLI</i> STRAINS AFTER 24 H OF CO-CULTIVATION, WITH AGS OR MKN28 CELLS.	74
FIGURE 22. APOPTOSIS AND LIVE/DEAD ANALYSIS OF AGS AND MKN28 CELLS INFECTED WITH <i>P. ACNES</i> , <i>H.</i> <i>PYLORI</i> OR <i>E. COLI</i> ASSESSED BY ANNEXIN V/PI STAINING AND FLOW CYTOMETRY	75
FIGURE 23. KINETICS OF <i>MICA</i> , <i>MICB</i> AND <i>IL15</i> MRNA EXPRESSION IN AGS STIMULATED WITH 1, 5, 10 AND 50MM OF SCFAS AND HCL AFTER 4 AND 24H.....	76
FIGURE 24. REPRESENTATION OF HISTOGRAMS SHOWING MICA/B EXTRACELLULAR PROTEIN EXPRESSION IN AGS CELLS AFTER 4H OF SCFAS AND HCL STIMULATION FOLLOWED BY 4H OF RESCUE IN DMEM MEDIUM.	77
FIGURE 25. MICA/B ICC OF AGS CELLS STIMULATED WITH SCFAS OR HCL FOR 4H FOLLOWED BY 4H RESCUE IN DMEM.	78
FIGURE 26. APOPTOSIS AND LIVE/DEAD ANALYSIS OF AGS CELLS TREATED WITH THE DIFFERENT SCFAS FOR 4H FOLLOWED BY 4H RESCUE IN DMEM, ASSESSED BY ANNEXIN V/PI STAINING BY FLOW CYTOMETRY.	80
FIGURE 27. MRNA EXPRESSION OF <i>MICA</i> , <i>MICB</i> AND <i>IL15</i> IN AGS CELLS AFTER 4H OF STIMULATION WITH 5MM OF SCFAS OR HCL USED AS A NEGATIVE CONTROL.	81
FIGURE 28. MRNA EXPRESSION OF <i>MICA</i> , <i>MICB</i> AND <i>IL15</i> IN MKN28 CELLS AFTER 4H OF STIMULATION WITH 5MM SCFAS OR HCL USED AS A NEGATIVE CONTROL.	82

FIGURE 29. OVERALL MICA/B PROTEIN EXPRESSION WAS ASSESSED IN AGS AND MKN28 CELLS BY FLOW-CYTOMETRY AFTER SCFAS STIMULATION FOR 4 H FOLLOWED BY 4 H RESCUE IN DMEM WITHOUT SCFAS.	83
FIGURE 30. EXTRACELLULAR MICA/B PROTEIN EXPRESSION WAS ASSESSED IN AGS AND MKN28 CELLS BY FLOW-CYTOMETRY AFTER SCFAS STIMULATION (5MM) FOR 4 H FOLLOWED BY 4 H RESCUE IN DMEM WITHOUT SCFAS.	84
FIGURE 31. MICA/B ICC OF AGS CELLS STIMULATED WITH SCFAS AND HCL FOR 4H FOLLOWED BY 4H RESCUE IN DMEM MEDIUM WITHOUT SCFAS.	85
FIGURE 32. APOPTOSIS AND LIVE/DEAD ANALYSIS OF AGS CELLS TREATED WITH THE DIFFERENT SCFAS OR HCL FOR 4H FOLLOWED BY 4H RESCUE ASSESSED BY ANNEXIN V/PI STAINING AND FLOW CYTOMETRY IN AGS AND MKN28 CELLS.	86
FIGURE 33. CACO-2 MRNA EXPRESSION OF <i>MICA</i> , <i>MICB</i> , AND <i>IL15</i> AFTER 24H OF STIMULATION WITH 5MM OF SCFAS OR HCL USED AS A NEGATIVE CONTROL.	88
FIGURE 34. EXTRACELLULAR MICA/B PROTEIN EXPRESSION WAS ASSESSED IN CACO-2 CELLS BY FLOW-CYTOMETRY AFTER SCFAS STIMULATION FOR 24H.	88
FIGURE 35. OVERALL MICA/B PROTEIN EXPRESSION WAS ASSESSED IN CACO-2 CELLS BY FLOW-CYTOMETRY AFTER SCFAS STIMULATION FOR 24 H.	89
FIGURE 36. MICA/B ICC OF CACO-2 CELLS STIMULATED WITH SCFAS AND HCL FOR 24H.	90
FIGURE 37. APOPTOSIS AND LIVE/DEAD ANALYSIS OF CACO-2 CELLS TREATED WITH THE DIFFERENT SCFAS OR HCL FOR 24H ASSESSED BY ANNEXIN V/PI STAINING AND FLOW CYTOMETRY.	91
FIGURE 38. BODY WEIGHT AND COLON PARAMETERS IN CONTROL MICE VS. TREATED WITH DSS (WT AND KO)..	95
FIGURE 39. GUT MACROSCOPY AND COLON LENGTH IN CONTROL AND KO MICE TREATED WITH DSS (WT AND KLRK1-/-).	96
FIGURE 40. LAMINA PROPRIA IMMUNE CELL REGIONALIZATION ALONG THE MURINE GIT.	98
FIGURE 41. INTRAEPITHELIAL IMMUNE CELL REGIONALIZATION ALONG THE MURINE GIT.	99
FIGURE 42. HEAT MAP MATRIX REPRESENTING THE CORRELATION BETWEEN TLRs (TLR2, TLR4 AND TLR5) AND THE NKG2D SYSTEM (KLRK1 RECEPTOR, RAE1 AND MULT1 LIGANDS AND IL15) IN WT AND KLRK1 KO MICE.	103
FIGURE 43. COMPARATIVE MICROBIOTA ANALYSES OF WT AND KLRK1-/- MICE.	104
FIGURE 44. DIAGRAM REPRESENTING THE MAIN DIFFERENCES FOUND BETWEEN WT AND KLRK1-/- MICE ALONG THE GIT AND FECES IN TERMS OF BACTERIA GENERA RELATIVE ABUNDANCE.	105
FIGURE 45. CLADOGRAMS REPRESENTING LEfSE OUTPUT SHOWING TAXONOMIC REPRESENTATION OF STATISTICALLY DIFFERENCES IN MICROBIOTA COMPOSITION BETWEEN WT AND KLRK1-/- MICE.	107

List of tables

TABLE 1. BACTERIA SPECIES AND STRAINS USED FOR IN VITRO INFECTION ASSAYS IN THIS STUDY.....	50
TABLE 2. CONCENTRATION OF SCFAS IN THE SUPERNATANT OF CHALLENGED AGS CELLS ASSESSED BY GC-MS.....	81
TABLE 3. CELL COUNTS AND VIABILITY IN CACO-2 CELLS AFTER 4 AND 24H OF TREATMENT WITH 5 OR 10MM SCFAS OR HCL.....	91
TABLE 4. LIST OF ANTIBODIES USED FOR GIT IMMUNOPHENOTYPING IN MOUSE.....	92
TABLE 5. FREQUENCIES OF THE DIFFERENT IMMUNE CELL POPULATIONS IN THE LAMINA PROPRIA AND INTRAEPITHELIAL COMPARTMENTS ALONG THE GIT, IN WT AND KLRK1 -/- (KO) MICE.....	93
TABLE 6. FREQUENCIES OF DIFFERENT IMMUNE CELL POPULATIONS IN THE COLON LAMINA PROPRIA OF WT CONTROL MICE, OR TREATED WITH DSS (WT AND KLRK1 -/- (KO)) MICE.....	94
TABLE 7. RELATIVE GENE EXPRESSION TO HOUSEKEEPING GENE (HKG) (HPRT) ALONG THE GIT.....	101
TABLE 8. READS PER SAMPLE AND OTUS ALONG THE GIT IN WT AND KLRK1-/- (KO) MICE.....	104
TABLE 9. LDA EFFECT OF THE DISCRIMINANT BIOMARKERS FOUND FOR WT AND KLRK1-/- (KO) MICE ALONG THE GIT AND FECES MICROBIOTA ANALYSIS.....	108

Abstract (English)

The human gastrointestinal tract (GIT) represents the largest reservoir of commensal bacteria as well as the largest immune system of the body. Moreover, microbes are crucial for the development of the immune system. However, alterations in either the microbiota or the immune system may lead to gastrointestinal (GI) disorders. The natural killer group 2 member D (NKG2D) system is critical in the recognition of cell stress due to cell transformation or infection. Recently, it has been demonstrated that gut microbiota can modulate the expression of NKG2D ligands. Interestingly, the activation of the NKG2D has been associated with GI diseases, such as celiac disease (CeD) or inflammatory bowel disease, wherein the microbiota is also impaired. In this study, we have identified *Propionibacterium acnes* being associated with lymphocytic gastritis, a chronic form of gastritis often associated to CeD. Moreover, we have seen that patients suffering from LyG show an activation of the NKG2D system, which does not happen in the gastritis triggered by *Helicobacter pylori*. Using gastric epithelial cell (EC) lines, we demonstrated that *P. acnes* and the microbial products short-chain fatty acids, can induce the expression of NKG2D ligands *in vitro*. However, *H. pylori* omitted or even repressed their expression. Interestingly, in lymphocytic colitis, a pathology presenting similar features with LyG, the NKG2D system is not activated, maybe due to differences in the microbiota composition and immune cells found in both organs. Moreover, Caco-2 colon ECs also showed a different NKG2D system response when challenged with SCFAs compared to gastric ECs, suggesting this system plays a role in the gut that is location-dependent. Finally, using a mouse model lacking the NKG2D receptor, we saw that the NKG2D system activity is linked to TLRs expression along the GIT, that is location and genotype-dependent. Interestingly, we found subtle differences in the microbiota that were NKG2D-dependent. Thus, we could demonstrate that NKG2D system is important in the modulation of the gut microbiota and this system could be a target in the treatment of GI disorders.

Abstract (German)

Der Verdauungstrakt stellt sowohl das größte Reservoir für kommensale Bakterien und andere Mikroorganismen, als auch das größte immunologische Organ des menschlichen Körpers dar. Diese Mikroorganismen sind maßgeblich an der Entwicklung des Immunsystems beteiligt, weshalb Veränderungen der Darmflora bzw. intestinalen Mikrobiota, sowie Störungen des Immunsystems, schwerwiegende Krankheiten des Magen-Darm-Trakts auslösen können. Der immunologische Abwehrmechanismus rund um den Rezeptor NKG2D (natural killer group 2, member D) ist dabei wesentlich zur Erkennung von Zellstress, der durch zelluläre Veränderungen oder aber auch durch Infektion ausgelöst werden kann. Studien haben gezeigt, dass je nach Zusammensetzung der intestinalen Mikrobiota, diese die Expression der NKG2D Liganden beeinflussen kann. Dabei konnte ein Zusammenhang der Aktivierung des NKG2D Systems mit Krankheiten des menschlichen Verdauungstraktes, sowie Zöliakie oder chronisch-entzündlichen Darmerkrankungen, hergestellt werden. Diese Krankheiten sind ebenfalls mit einer Veränderung der Darmflora assoziiert. Die hier durchgeführte Studie, über den Aufbau der Magenmikrobiota, konnte zeigen, dass das grampositive Bakterium *Propionibacterium acnes* mit der lymphozytären Gastritis assoziiert ist. Hierbei handelt es sich um eine chronische Form der Gastritis, die häufig gemeinsam mit der Zöliakie auftritt. Weiter konnte diese Studie zeigen, dass die lymphozytäre Gastritis neben einer Veränderung der Mikrobiota, im Gegensatz zu einer *Helicobacter pylori* induzierten Gastritis auch eine Aktivierung des NKG2D Systems zur Folge hat. Zusätzlich konnte mittels Zellkulturen von Magen-Epithelzellen gezeigt werden, dass sowohl *P. acnes* Zellen, als auch kurzkettige Fettsäuren, die Expression der NKG2D Liganden *in vitro* stimulieren können, während eine Behandlung der Epithelzellen mit *H. pylori*, je nach Stamm, keinen bzw. einen reprimierenden Effekt auf deren Expression hatte. Untersuchungen der lymphozytären Kolitis, einer entzündlichen Erkrankung des Kolons, die ähnliche pathologischen Muster der lymphozytären Gastritis aufweist, ergaben wiederum keine Aktivierung des NKG2D Systems. Dieser Unterschied könnte auf die unterschiedliche Zusammensetzung der Mikrobiota einerseits und der Immunzellen beider Organe andererseits, zurückzuführen

sein. Die unterschiedliche Reaktion des NKG2D Systems in Magen- und Kolon-Epithelzellen auf kurzkettige Fettsäuren als Stimulus, läßt ebenfalls den Schluss zu, dass die Bedeutung dieses immunologischen Abwehrmechanismus organspezifisch unterschiedlich ist. Abschließend konnte in einem Mausmodell gezeigt werden, dass die Aktivierung des NKG2D Systems mit der Expression von Toll-ähnlichen Rezeptoren (TLRs) verbunden ist. Genetisch veränderte Mäuse ohne NKG2D Rezeptor, zeigten dabei wiederum, dass die Zusammenhänge zwischen NKG2D System und TLR Expression dabei gewebsspezifische und auch genotypische Unterschiede aufweisen. Diese Untersuchungen zeigen, dass das NKG2D System entscheidenden Einfluss auf die Zusammensetzung der intestinalen Mikrobiota hat und somit auch als einen wichtigen therapeutischen Ansatz für die Behandlung von Magen-Darmerkrankungen bietet.

I. Introduction

1.The human gastrointestinal tract

The gastrointestinal tract (GIT) is the largest reservoir of commensal bacteria in the human body (1). Food intake allows the entry of exogenous microorganisms and nutrients in the GIT, supporting the growth and survival of both the host and commensals. In fact, the intestine represents the largest body-surface, with an area of about 300 m² in adults (2). Therefore, a healthy gut is important to perform digestive and absorptive functions, while maintaining a barrier against microbes present in the lumen. For this reason, highly specialized barrier defenses have evolved. The barrier is comprised of a stratified mucous layer, a single layer of columnar epithelial cells (ECs) (stratified squamous epithelium in the case of the esophagus), and a lamina propria, populated by immune cells that actively participate in homeostatic responses against microbiota without triggering an unnecessary inflammatory response (2).

1.1. Anatomy and function of the GIT

1.1.1. Stomach

The stomach is located in the upper left quadrant of the abdomen and receives food from the esophagus. The stomach is divided in three regions: fundus, corpus and antrum. The stomach has a surface area of about 500 cm², corresponding to a volume of 1 L (3). The mucosa of the stomach is represented by a simple columnar epithelium containing numerous tubular gastric glands. These gastric glands are open at the surface of the mucosa and are known as gastric pits (3). Five different types of cells compose the gastric glands: mucous, parietal, chief, enteroendocrine and stem cells.

1.1.2. Small intestine

The small intestine is divided in three main portions, that are, from proximal to distal: duodenum, jejunum and ileum. The small intestine presents the general epithelial structure of the GIT, with a single layer of columnar ECs.

The small intestine, with its characteristic villous structure, holds the greatest epithelial surface, which in average is about 30 m² (3). This feature is important for favoring the digestion and absorption of nutrients. However, this large surface area makes the small intestinal epithelium more exposed to the microbiota and therefore, more susceptible to pathogen entry (2). Nevertheless, the bacterial load in the small intestine is not as great as in the large intestine, partly because of peristalsis moving the content quickly, including microbes. On the other hand, the duodenum receives bile salts from the gall and acid from the stomach, both of them with antimicrobial capacities (2).

1.1.3. Large intestine

The large intestine is the final portion of the GIT. It is divided in the colon (ascending, transverse, descending, sigmoid) and rectum.

The epithelial layer of the large intestine shared the same characteristics as the ones found in the rest of the GIT, but with some particular characteristics: The large intestinal mucosa has a great number of goblet cells and it does not present villi (3).

1.2. Gut mucosal barrier

1.2.1. Lumen

The lumen is the hollow space at the center of the GIT, through which food passes. In the lumen we find the greatest load of commensal bacteria (4).

Events such as changes in diet, antibiotic exposure or an aberrant gastrointestinal (GI) motility alter the lumen community drastically. However, the intestinal crypts and the mucosa, with a more stable microbial community, serve as reservoirs to replenish

the lumen bacteria (5), although a general divergence between mucosal and luminal microbial communities has been observed (6).

The lumen also contains antibodies, such as soluble Immunoglobulin A (sIgA), which is the first line of defense and protects the intestinal epithelium from pathogens and toxins. sIgA blocks the access of those pathogens from the lumen to the epithelium trapping them in the mucus, where they will be later removed by peristalsis in a process called "immune exclusion" (7).

1.2.2. Mucous layer

Mucus is the first line of defense against microbes and creates a boundary between the gut lumen and the epithelium. It is produced continuously by goblet cells in the epithelium. Mucus consists of mucins and antimicrobial peptides (AMPs). Mucin is composed of carbohydrate-rich glycoproteins and glycolipids. Mucus production is modulated by microbial products, such as microbial-associated molecular pattern (MAMPs) and short-chain fatty acids (SCFAs) (8, 9). Thickness and structure of gut mucus differs along the GIT: While in the proximal small intestine it is a single discontinuous and relatively thin mucous layer, it becomes thicker and continuous in the terminal ileum and colon, which present two layers of mucus. The mucus is stratified in two functionally different layers in the colon: a compact inner layer, which is hardly populated by bacteria; and an outer layer, loosely structured and densely populated by commensals (10). Both mucous layers have a similar MUC2 composition. However the differences reside in the distinct proteolytic cleavage of MUC2's polypeptide backbone in the outer layer, resulting in an expanded volume (10). This architecture correlates with the local bacterial load (10) and provides an anchor where the commensals can establish biofilms that will exclude pathogens (11). In contrast with the outer mucous layer, the inner mucous layer has a compact physicochemical structure and functions as a reservoir for microbicidal products of the epithelium, including antimicrobial peptides, such as Reg-IIIγ (12) and sIgA (13).

Moreover, the distinct architecture of the mucus layer will define different habitats for specific microbial communities along the GIT (5).

Furthermore, mucin glycans are a source of nutrients for some commensals, such as *Bifidobacterium* and *Bacteroides* spp. These bacteria have the capacity of fermenting these complex mucin glycans to produce SCFAs. The production of SCFAs result in an advantage for the host, since they are toxic for some pathogens (14), but also some SCFAs, especially butyrate, are the main nutrient source for colonocytes.

Variation in mucin expression may change in the GIT when an inflammatory condition is present (15), such in IBD (16), *H. pylori*-gastritis (HpG) (17-19) or in intestinal metaplasia of gastric mucosa (20), where intestinal rather than gastric mucins are produced in the stomach (21).

1.2.3. Epithelium

A single layer of columnar ECs composes the GIT epithelium, as previously mentioned. These cells are linked by tight junctions and are the first line of defense against invading microbes. Therefore, it constitutes an active sensor for the dialogue between the host and the microbiota. In fact, the GI epithelium is considered an active participant in innate immunity (22). In this sense, the epithelial barrier is able not only to restrain physically the microbiota from the lamina propria, but also it secretes pro-inflammatory cytokines, reactive oxygen species, AMPs and IgA in response to pathogen invasion and metabolic stress (23-27).

1.2.4. Lamina propria

The lamina propria constitutes a layer of loose connective tissue that is found beneath the epithelium. It contains blood and lymph vessels and parts of the GIT nervous system (28). The lamina propria harbors large numbers of cells, including various lymphocyte populations, macrophages, dendritic cells (DCs) and IgA-producing plasma cells (29), summarized as gut-associated lymphoid tissue (GALT) (30). However, the lamina propria and the epithelium represent very distinct immunological compartments. The immune cells may be organized in specialized

lymphoid structures, such as Peyer's patches, cryptopatches or isolated lymphoid follicles in the gut (29), or are represented in a scattered form throughout the lamina propria, depending on the region along the GIT. These specialized immune structures are going to be essential in sensing the gut microbiota and regulating immune responses (29, 31).

In the recent years it has been widely reported that exposure of immune cells to bacteria is essential to maintain proper immune functions in the gut (32-35). However, either excessive or limited contact with commensals will have dramatic consequences, such as an excessive inflammatory reaction or impaired gut development and function, respectively (31, 32, 36).

1.3. Chronic inflammatory diseases of the GIT associated with dysbiosis

1.3.1. Inflammatory bowel disease (IBD)

IBD comprises two different pathologies: Crohn's disease (CD) and ulcerative colitis (UC). CD may be suffered throughout the GIT, from mouth to anus, while UC is restricted to the large intestine. Both diseases share symptoms ranging from chronic inflammation, pain, vomiting, diarrhea to other complications, including severe weight loss, behavioral changes as well as cancer (37).

IBD is a multifactor disease, where both a genetic predisposition and environmental factors have an implication in its development and outcome, although the genetic susceptibility factors cannot explain the incidence in most of the cases (38). Among the environmental factors, diet, antibiotic treatment, social status and microbial exposure have been related to the diseases (39). Interestingly, most of these factors are involved in the microbial composition of the gut. In fact, several studies investigating stool or mucosa samples, showed that general dysbiosis and not a specific pathogen, is associated with IBD (39-44). In general, people suffering from IBD show a decrease in microbial diversity compared to healthy controls (45), with a decrease in the phyla Bacteroides and Firmicutes and an increase in

Gammaproteobacteria (44). Among the strategies to treat IBD, TNF- α therapy is widely used in patients with CD or UC, where mucosal healing leads to fewer hospitalization and better quality of life (46).

1.3.2. Celiac Disease

Celiac disease (CeD) has been classically described as a chronic immune-mediated enteropathy of the small intestine characterized by villous atrophy, crypt hyperplasia, and T-lymphocyte infiltration of the epithelium (47). The main trigger factor of CeD is the ingestion of gluten in susceptible individuals bearing the histocompatibility complex II class human leukocyte antigen (HLA) DQ2 or DQ8 haplotype (48). However, only 2-5% of people carrying the HLA-DQ2/8 susceptibility genes develop CeD. This fact suggests that additional environmental factors may contribute to disease development (49).

It has been recently stressed that not only gluten, but also the microbiota is involved in the outcome of CeD (50). Several studies point towards differences in both fecal and duodenal microbiota in CeD patients compared to healthy controls (51-63). Particularly, patients suffering from CeD show an increase in Proteobacteria and a decrease in Firmicutes compared to healthy controls (59, 62). Further evidences of an implication of the gut microbiota in CeD development is related to factors involved in shaping the gut microbiota from birth, such as breastfeeding, delivery mode, diet, antibiotic exposure or probiotic use and the disease development later in life (50).

1.3.3. *H. pylori* gastritis

H. pylori colonize the stomach of about 50% of the human population and frequently persist in the gastric mucosa for decades, despite a strong humoral and cellular immune response at the local and systemic level (64, 65). *H. pylori* is normally acquired during childhood (66) and many people carrying *H. pylori* do not present any

symptoms. However, several colonized individuals develop clinical symptoms. Chronic inflammation due to *H. pylori* infection leads to different gastroduodenal pathologies, ranging from peptic or duodenal ulcer to gastric cancer or MALT lymphoma (67, 68). It is not clear which factors determine the different outcomes of *H. pylori* infection, however differences in the presence and expression of specific bacterial virulence factors and the host immune status appear to be related to the outcome. Additionally, during its long co-evolution with humans, *H. pylori* has developed complex strategies to evade the host immune response (69). Among these strategies, *H. pylori* is able to avoid the effect of the acidic gastric pH and motility, due to production of urease (which hydrolyzes urea into carbon dioxide and ammonia) and its flagella (which allows the bacterium to swim in the mucus to reach zones with a more neutral pH) (64). Once in the mucus, *H. pylori* adheres tightly to the gastric ECs. Treatment of HpG is not trivial, and a combination of various antibiotics and acid suppressants has been traditionally used to eradicate the infection (70-73). Effectiveness is compromised due to the rapid emergence of antibiotic-resistance of *H. pylori* or due to compliance problems of the patient (74). Therefore, alternative treatments are needed and some have been already suggested, as the use of probiotics. The idea behind is to avoid *H. pylori* to adhere to the gastric epithelium or the production of antimicrobial molecules that can directly affect the viability of *H. pylori* (75-77). Successful *H. pylori* eradication cures chronic gastritis, reverses mucosa inflammation and cures symptoms in patients showing dyspepsia, peptic or duodenal ulcer and also gastric MALT lymphomas.

1.3.4. Lymphocytic gastritis

Lymphocytic gastritis (LyG) is a rare form of gastritis that accounts for up to 4.5% of chronic gastritis cases. Symptoms range from abdominal pain and dyspepsia to severe cases with protein-losing gastro-enteropathy, weight-loss and anemia (78). LyG is histologically characterized by an increased number of CD8+ intraepithelial lymphocytes (IELs). Normal range is below 8 IELs per 100 ECs and increases around

25 per 100 ECs in LyG cases. These IELs show typically a cytotoxic phenotype with granzyme B and TIA 1 expression (79, 80). LyG was initially reported in the context of "varioliform gastritis" and seems to be a histopathologic syndrome rather than a single disease (81). Up to 45% of LyG cases are associated with CeD. In these cases, IELs are normally found in the gastric antrum. Several other cases are though to be associated with the previous describe HpG, although *H. pylori* is often not detectable (82). Rare causes include CD, HIV infection, common variable immunodeficiency or ticlopidine use (78). Nevertheless, more than 20% of cases have an unknown etiology not associated with any of the former mentioned conditions. Interestingly, antibiotic therapy used for HpG cases seems to be effective in the treatment of LyG, suggesting an alternative bacterial cause for the disease (83-85). Recently our group has shown through comparative microbiota analysis that LyG is characterized by an overabundance of *Propionibacterium acnes*. Moreover, we have identified that the NKG2D system and the pro-inflammatory cytokine IL15 to be significantly induced in LyG patients, which might be responsible for IELs recruitment, the typical phenotype found in LyG. A proposed model of the molecular mechanism triggered in LyG patients is presented in Fig. 1.

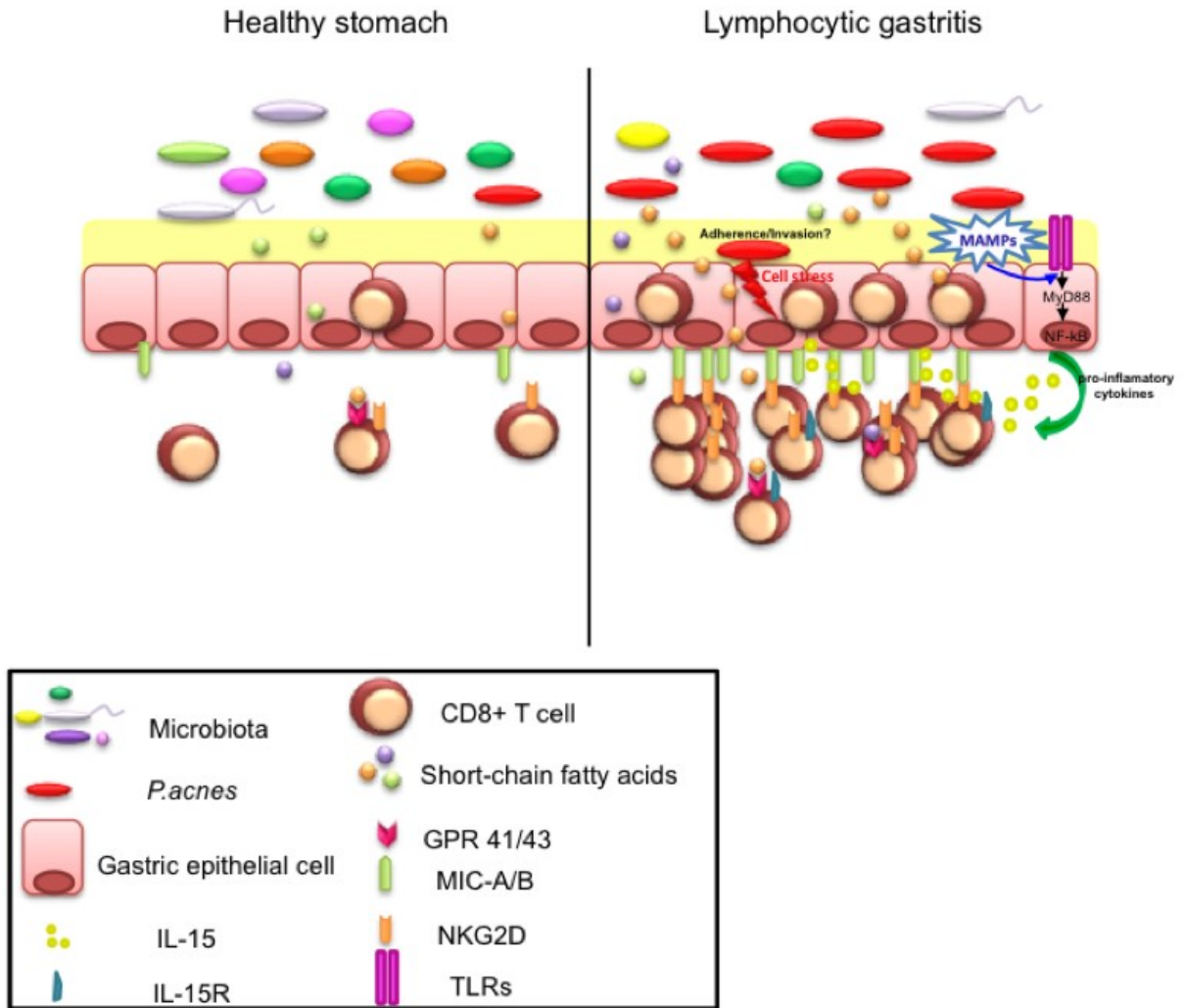


Figure 1. Representation of the molecular mechanisms triggering LyG, where the NKG2D system is highly activated due to the presence of *P. acnes* and the production of microbial metabolites, such as SCFAs.

2. Gut microbiota

2.1 Definition

The gut microbiota is defined as all those microbial species, including bacteria, archaea, viruses, and unicellular eukaryotes, living in the GIT (86).

2.2. Composition, distribution and abundance

The human gut harbors around 100 trillions of microorganisms, most of which belong to the domain Bacteria. However, this population of microorganisms is very diverse and includes also members of the domains Archaea and Eukarya, as well as viruses (31). Although it has been largely estimated that bacteria outnumbered human cells by a ratio of 10:1, Sender, R et al. have recently revisit this statement and came to the conclusion that the ratio bacterial cells: human cells is more like 1:1 (87).

Among all the tissues in a vertebrate body, the GIT harbors the most diverse and abundant bacterial community. In humans, the GI community varies, beginning at the upper tract with about 10^1 bacteria, where the composition is affected mainly by food components (50) and concluding with approximately 10^{14} cells/g in the colon, represented by ~1000 different species, which have been well characterized (88-90). From those 1000 species, each individual will be colonized by about 15% of them (91), giving an impression of they high interindividual variability in the gut microbiota composition.

In the gut, bacteria belong predominantly to the phyla Firmicutes, Bacteroidetes and Actinobacteria (6, 91-93). However, under dysbiosis, presence of the phylum Proteobacteria may also increase (94-96). Interestingly, although Firmicutes and Bacteroidetes dominate the gut, their relative abundance may vary within individuals, which seems to be related to dietary effects (97, 98). Importantly, microbiota alterations due to over- or malnutrition are known to have profound consequences for immune function and health (98-101). A detailed characterization of the human gut microbiota is feasible due to metagenomic approaches, which are useful to identify the members playing an important role in gut homeostasis (91, 102, 103).

2.3. Host-microbial interactions

The human gut is a complex ecosystem wherein microbiota, host and nutrients interact intensively (Fig. 2). This host-microbe relationship was considered for years only from a pathogenic perspective. However, in the last years plenty evidence emerged of the beneficial effect of the microbiota on hosts health (1, 104-106). In fact, this host-microbe relationship coexists, under physiological conditions, in a homeostatic scenario (28). However, environmental factors can influence the immune function and bacterial composition, which will disrupt this homeostasis and lead to a proinflammatory response (50, 104, 105, 107).

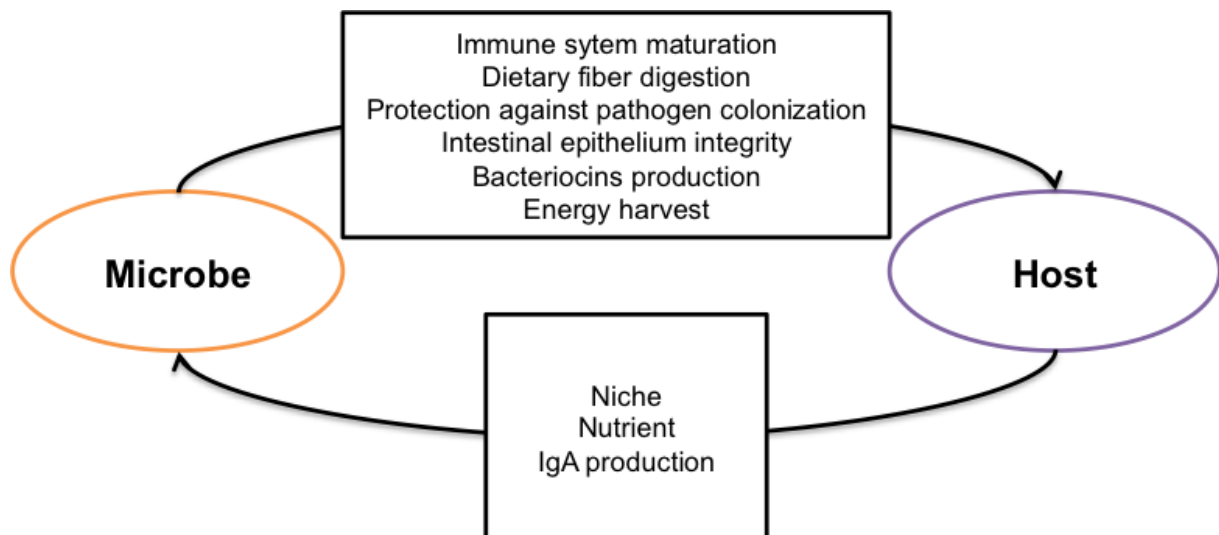


Figure 2. Scheme representing some features of the host-microbe interplay.

2.3.1. Functions of the microbiota in the GIT

The indigenous microbiota is responsible for diverse functions in the gut, such as the metabolization of non-digestible dietary compounds (108-110), the synthesis of vitamins (111), the bioconversion of xenobiotics, the priming and shaping of the immune system (2, 32, 33) and the maintenance of the intestinal mucosal barrier (112, 113). They also protect from pathogen colonization by occupying specific niches and creating biofilm networks, which will restrict the colonization of potential

pathogens, a process named colonization resistance (2, 114). At the same time, the gut microbiota benefits from the nutrient-rich environment of the gut (2, 110) (Fig.3).

2.3.2. Homeostasis vs. dysbiosis

Despite all the benefits stated above, the microbiota is not innocuous and under specific conditions that compromise the host immune system, bacterial species can reach the host tissue and cause disease (2). Furthermore, dietary changes, antibiotic exposure or invasive pathogens can disturb the metabolic network of the gut microbiota, break the homeostatic status of the host and lead to the overgrowth of certain commensal species that can then behave now as pathogens, named pathobionts. This imbalance of the homeostasis is called dysbiosis and it can trigger undesired immune responses that will end in GIT disorders (113).

The term dysbiosis has been widely associated with several GI diseases, such as IBD (45, 115, 116), CeD (51-54, 56) or colon cancer (117-121). But dysbiosis is not just restricted to the gut, since it has been related to many other extraintestinal pathologies and disorders, including rheumatoid arthritis, diabetes, multiple sclerosis, atopic dermatitis, asthma, obesity, autism (122), metabolic syndrome (123) and different types of cancer (124-127). Whether dysbiosis is a cause or consequence of a disturbed host-microbe interaction remains elusive, but understanding the features influencing the composition of the microbiota will possibly enable the development of new therapies for those diseases.

2.3.2. Association of the microbiota with inflammatory diseases

In the last years, the incidence of infectious diseases has dropped in the industrialized countries. However the frequency of allergic and autoimmune disorders increased, such as CeD, IBD or asthma. This fact has been related to a reduced environmental exposure to microbes early in life, known as the "hygiene hypothesis" (128). During the early stages of life, when the immune system is developing, it is crucial that the host is challenged with microbial stimuli to ensure the full and proper

development of the GI and extra-intestinal systems (129). The consequences usually emerge during adolescence or early-adulthood. For example, caesarean section delivery, wherein the infant gut is colonized predominantly by clostridia, has been linked to an increased risk of coeliac disease (130, 131), type 1 diabetes mellitus (132, 133), and asthma (134, 135) compared to vaginal delivery, wherein bifidobacteria are the dominant gut microbes (61, 107, 136-138).

2.3.3. Pathobionts associated with GI inflammatory diseases: *H. pylori* and *P. acnes*

It is a challenge for the immune system to distinguish between harmless commensals from dangerous or opportunistic pathogens, since both present the same pattern recognition receptors (PRRs) (139, 140). Though most of the host-microbe associations within the GIT are symbiotic or commensal, some resident bacteria have potential to cause disease, which is known as pathobiont (141). Interestingly, almost every commensal may have pathogenic potential when the host is immunocompromised or in a nutrient-deprived state (5). Therefore the same microorganisms could be both beneficial and hazardous (141). *Helicobacter hepaticus* is a good example of pathobiont in animal models. *H. hepaticus* cause chronic inflammatory responses in mice (similar to human IBD) only when genetic or environmental conditions are altered in the host (32, 142). Similarly, other *Helicobacter* species in human, such as *H. cinaedi*, *H. fennelliae* or *H. canadensis* have been related to enterocolitis, diarrhea, and bacteremia only in a portion of infected patients (143, 144).

2.3.3.1. *Helicobacter pylori*

A good example for a pathobiont is *H. pylori*, which colonizes about 50% of the population as a commensal of the stomach. *H. pylori* was discovered in the '80s and since then, this Gram- negative microaerophilic bacterium has been paid much attention (74). However, *H. pylori*-host interactions could have different outcomes

depending on the bacterial strain that colonizes the stomach, the host immune status and susceptibility and also the age of the individual (145). *H. pylori* is often acquired in childhood by oral ingestion, generally transmitted by the mother (64, 146), and may cause acute or chronic gastritis in adulthood, gastric or duodenal ulceration and even gastric cancer or lymphoma in the most severe cases at a later age (147). By contrast, *H. pylori* is also known to confer protection against asthma and possibly infections in early life (148, 149). Additionally, *H. pylori* has been reported to be a safeguard against reflux-associated complications, metaplasia and neoplasia at the gastroesophageal junction (150).

H. pylori displays several unique features to successfully colonize the hostile stomach (Fig. 3). One intensively studied is the production of the enzyme urease, which is able to hydrolyze urea into ammonia and carbamate, increasing the gastric pH and permitting colonization of the gastric epithelium (151-154). Additionally, *H. pylori* presents an extraordinary mobility due to its flagella (155). Among its virulence factors, the vacuolating cytotoxin A (VacA), and the cytotoxin associated gene A (CagA) are the most studied and well-characterized virulence factors.

VacA is not only capable of induce vacuolization of ECs, but is also involved in multiple cellular activities. For example, VacA is able to form membrane-channels, release cytochrome c from mitochondria leading to apoptosis, and bind to cell-membrane receptors followed by initiation of a proinflammatory response (156). Additionally, VacA inhibit activation and proliferation of T-cells and B-cell subsets (157, 158). VacA is associated with several clinical outcomes, such as peptic ulcer and gastric cancer (159). CagA is encoded by the *cag* pathogenicity island and is injected into gastric ECs by type IV secretion (160). Transmission of CagA directly to the ECs affects cellular tight junctions, cellular polarity, cell proliferation and differentiation, cell scattering, induction of inflammation and cellular elongation (161-172). CagA positive strains cause more severe disease, and are also implicated in the development of gastric cancer (173) and are generally more prevalent in East Asian countries (174).

2.3.3.2. *Propionibacterium acnes*

P. acnes is an anaerobic-aerotolerant, rod-shaped Gram-positive bacterium that is part of the normal skin microbiota (175) and is well known for its implication in acne vulgaris (176). However, *P. acnes* can also be found in the oral cavity, the conjunctiva (177) or the GIT (178) (Fig. 3).

Beyond acne vulgaris, *P. acnes* has been associated with different inflammatory conditions and post-surgical infections (179). In fact, it has been isolated from patients with primary biliary cirrhosis (180), prostate cancer (181, 182) or sarcoidosis (183).

It has been demonstrated that *P. acnes* possesses a potent immunostimulatory activity, able to induce the secretion of proinflammatory cytokines and the stimulation of T- cells (184, 185). Recently, *P. acnes* strains have been classified into different phylotypes (Type I-1a, 1b and 2, type II and type III) using a multilocus sequence typing (MLST) approach (186), which allows to differentiate the strains according to single-nucleotide polymorphism (SNPs) in housekeeping genes (187).

Interestingly, some *P. acnes* strains have been attributed also with probiotic effects. Thus, *P. acnes* is able to produce SCFAs from non-digestible carbohydrates due its anaerobic metabolism (188, 189), which may play beneficial roles for the host.

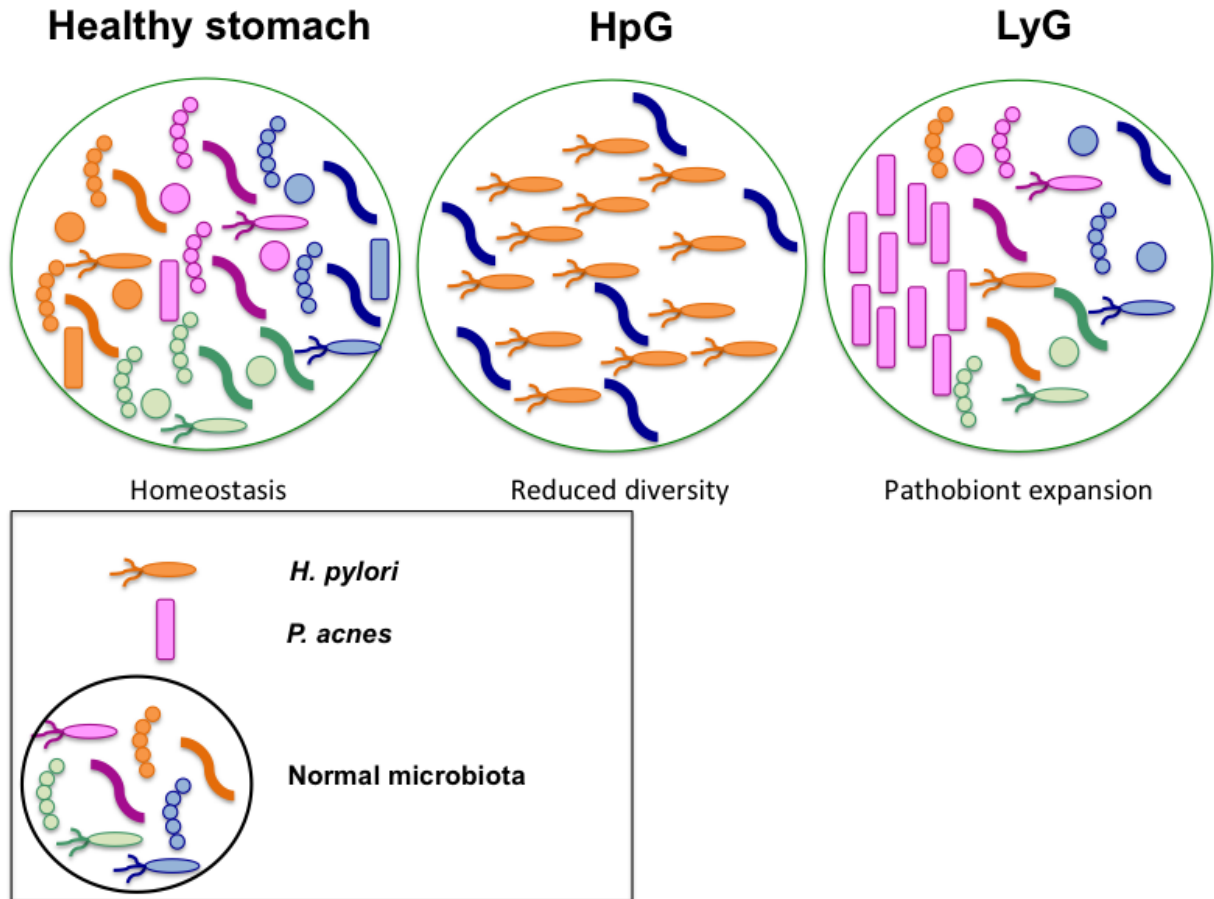


Figure 3. Graphic representation of the stomach microbiota under homeostasis, in HpG and LyG. Note the difference between HpG and LyG pathologies. While in HpG we have a typical infection due to *H. pylori* (presence/absence of *H. pylori* determines disease), in LyG the disorder is more related to the expansion of the pathobiont *P. acnes*.

2.4. Microbial metabolites: Short-chain fatty acids (SCFAs)

2.4.1. Definition, composition and concentration.

SCFAs are carboxylic acids characterized by the presence of an aliphatic tail with a length from two to six carbons (190). Acetate (C2), propionate (C3), and butyrate (C4) are the most abundant (95%) in the human gut and are present in a molar ratio of 60:25:15, respectively (191). However, the luminal concentrations of intestinal SCFAs are prone to change by the site of fermentation, host genotype and the amount of fiber ingested, which affects the composition of the microbiota (100, 192). Thereafter,

the total concentration of SCFAs will decrease from 70 to 140 mM in the proximal colon to 20 to 70 mM in the distal colon (193, 194).

2.4.2. Metabolization, transport, absorption and signal transduction of SCFAs.

SCFAs are the major products obtained after fermentation of dietary complex carbohydrates by specific members of the gut microbiota. The major source for SCFAs production are plant cell wall polysaccharides (named dietary fiber), as well as resistant starches that escape digestion in the small intestine (195). Additionally, protein, mucus, sloughed cells and GI secretions may also contribute to SCFAs production (195). Certain bacterial species possess specific enzymes involved in the production of different SCFAs using alternative pathways (190). Interestingly, interaction within the microbiota may also control the proportion of SCFAs in the gut lumen. For example, it is known that members of the phylum Bacteroidetes degrade butyrate and propionate into acetate, while species belonging to the phylum Firmicutes use acetate as a substrate to generate propionate and butyrate (196).

SCFAs can exist as ionized or unionized form. The first case is the most common form and is absorbed by the transporters monocarboxylate transporter 1 (MCT-1) and the sodium-coupled monocarboxylate transporter 1 (SMCT-1). Both transporters are generally expressed along the GIT on ECs. Additionally, MCT-1 is found on lymphocytes, suggesting a role of SCFAs on these cells (197). SCFAs in their unionized form can passively cross the epithelial barrier.

Once SCFAs cross the epithelial barrier they can exert different functions and modulate biological responses of the host mainly by two different mechanisms: histone deacetylase (HDAC) inhibition (mostly by butyrate) to modulate gene expression (198, 199), and signaling through the G-protein-coupled receptors (GPCRs). GPRs activated by SCFAs are GPR41, GPR43, and GPR109A and have distinct affinities for the different SCFAs (200-202). Upon binding GPR41, GPR43 or GPR109A, SCFAs exert both their metabolic and immune-related effects (203).

GPR43 is expressed along the GIT, but also on immune and nervous cells; whereas, GPR41 is found mainly in colonocytes (190). GPR109A is expressed not only on immune cells, but also on adipocytes (204).

2.4.3. Role of SCFAs in the GIT

In the recent years, the gut microbiota has been attributed with an extensive range of functions to keep host health and homeostasis in the gut. We now know that these effects are, at least in part, due to SCFAs production (190). In fact, SCFAs deficiency may affect the outcome of different pathologies, both intestinal and extraintestinal (205-207). For example, it has been recently reported that the amount of butyrate significantly decreased in the intestinal tissue after allogenic bone marrow transplantation in patients that experience graft-versus-host disease (GvHD). By increasing the amount of butyrate or by specifically altering the microbiota with high-butyrate producing Clostridia, GvHD severity was decreased (208).

SCFAs are also known to be an important energy source for the host, especially for colonocytes (209), thus, they play a central role in the physiology and metabolism of the gut. Gut cell proliferation, cell differentiation, apoptosis, mucin production and lipid metabolism seem to be largely mediated by SCFAs (189, 208, 210, 211).

Interestingly, SCFAs also play a notable role on host immune responses (212-214) (104, 191, 215-217). SCFAs modulate anti-inflammatory responses by inhibiting the release of pro-inflammatory cytokines (218), or modulating immune cell chemotaxis (219, 220). Other immune functions of SCFAs include regulation of autophagy (221), regulation of T cell differentiation (215), development of regulatory T cells (222, 223) and stimulation of heat shock protein production (224).

SCFAs exert antimicrobial activities by for example, modifying the pH or promoting the secretion of antimicrobial peptides by the host (225, 226), even at micromolar concentrations (227). Interestingly, this effect seems to be innocuous for the bacteria that produce SCFAs, while affecting other microorganisms (225), thereby shaping the

gut microbiota composition and maintaining homeostasis.

SCFAs are also able to promote intestinal epithelial barrier integrity (228) by the stimulation of mucin production (229). This fact prevents the luminal microbes to reach the intestinal epithelium, avoiding aberrant inflammatory responses, as seen in dysbiotic diseases such as IBD, characterized by increased gut permeability (230) (Fig. 4).

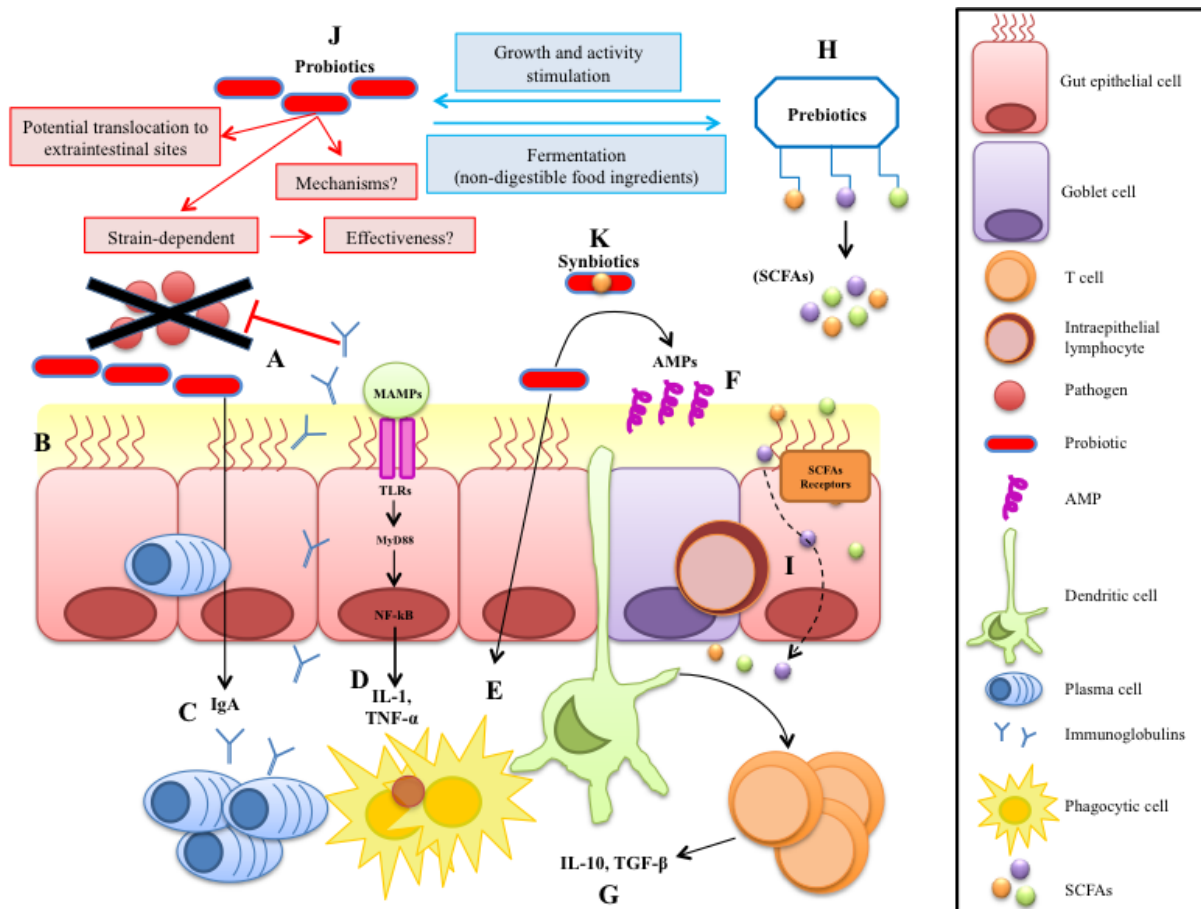


Figure 4. Potential microbial strategies to improve gut mucosal immunity (modified from Montalban-Arques, et al., 2015 (189)). (A) Competitive exclusion for binding sites and translocation, (B) enhanced barrier function by reversing the increased intestinal permeability, (C) enhanced mucosal immunoglobulin IgA response to enteral antigens, (D) reduction of secretion of inflammatory mediators, (E) stimulation of innate immune functions, (F) stimulation of the release of AMPs at the mucosal layer, (G) release of anti-inflammatory mediators by regulatory immune cells. (H) The non-digestible dietary components (prebiotics) produce metabolic health-enhancers like SCFAs; (I) SCFAs diffuse through the enterocytes to

improve mucosa barrier functions. (J) In contrast, probiotics have been suggested to confer several health benefits on the host. However, the mechanisms of action are not well understood. (K) Synbiotics are a mix of pre- and probiotics, thus the mode of action are difficult to be defined.

3. The gut Immune system

3.1. Development of the immune system by the gut microbiota

Microbes are crucial for the development of the immune system. At the same time, a healthy gut is necessary for the maintenance of homeostasis (231). Alterations in either gut microbiota or the immune system may lead to GI disorders.

The development of the immune system begins *in utero*. Thereby the mother can transfer through the placenta immune cells and modulate immune responses in the fetus (232). Interestingly it has recently reported that there is a selective intrauterine contract with microbes and microbial components (136, 233-237). This first contact will have implications for infant health (238, 239).

During birth the baby will be colonized by microbes originating by the maternal vaginal flora or by members of the skin microbiota if delivered by Caesarean section, which will determine the initial colonizers of the baby's GIT (240). This pioneer bacterial species will play an important role in the predisposition to develop allergies or autoimmune diseases later in life (241). Breastfeeding is another main driving force in determining gut colonization patterns early after birth (242, 243). Apart of being the sole source of nutrition for the first months of life, breast milk is also a source of specific nutrients for the infants gut microbiota as well as microbes directly (233). Thereby, breastfeeding exert various immunoprotective roles to the infant, by modulation of the baby gut microbiota or transfer IgA antibodies from the mother.

Microbial antigens that are bound by sIgA could be handled by the innate immune system in a 'tolerogenic' mode, favoring the establishment of regulatory immune networks in the infant that will promote mutualistic relationships with the microbiota.

Thus, sIgA has a dual role in infant-gut-microbiota homeostasis: direct immunomodulation by shaping the infant's immune repertoire as well as selection of microbiota composition (2).

The intestinal microbiota is also essential for the development of the gut-associated lymphoid tissue (GALT), which is composed by Peyer's patches (in the distal ileum), isolated lymphoid follicles (ILFs) and mesenteric lymph nodes (MLNs). Peyer's patches and MLNs develop before birth, while ILFs develops postnatally (244).

Central for the host-microbe tolerance is the seeding of the GIT epithelium with IELs, already before birth (2). These "innate" immune-cells can rapidly respond against microbial insults. Throughout life IELs will play an important role in keeping gut homeostasis and an intact epithelial barrier (245).

3.2. Microbial recognition by Toll-like receptors (TLRs)

Innate immune receptors, such as TLRs seem to play a key role in the communication between the host and the microbiota that will lead to tolerance (246). In mammals, TLRs include at least 11 members, from which TLR1-9 are conserved between mice and human (247). TLR recognize microbial-associated molecular patterns (MAMPS), present in both commensal and pathogenic bacteria (248). For example, TLR2 recognizes peptidoglycan (PG), TLR4 bacterial lipopolysaccharide (LPS), and TLR5 recognized bacterial flagellin (31). TLRs are found extra- and intracellularly on various cells in the gut, including epithelial and immune cells (249).

One of the challenges for the immune system is how to differentiate between commensals and pathogens, so then an inflammatory response is not trigger unnecessarily. One of the mechanisms that have been proposed is the compartmentalization and restricted expression of TLRs, as well as the expression of inhibitors of the TLR signaling cascades (250). Thus, non-invasive bacteria, mainly acting on TLRs expressed on the apical epithelial surface, will generally induce minimal immune activation, while invasive pathogens may trigger a more potent inflammatory response activating TLRs on the basolateral membrane of gut ECs. This mechanism has been reported for example in the case of TLR5 (251, 252).

Interestingly in the case of TLR5, certain flagellins are able to activate it (253), while others do not (254). That is the case for *H. pylori*, which evades immune-recognition and persists in the host (255). Another proposed mechanism is the hyporesponsiveness of TLRs due to constant exposure to TLRs ligands (256).

3.3. NKG2D system

3.3.1. NKG2D receptor

The natural killer group 2 member D (NKG2D) is a lectin-like, type 2 transmembrane activating receptor, which is associated with its adaptor molecule DAP10 (DAP10 and/or DAP12 in case of mice) (257). After receptor engagement, signal transduction and cellular activation is initiated. An arginine positively charged in the transmembrane domain of NKG2D associates with a negatively charged aspartic acid located in the transmembrane domain of the adaptor molecule DAP10. DAP10 contains an YXXM tyrosine-based motif, similar to those found in the co-stimulatory molecule CD28. The YXXM recruits and activate the p85 subunit of phosphoinositide 3-kinase (PI3-K) and the growth factor receptor-bound protein 2 (Grb2) (258-260). In humans, each NKG2D associates with two homodimers of DAP. However, in mice two isoforms of NKG2D exists, as a result of alternative splicing. The shorter variance of NKG2D (NKG2D-S), which lacks 13 amino acids in the N-terminus of the cytoplasmic domain, can bind both DAP10 and DAP12 adaptor molecules. Unlike DAP10, DAP12 contains an immunoreceptor tyrosine based activation motif (ITAM) that recruits and activates ZAP70 and Syk tyrosin kinases to further phosphorylate downstream effectors that trigger cell activation (257). NKG2D is expressed constitutively on NK cells in both human and mice. NKG2D is found also on many T cells, including all CD8⁺ T cells in humans (only in activated CD8⁺ T cells in mice), subsets of CD4⁺, $\gamma\delta$ T and NKT cells as well as macrophages (261). NKG2D receptor expression levels can be upregulated in the presence of IL15 (262). NKG2D receptor is highly conserved and its similarity between humans and mice is about 70%.

3.3.2. NKG2D ligands

The NKG2D receptor has the ability to engage multiple ligands, in both humans and mice, all of which are related to MHC class I molecules (261, 263, 264). In humans, the NKG2D ligands (NKG2DLs) include the MHC class I chain-related proteins A and B (MICA and MICB) and up to six different UL16-binding proteins (ULBP1 to 6), also known as RAET1 proteins (261). In mice there are no orthologous to the human MICA and MICB genes. However, there are orthologous for the ULBP family, corresponding to three different subfamilies, known as retinoic acid early inducible-1 proteins (Rae1), murine UL16-binding protein-like transcript 1 protein (Mult1) and H60 proteins. Rae1 comprises five different isoforms (α , β , γ , δ and ϵ), Mult1 just one and H60 present three different isoforms (a, b and c). It is important to note that not all mouse strains express all the isoforms (257, 261). The NKG2DLs present different structures and their conformation enables them to bind to the NKG2D receptor with different affinities. While, some of the ligands are transmembrane proteins, others are glycosylphosphatidylinositol (GPI)-anchored (261) (Fig. 5).

There are several hypotheses why so many different NKG2DLs exist and about the functional redundancy of them (261, 264):

- a)** It could be that different kinds of stress induce the expression of different ligands (265-268).
- b)** Evolutionary selection pressure might have led to the development of redundant ligands for the same receptor in order to recognize pathogens that have developed strategies to evade the immune system, such as some viruses (269-271).
- c)** Like pathogens, tumor cells have also evolved mechanisms to avoid NKG2D-mediated immune response. One such mechanism consists in shedding NKG2DLs from the EC surface. These shed ligands can bind to NKG2D and downregulate its expression, triggering anergy in NK and T cells expressing the receptor (272). It has been also reported that transformed cells have the ability to switch off the expression of NKG2DLs as they progress (273, 274). Therefore, by the acquisition of multiple NKG2DLs, the host is provided with a fail-safe alert mechanism.

d) Since the ligands have different affinities for the receptor, the response triggered might vary. It has been proposed that these differences may represent a mechanism to regulate the magnitude of the immune response when recognized by the receptor (275).

e) It is plausible that some NKG2DLs may have unique tissue-specific functions not necessarily involved in immune surveillance (264). Thereby, some NKG2DLs are constitutively expressed in healthy ECs, like along the GIT, where contact with bacteria is permanent (276). Moreover, it seems that NKG2DL diversity is related to functional singularities for specific cell types and tissues, as is the case for MICA in the gut or for ULBP4 in the skin (277).

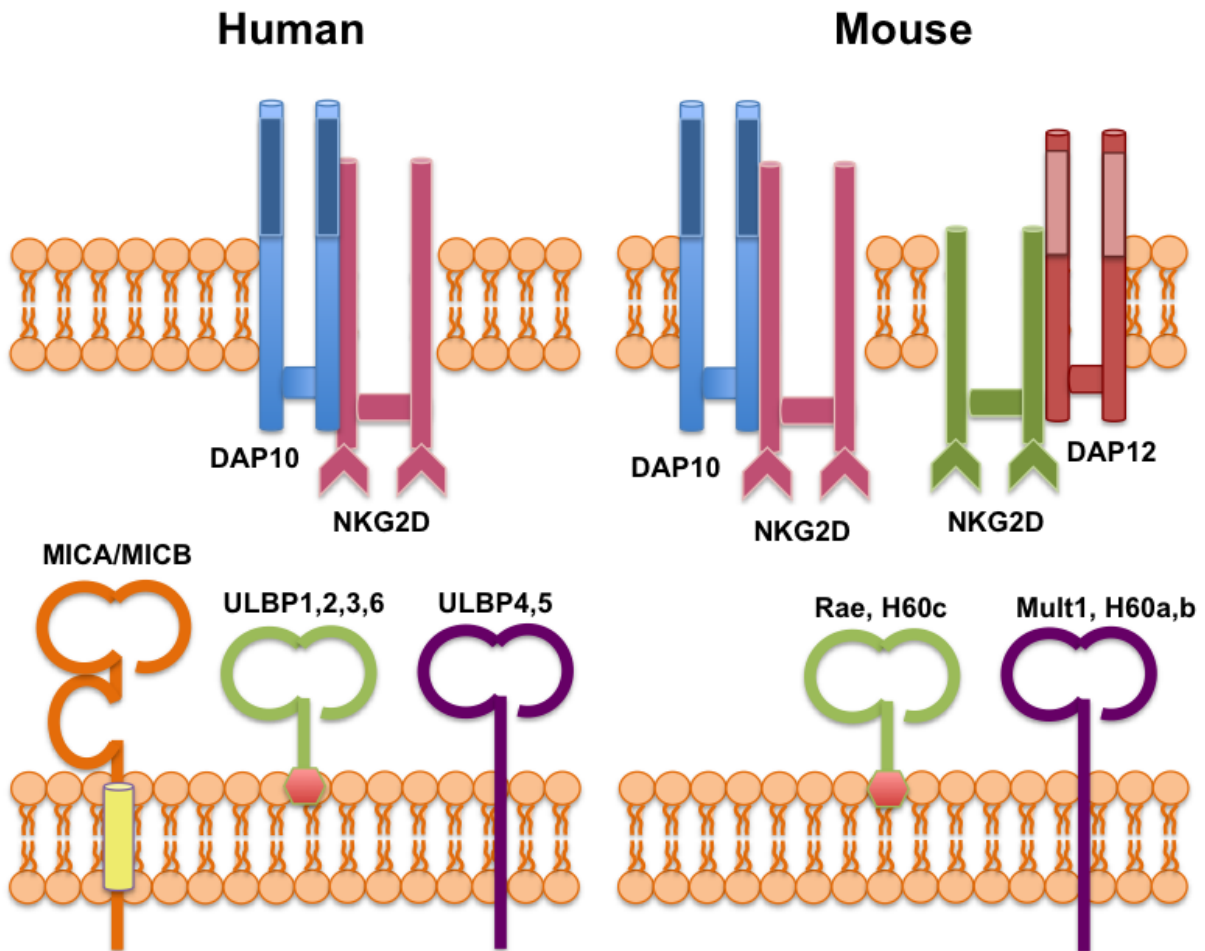


Figure 5. Representation of the different molecular structures of the NKG2D receptor and its ligands in human and mouse.

3.3.3. Interleukin 15

IL15 is a cytokine belonging to the IL 2 family, which includes IL2, IL4, IL7, IL9, IL15 and IL21 (278). In fact, IL2 and IL15 share many functions, for example the stimulation of T cell proliferation and generation of cytotoxic T lymphocytes (278). However, unlike IL2, IL15 plays a role in prolonging responses of memory T cells to pathogens (278).

IL15 is a 14-15 KDa glycoprotein mainly produced by macrophages and non-lymphoid cells. Its expression is regulated at the transcription, translation and intracellular trafficking levels. Aberrant of any of this regulation steps results in increased IL15 production, which will trigger excessive lymphocyte activation, leading to autoimmune and chronic inflammatory diseases, such as CeD (85), IBD (279, 280) or LyG (281).

The IL15 receptor is composed of three different subunits. The α subunit is specific for IL15 and the other two (β or CD122 and γ or CD132) are shared with IL2. IL15 and IL15R α receptors are co-expressed in the same cell. IL15R α binds IL15, both are shuttled to the cell surface as a complex. Thereby, IL15R α modulates the expression of IL15. Once on the cell surface, the IL15-IL15 α complex binds to the IL15R $\beta\gamma$ subunits expressed on immune cells. The complex is shuttled between immune cells in a cell-cell interaction dependent manner (278). This form of cytokine delivery is known as trans-presentation and comprises the formation of an immunological synapse that limits the exposure of circulating IL15 (282, 283). In consequence, IL15 coordinates the response of innate and adaptive immune cells for host protection (284-287).

IL15 is produced by GI ECs (288) and is a potent stimulator of IELs (289). Therefore, IL15, which is increased in several GIT pathologies, is considered a very important modulator of the homeostasis of the intestinal barrier in general and for the function of the NKG2D system in particular.

A summary of the main characteristics associated with each region of the GIT related to function, microbial composition and abundance; pH, SCFAs concentration, CD4+ and CD8+ T cells abundance, and NKG2D system expression along the GIT can be found in Fig. 6.

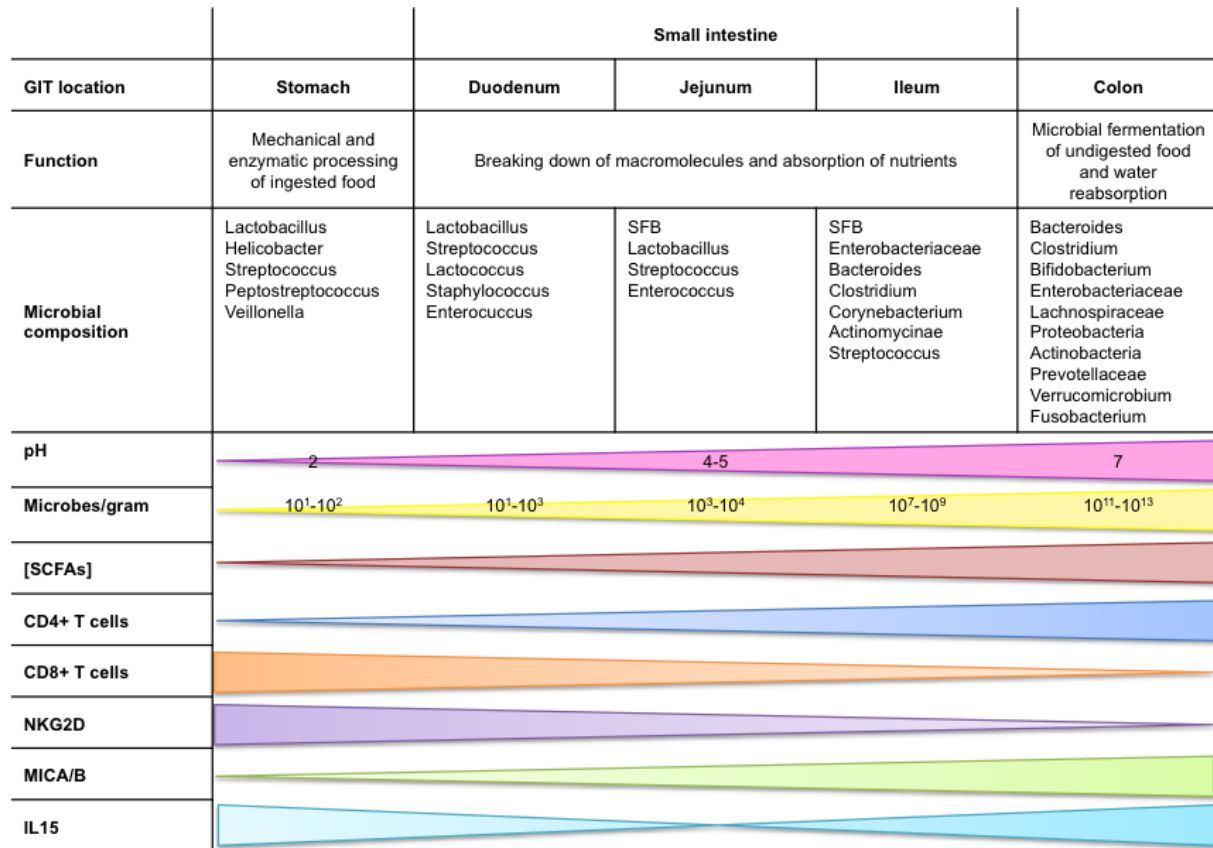


Figure 6. Spatial characteristics of the GIT including function, microbial composition, pH, SCFAs concentration, CD4+ and CD8+ T cells abundance, and NKG2D system expression along the GIT.

3.3.4. Intraepithelial lymphocytes

IELs are predominantly CD8+ T cells belonging to the T cell receptor (TCR) lineages TCR $\alpha\beta$ + and TCR $\gamma\delta$ + (290). In the human small intestine, TCR $\gamma\delta$ + IELs represent about 10% of the IELs, although the numbers increase dramatically under certain inflammatory conditions (291), such as CeD or LyG. Additionally, IELs do not need

priming. In contrast to other T cells, IELs are activated when encountering antigens, triggering the release of cytokines and killing the infected cells (292). IELs are settled between the basolateral surfaces of ECs (293) along the GIT. IELs can express effector cytokines and chemokines, such as IFN γ , IL2, IL4, IL17 or CXCR-3 (294-296), (297-302). IELs present a high cytotoxic activity, denoted by the high presence of cytoplasmic granules (300). Additionally, IELs express both activating and inhibiting NK cells receptors, such as NKG2D and NKG2, respectively. These hallmarks make the IELs behave as stress-sensing immune cells (303, 304).

The characteristic location of the IELs makes them to play a double role in the immune response. These cells need to provide immediate protection against pathogens, while avoiding unnecessary inflammatory immune response against commensals and self-antigens (292). IELs are also known to produce innate antimicrobial factor, such as Reg-III γ , in response to those commensals that penetrate the epithelium (245). However, the primary function of IELs seems to be to keep epithelial integrity (305-310). It has been reported that the secretion of TGF β by IELs has a direct role in protecting the integrity of the epithelium (294). TGF β production is increased when the inhibitory receptor NKG2A is expressed in IELs, while inhibiting the activating receptor NKG2D (311). Therefore, certain IELs control the number and activation of cytotoxic IELs, maintaining thereby a homeostatic condition in the epithelium. Interestingly, IELs are able to sense and eliminate transformed, injured and infected ECs (292).

Despite the beneficial effects of IELs, they are also directly associated to disease severity in GI pathologies, such as IBD, CeD or LyG (312-317). In these cases, the pro-inflammatory cytokine IL15, expressed by the ECs, seems to play a major role in driven a potent cytotoxic response against target ECs, via the activation of the NKG2D system (85).

3.3.5. The diverse roles of the NKG2D system

The natural-killer group 2 member D (NKG2D) system has been classically associated with the regulation of the immune response during "stressed-self"

conditions such as heat shock, DNA damage, oxidative stress, tumorigenesis, infection and autoimmune disorders (85, 265, 318-324). However, recent data reports expression of NKG2DLs in diverse immune cells (325, 326) and ECs (276), which suggests that the role of the NKG2D system may have been oversimplified (327).

3.3.5.1. Infection

The activation of the NKG2D system has also been reported in cases of infection. For example, pathogenic adherent *E. coli* associated with diarrhea can trigger rapid MICA expression on Caco-2 colon ECs by the interaction of its afimbrial adhesin AfaE with the adhesin receptor CD55, which may be related to the pathogenesis of CD (323). In our group we have identified the pathobiont *P. acnes* to induce the mRNA and protein expression of the NKG2DLs MICA and MICB in a strain-dependent way in gastric EC lines.

However, some pathogens, especially viruses, have developed strategies to evade NKG2D-mediated recognition through immunoevasins or micro-RNAs (mi-RNAs) (328). For instance, the glycoprotein UL16 of the Human cytomegalovirus (HCMV) is able to block the surface expression of several NKG2DLs (271, 277). We have recently seen, using an *in vitro* approach with gastric ECs, that *H. pylori* either does not induce or inhibit the mRNA expression of *mica*, *micb* and *il15*, in a strain-dependent manner. Additionally, MICA/B surface protein expression was also downmodulated in gastric ECs (281). This capacity to block the activation of the NKG2DLs may be directly related to the role that *H. pylori* it presents in inducing gastric neoplasia induction and progression.

3.3.5.2. Cell transformation

The majority of studies in regard of the NKG2D function have been related to cell transformation and tumor progression. Most transformed cells express NKG2DLs constitutively (329) and therefore, are susceptible to be killed by immune cells expressing the NKG2D receptor.

Interestingly, high levels of MICA have been reported to be associated with a good prognosis in colorectal cancer (330). In mice, Mult1 and Rae1 ligands were found on primary tumors and were expressed in higher amounts in NKG2D-deficient mice, supporting the idea that NKG2D favors the loss of NKG2DLs on primary tumors (321).

3.3.5.3. Inflammatory and autoimmune diseases

Constitutive expression of MICA in intestinal epithelial cells (IECs) has been associated with GIT inflammatory diseases, such as CeD, IBD or LyG (85, 281, 324, 331). In these disorders, ECs are attacked by NKG2D+ IELs, leading to an impaired epithelium. Interestingly, those diseases are characterized by a dysbiotic microbiota (50, 116), suggesting a link between epithelial homeostasis, microbiota composition and a proper NKG2D system function.

Other extraintestinal autoimmune diseases have been linked to NKG2D system overactivation. For example, type 1 diabetes is associated with MICA expression (332) in humans. In rheumatoid arthritis patients, high levels of IL15 are detected (333), along with higher expression of MICA and MICB (334). Multiple sclerosis susceptibility has been linked with the MICB allele MICB*004 (335). Additionally, high levels of MICB, but not MICA are found in multiple sclerosis patient's sera (336). Moreover, it was also demonstrated by Guerra et al., that NKG2D plays a role in an experimental murine model of autoimmune encephalitis, which resembles human multiple sclerosis (337).

3.3.5.4. Other types of cell stress that activate the NKG2D system

It has been shown in *in vitro* assays, using different cell lines or fibroblasts, that DNA damage produced by irradiation or drugs is associated with the induction of NKG2DLs, in both mice and humans (265, 326, 338). The expression of MICA and MICB has also been related to the heat-shock stress pathway (339). Heat-shock

induces MICA/B through Sp1 and Hsf-1, which is often related to cell transformation (340).

3.3.5.5. The NKG2D system is also active under a physiological status.

Despite the different roles of the NKG2D system mentioned above, NKG2DLs expression must not only be a response of "cell stress" to generate a cytotoxic immune response (327). Several authors have reported expression of NKG2DLs under physiological conditions. For example, Nomura, MJ et al., found Rae1 transcripts in mouse embryonic brains (341) and Gourzi et al., (342) reported the same ligand in class-switching B cells in the spleen. Some, but not all NKG2DLs have also been found in cells of the bone marrow in both humans and mice (343, 344). MICA is expressed in the trophoblast during normal pregnancy (345).

Interestingly, it is likely that the NKG2D system plays a role in development, since the developmental signaling molecule retinoic acid has been shown to induce the expression of Rae1 in mice and MICA in human cell types *in vitro* (341, 346).

3.3.6. *The interplay between the NKG2D system and cytokines*

Cells are able to communicate with each other through extracellular small proteins known as cytokines. Cytokines are secreted by different cells and intervene in the regulation of host immune responses to inflammation, infection or trauma (347). Cytokines can be grouped into innate and adaptive cytokines and also into pro- and anti-inflammatory cytokines (278). Stimulation of NK and T cells by cytokines can significantly affect their cytotoxic activity (327). In fact, cytokines and the NKG2D system modulate the immune response reciprocally (302). Several studies have reported that cytokines such as IL2 (348, 349), IL15 (350, 351), or the combination of IL15 and TNF α (333) are able to increase the expression of NKG2D receptor. However, other cytokines have been implicated in the downregulation of the NKG2D on NK and T cells, such as IL21 (352, 353) or TGF β (85, 354).

Cytokines are not only able to modulate the expression of the NKG2D receptor, but also the NKG2DLs. Thereby, IFN γ has been reported to downregulate MICA and ULBP2 in tumors (355, 356), while IFN α can induce the expression of these two ligands (357, 358). However, in patients with CD, IFN γ upregulates MICA in IECs (359, 360). On the other hand, engagement of NKG2D and any of its ligands, induce the expression of cytokines that will trigger the activation of the immune response, as it is the case for IL15, as discussed before. For a review see (302) and (Fig. 7).

Taking the role of cytokines on the expression of the NKG2D system, it is plausible that these molecules are appealing targets for immunotherapy. However, more knowledge is needed for a complete understanding of their role in the NKG2D system modulation depending on the scenario.

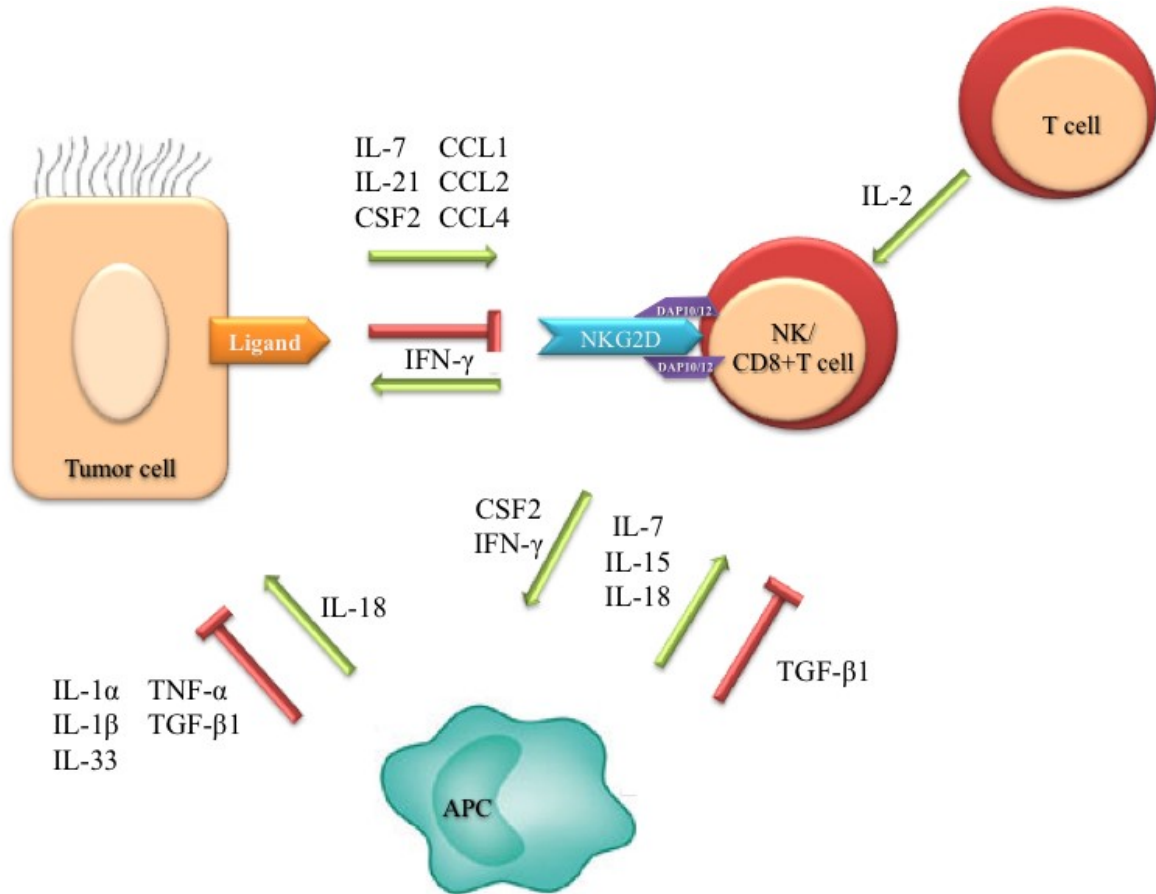


Figure 7. Interplay between cytokines and the NKG2D system in the tumor microenvironment. Within the tumor microenvironment, cytokines play a significant role in the regulation of the cytotoxic and cytolytic activity against tumor cells. Antigen- presenting cells (APC), DCs, and macrophages, can up- or downregulate the expression of NKG2D and NKG2DLs on the surface of ECs, leading to tumor elimination or tumor-cell resistance, respectively. The different output effects depend on the developmental stage of the tumor. Cytokines produced by NKG2D+ cells modulate ligand expression on the target cell and stimulate APC to exert antitumor effects.

3.3.7. Association of the NKG2D system with the microbiota.

It has been reported that members of the microbiota, such as *Akkermansia muciniphila* are able to reduce the expression of NKG2DLs as well as IL15 on IECs, while germ-free and ampicillin-treated mice presented an increased surface expression of NKG2DLs. These results suggest that the commensal microbiota plays

a protective role by downregulating the NKG2DLs on IECs (361). In our group we found that *P. acnes*, which is overrepresented in LyG, is able to increase the expression of MICA and MICB both at the mRNA and protein levels in gastric ECs (281). Moreover, the microbial metabolites SCFAs (propionate and butyrate) were also found to stimulate the transcripts and protein of the same NKG2DLs *in vitro* on gastric ECs (281) (Fig. 8). Previously, Andresen, L et al., reported the induction of MICA/B expression due to propionate stimulation on different cancer cells and activated T lymphocytes, suggesting a prophylactic role of propionate in cancer (362). Additionally, some studies have shown a link between TLR signaling and NKG2DLs expression. For example Hamerman et al. reported that RAE-1 proteins are upregulated on the surface of macrophages that are stimulated with TLR ligands. Thereby, TLR signaling through the adaptor protein MyD88, induce the transcription of Rae1 ligands, establishing a direct communication between infected macrophages and NK cells (363). In a different work, Zhou et al., stated that TLR3 signaling induces the expression of Rae1 on IECs and the expression of NKG2D on IELs by IL 15 derived from those TLR3- activated IELs, leading to tissue injury through the NKG2D pathway. These results suggest that TLR signaling is able to break down self-tolerance by the aberrant induction of NKG2DLs (304).

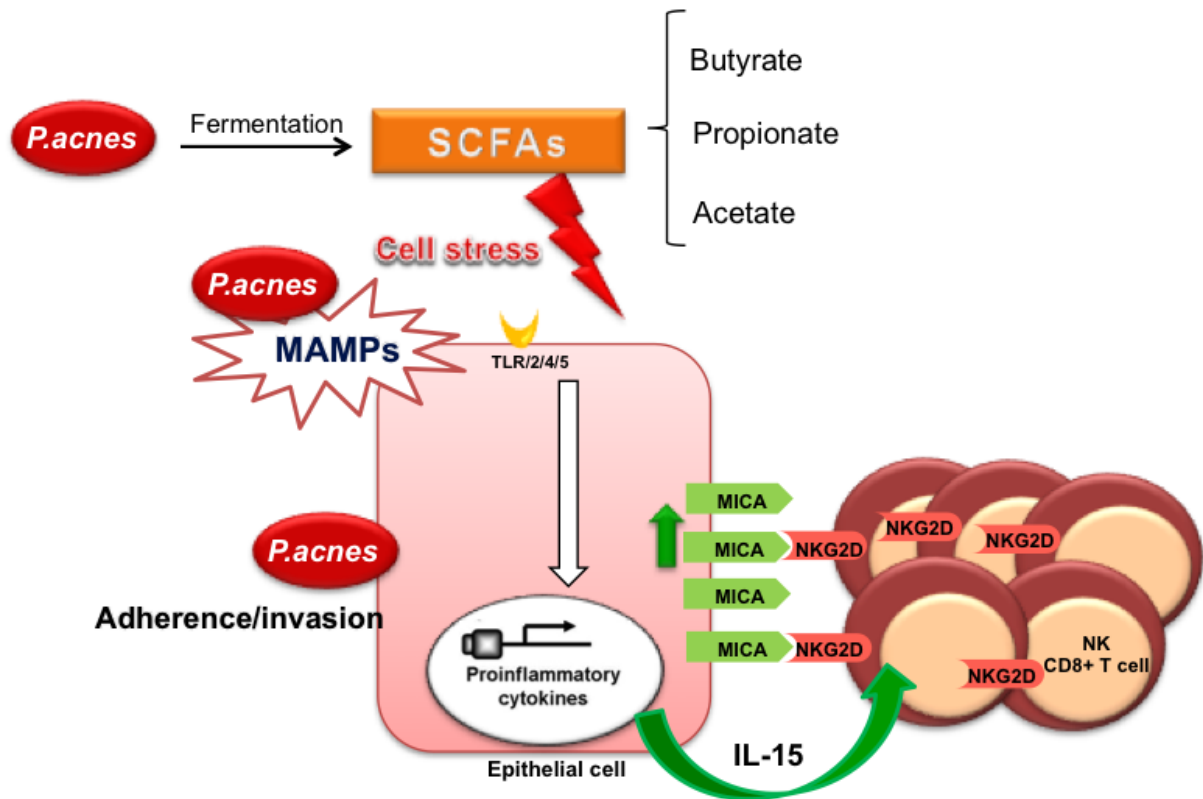


Figure 8. Scheme representing the possible activation of the NKG2D system due to *P. acnes* and the SCFAs through adherence, invasion, TLR signaling or direct cell stress.

We have recently identified a positive correlation between the expression of TLRs and the NKG2D system along the GIT that are NKG2D receptor-dependent (Montalban-Arques et al., unpublished data). Therefore, it seems that the role of the NKG2D system may have been oversimplified and it may play a role in sensing gut microbiota under health and disease conditions.

3.3.8. Phylogenetics of the NKG2D system: A matter of mammals.

Classic MHC class I molecules are found in all jawed vertebrates, from fish to mammals (364-366). However, MIC and ULBP molecules are restricted to placental and marsupial mammals (367). Consistently, the receptor NKG2D is also just found in placental and marsupial mammals (368). Thus, the NKG2D system seems to play an

important role for mammals and this role is, at least in part, unique in this group of vertebrates.

II. Aims

1. To decipher the molecular players in the pathology of LyG.
2. To study the expression of the NKG2D system along the GIT under health and disease conditions.
3. To investigate the role the gut microbiota plays in the activation of the NKG2D system in the GIT.

III. Materials and Methods

1. Human samples.

Formalin-fixed and paraffin-embedded (FFPE) GI biopsies from stomach, duodenum, ileum and colon collected between the years 2007 and 2015 were derived from the files of the Institute of Pathology at the Medical University of Graz. *H. pylori* carriage was determined by Warthin-Starry staining (369) and/or immunohistochemistry using an anti-*H. pylori* antibody (clone SP48; Ventana, AZ, USA). The following entities were used: Healthy corpus (n=17), healthy duodenum (n=10), healthy ileum (n=8), healthy colon (n=12), corpus biopsies of corpus-dominant LyG in the absence of CeD (n=23), corpus biopsies of *H. pylori*- gastritis (HpG) cases (n=17), duodenal biopsies with proven CeD without concomitant LyG or HpG (n=11), duodenal biopsies of HpG cases (n=4), ileum biopsies with CD (n=11), colon biopsies of UC cases (n=8) and colon biopsies with lymphocytic colitis (LyC) (n=10). Detailed clinical information and analyses performed on specimens are indicated in the appendix section (Appendix 1).

2. Mouse colony.

Wild type and *Klrk1*^{-/-} mice (C57BL/6) (321) were genotyped as previously described. All mice were bred and maintained in the animal facility at Imperial College London in a specific pathogen-free environment. Animal work was carried out in compliance with the British Home Office Animals Scientific Procedures Act 1986. Mice used in this study are compiled in Appendix 2.

3. Cell lines and culture.

AGS (human stomach adenocarcinoma cell line) and KATO III (human stomach carcinoma cell line) were purchased from CLS Cell Lines Service GmbH (Eppenheim, Germany). MKN28 cells (human stomach adenocarcinoma cell line) cells were originally obtained from JCRB (Japanese Collection of Research Bioresources, <http://cellbank.nibio.go.jp/>) and kindly provided by Dr. S. Wessler (370). Caco-2 (human epithelial colorectal adenocarcinoma cell line) was obtained from the Center of Medical Research (ZMF), Medical University of Graz, Austria. AGS and MKN28 cells were cultured in DMEM high glucose (4.5 g/L) (Gibco, UK), KATO III in DMEM/Ham's F12 medium (Gibco, UK) and Caco-2 in MEM (GE healthcare, Austria), supplemented for each cell line with 10% fetal bovine serum (Gibco, UK) and 2 mM L-glutamine (PAA, Austria). In the case of Caco-2, MEM non-essential amino acids solution (NEAA) (Gibco, USA) was added at a final concentration of 1%. For further stimulation or infection, 1.5×10^5 cells were seeded per well into 6-well plates in a final volume of 3ml cell culture medium and grown to 80% confluence in a water-saturated atmosphere of 95% air and 5% CO₂ at 37°C. Cell viability was examined by CASY cell counter.

4. Bacteria strains and culture.

P. acnes strains were kindly provided by Dr. B. Mayo (178) and cultured under anaerobic conditions (GenBox anaer, Biomérieux, France) on Columbia blood agar plates (Biomérieux) at 37°C for 3 days. *E. coli* strains were routinely cultured on Columbia blood agar plates at 37°C under aerobic conditions overnight. *H. pylori* strains were kindly provided by Dr. M. Blaser (371) and cultured under microaerophilic conditions (GENbox microaer, Biomérieux, France) on Columbia blood agar plates at 37°C. Detailed bacteria strains used for infection *in vitro* assays are provided in Table 1.

Bacteria strains used in this study		
Species	Strain	Source
<i>P. acnes</i>	PA-1.1	Delgado, S et al. 2011(178)
	PA-1.2	
	PA-1.3	
	PA-2.2	
<i>H. pylori</i>	SS1	Lee, A. et al. 1997 (372)
	PMSS1	Thompson, L.J. et al. 2004 (373)
<i>E. coli</i>	DH5-α	Woodcock, D.M. et al. 1989 (374)
	30083	DMSZ, Braunschweig, Germany

Table 1 Bacterial strains used for *in vitro* infection assays in this study.

5. Histology and immunohistochemistry.

5µm thick sections of FFPE gastric biopsies corresponding to healthy corpus, LyG and HpG were stained with monoclonal mouse anti-human CD8 (clone C8/144B; dilution 1:30; Dako), monoclonal mouse anti-human CD4 (clone 4B12; dilution 1:20;

Labvision, Fremont, USA) and polyclonal goat anti-human MICA (clone F-6; dilution 1:200; Santa Cruz Biotech, CA, USA) antibodies according to the suppliers specifications.

6. Cytospin and immunocytochemistry.

100µl of AGS cells in DMEM high glucose (4.5g/l) were added to the slide chamber and spin for 5minutes at 1000rpm in a Cellspin I Cytocentrifuge (Tharmac, Waldsolms, Germany). Cells were concentrated and immobilized on a microscope slide. Slides were further fixed by immersion in slide-containers with formalin 10% for 10 minutes. Subsequently they were air-dried prior staining with the MICA Ab (R&D systems, MN, USA) as described above.

7. SCFAs stimulation.

Cell lines were stimulated with 5mM (191, 225, 375) of propionic acid ACS reagent ≥99.5%, butyric acid ≥99%, acetic acid or hydrochloric acid 37% (HCl) (Sigma Aldrich, USA), used as a negative control, for 4 and 24h.

Subsequently cells were harvested and placed in 500µl Trizol (Invitrogen, CA, USA) for further RNA isolation. Cells used for short-time MICA/B protein expression were rescued after 4h of stimulation with SCFAs and left in DMEM high glucose medium (10% FBS, 2mM L-glutamine) without additional SCFAs for another 4h before being analyzed by flow cytometry. For 24h protein expression analysis no rescue was carried out. Experiments were performed in triplicates and repeated at least twice. pH was monitored using Test Strips (Macherey-Nagel, Germany).

8. Bacterial infection assay.

Prior to the infection assays a single *E. coli* colony was transferred into a 15 ml tube containing 3ml Brucella broth (Roth, Germany) and incubated with gentle agitation

(100 rpm) at 37°C for 4h. For *P. acnes*, a bacterial suspension with an optical density (OD₆₀₀) of 0.1 was cultivated into 6-well plates using 3 ml DMEM high glucose (4.5 g/l) (GE healthcare, Austria) per well for 24h. In the case of *H. pylori*, no liquid culture was prepared prior to the infection, due to the slow growth rate under this condition. Subsequently, the OD₆₀₀ was measured for each strain and a multiplicity of infection (MOI) 1:50 was calculated to infect AGS or MKN28 cells. The same conditions applied for living bacteria were also used to challenge cells with heat-inactivated bacteria and conditioned supernatant. *P. acnes* or *E. coli* were heat-inactivated by heating at 80°C for 20 minutes. Supernatant was obtained by centrifugation of the liquid culture (OD₆₀₀ of 0.1) at 4500 rpm for 15 minutes at 4°C and subsequent filtering by using a 0.22µm PVDF syringe filter (Fisherbrand, UK). Cell lines were infected for 4, 8 and/or 24h. OD₆₀₀ and colony-forming units per ml (CFU/ml) were monitored after each infection time point.

9. Quantitative real-time PCR.

9.1. RNA isolation from human FFPE samples and human cell lines

Total RNA from FFPE samples was isolated using the RNeasy FFPE kit (Qiagen, Hilden, Germany); RNA from ECs was extracted by using TRIzol (Invitrogen, CA, USA) and the PureLink RNA mini kit (Invitrogen, CA, USA) according to the manufacturer's specifications. RNA purity was assessed by a Nanodrop (Thermo Scientific). A 260/280 and a 260/230 ratio of ~2.0 was accepted as "pure" for RNA. 1 µg of total RNA was used for cDNA synthesis with the gene Amp RNA PCR kit (Applied Biosystems, CA, USA). Real-time PCR was performed with an ABI PRISM 7900HT instrument (Applied Biosystems) using SYBR Green Universal PCR Master Mix (Applied Biosystems, UK) core reagent. Reaction mixtures were incubated for 10 min at 95 °C, followed by 40 cycles of 15 s at 95 °C, 1 min at 60 °C, and finally 15 s at 95 °C, 1 min at 60 °C, and 15 s at 95 °C. The oligonucleotide primers used are shown in Appendix 3A. For each mRNA target, gene expression was normalized by using β-actin as a house-keeping gene, and calculated using the Pfaffl method (376).

Each PCR reaction was performed in triplicate and analyses were repeated at least twice.

9.2. RNA isolation from mouse gut samples

Gut tissues from mice were collected in a 1.5 ml eppendorf tubes containing 500 μ l RNA later (Sigma, USA) and kept at 4°C for 24h to let RNA later to penetrate into the tissue. Afterwards, the samples were stored at -80°C until processed for RNA isolation. RNA later was removed by thawing the samples and spin them down at 3000x g. Total RNA from mouse gut samples was isolated using the Qiagen RNeasy plus Mini Kit (Qiagen, Germany) following the manufacture's specifications. RNA quality and quantity was determined spectrophotometrically by using a NanoDrop instrument (ThermoScientific) as described above. 1750 ng of RNA was used for cDNA synthesis with the gene Amp RNA PCR kit (Applied Biosystems, CA, USA). Real-time PCR was performed with an ABI 7500 FAST Real Time PCR (Applied Biosystems) using SYBR Green or TaqMan Universal PCR Master Mix (Applied Biosystems, UK) core reagents. Reaction mixtures were incubated for 10 min at 95 °C, followed by 40 cycles of 15 s at 95 °C and 1 min at 60 °C in the case of TaqMan and 20 s at 95°C, followed by 3 s at 95°C and 30 s at 60°C in case of Sybr Green. The oligonucleotide primers used are shown in Appendix 3B. For each mRNA target, gene expression was normalized by using HPRT as a house-keeping gene, and calculated using the Pfaffl method (376). Each PCR reaction was performed in triplicate and analyses were repeated at least twice.

9.3. DNA isolation from FFPE human samples

For DNA extraction FFPE blocks were cut into 5 μ m thick sections. The first 5 sections were discarded and the subsequent 10 sections were sampled, incubated with 400 μ l xylene and centrifuged at 13,000 rpm in a table-top centrifuge at room

temperature (RT) for 10 min. Xylene was discarded and this step was repeated 3 times. Thereafter, 400 µl absolute ethanol were added, the mixture gently vortexed and centrifuged at 13,000 rpm in a table-top centrifuge at RT for 10 min. This step was repeated 2 times and the pellet was air-dried for 2 h. Thereafter, samples were subjected to mechanical lysis with a MagnaLyser Instrument (Roche Diagnostics, Mannheim, Germany). Tissue pellets were mixed with 230 µl bacterial lysis-buffer and transferred to MagnaLyser tubes and centrifuged at 6500 rpm for 20 s. Thereafter, 5.75 µl lysozyme (100 mg/ml) were added and the mixture was incubated at 37°C for 30 min. Subsequently, 20 µl proteinase K were added according to the MagNA Pure protocol and the mixture was incubated at RT overnight. Then, samples were incubated at 95°C for 10 min, spun down and placed on ice for 5 min. Finally, samples were centrifuged at 13,000 rpm in a table-top centrifuge and 100 µl of the lysates were transferred into MagnaPure sample tubes and further processed according to the manufacturer's specifications. Total DNA was isolated with the MagNA Pure LC DNA Isolation Kit III (bacteria, fungi) in a MagNA Pure LC 2.0 Instrument (Roche Diagnostics). For amplification of *P. acnes* 16S rRNA gene, primers PA74F: TTTTGTGGGGTGCTCGAG and PA216R: CCAACCGCCGAACTTTC were used. 50 ng total DNA extracted from the FFPE specimens was used as a normalized input for real-time PCR amplification. Each PCR reaction was performed in triplicate and analyses were repeated three times. This methodological description was also published in a similar fashion in an original article (281).

10. Lamina propria and intraepithelial lymphocyte isolation

Mice were dissected and the GIT isolated and placed on a bucket of ice covered with aluminum foil and sprayed with cold PBS. The stomach, small intestine, caecum and large intestine were cleaned from fat, connective tissue, mucus and content before cut into 1cm pieces and placed in individual 50ml tubes containing 5ml cold PBS. Later, each section of the GIT was place in a 50ml tube containing 10ml of warm (37°C) HBSS (PAA, USA), 2% FBS (Gibco, UK), 1mM EDTA and 1mM DTT (Sigma,

USA). Samples were incubated for 30 minutes at 37°C and 200 rpm. After the first wash IELs remain in the supernatant, which was kept on ice. This wash step was repeated twice, the second time just for 15 minutes. Right after collecting the supernatant from the second wash, samples containing IELs were centrifuged at 800g for 10min and resuspended with 3% BSA (GE Healthcare, USA), and kept on ice. Tubes containing tissue were washed once with 50 ml PBS before enzymatic digestion, to remove any EDTA residue. Thereafter PBS was discarded and 15ml pre-warmed RPMI containing 10% FBS, 15mM Hepes (Sigma, USA), collagenase VIII (100U/ml) (Sigma, USA) or collagenase IV (0.5mg/ml) (Sigma, USA) in the case of the stomach and DNase (Sigma, USA) 50U/ml was added to each sample for enzymatic digestion. Prior to digestion, stomach tissue was chopped into smaller pieces using scissors and tweezers to facilitate the enzymatic digestion. After 45 minutes at 37°C and 200 rpm samples were vortexed and the digestion was finished passing the content through a 20 ml syringe several times. Then, the suspension was filtered on a 100µm nylon strainer to remove tissue debris. Using the piston of a 2ml syringe tissue was gently massaged and washed through with 3% BSA/PBS supplemented with 5mM EDTA to inhibit collagenase activity. Thereafter samples were centrifuged at 800g for 10 minutes and supernatant was discarded. Cells were then resuspended in 4ml of 40% percoll (VWR, UK) and layered on top of 4ml 80% percoll, in a 15ml tube to enrich the cell fraction. Samples were subjected to a density gradient centrifugation at 600g for 20 minutes at 20°C (Acc5, Dec3) (Appendix 7).

11. Flow cytometry

11.1. Cell lines and staining

AGS and MKN28 cells were harvested using ice-cold PBS, as trypsin cleaves surface NKG2DLs giving false negative results (377). Harvested gastric epithelial cells were incubated at 4°C for 30 minutes with 5 µl (0.125 µg) of the anti-human monoclonal MICA/B Alexa Fluor® 647 Ab (clone 6D4, mouse IgG2a, kappa; BioLegend) diluted in 45 µl PBS. Subsequently, cells were washed twice in PBS. For the detection of

intracellular MICA/B protein, cells were fixed adding 500µl of IC fixation buffer (eBioscience, CA, USA) to the cells and incubated for 30 minutes in the dark at room temperature. Subsequently, cells were permeabilized using 1X permeabilization buffer (eBioscience, CA, USA) and stained using 5 µL (0.125 µg) of Ab diluted in 1X permeabilization buffer in a final volume of 50 µl. Thereafter, cells were incubated for 30 minutes in the dark at room temperature. Then, cells were washed twice in 1X permeabilization solution and resuspended in PBS for analyses. Additionally, 7-AAD viability staining solution (eBioscience) or Annexin V Apoptosis Detection Kit APC (eBioscience) were used, following the manufacturer's recommendations to check cell viability and apoptosis. Cells were analyzed on a FACS bench-top cytometer (BD™ LSRII) according to the supplier's recommendations and the results were calculated using FlowJo version 9.3.1 or higher (TreeStar, Oregon, USA).

11.2. Mouse lymphocytes

Lymphocytes obtained from enzymatic-dissociated mouse GIT were plated in a 96 well V-bottomed plate and pre-incubated with an anti-mouse FcR blocking Ab CD16/CD32 (clone 2.4G2) (BD Pharmingen) and live/dead fixable Aqua dead cell stain kit (Life Technologies, CA, USA), before staining with a cocktail of specific mAbs (A detailed description of the flow monoclonal antibodies used is shown in Appendix 5). When intracellular staining was required, cells were permeabilized and stained using a Fixation/Permeabilization Kit (eBioscience). Qdot 605 conjugated streptavidin (Life Technologies, CA, USA) was used to reveal biotinylated antibodies. The relevant fluorescence-minus-one labeling conditions including the appropriate isotype mAb were used as control. Samples were acquired on an LSR Fortessa flow cytometer (BD) and analyzed with FlowJo version 9.3.1 or above (TreeStar, Oregon, USA).

12. Gut microbiota analysis

Mouse gut samples (stomach, small intestine, caecum and colon,) and feces were subjected to mechanical lysis with a MagNA Lyser Instrument (Roche Diagnostics, Mannheim, Germany) and total DNA was isolated with the MagNA Pure LC DNA Isolation Kit III (bacteria, fungi) in a MagNA Pure LC 2.0 Instrument (Roche Diagnostics). Therefore, tissue pellets were mixed with 230 μ l bacterial lysis-buffer and transferred to MagnaLyser tubes and centrifuged at 6500 rpm for 20 s. Thereafter, 5.75 μ l lysozyme (100 mg/ml) were added and the mixture was incubated at 37°C for 30 min. Subsequently, 20 μ l proteinase K were added according to the MagNA Pure protocol and the mixture was incubated at RT overnight. Then, samples were incubated at 95°C for 10 min, spun down and placed on ice for 5 min. Finally, samples were centrifuged at 13,000 rpm in a table-top centrifuge and 100 μ l of the lysates were transferred into MagnaPure sample tubes and further processed according to the manufacturer's specifications.

DNA quality and concentration was determined spectrophotometrically via a NanoDrop ND-3300 instrument and the PicoGreen® assay (ThermoScientific, Delaware, USA). Only specimens yielding a wavelength ratio >0.8 at 260/280 and ≈ 2 at 260/230 nm, respectively, were considered for further analyses. For amplification of the bacterial 16S rRNA gene FLX one-way fusion primers (Lib-L kit, Primer A, Primer B; Roche 454 Life Science, Branford, CT) with the template-specific sequence F27 and R357 (Table S2) targeting the V1-2 region of the 16S rRNA gene were used (amplicon length 349 bp). Primers were chosen based on their performance enabling superior community capture and taxonomic resolution (378). PCR amplification was performed as described (379). Reactions for each sample were performed in triplicates, amplification products were visually quality checked on agarose-gels and only specimens resulting in a reliable PCR amplification were further used.

Amplicons were gel-purified, pooled and sequenced with the GS FLX Titanium Sequencing Kit XLR70 (Roche 454 Life Science, Branford, CT, USA) as described (379). For microbiota analysis raw files from 454 FLX pyrosequencing were processed with MOTHUR v.1.31.2 according to the standard 454 SOP of MOTHUR

(380). Sequencing errors were reduced using MOTHUR's implementation of PyroNoise (381), and the command pre.cluster (382) was used to remove sequences that arose due to pyrosequencing errors. Chimeras were removed with UCHIME (383) and non-bacterial contaminants were removed using the Ribosomal Database Project (RDP) reference (384). The high quality reads were aligned to the SILVA database (385, 386). For operational taxonomic unit (OTU) based analyses, the processed fasta files from MOTHUR were introduced into QIIME v.1.7.0 (387). OTUs were formed by clustering the sequences with uclust (388) using a similarity score of 97%; (OTU 97% ID) and taxonomy was assigned by using the RDP-classifier and Greengenes reference OTUs. A de-novo OTU picking strategy was employed. The biomarker discover program LEfSe (linear discriminant analysis effect size) was used to determine differentially abundant OTUs (389). This methodological description was also published in a similar fashion in an original article (281).

13. DSS- induced colitis

Acute colitis was induced by 2% (weight/volume) dextran sulfate sodium (DSS) (molecular weight 36-50Kda; MP Biochemicals, Inc. OH, USA) dissolved in 100ml drinking water. Treatment with DSS was for 5 days followed by 3 days of recovery with sterile water. Mice were monitored each day for body weight, stool consistency and possible presence of blood in stools. Water consumption was also monitored in each cage every day.

On day 8 after the initiation of DSS- treatment, mice were sacrificed and gut was removed. Colon length and weight were measured with and without fecal content. Colon tissue was taken for flow cytometry analysis or histology and for RNA isolation. Information about mice used and groups, measurements and other details can be found in Appendix 4.

14. SCFAs measurements by GC-MS.

Acetate, propionate and butyrate levels from culture supernatants were measured by Gas Chromatography Mass Spectrometry (GC-MS) using a Thermo Scientific DSQ II™ Series Single Quadrupole GC-MS by electron ionization instrument. 500 µl supernatant were mixed with 500 µl H₃PO₄ (0.5%), internal standards (ISTD: 200 µl dC₂ [500 µM] and 200 µl dC₄ [500 µM]) and 600 µl methyl tert-butyl ether (MTBE). After centrifugation (10 min; 2.500 rpm; RT) 150 µl of the organic phase were used for the measurement. A calibration curve was created with increasing ISTDs mixed with H₃PO₄ (0,5%) for the analysis. This methodological description was also published in a similar fashion in an original article (281).

15. Statistical analysis

Statistical analyses were performed with GraphPad Prism 5 software. The D'agostino & Pearson test was used to assess the normality of distribution of investigated parameters. Data were expressed as mean ± standard deviation, if not indicated otherwise. When samples were normally distributed (human samples) an unpaired t-test or a one-way ANOVA followed by a post hoc Tukey's or Dunnett's test for multiple comparisons was applied. In cases where samples were not normally distributed (mouse samples), a Kolmogorov-Smirnov test was used. Differences between expression of sample groups with $p < 0.05$ were considered statistically significant. Spearman's correlation was used to analyze the association between gene expression of the players of the NKG2D system and TLRs in mouse samples.

16. Ethics statement.

Usage of tissue specimens was approved by the institutional review board of the Medical University of Graz (EK-23-212ex10/11).

IV. Results

1. LyG is not associated with *H. pylori* infection but shows an overabundance of *P. acnes*.

In order to investigate the gastric microbiota in LyG and to discern a possible bacterial cause of the disease, gastric corpus biopsies originating from LyG, HpG and healthy controls were subjected to 16S rRNA gene profiling. From the results, we extracted that although microbial richness was not different between the entities analyzed, which indicates how many taxa are detectable, diversity and evenness were significantly lower in both gastric pathologies (HpG and LyG), what tells us that there are some bacteria that dominate the microbial community (281). Further, at the phylogenetic level, HpG showed a significant relative increase of Proteobacteria compared to healthy controls and LyG, from which almost 90% of proteobacterial reads originated from *H. pylori*. Thus, *H. pylori* was the overall dominant bacterium in HpG. On the other hand, LyG showed a significant relative increase of Actinobacteria and a significant relative decrease in Bacteroidetes compared to healthy controls. *P. acnes* represented around 80% of Actinobacteria in LyG. Therefore, only two significant OTU-level taxonomic associations with disease entities could be discerned: *H. pylori* was significantly increased in HpG compared to LyG and healthy controls, whereas *P. acnes* was significantly increased in LyG compared to HpG and healthy controls. Collectively, these data indicate that LyG is not associated with *H. pylori* infection but shows significantly increased *P. acnes* loads (281). This finding was further validated by qPCR, where *P. acnes* abundance was measured using specific primers targeting 16S rRNA gene sequences, where we could corroborate that the abundance of *P. acnes* in LyG patients is significantly higher compared to controls and HpG patients (Fig. 9).

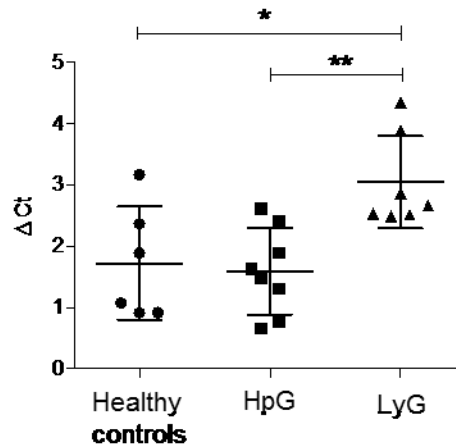


Figure 9. *P. acnes* specific qPCR in healthy controls vs. HpG and LyG human FFPE stomach biopsies. (n=6-7) * $p < 0.05$, ** $p < 0.01$; one-way ANOVA and post-hoc Tukey's test.

Moreover, a significant correlation of abundance determined by 16S NGS and load determined by qPCR was evident validating the microbiota analysis results (Fig. 10). This proved that no bias or error was introduced during the NGS and later data analysis, and that *P. acnes* overabundance is a true meaningful finding in LyG patients.

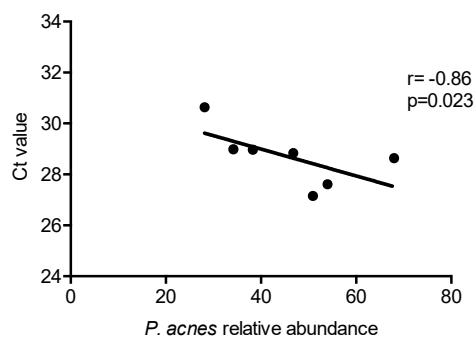


Figure 10. Validation of NGS results by qPCR. Spearman correlation analysis (non-parametric) of samples with paired 16S rRNA gene sequencing and qPCR data shows a significant correlation of relative abundance and load (Ct value).

2. The NKG2D/NKG2D ligand system is induced in lymphocytic gastritis.

The NKG2D/NKG2DL system and the pro-inflammatory cytokine IL15 are the major determinants for IEL recruitment in the gut. Upregulation of both factors leads to intraepithelial lymphocytosis and subsequently to villus atrophy in CeD (85, 324). The phenotypic similarities between LyG and CeD prompted us to investigate the involvement of this cell-stress sensing system in LyG. First, we comparatively assessed the number of CD8⁺ and CD4⁺ lymphocytes in gastric corpus specimens from LyG, HpG and healthy controls via immunohistochemistry (IHC) (Fig. 11).

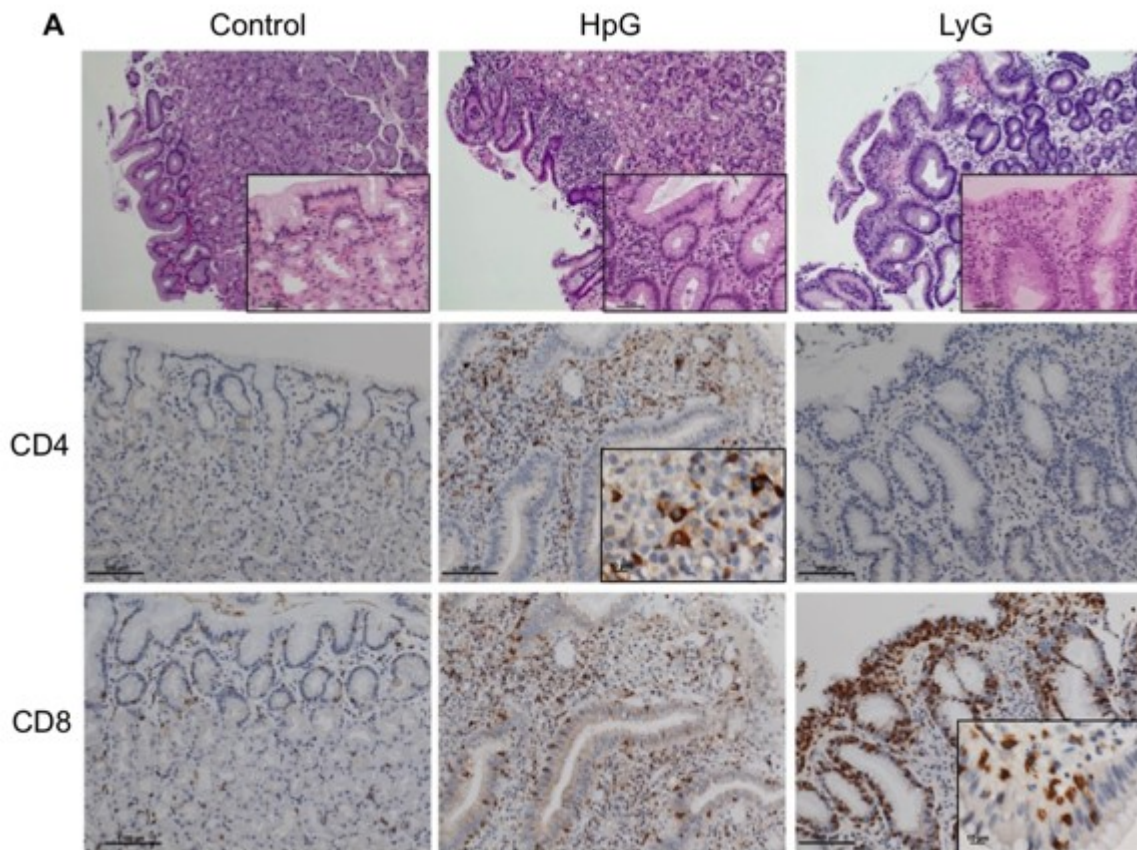


Figure 11. H&E and immunohistochemical staining of CD4⁺ and CD8⁺ T-cells in human gastric corpus biopsies of healthy controls, HpG and LyG cases. (Magnification: upper panels 100X, insets 400X; middle and lower panels 200X; IHC insets 600X).

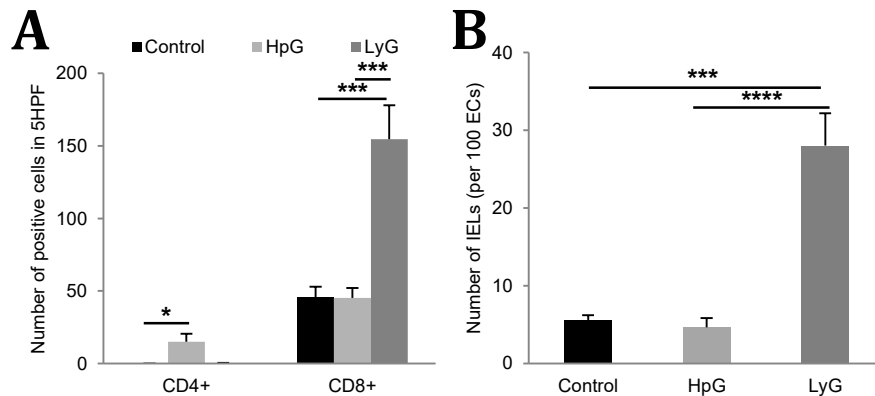


Figure 12. Bar charts representing (A) the average number of CD4⁺ and CD8⁺ T cells in 5 HPF and (B) the number of IELs per 100 ECs in controls, HpG and LyG patients. * p<0.001, ****p<0.0001; one-way ANOVA and post-hoc Tukey's test.**

LyG cases showed a significant increase of CD8⁺ lymphocytes compared to HpG and healthy controls (Fig. 12A). These CD8⁺ T cells were mainly IELs (Fig. 12B). The average CD8⁺ IEL count was 28.04±4.15 per 100 ECs in LyG compared to 5.6±0.62 in healthy controls and 4.64±1.18 in HpG. In contrast, HpG showed a significant increase of CD4⁺ T-cells (14.4±5.65 in 5 HPF) compared to healthy controls, the CD4⁺ T cells were mainly present in the lamina propria (Fig. 12A).

Next we comparatively assessed the expression of *nkg2d*, *nkg2d* ligands (*mica*, *micb*, *ulbp1*, *ulbp2*, *ulbp3* and *ulbp4*) and *il15* by qRT-PCR. Gastric corpus biopsies of LyG showed a significant overexpression of *nkg2d* (Fig. 13A) and *il15* (Fig. 13B) mRNA compared to HpG and healthy controls, *mica* levels were also significantly increased compared to healthy controls (Fig. 13C). *micb* and *ulbp1-4* mRNA expression was slightly repressed in LyG (Fig. 13D-H). Of note HpG showed no significant induction of assessed markers compared to healthy controls, which correlated with the observed absence of CD8⁺ T-cell infiltration in HpG.

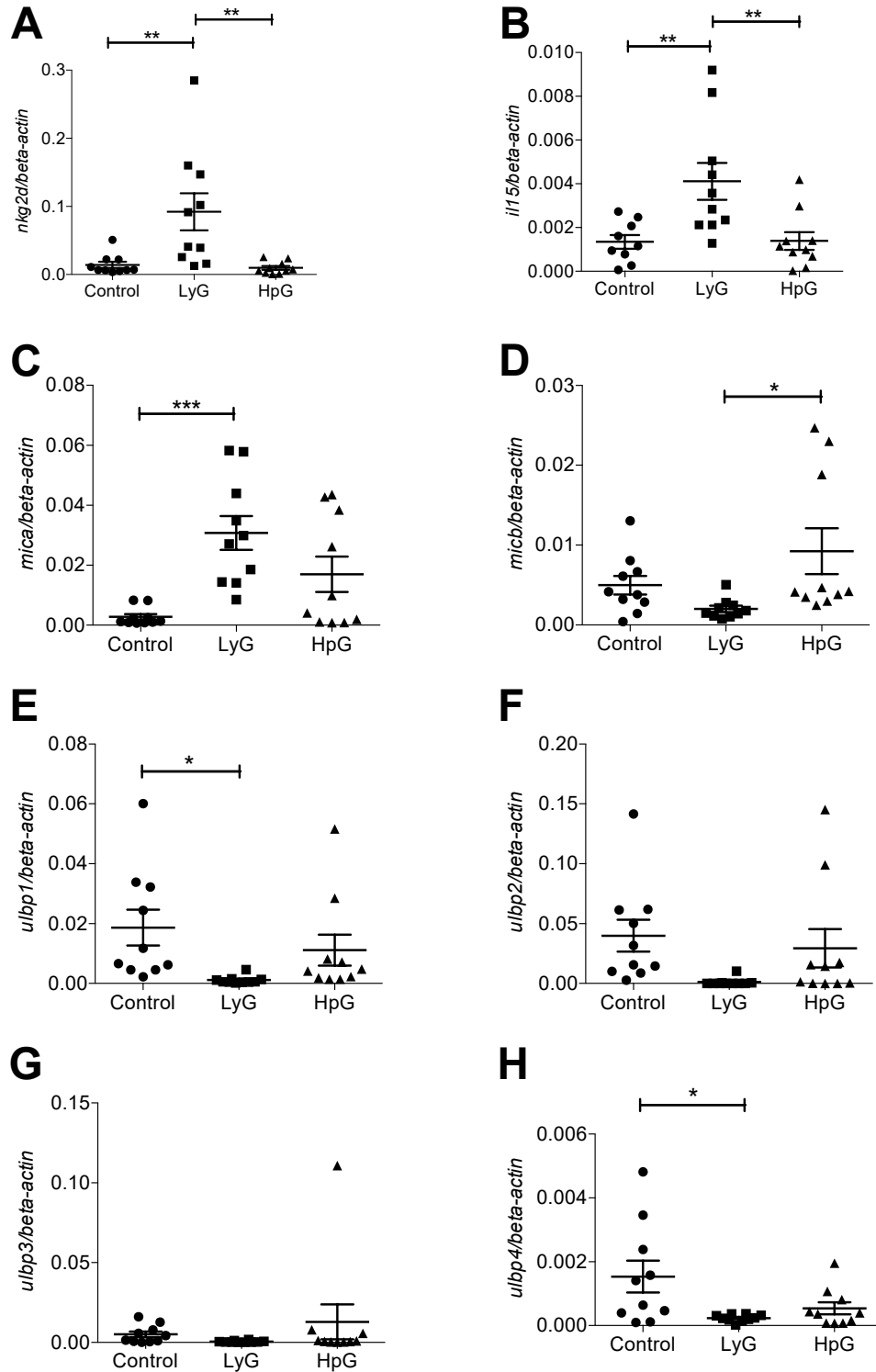


Figure 13. Gene expression analysis of the NKG2D/NKG2D ligand system and IL15 in FFPE stomach biopsies from controls, HpG and LyG patients. (n=10). Data represent the mean \pm SEM. *p<0.05, **p<0.01, *p<0.001, by One-way ANOVA and *post-hoc* Tukey's test.**

Gastric corpus biopsies of LyG showed also a pronounced staining with a MICA/B Ab in areas wherein IELs were increased, indicating epithelial specific induction of the system (Fig. 14). Taken together, these data indicate that the NKG2D/NKG2DL system and the pro-inflammatory cytokine IL15 are induced in LyG suggesting that these factors are important for CD8⁺ IEL recruitment and disease pathogenesis. Interestingly, the NKG2D/NKG2DL system and IL15 are not induced in HpG pointing towards deviating mucosal immune reactions and pathogenesises of both diseases.

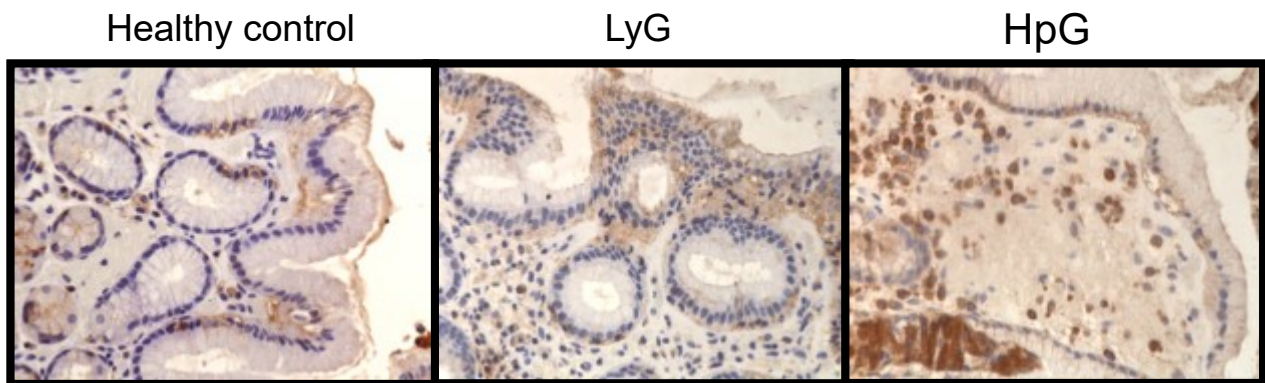


Figure 14. MICA/B IHC in healthy controls, LyG and HpG stomach FFPE samples. LyG samples revealed a marked staining in ECs where the concentration of intraepithelial lymphocytes is higher. In the case of HpG and healthy controls, MICA/B staining is concentrated in the basolateral region of the ECs. Note that some immune cells in the lamina propria also express MICA/B. (400X).

3. The GIT displays ubiquitous expression of the NKG2D system

Groh et al., have previously shown that MICA is constitutively expressed on GI ECs (276), however no studies followed this finding, and therefore little is known about the presence of the NKG2D system under physiological conditions along the GIT. Using FFPE biopsies from stomach corpus, duodenum, terminal ileum and colon from healthy patients (n=8-12), we were able to measure the mRNA expression of the NKG2D receptor, as well as the ligands MICA, MICB and the pro-inflammatory cytokine IL15 by qRT-PCR. From the results, it arose that all the main players of the NKG2D system (NKG2D receptor, MICA and MICB ligands and IL15) were present

along the GIT (Fig. 15A-D), the expression of the NKG2D receptor higher in the stomach compared to colon (Fig. 15A). This is consistent with previously published data showing that CD8⁺ cytotoxic T cells are more abundant in the stomach compared to lower GIT (390). In contrast, both ligands MICA (Fig. 15B) and MICB (Fig. 15C), and IL15 (Fig. 15D) show increased expression from upper to lower GIT. Although it was not significantly different in the case of MICB, we could still see a tendency towards increased expression in colon. This sequential increment in the expression of MICA and IL15 from stomach to colon is consistent with the increase of bacterial load and microbial metabolites, such as SCFAs from upper to lower GIT (28).

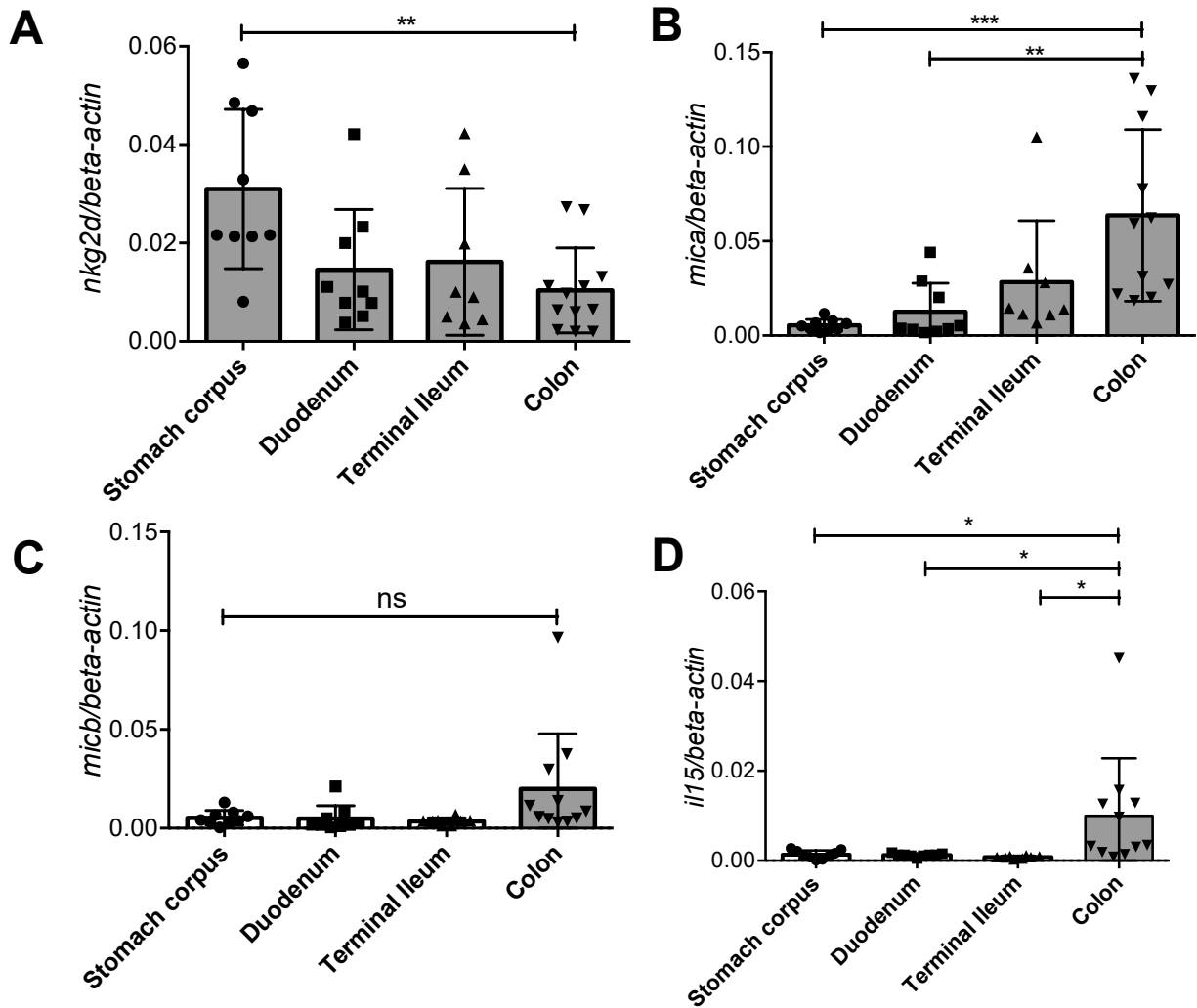


Figure 15. *nkg2d* (A), *mica* (B), *micb* (C), and *il15* (D) mRNA expression in human mucosal biopsies of healthy individuals determined by qRT-PCR analyses. (n=8-12). Data represent the mean \pm SEM. * $p < 0.05$, ** $p < 0.01$, *** $p < 0.001$, by One-way ANOVA and *post-hoc* Tukey's test.

4. The NKG2D system expression is altered in GI diseases characterized by dysbiosis.

We have previously reported that in LyG, NKG2D as well as MICA ligand and IL15 were overexpressed in the stomach. Furthermore, we showed through microbiota analysis, that LyG is characterized by an overabundance of *P. acnes*, giving insights into a dysbiotic pathology, more than a typical infectious disease. In order to clarify

the relation of NKG2D system regulation and dysbiotic GI pathologies paradigmatic diseases of the GIT that are characterized by an aberrant microbiota were analyzed in terms of the NKG2D system expression (Fig. 16).

In regard to the NKG2D receptor, the expression was significantly higher in LyG (Fig. 16A) and CD (Fig. 16C) compared to their controls (Stomach corpus and terminal ileum, respectively), while in HpG, NKG2D receptor was downregulated (Fig. 16A). The same pattern was observed for MICA in both LyG (Fig. 16E) and CD (Fig. 16G). However, LyC and UC showed lower expression levels compared to healthy colon (Fig. 16H). In contrast, MICB ligand showed generally less expression levels as MICA (Fig. 16I-L), although it was also significantly higher in ileum of CD compared to controls (Fig. 16K). The pro-inflammatory cytokine IL15 exhibited a higher expression in LyG compared to healthy controls and HpG (Fig. 16M). CD also presented higher levels of IL15 than the controls (Fig. 16O), in contrast to the pattern displayed in the colon, where controls showed increased levels of IL15 in comparison with the two diseases analyzed (LyC and UC) (Fig. 16P). These results show that the three key players of the NKG2D system: NKG2D receptor, MICA ligand and IL15 are expressed together in consonance and that expression is upregulated in diseases like LyG or CD, while colon inflammatory diseases like LyC or UC show an inhibition. Although there was a trend in the upregulation of NKG2D, MICA and IL15 in the case of CeD, this was not significantly different to healthy duodenum in any of the cases (Fig. 16B,F,J,N). The lack of a significant induction of assessed markers in CeD samples could be explained by the fact that in higher grade CeD (our samples were mainly Marsh III and above; see Tab. 1) NKG2D/NKG2DL become down-regulated (391).

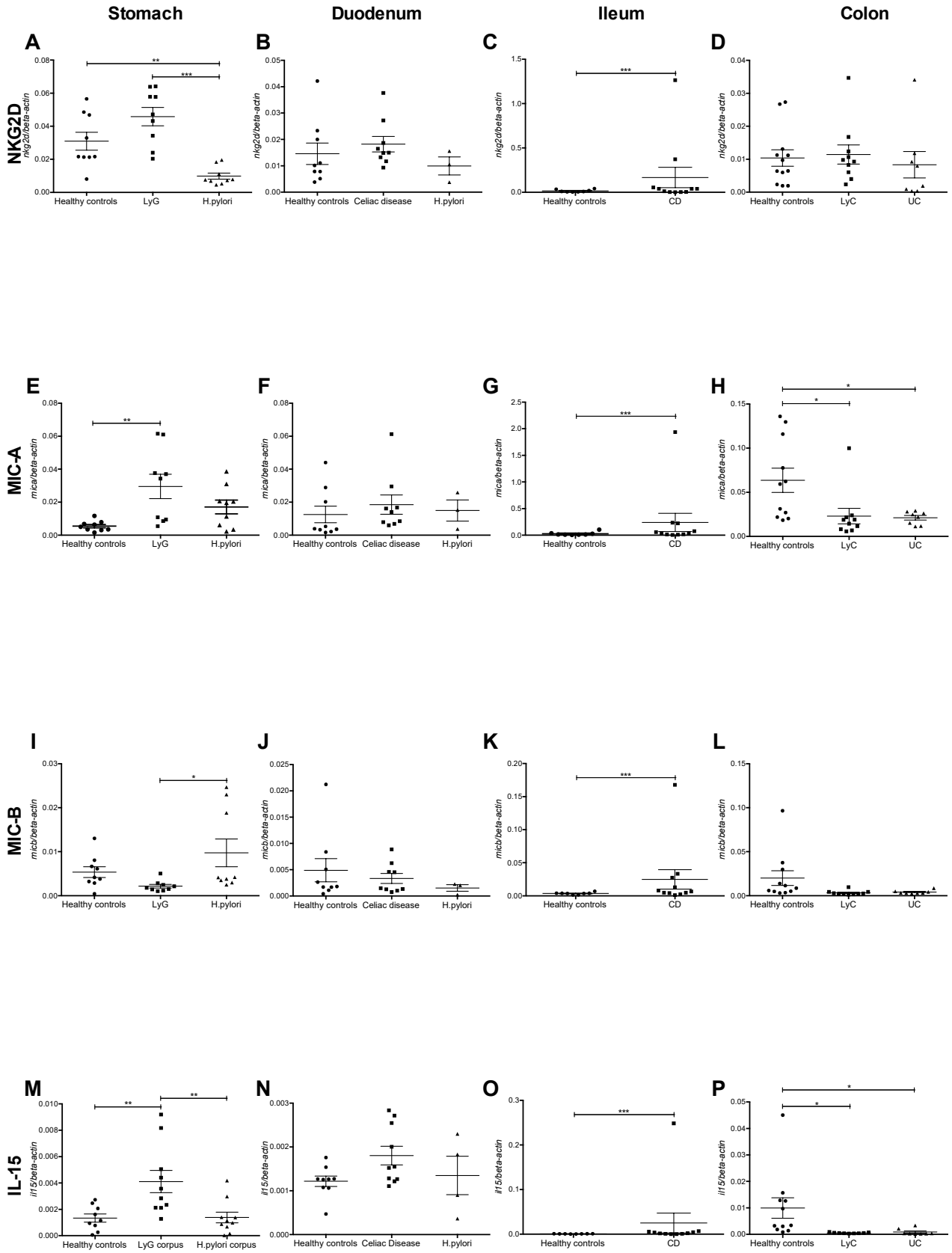


Figure 16. *nkg2d* (A-D), *mica* (E-H), *micb* (I-L) and *il15* (M-P) mRNA expression in human mucosal FFPE biopsies of stomach (healthy, LyG, HpG), duodenum (healthy, CeD and HpG) ileum (healthy and CD) and colon (healthy and UC) by qRT-PCR analyses. (n=8-12). Data represent the mean \pm SEM. *p<0.05, **p<0.01, ***p<0.001, by One-way ANOVA and *post-hoc* Tukey's test.

A summary of the main findings in terms of CD4 and CD8 expression, and NKG2D system (NKG2D, MICA, MICB and IL15) in the different GI pathologies analysed in this study compared to healthy status can be found in Figure 17.

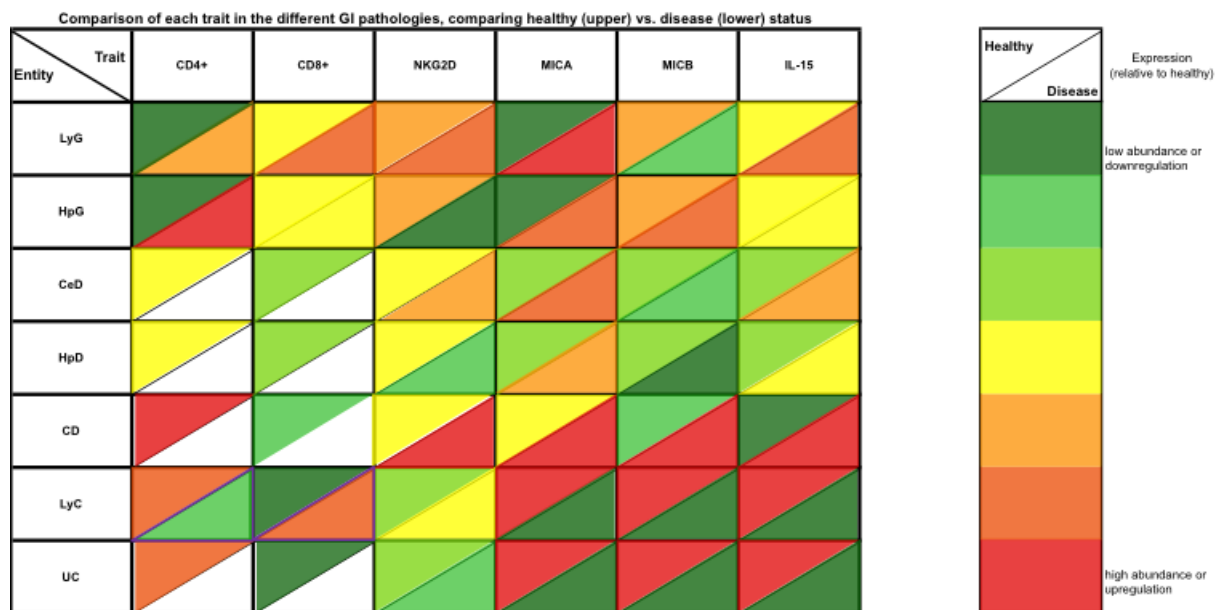


Figure 17. Summary heat-map representing the mRNA or protein expression of the main players in the NKG2D system activation, in the different GI pathologies tested in this study, comparing healthy (upper quadrant) vs. disease (lower quadrant) status.

5. Gastric ECs respond to different *P. acnes* strain stimuli by induction of the NKG2D system, but not to *H. pylori*.

It has been shown that microbes are able to induce NKG2DLs in certain cell lines, however human stomach epithelia have not been investigated for their responsiveness thus far (361, 362). In a first approach, we challenged AGS cells with the active form; the supernatant or heat-inactivated *P. acnes* (PA-1.1) and *E. coli* (DH5 α). After 24h, we measured the mRNA expression of *mica*, *micb* and *il15* by

qPCR. From the results, we could conclude that only the active forms of the bacteria (both *P. acnes* and *E. coli*) were able to induce the expression of the NKG2DLs. Moreover, we saw that *E. coli*, but not the *P. acnes* strain used, was able to induce a pro-inflammatory response (Fig. 18).

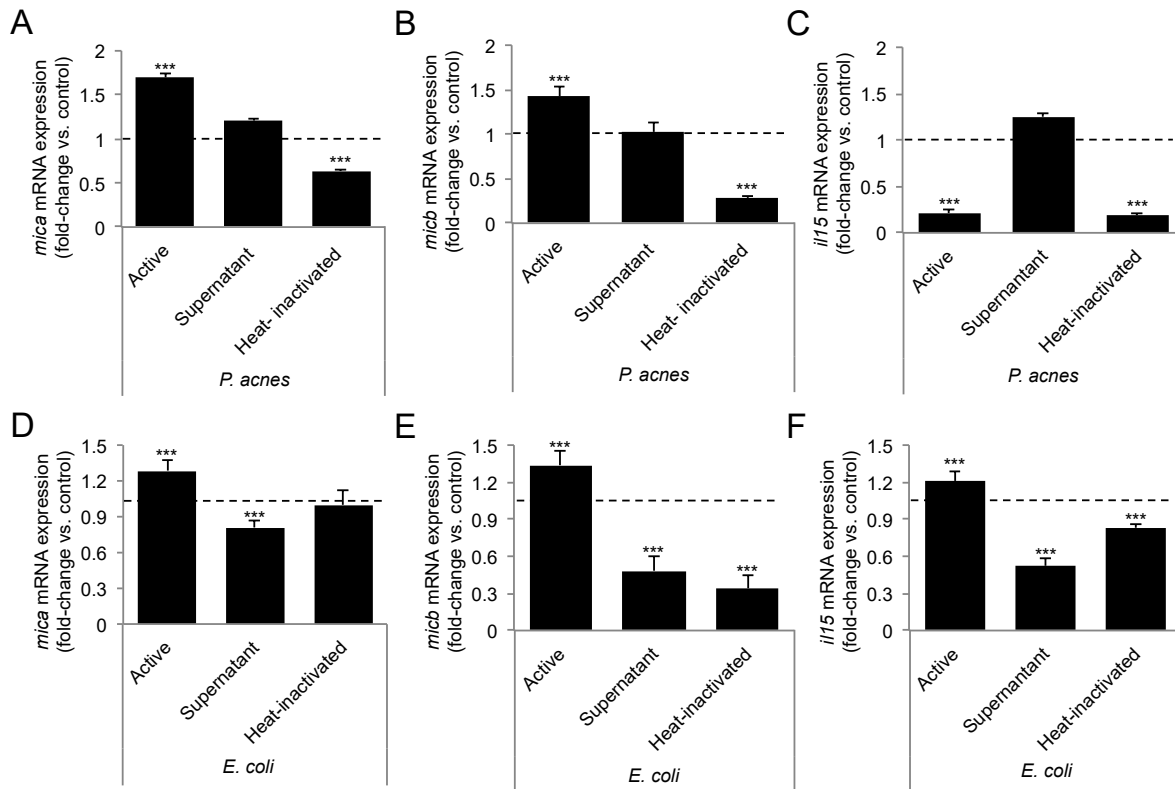


Figure 18. *mica*, *micb* and *il15* mRNA expression in AGS cells challenged for 24h with the active form, supernatant or heat- inactivated *P. acnes* (A-C) and *E. coli* (D-F)

Afterwards, we challenged AGS and MKN28 gastric EC lines with *P. acnes* strains isolated from the human stomach, with two different *H. pylori* strains (PMSS1 and SS1) and a native *E. coli* strain (DSM 30083) as control for 24 h (MOI 1:50). After 24h challenge *mica*, *micb* and *il15* expression was measured by qRT-PCR. In both cell lines, live *P. acnes* induced *mica* and *micb* ligands, while neither *H. pylori* or *E. coli* strains were able to do so. In fact, they showed lower levels of *mica* and *micb* mRNA expression compared to control conditions (Fig. 19A and B). In the case of *il15* mRNA, induction in a strain dependent manner was observed and the expression

was similar in both cell lines tested. While PA-1.1 showed a repression of IL15, PA-2.2 showed a strong induction of this pro-inflammatory cytokine. Neither *H. pylori* nor *E. coli* show a difference in *il15* mRNA expression compared to control conditions in AGS cells; while in MKN28 *E. coli* was able to induce in some extent an inflammatory response (Fig. 19C).

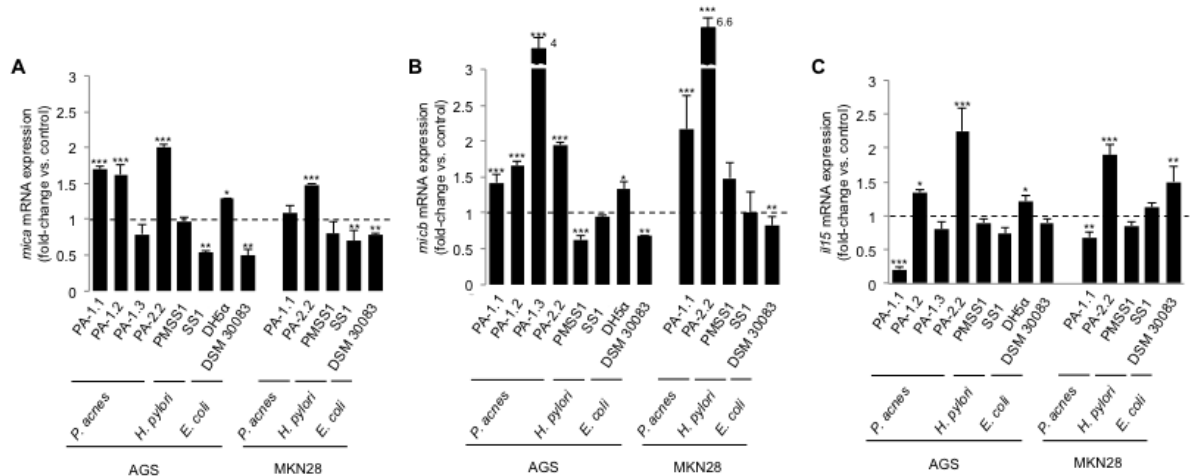


Figure 19. *mica*, *micb* and *il15* mRNA expression in AGS and MKN28 cells after 24h of infection with *P. acnes* (strains PA-1.1 and PA-2.2), *H. pylori* (strains PMSS1 and SS1) and *E. coli* (DSM 30083). Bars show the mean \pm SEM. * $p < 0.05$, ** $p < 0.01$, *** $p < 0.001$ by One-way ANOVA and *post-hoc* Dunnett's test.

Later on, we analyzed extracellular and overall MICA/B protein expression in both gastric cell lines (AGS and MKN28) after the infection with *P. acnes*, *H. pylori* or *E. coli* for 24h. From the results we can conclude that both cell lines behave in a similar way, being *P. acnes* the only bacterium capable of inducing extracellular MICA/B (Fig. 20B). Of note, *H. pylori* has no effect on AGS cells, but induce a strong repression of extracellular MICA/B protein on MKN28 cells (Fig. 20B). Intracellular MICA/B protein remained stable among the different bacteria stimuli used in both cell lines tested (Fig. 20A).

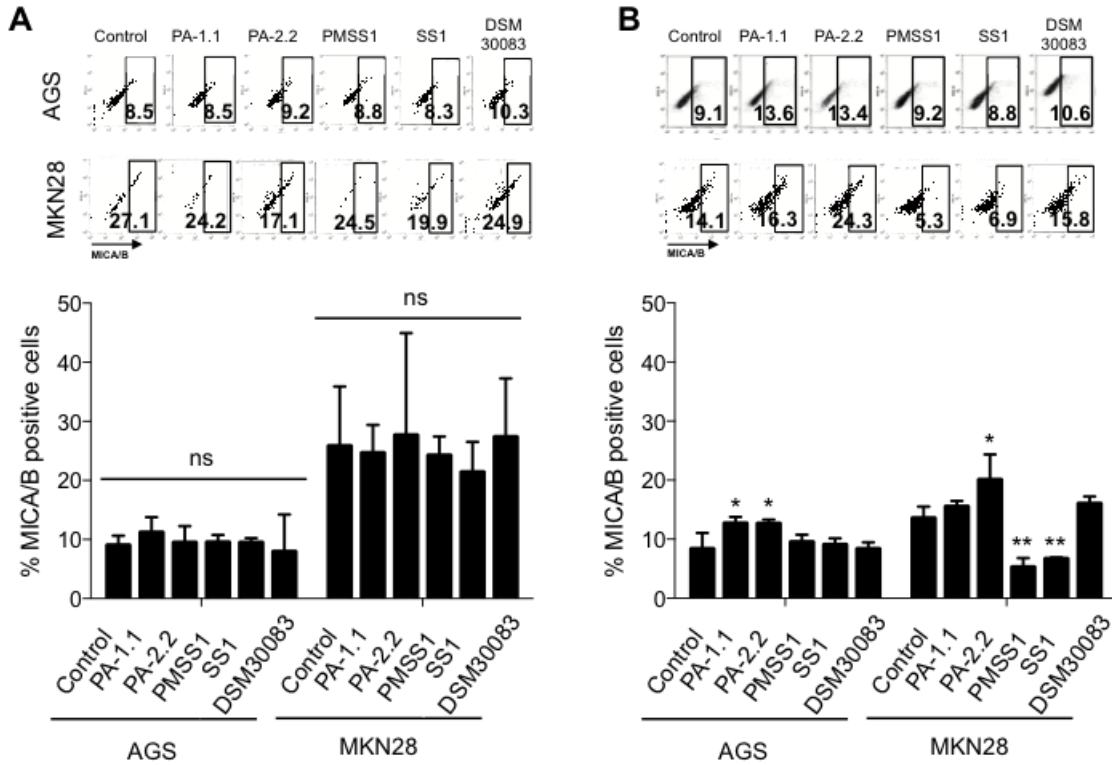


Figure 20. MICA/B protein expression was assessed in AGS and MKN28 cells by flow-cytometry after 24h of infection with *P. acnes* (PA-1.1 and PA-2.2 strains), *H. pylori* (PMSS1 and SS1 strains) or *E. coli* (DSM 30083 strain). Representative dot plots and bar charts of overall (A) and extracellular (B) MICA/B protein expression, respectively. Bar charts represent the mean values of percentages of MICA/B positive cells \pm SD of three independent experiments. * $p < 0.05$, ** $p < 0.01$, by One-way ANOVA and *post-hoc* Dunnett's test. No change in overall MICA/B protein expression is appreciated in any of the cases. 10000 events were analyzed.

Growth of assessed strains determined by CFU plating was not significantly different between the *P. acnes* strains or the *H. pylori* strains used after 24 h of co-cultivation. *E. coli* showed higher CFU/ml due to its higher growth rate in both AGS and MKN28 cell lines (Fig. 21A and B, respectively).

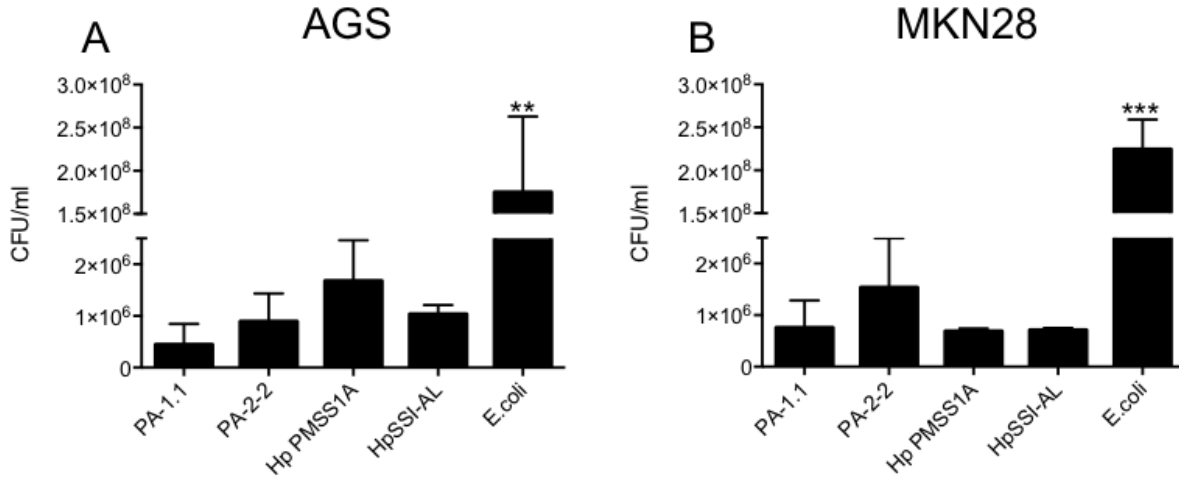


Figure 21. Colony forming units per ml (CFU/ml), of *P. acnes*, *H. pylori*, and *E. coli* strains after 24 h of co-cultivation, with AGS (A) or MKN28 (B) cells. Bars show the mean \pm SD. ** $p < 0.01$, *** $p < 0.001$ by One-way ANOVA and *post-hoc* Tukey's test.

Viability of the gastric cell lines used in these experiments was assessed by flow cytometry using an Annexin V/PI assay (Fig. 22).

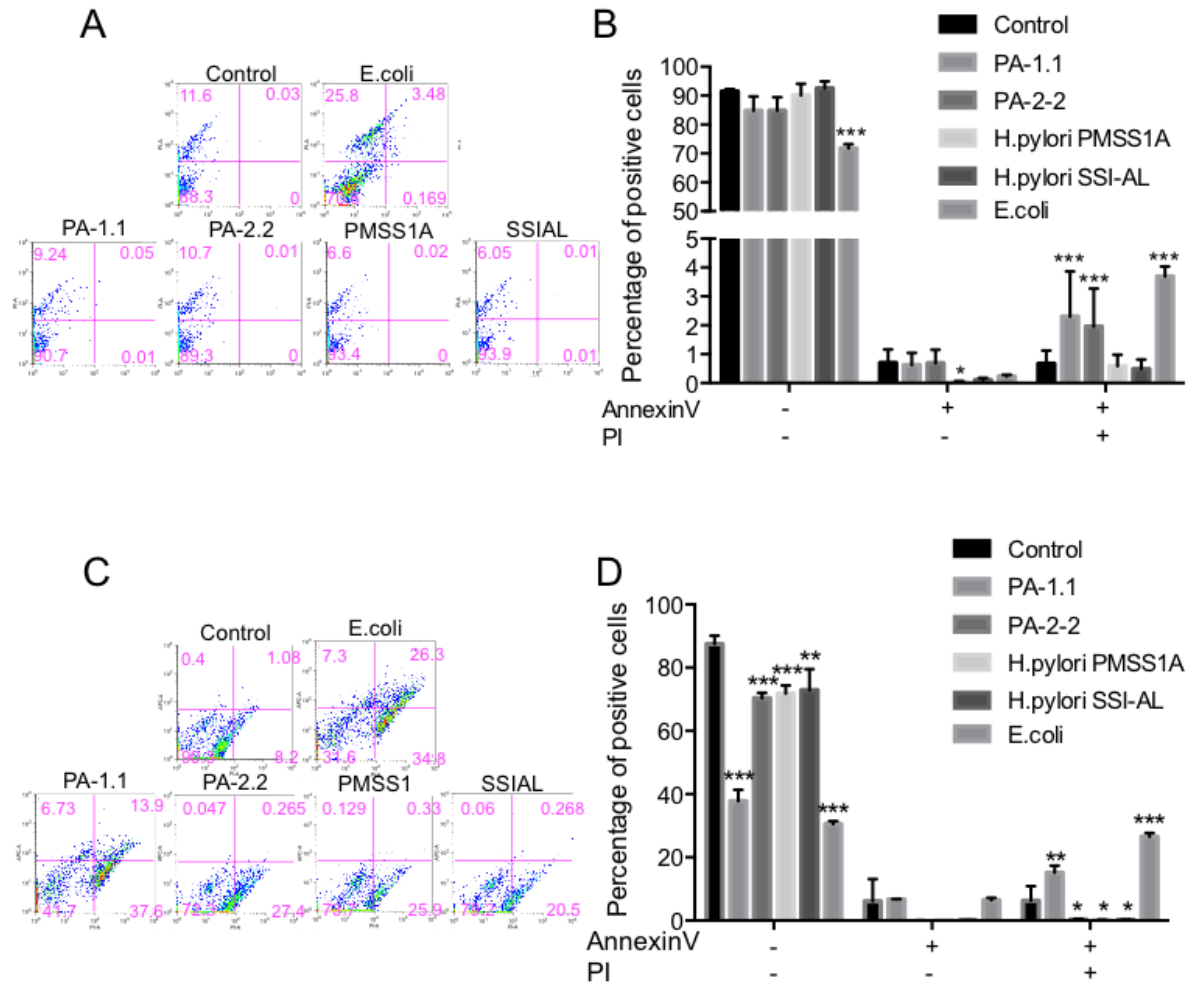


Figure 22. Apoptosis and live/dead analysis of AGS (A and B) and MKN28 (C and D) cells infected with *P. acnes*, *H. pylori* or *E. coli* assessed by Annexin V/PI staining and flow cytometry. Bar chart (B and D) representation of three independent Annexin V/PI assays showing the percentage of viable (Annexin V⁻/PI⁻), apoptotic (Annexin V⁺/PI⁻) and dead (Annexin V⁺/PI⁺) cells, respectively. Bars show the mean \pm SD. * $p < 0.05$, ** $p < 0.01$, *** $p < 0.001$, by one-way ANOVA and *post-hoc* Dunnett's test.

6. Gastric ECs respond to SCFAs by induction of the NKG2D system.

6. 1. Initial test using different concentrations of SCFAs at different time points

It has been recently reported that SCFAs, including propionate derived from *P. acnes*, are potent inducers of NKG2DLs (362). First, we stimulate AGS cells with different

concentration (1, 5, 10 and 50 mM) of SCFAs (acetate, propionate and butyrate) and HCl used as a negative control to study the effect of SCFAs in the expression of the NKG2D system in AGS cells. After 4 and 24h samples were taken and RNA isolated to measure the gene expression of *mica*, *micb* and *il15* (Fig. 23). From the results, we can extract that 4h stimulation with SCFAs is enough to induce robust expression of NKG2DLs and IL15 in a range between 5 to 10 mM.

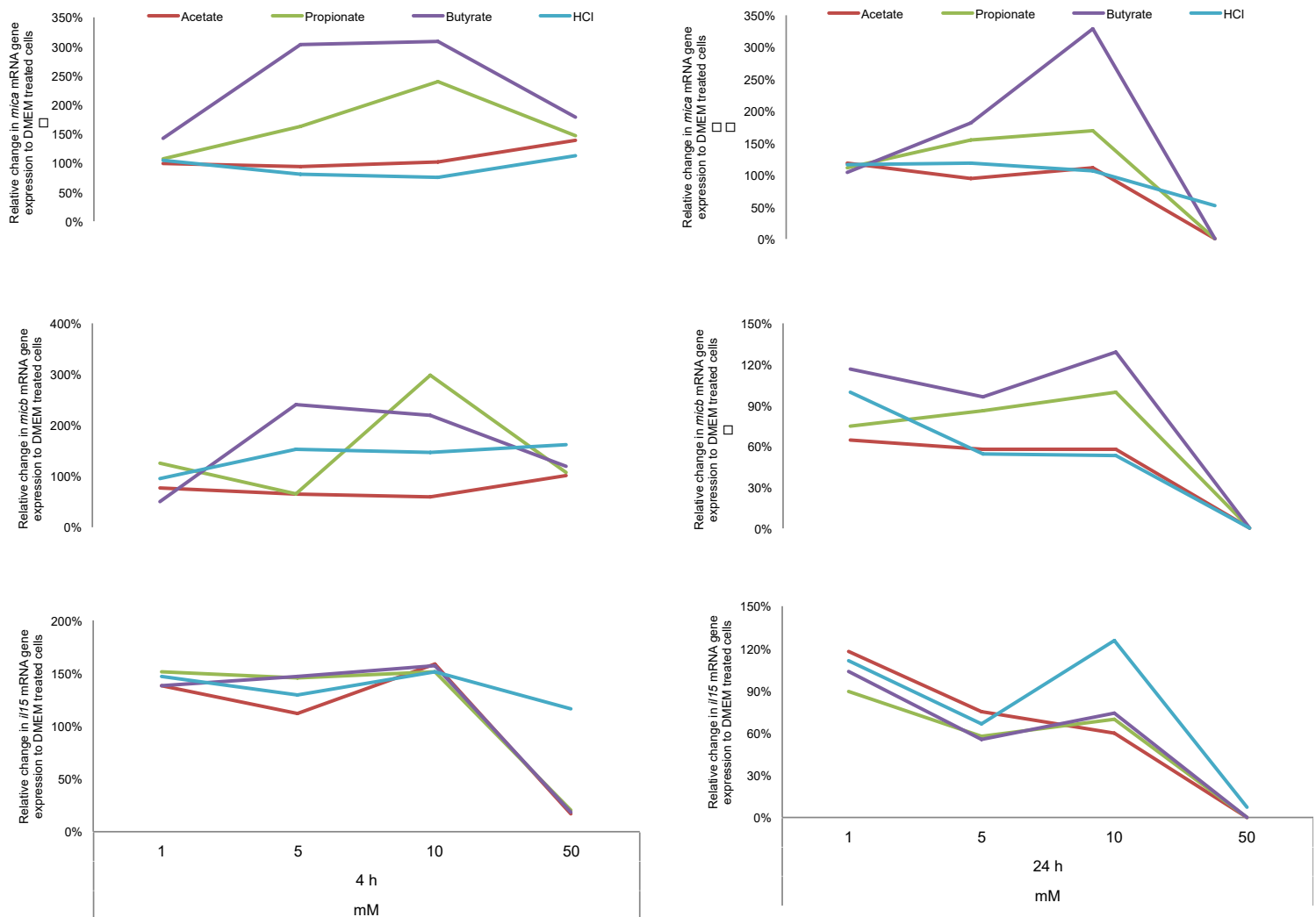


Figure 23. Kinetics of *mica*, *micb* and *il15* mRNA expression in AGS stimulated with 1, 5, 10 and 50mM of SCFAs and HCl after 4 and 24h.

Afterwards, we measured the MICA/B extracellular protein expression using three different concentrations of SCFAs and HCl: 0.5, 5, and 50mM for 4h followed by 4h of rescue to let the protein being expressed (Fig. 24). From the results we can conclude that the highest concentration of SCFAs (50mM) induced a potent cell stress

response reflected in high expression of MICA/B as seen in the histograms and by immunocytochemistry (ICC) of MICA/B, that compromise cell structure and viability, as it is appreciated in the ICC pictures (Fig. 25).

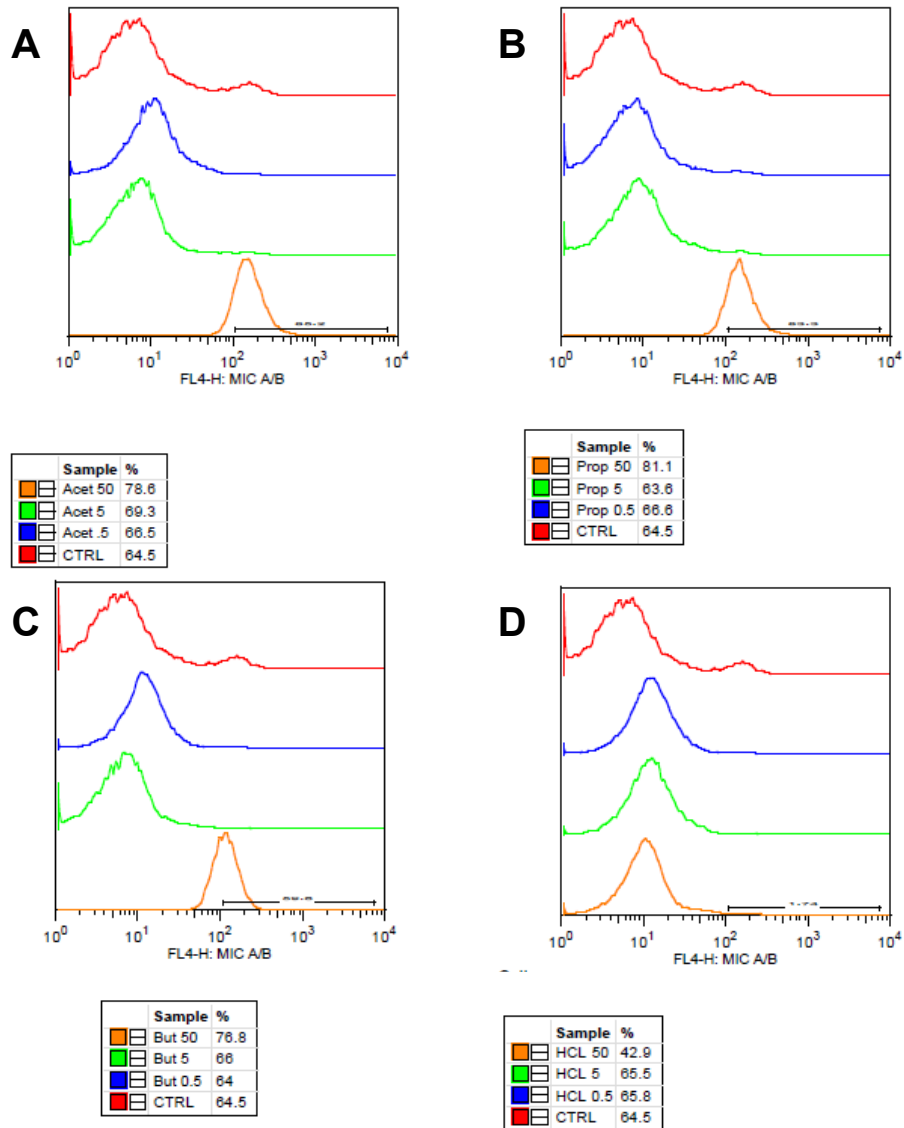


Figure 24. Representation of histograms showing MICA/B extracellular protein expression in AGS cells after 4h of SCFAs and HCl stimulation followed by 4h of rescue in DMEM medium.

Additionally, we performed ICC of AGS cells (Fig. 25) in order to study the localization and intensity of the proteins MICA/B after the stimulation with the different concentrations of the SCFAs analyzed. From the pictures, we can see a strong

surface staining in the cells stimulated with SCFAs, specially those stimulated with 5mM of propionate and butyrate. We can also see that the viability of cells was compromised when using 50mM of SCFAs or HCl.

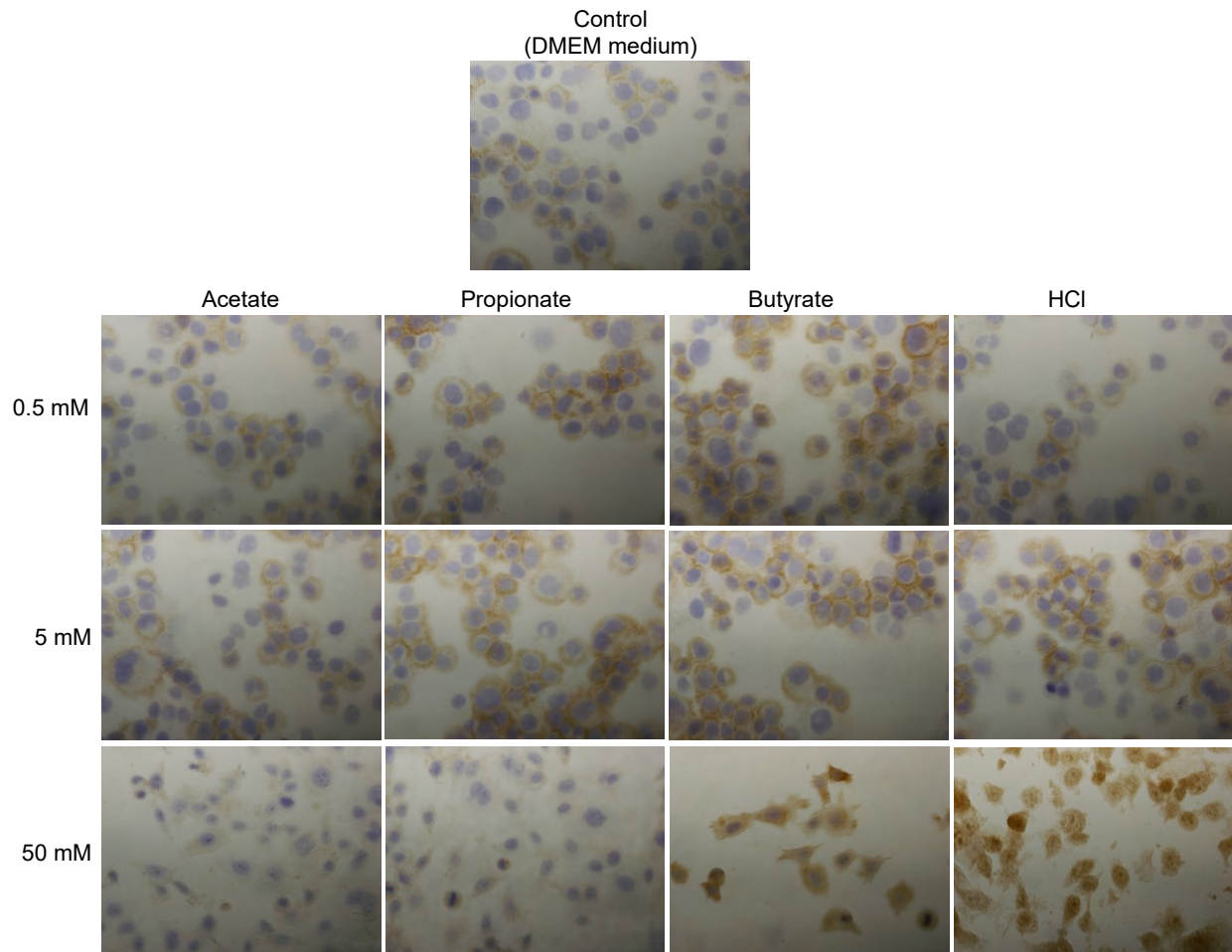
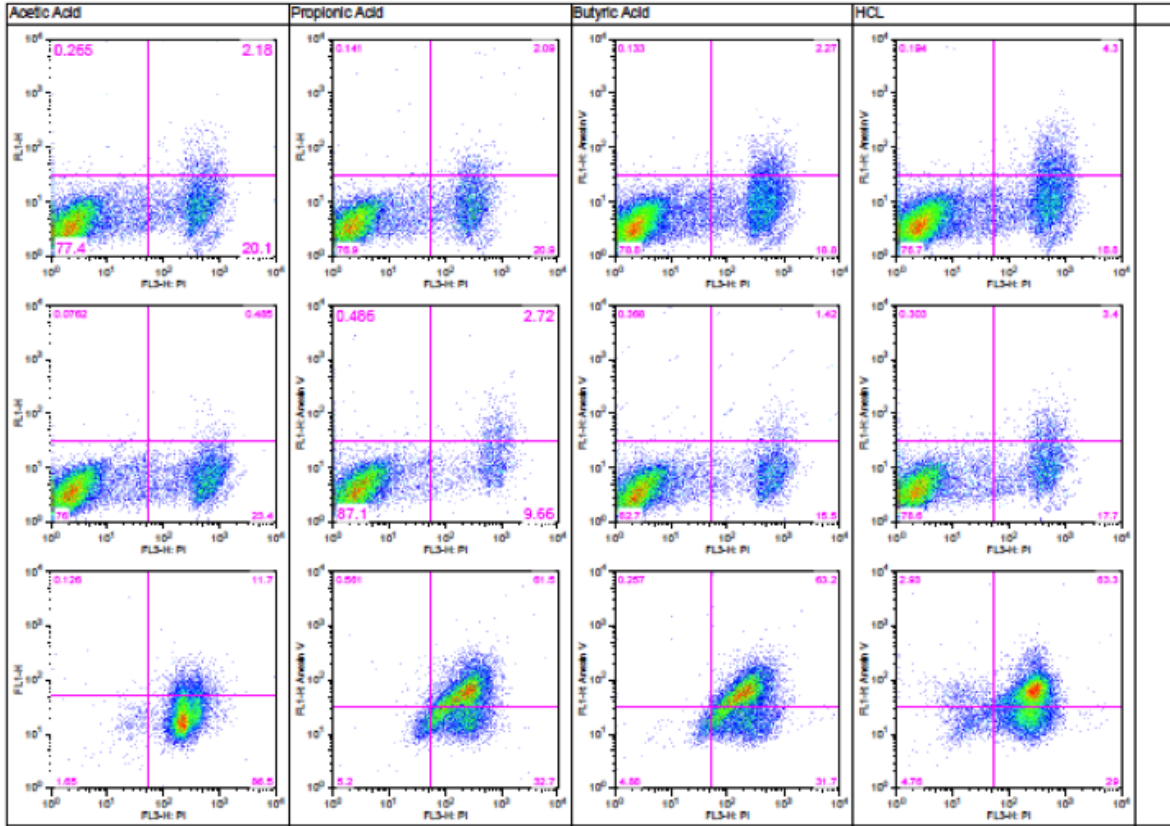
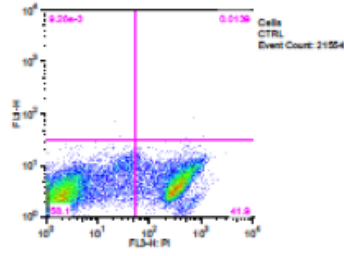


Figure 25. MICA/B ICC of AGS cells stimulated with SCFAs or HCl for 4h followed by 4h rescue in DMEM (400X magnification).

This effect was further corroborated with an apoptosis/necrosis assay using Annexin V and propidium iodide (PI) (Fig. 26). From the results, we established 5 mM as the most suitable concentration to study the NKG2D system expression *in vitro*, since it was enough to trigger the NKG2DLs response without compromising the cell viability.

A



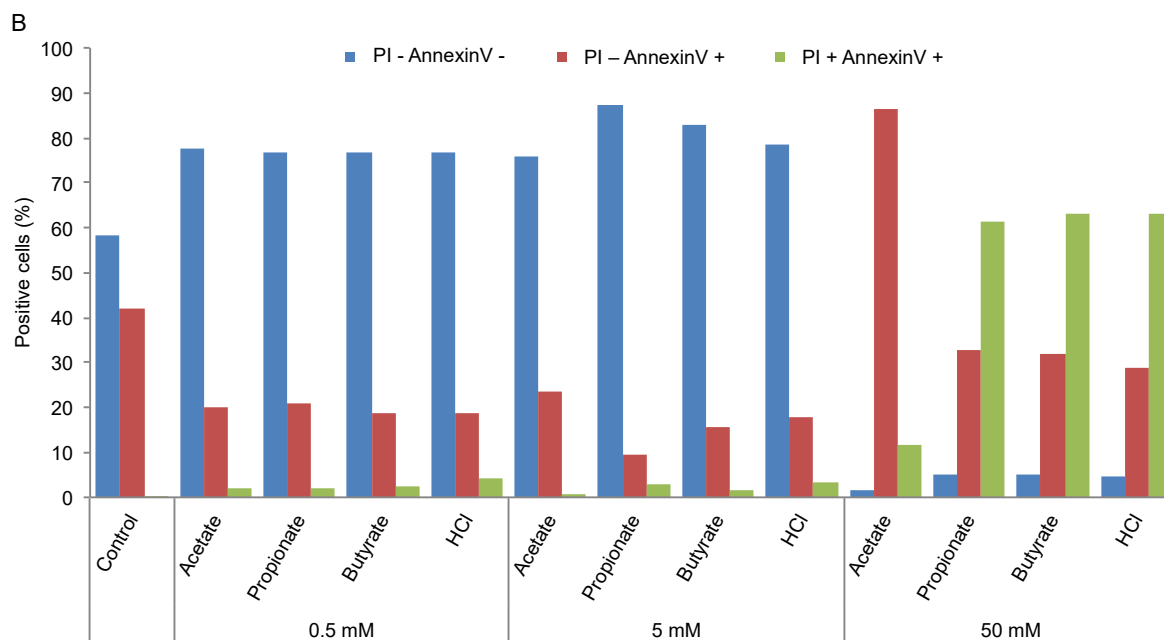


Figure 26. Apoptosis and live/dead analysis of AGS cells treated with the different SCFAs for 4h followed by 4h rescue in DMEM, assessed by Annexin V/PI staining by flow cytometry. A. Dot plots representation. From left to right: acetate, propionate and butyrate or HCl at 0.5 (upper panel), 5 (middle panel) or 50mM (lower panel). B. Bar chart representation extracted from the dot plots.

6. 2. AGS and MKN28 gastric ECs lines challenged with 5mM SCFAs or HCl for 4h (gene and protein expression)

SCFAs could be reliably detected in supernatants after 24h AGS challenge with *P. acnes* (Table 2).

Concentration of SCFAs in the supernatant of challenged AGS cells assessed by GC-MS.			
Sample (supernatant)	Acetate [µM]	Propionate [µM]	Butyrate [µM]
DMEM (Control)	50.6-56.0	0.7-9.0	n.d.
PA-1.1	5982.54-6728.20	406.10-585.61	172.53-392.42
PA-1.2	3061.82-3324.37	202.35-235.49	43.03-73.85
PA-1.3	4158.31-4290.41	223.87-228.14	20.89-30.08
PA-2.2	2223.80-2387.95	151.11-166.20	7.73-13.32
<i>E. coli</i> DH5α	1835.34-1912.58	38.92-52.80	4.52.6.45

Table 2. Concentration of SCFAs was measured by GC-MS in the supernatant of AGS cells after 24h of infection with the different strains used. n.d., not detected; indicated is range.

However, their concentration was about 1 to 2 log-phases lower than the concentration normally needed to reliably induce NKG2DLs in vitro (362, 392, 393). Thus, it is reasonable to speculate that also other factors, such as direct bacterium/cell contact or other metabolites, contributed to the observed ligand induction in our challenge experiments (323). To assess the net-effect of propionate and also the effect of the potent NKG2DL inducer butyrate, AGS and MKN28 cells were challenged with 5 mM SCFAs and HCl as control for 4 h and *mica*, *micb* and *il15* expression were assessed by qRT-PCR. In AGS cells, propionate induced significantly *mica* (1.61 ± 0.01) and *il15* (1.46 ± 0.04), whereas butyrate significantly induced *mica* (2.54 ± 0.02), *micb* (2.39 ± 0.02) and *il15* (1.47 ± 0.01) expression. Neither acetate nor HCl changed expression of the assessed genes in AGS cells (Fig. 27A-C).

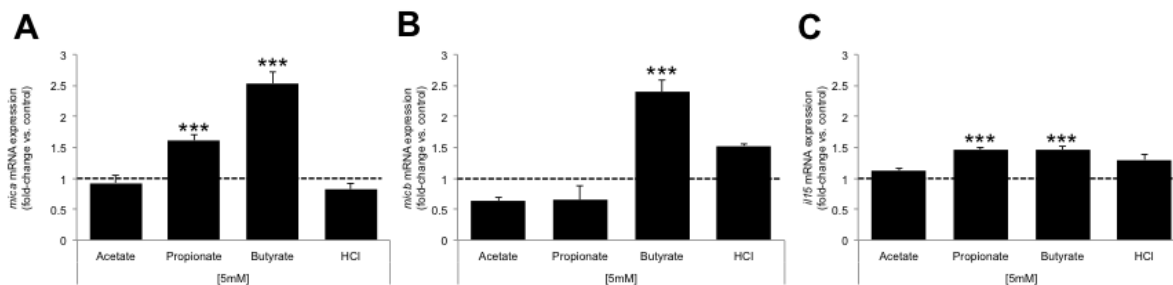


Figure 27. mRNA expression of *mica*, *micb* and *il15* in AGS cells after 4h of stimulation with 5mM of SCFAs (acetate, propionate, butyrate) or HCl used as a negative control. (*p<0.05; **p<0.01, * p<0.001 by one-way ANOVA and post-hoc Dunnett's test).**

In MKN28 gastric ECs, as in AGS cells, propionate (2.11 ± 0.1) and butyrate (2.66 ± 0.1) induced the expression of *mica* (Fig. 28A). Similarly, both propionate (2.08 ± 0.11) and butyrate (2.61 ± 0.04) induced the gene expression of *micb* (Fig. 28B). However, *il15* was not induced in any of the case. On the contrary, we detected certain levels of repression with all stimuli used but butyrate (Fig. 28C).

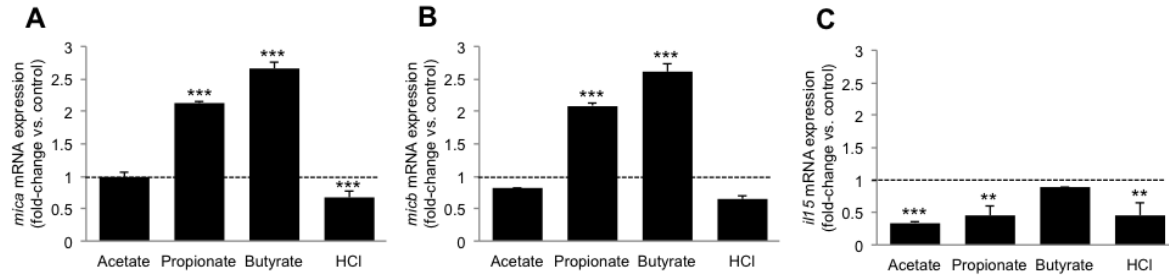


Figure 28. mRNA expression of *mica*, *micb* and *il15* in MKN28 cells after 4h of stimulation with 5mM SCFAs (acetate, propionate, butyrate) or HCl used as a negative control. (* $p < 0.05$; ** $p < 0.01$, *** $p < 0.001$ by one-way ANOVA and post-hoc Dunnett's test).

Of note, NKG2DL expression is differently regulated on mRNA and protein level (257). Thus, we wanted to investigate whether the challenge with SCFAs also translates into increased protein expression of NKG2DLs, which would be necessary for recruitment of NKG2D receptor-bearing lymphocytes to the ligand overexpressing epithelium. By using flow-cytometry and a MICA/B Ab, challenge of AGS and MKN 28 cells with 5 mM acetate, propionate, butyrate or HCl for 4 h did not alter overall ligand expression (Fig. 29).

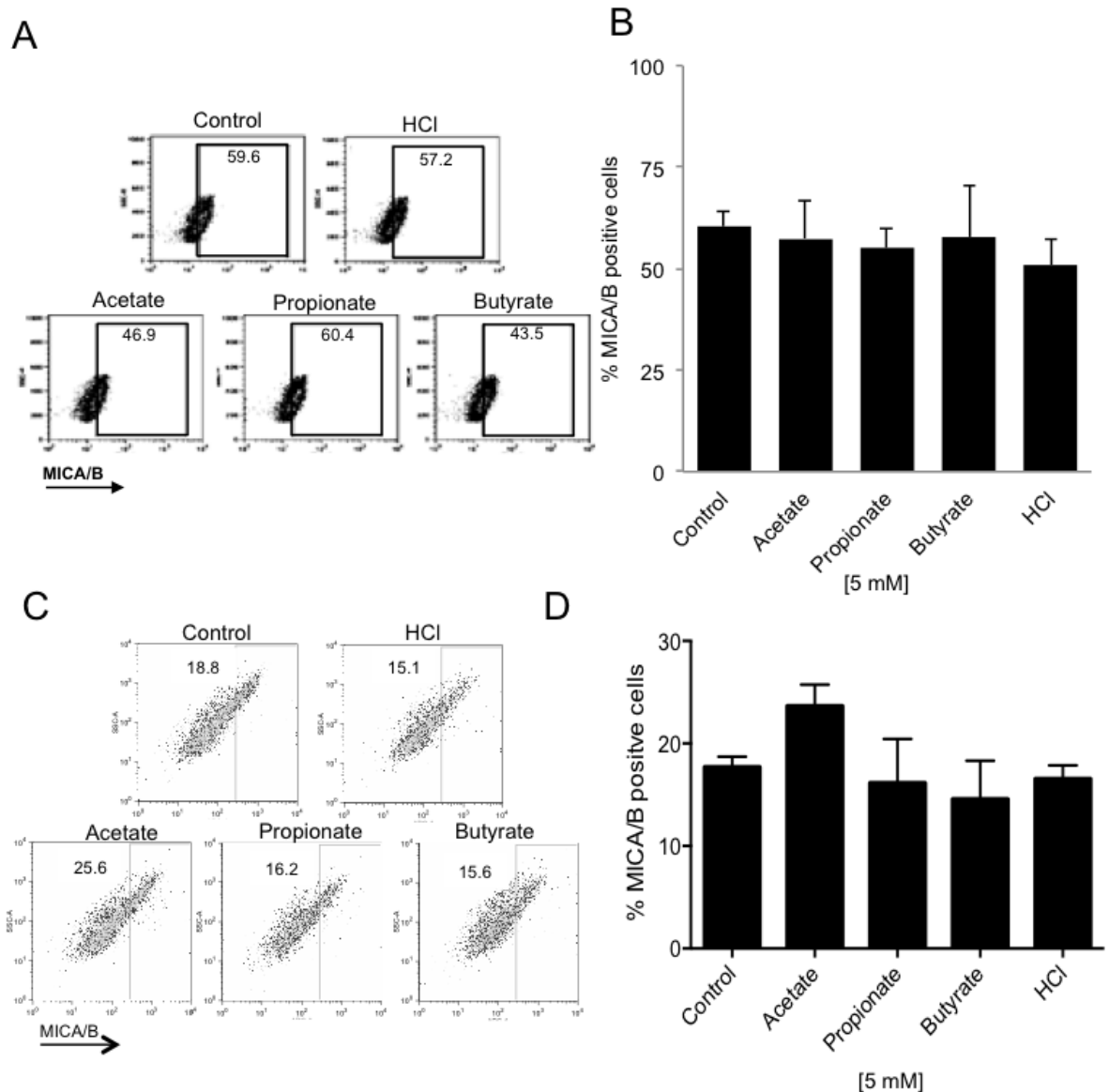


Figure 29. Overall MICA/B protein expression was assessed in AGS (A and B) and MKN28 (C and D) cells by flow-cytometry after SCFAs stimulation for 4 h followed by 4 h rescue in DMEM without SCFAs. (A and C) Representative pictures of dot plots and bar charts (B and D) represent the mean values of percentages of MICA/B positive cells \pm SD of three independent experiments. No change in overall MICA/B protein expression is appreciated in any of the cases. 10000 events were analyzed.

However, propionate and butyrate enhanced significantly extracellular protein expression of MICA/B on AGS cells and MKN28 cells (Fig. 30).

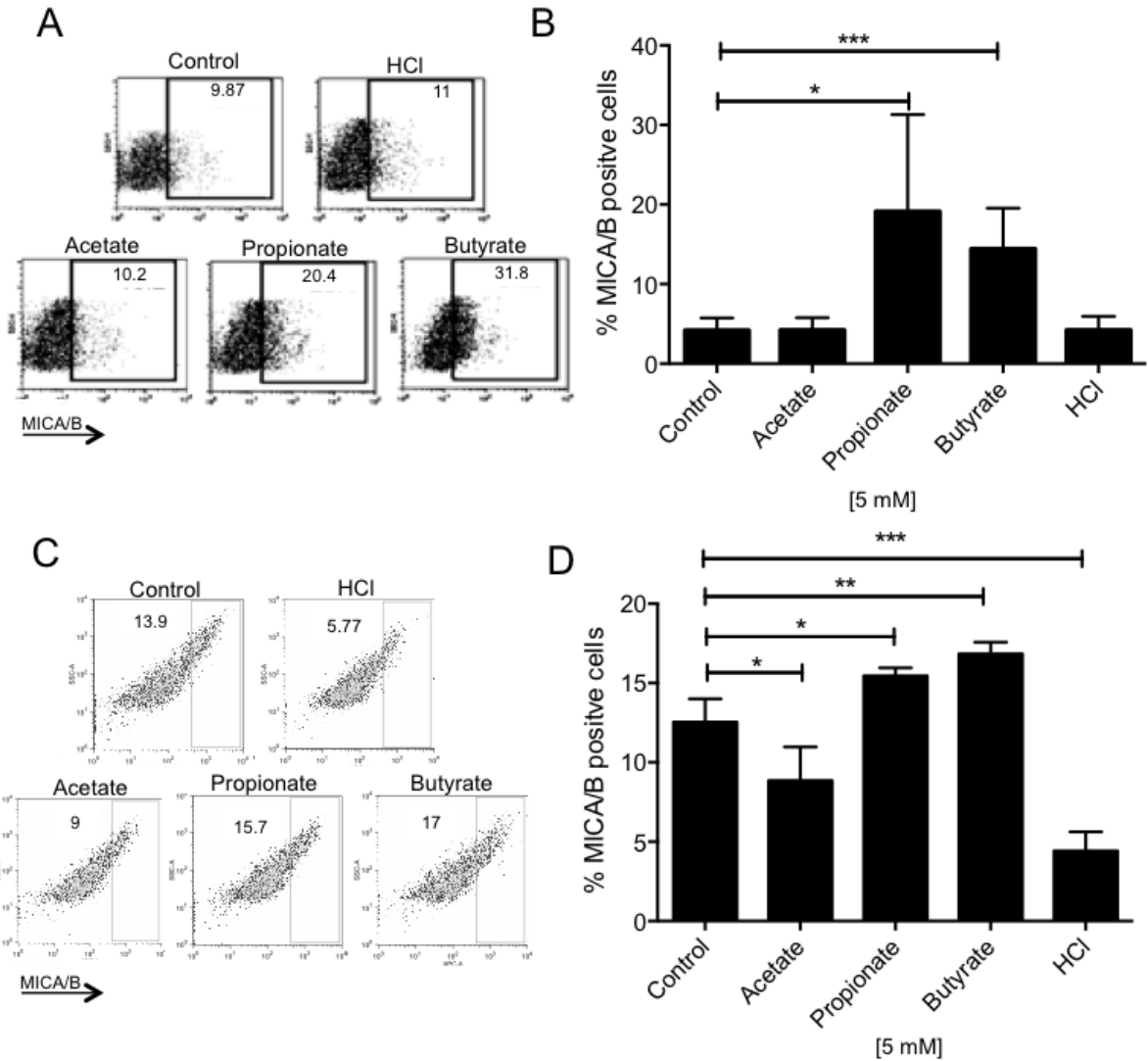


Figure 30. Extracellular MICA/B protein expression was assessed in AGS (A and B) and MKN28 (C and D) cells by flow-cytometry after SCFAs stimulation (5mM) for 4 h followed by 4 h rescue in DMEM without SCFAs. 10000 events were analyzed. (B) Bar charts represent the mean values of percentages of MICA/B positive cells \pm SD of three independent experiments (* $p < 0.05$; *** $p < 0.001$; one-way ANOVA and post-hoc Dunnett's test).

Additionally, AGS cells stimulated with 5mM of SCFAs or HCl were stained with a MICA/B Ab and ICC was performed in the same set of samples to support the results obtained by flow cytometry (Fig. 31A). ICC was scored according to staining intensity (Fig. 31B) and MICA/B cellular localization (Fig. 31C).

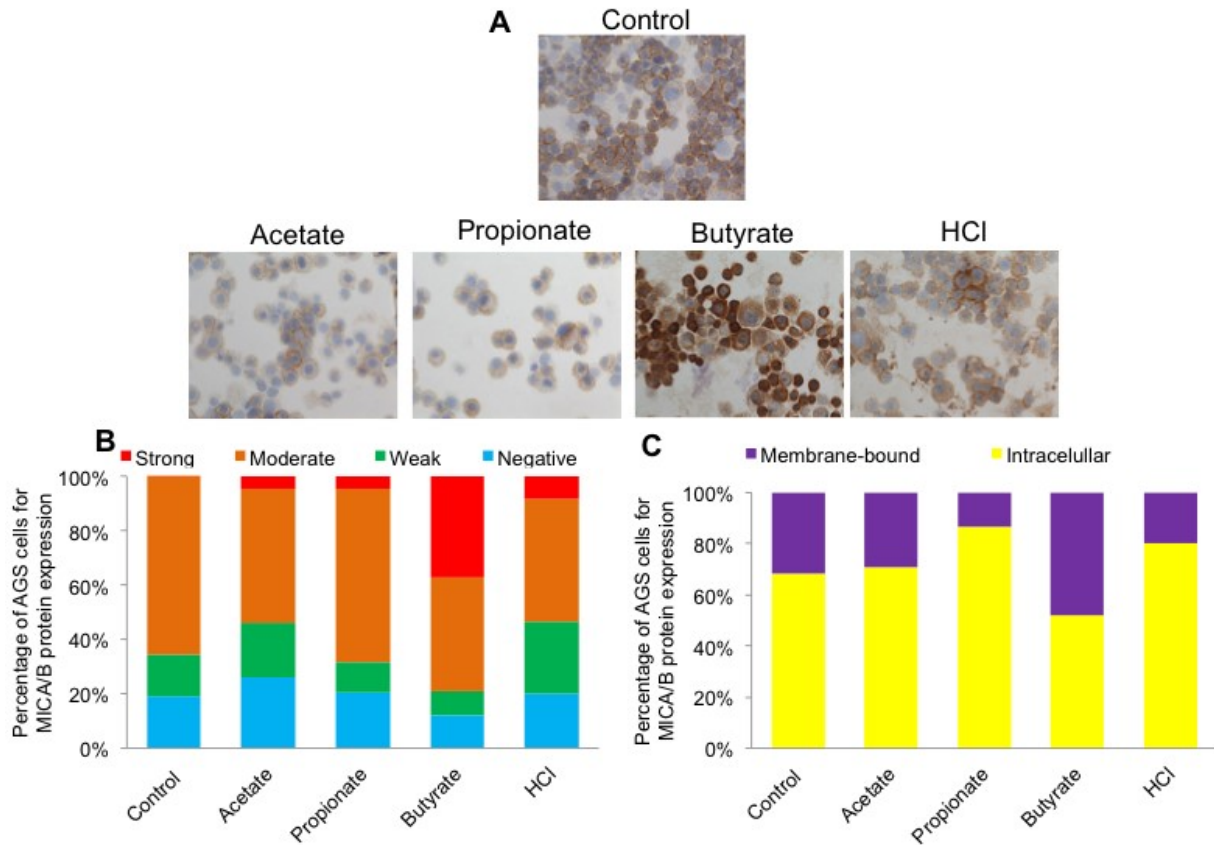


Figure 31. MICA/B ICC of AGS cells stimulated with SCFAs and HCl for 4h followed by 4h rescue in DMEM medium without SCFAs. Each bar represents the average relative counts of 5 HPF). Representation of three independent experiments.

Of note SCFA stimulation under these conditions did not influence AGS cell viability (Fig 32).

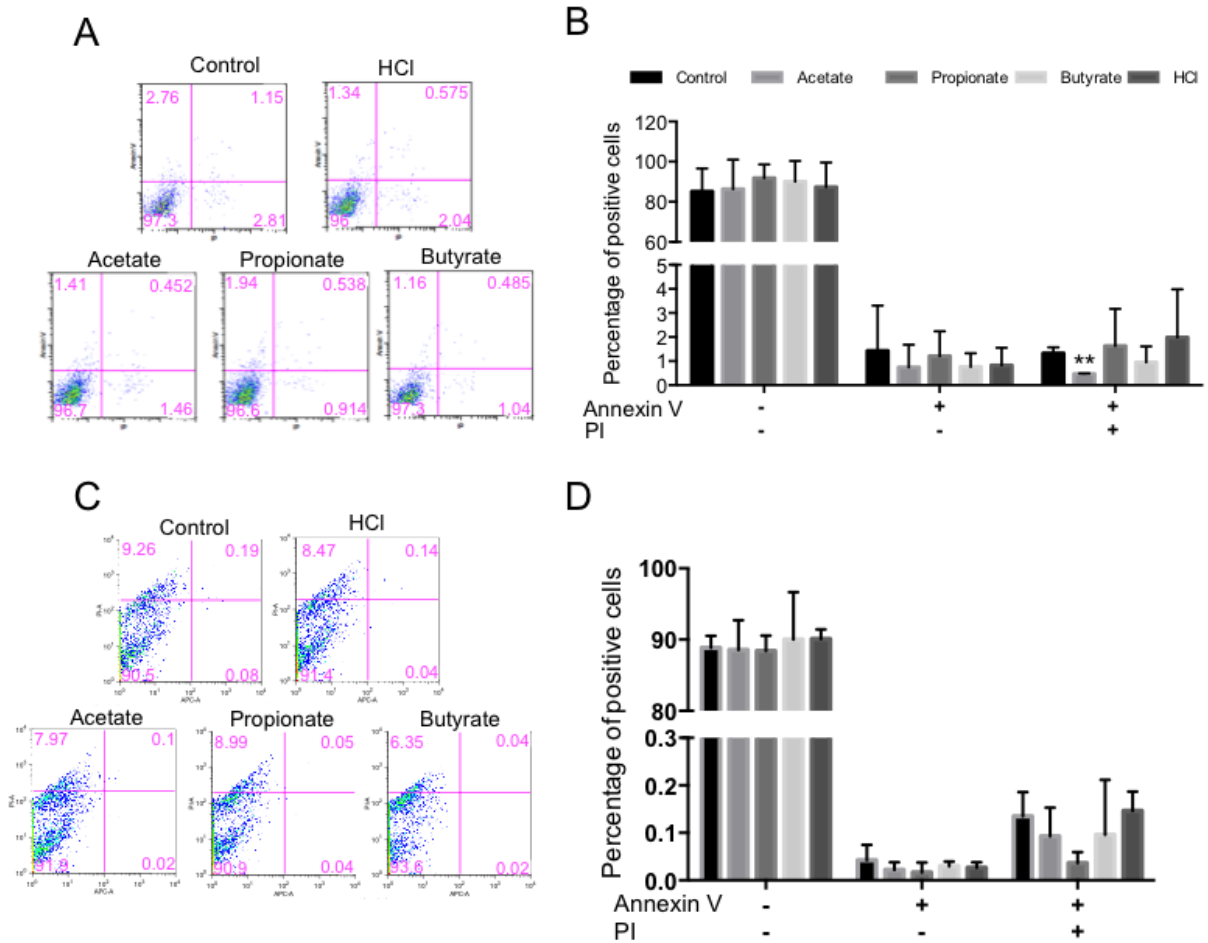


Figure 32. Apoptosis and live/dead analysis of AGS cells treated with the different SCFAs or HCl for 4h followed by 4h rescue assessed by Annexin V/PI staining and flow cytometry in AGS (A and B) and MKN28 (C and D) cells. Bar charts represent three independent Annexin V/PI assays showing the percentage of viable (Annexin V-/PI-), apoptotic (Annexin V+/PI-) and dead (Annexin V+/PI+) cells (B and D). Bars show the mean \pm SD. ** $p < 0.001$, by one-way ANOVA and *post-hoc* Dunnett's test.

In summary, these data indicate that live *P. acnes*, including its main metabolite propionate as well as the SCFA butyrate are potent inducers of NKG2DLs and modulate *il15* mRNA expression in the human stomach epithelial AGS cell line. In addition, both SCFAs enhance membrane-specific protein levels of NKG2DLs. Taken together, either direct interaction of bacteria with gastric epithelia or the bacterial metabolites SCFAs might therefore contribute to over-activation of the system and disease pathogenesis.

7. NKG2D ligands and IL15 expression is differentially modified by microbial metabolites in the upper and lower GI ECs.

We showed that gastric ECs respond to different *P. acnes* strains and microbial fermentation products by the induction of NKG2DLs *in vitro*, which would be necessary to increase CD8⁺ T cell infiltration into the epithelium. Indeed it was reported by Andresen, L et al., that *P. acnes* and microbial fermentation end-products, namely SCFAs, like butyrate and propionate, were able to induce NKG2DLs in various tumor cell lines (362).

As we previously did with AGS and MKN28 gastric ECs, we challenged Caco-2 colon ECs with 5mM acetate, propionate and butyrate, corresponding to a physiological GIT concentration of SCFAs (191) and HCl used as a negative control in order to compare the behavior exhibited in the upper and lower GIT ECs upon SCFAs stimulation and to understand how the microbial metabolites are affecting the host immune response along the GIT. First, mRNA expression of the ligands MICA and MICB and the cytokine IL15 was measured by qRT-PCR after 24h of stimulation (no effect was seen after 4h as in the case of AGS). After 24h, only butyrate was able to induce upregulation of the NKG2DLs MICA (2.65+/- 0.038) and MICB (2.6+/- 0.0012) and the (9.37+/- 0.0016) (Fig. 33).

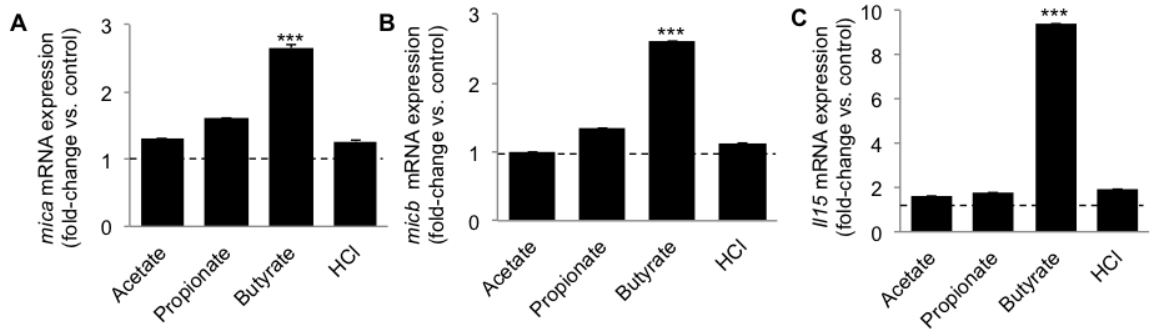


Figure 33. Caco-2 mRNA expression of (A) *mica*, (B) *micb*, and (C) *il15* after 24h of stimulation with 5mM of SCFAs (acetate, propionate, butyrate) or HCl used as a negative control. ($p < 0.001$ by one-way ANOVA and post-hoc Dunnett's test).**

Next, as previously done with gastric cell lines, we determined levels of MICA/B by flow cytometry in Caco-2 colon ECs (Fig. 34). In this case, not only butyrate (3.1+/-0.55), but also HCl (2.68+/-0.38) were able to induce the surface expression of MICA/B ligands, probably because HCl is not normally found in the colon, thus representing a certain level of stress on colonocytes.

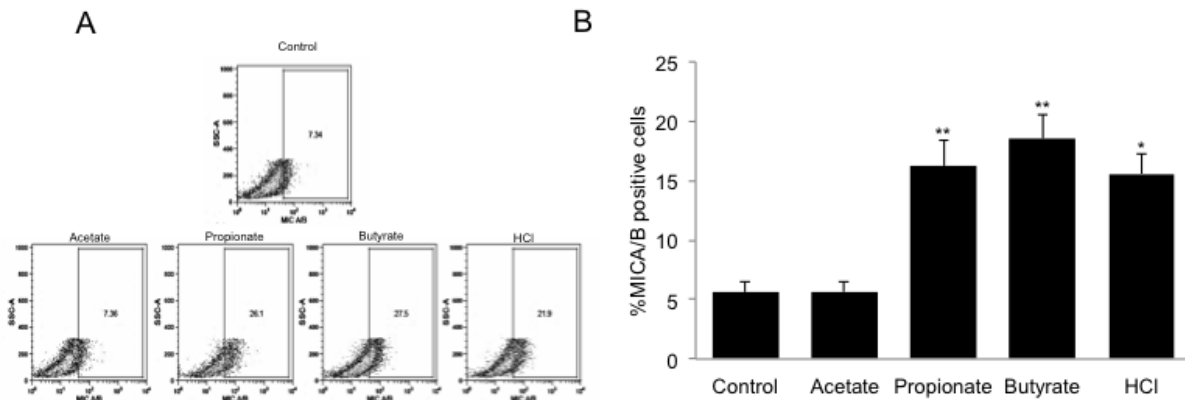


Figure 34 (A) Extracellular MICA/B protein expression was assessed in Caco-2 cells by flow-cytometry after SCFAs stimulation for 24h. Significant induction of cell-surface specific MICA/B protein expression due to treatment with 5 mM butyrate, propionate and HCl. 10000 events were analyzed. (B) Bar charts represent the mean values of percentages of MICA/B positive cells \pm SD of three independent experiments (* $p < 0.05$; ** $p < 0.01$; * $p < 0.001$; one-way ANOVA and post-hoc Dunnett's test).**

However, intracellular levels of MICA/B in Caco-2 cells stay unchanged among the different treatments as previously shown for AGS and MKN28 cells (Fig. 35).

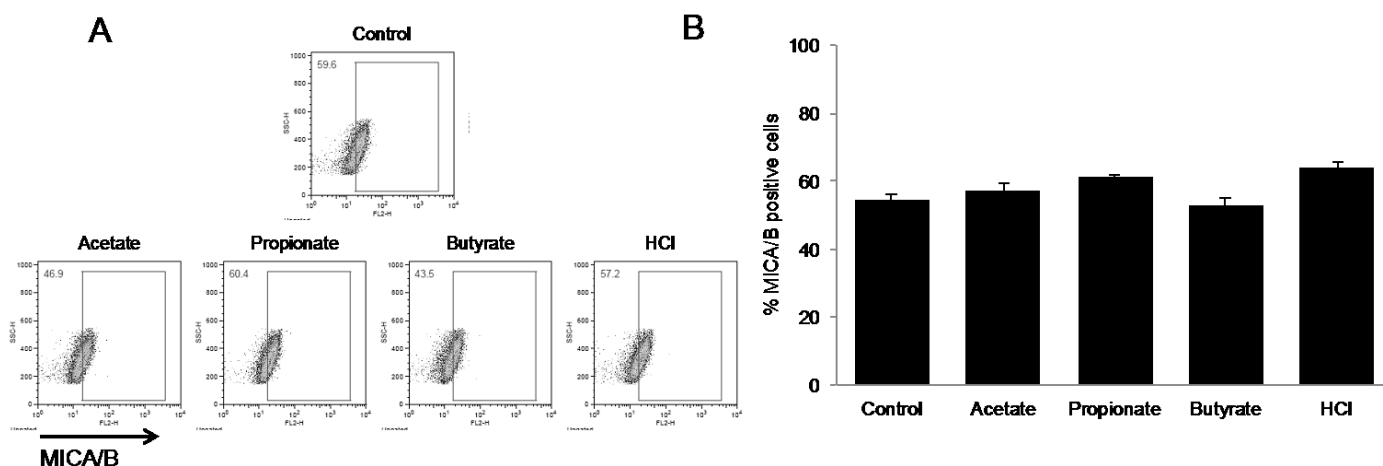


Figure 35. Overall MICA/B protein expression was assessed in Caco-2 cells by flow-cytometry after SCFAs stimulation for 24 h. A) Representative pictures of dot plots and bar charts B) represent the mean values of percentages of MICA/B positive cells \pm SD of three independent experiments. No change in overall MICA/B protein expression is appreciated in any of the cases. 10000 events were analyzed.

Finally, we assessed the protein expression of MICA/B ligands in Caco-2 by ICC in order to show how these ligands are localized within the cells. From the ICC pictures, we can see that Caco-2 cells treated with propionate, butyrate and HCl showed a stronger staining with MICA/B Ab, being more prominent around the cell membrane (Fig. 36A and C). Additionally, we scored staining intensity and localization in a semi quantitative way with each stimulus used and we found that butyrate triggers the most prominent expression of MICA/B ligand on Caco-2 cells (Fig. 36B).

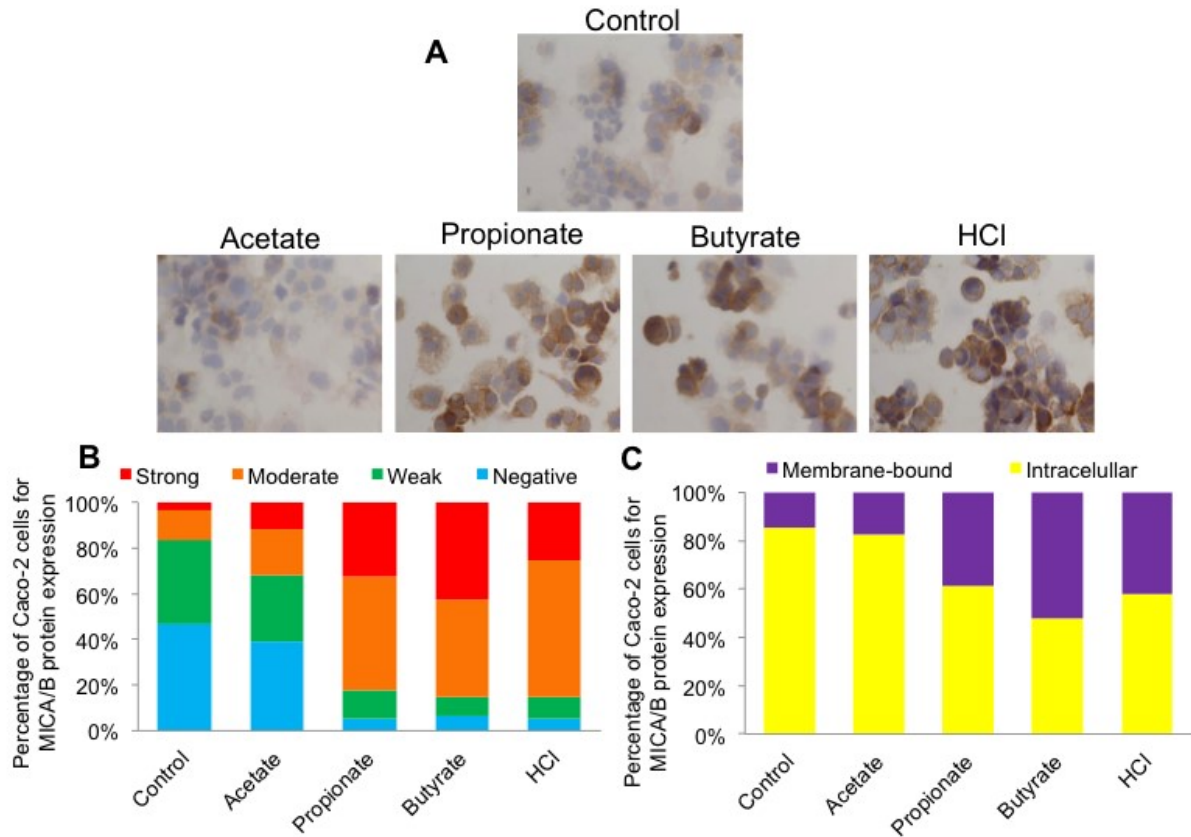


Figure 36. MICA/B ICC of Caco-2 cells stimulated with SCFAs and HCl for 24h. A) ICC was performed in the same set of samples to support the results obtained by flow cytometry. B) Caco-2 cells were scored according to the staining intensity. C) Positive cells were classified according to MICA/B cellular localization (cytoplasmatic vs. cell-membrane dominant; each bar represents the average relative counts of 5 HPF). Representation of three independent experiments.

Treatment of Caco-2 cells with 5 mM acetate, propionate, butyrate or HCl for 24h showed increased levels of live cells and decreased necrotic cells compared to controls. Additionally, butyrate significantly decreases the percentage of apoptotic cells compared to control conditions (Fig. 37 and Table 3).

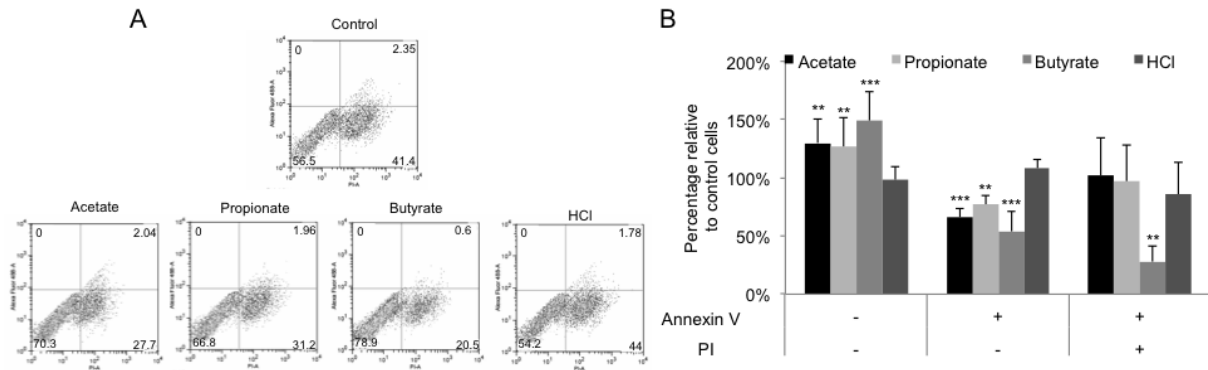


Figure 37. (A) Apoptosis and live/dead analysis of Caco-2 cells treated with the different SCFAs or HCl for 24h assessed by Annexin V/PI staining and flow cytometry. (B) Bar chart representation of three independent Annexin V/PI experiments showing the percentage of viable (Annexin V-/PI-), apoptotic (Annexin V+/PI-) and dead (Annexin V+/PI+) cells, respectively. Bars show the mean \pm SD, (* p <0.05; ** p <0.01; * p <0.001; one-way ANOVA and post-hoc Dunnett's test).**

Time	Stimulus	5 mM			10 mM		
		Total cell count	Viable cells	Viability (%)	Total cell count	Viable cells	Viability (%)
4h	Control	5,60E+05	5,40E+05	96,8	5,60E+05	5,40E+05	96,8
	Acetate	5,50E+05	5,30E+05	95,8	2,60E+05	2,30E+05	90
	Propionate	3,40E+05	3,40E+05	93,6	8,80E+05	8,60E+05	97,3
	Butyrate	3,70E+05	3,50E+05	94,6	3,70E+05	3,40E+05	91,4
	HCl	6,20E+05	6,00E+05	96,4	1,90E+05	1,60E+05	85,5
24h	Control	4,40E+05	3,60E+05	88,3	4,40E+05	3,60E+05	88,3
	Acetate	4,20E+05	3,90E+05	92,5	6,20E+05	5,90E+05	95
	Propionate	3,50E+05	3,20E+05	90,8	1,30E+05	1,00E+05	80,2
	Butyrate	4,70E+05	4,30E+05	91,9	3,80E+05	3,50E+05	92,4
	HCl	4,20E+05	3,50E+05	90,2	2,20E+05	2,00E+05	90,9

Table 3. Cell counts and viability in Caco-2 cells after 4 and 24h of treatment with 5 or 10mM SCFAs or HCl.

8. NKG2D deficiency in mice is not affecting the immune cell populations under homeostatic conditions neither in the lamina propria nor in the intraepithelial compartment.

Lamina propria and intraepithelial lymphocytes (LPLs and IELs, respectively) were isolated from the stomach, small intestine, caecum and colon of NKG2D mutant (*klrk1*^{-/-}) and WT mice as described in the Materials and Methods section. Later, both LPLs and IELs were stained for multiparameter flow cytometry using an Ab cocktail as shown in Table 4:

Ab	Fluorophore	Clone	Company
CD45	AF700	30-F12	biolegend
CD3	BUV737		BD
CD4	BV711		biolegend
CD8	BUV395		BD
CD11b (Mac1)	PerCP-Cy5.5	M1/70	ebio
CD19	BV650	6D5	biolegend
CD27	PE-Cy7	LG.7F9	ebio
CD122	AF647	TM-beta1	Serotec
gdTCR	BV421	GL3	BD
NKG2D (CD 314)	biot	A10	ebio
NKp46	FITC	29A1.4	ebio
NK1.1	PE-CF594	PK136	BD

Table 4. List of antibodies used for GIT immunophenotyping in mouse.

5 mice were analysed per genotype. From the results we can extract that the absence of the NKG2D receptor (named KLRK1 in mouse) does not influence the immune cell populations neither in the lamina propria or intraepithelial compartment along the GIT (Table 5). The only case a statistically significant difference between WT and KO mice could be found was lamina propria CD4⁺ T cells from the small intestine, which are lower in *Klrk1*^{-/-} compared to WT mice.

		LPLs			IELs		
		WT	KO	P value	WT	KO	P value
		Mean ± SEM			Mean ± SEM		
Stomach	CD4	2.524 ± 1.010	4.472 ± 2.032	0.4157	9.990 ± 5.209	6.035 ± 2.543	0.5205
	CD8	11.41 ± 2.859	14.63 ± 2.415	0.4149	14.80 ± 4.543	30.23 ± 6.195	0.0914
	CD11b	49.60 ± 13.64	42.46 ± 13.39	0.7185	13.88 ± 6.275	22.18 ± 13.88	0.6054
	CD19	10.12 ± 5.146	4.658 ± 2.274	0.3601	11.10 ± 5.300	12.87 ± 4.838	0.8134
	NK1.1	3.714 ± 2.397	5.826 ± 2.082	0.5246	0.8075 ± 0.2866	5.218 ± 2.348	0.1115
	NKp46	42.22 ± 13.48	24.47 ± 9.180	0.3082	8.468 ± 7.493	4.655 ± 2.654	0.6485
	CD122	26.17 ± 7.760	24.74 ± 7.020	0.894	28.62 ± 16.69	36.33 ± 11.16	0.7144
	γδT	2.120 ± 0.9231	9.056 ± 5.085	0.2164	25.43 ± 12.04	30.99 ± 10.47	0.7393
Small intestine	CD4	4.834 ± 0.8530	2.086 ± 0.7699	0.0438*	9.742 ± 4.783	5.760 ± 0.8960	0.4368
	CD8	16.38 ± 5.031	32.88 ± 11.23	0.2167	29.64 ± 6.902	33.79 ± 8.068	0.7064
	CD11b	33.90 ± 11.62	29.17 ± 13.41	0.7963	4.512 ± 1.188	25.31 ± 14.98	0.2037
	CD19	23.73 ± 9.344	12.72 ± 4.581	0.321	18.57 ± 5.532	20.82 ± 6.654	0.8016
	NK1.1	4.139 ± 2.095	2.524 ± 1.095	0.5138	1.760 ± 0.3168	1.347 ± 0.2505	0.3362
	NKp46	32.30 ± 10.52	16.36 ± 5.945	0.2236	N.D.	N.D.	-
	CD122	15.81 ± 7.958	20.41 ± 7.120	0.6778	14.67 ± 4.521	38.36 ± 15.12	0.1717
	γδT	2.708 ± 0.9294	14.74 ± 6.313	0.0961	18.19 ± 8.305	28.56 ± 12.15	0.5009
Caecum	CD4	5.960 ± 1.149	5.812 ± 2.154	0.9532	7.918 ± 4.832	4.140 ± 1.288	0.4716
	CD8	22.58 ± 2.623	22.75 ± 5.114	0.9771	23.06 ± 5.084	29.50 ± 5.644	0.4212
	CD11b	15.06 ± 3.215	16.49 ± 3.344	0.7657	2.342 ± 1.089	4.954 ± 2.154	0.3107
	CD19	18.38 ± 5.389	17.14 ± 6.599	0.8877	12.23 ± 3.910	10.60 ± 4.944	0.8018
	NK1.1	4.594 ± 0.7551	6.524 ± 1.715	0.3332	4.088 ± 1.393	6.012 ± 2.469	0.5164
	NKp46	17.02 ± 3.545	8.904 ± 3.680	0.151	1.265 ± 0.8595	1.762 ± 0.5818	0.6351
	CD122	11.25 ± 4.674	10.16 ± 3.807	0.86	6.930 ± 2.583	9.938 ± 3.793	0.5306
	γδT	3.318 ± 1.082	7.866 ± 3.704	0.2724	7.774 ± 2.862	13.24 ± 5.278	0.389
Large intestine	CD4	5.928 ± 0.5210	6.052 ± 1.950	0.9525	3.584 ± 0.6690	4.122 ± 0.7239	0.6001
	CD8	25.80 ± 3.815	22.42 ± 5.211	0.6145	39.60 ± 6.577	43.12 ± 8.595	0.7533
	CD11b	15.21 ± 3.182	16.27 ± 3.593	0.8304	3.126 ± 1.835	4.526 ± 1.736	0.5946
	CD19	21.42 ± 3.031	17.27 ± 6.605	0.5838	4.128 ± 2.576	8.990 ± 4.995	0.4122
	NK1.1	3.558 ± 0.7562	3.914 ± 0.8662	0.7648	4.784 ± 0.8546	3.928 ± 0.9736	0.5273
	NKp46	16.04 ± 4.814	12.12 ± 6.609	0.645	3.346 ± 0.8272	1.682 ± 0.6280	0.1478
	CD122	7.773 ± 2.766	11.42 ± 4.352	0.4993	9.096 ± 4.904	15.88 ± 9.255	0.5352
	γδT	3.038 ± 0.8679	4.935 ± 1.496	0.3045	9.580 ± 3.175	12.96 ± 4.560	0.5603

Table 5. Frequencies of the different immune cell populations in the lamina propria and intraepithelial compartments along the GIT, of WT and Klrk1^{-/-} (KO) mice. Mean ± SEM and p value are represented. *p<0.05 by unpaired t-test; n=5.

9. Induction of colitis by DSS does not trigger differences in immune cell populations.

Since we did not find prominent differences in immune cell populations between WT and Klrk1^{-/-} mice under physiological conditions, we next induced acute colitis by

administration of DSS (2%) in the drinking water. After 5 days of treatment followed by 3 days of recovery, we took colon samples for lymphocyte isolation and further immune characterization by flow cytometry. In summary, we could just discern differences in certain immune cell populations between control mice (non-treated with DSS) and mice treated with DSS, but no differences were found between genotypes. For instance, CD11b+IFN γ +, CD19+Rae1+, NK1.1+, and NK1.1+IFN γ + cells presented higher relative abundance in control mice compared to DSS-treated (both WT and Klrk1-/-) mice. On the contrary, CD19+ cells were more abundant in DSS treated mice compared to controls (Table 6).

	Control vs. WT DSS					Control vs. KO DSS					WT DSS vs. KO DSS				
	Mean 1	Mean 2	Diff.	SE of diff.	P value	Mean 1	Mean 2	Diff.	SE of diff.	P value	Mean 1	Mean 2	Diff.	SE of diff.	P value
CD3+	15.04	13.2	1.926	4.899	0.9189	15.04	13	2.044	4.899	0.9091	13.12	13	0.1183	4.381	0.9996
CD4+	20.63	26.77	-6.142	4.715	0.4185	20.63	29.42	-8.792	4.715	0.1881	26.77	29.42	-2.65	4.217	0.8074
CD4+IFN γ +	0	0.239	-0.239	0.2341	0.5772	0	0.3542	-0.3542	0.2341	0.3171	0.239	0.3542	-0.1152	0.2094	0.8482
CD4+NKG2D+	2.193	2.496	-0.303	2.154	0.9892	2.193	4.911	-2.718	2.154	0.4399	2.496	4.911	-2.415	1.926	0.4444
CD8+	26.35	36.03	-9.681	9.48	0.5771	26.35	28.69	-2.334	9.48	0.9672	36.03	28.69	7.347	8.479	0.6699
CD8+CD107a+	50.3	29.12	21.18	12.15	0.2267	50.3	44.18	6.117	12.15	0.8709	29.12	44.18	-15.07	10.87	0.3759
CD8+ γ δ T+	59.35	62.58	-3.233	9.331	0.9363	59.35	59.45	-0.1	9.331	>0.9999	62.58	59.45	3.133	8.346	0.9257
CD8+IFN γ +	0.1659	0.05455	0.1114	0.2044	0.8508	0.1659	0.3573	-0.1914	0.2044	0.6279	0.05455	0.3573	-0.3028	0.1828	0.2585
CD8+NKG2D+	1.696	1.321	0.3748	0.8222	0.8927	1.696	1.698	-0.0019	0.8222	>0.9999	1.321	1.698	-0.3767	0.7354	0.8668
CD11b+	41.73	28.02	13.71	7.575	0.205	41.73	33.08	8.642	7.575	0.5072	28.02	33.08	-5.067	6.775	0.7402
CD11b+F4/80+	19.24	32.85	-13.61	7.039	0.1686	19.24	17.68	1.554	7.039	0.9735	32.85	17.68	15.17	6.296	0.0756
CD11+IFN γ +	5.985	1.597	4.388	1.39	0.0193*	5.985	1.482	4.503	1.39	0.0166*	1.597	1.482	0.1155	1.243	0.9953
CD11b+Ly6G+	2.537	3.955	-1.418	2.479	0.8372	2.537	5.138	-2.601	2.479	0.5606	3.955	5.138	-1.183	2.218	0.8564
CD11b+Rae1+	21.3	25.3	-4.007	8.03	0.8731	21.3	18.03	3.268	8.03	0.9133	25.3	18.03	7.275	7.182	0.5821
CD19+	14.79	45.42	-30.62	5.274	0.0002***	14.79	39.98	-25.19	5.274	0.001***	45.42	39.98	5.433	4.717	0.5009
CD19+Rae1+	13.2	3.466	9.735	2.806	0.0108*	13.2	1.561	11.64	2.806	0.0031**	3.466	1.561	1.905	2.509	0.7337
NK1.1+	40.25	28.5	11.75	3.025	0.005**	40.25	24.27	15.98	3.025	0.0004***	28.5	24.27	4.233	2.706	0.2949
NK1.1+CD107a+	69.18	64.37	4.808	10.49	0.8917	69.18	73.33	-4.158	10.49	0.9176	64.37	73.33	-8.967	9.387	0.6166
NK1.1+IFN γ +	4.76	1.955	2.806	0.624	0.0016**	4.76	2.036	2.724	0.624	0.0021**	1.955	2.036	-0.0817	0.5581	0.9883
NK1.1+NKG2D+	50.48	46.85	3.625	7.574	0.8825	50.48	42.62	7.858	7.574	0.5674	46.85	42.62	4.233	6.774	0.8093
NK1.1+Rae1+	17.15	20.22	-3.078	9.399	0.9428	17.15	19.9	-2.757	9.399	0.9539	20.22	19.9	0.3217	8.407	0.9992

Table 6. Frequencies of different immune cell populations in the colon lamina propria of WT control mice, or treated with DSS (WT and Klrk1 -/- (KO)) mice. Represented is the mean of the group, the mean difference, the SE of the difference and the P value. *p<0.05, **p<0.01, ***p<0.001 by One-way Anova and post-hoc Tukey's test; n=4-6.

10. NKG2D absence does not have a strong influence in the acute colitis model.

During the time course of the DSS experiment, body weight of mice was monitored daily. At the end of the DSS treatment, we could see that the decrease in body weight (BW) was noticeable already during the recovery phase (days 6 to 8). However, no differences were found between WT and KO (klrk1-/-) mice treated with DSS (Fig.

38A). On the day 8, mice were sacrifice and colon isolated for further measurements. Relative colon weight to total BW was lower in WT treated with DSS compared to KO treated with DSS or control mice (Fig. 38B). Colon length was also shorter in DSS treated mice, although no statistically significant differences were found between WT and KO mice (Fig. 38C and Fig. 39). Finally, colon mass, measured as the ratio of mg of colon/ colon length showed no differences among the groups tested (Fig. 38D).

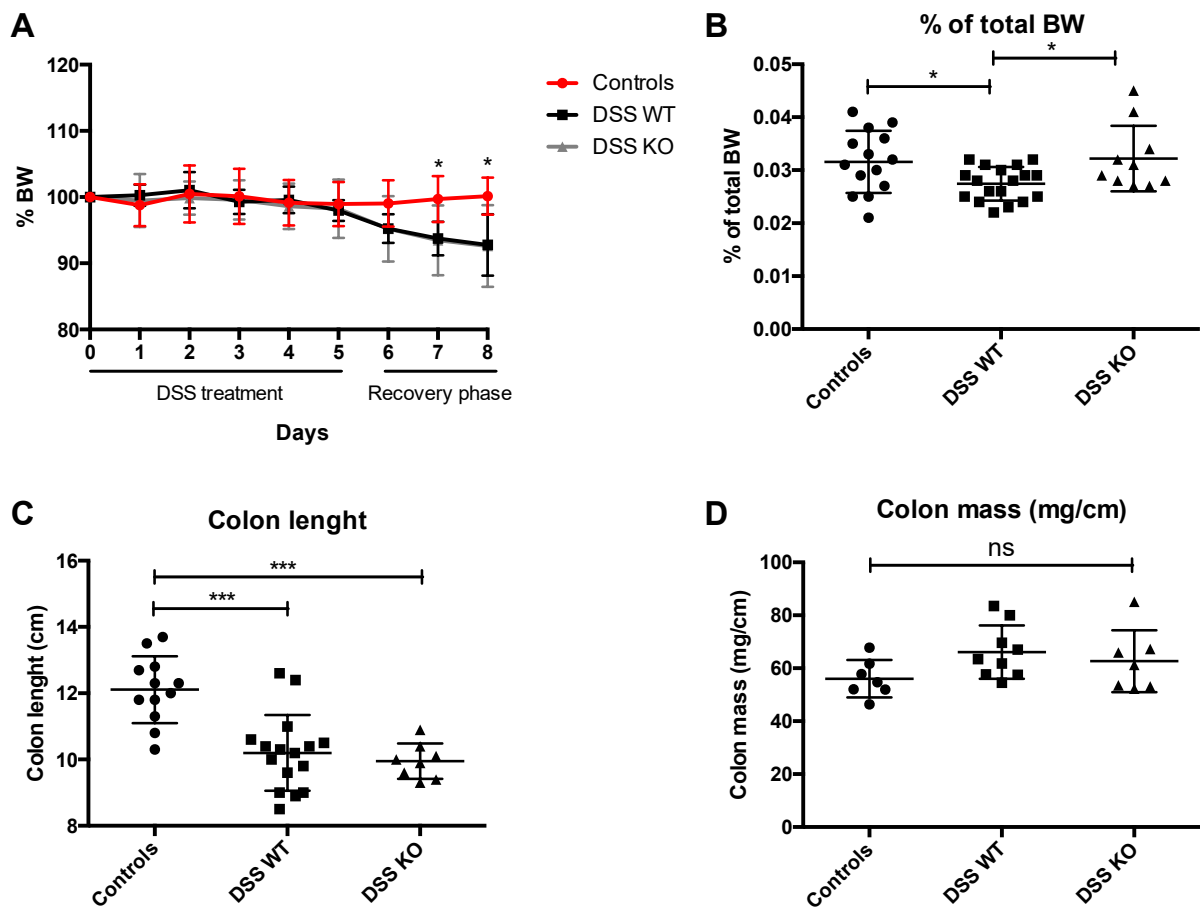


Figure 38. Body weight and colon parameters in control mice vs. treated with DSS (WT and KO). Total body weight evolution along the course of the experiment (A); percentage of colon weight relative to total body weight (BW) (B), colon length (C) and colon mass (D) at the end of the experiment (day 8). * $p < 0.05$, *** $p < 0.0001$ by One-way Anova and post-hoc Tukey's test.

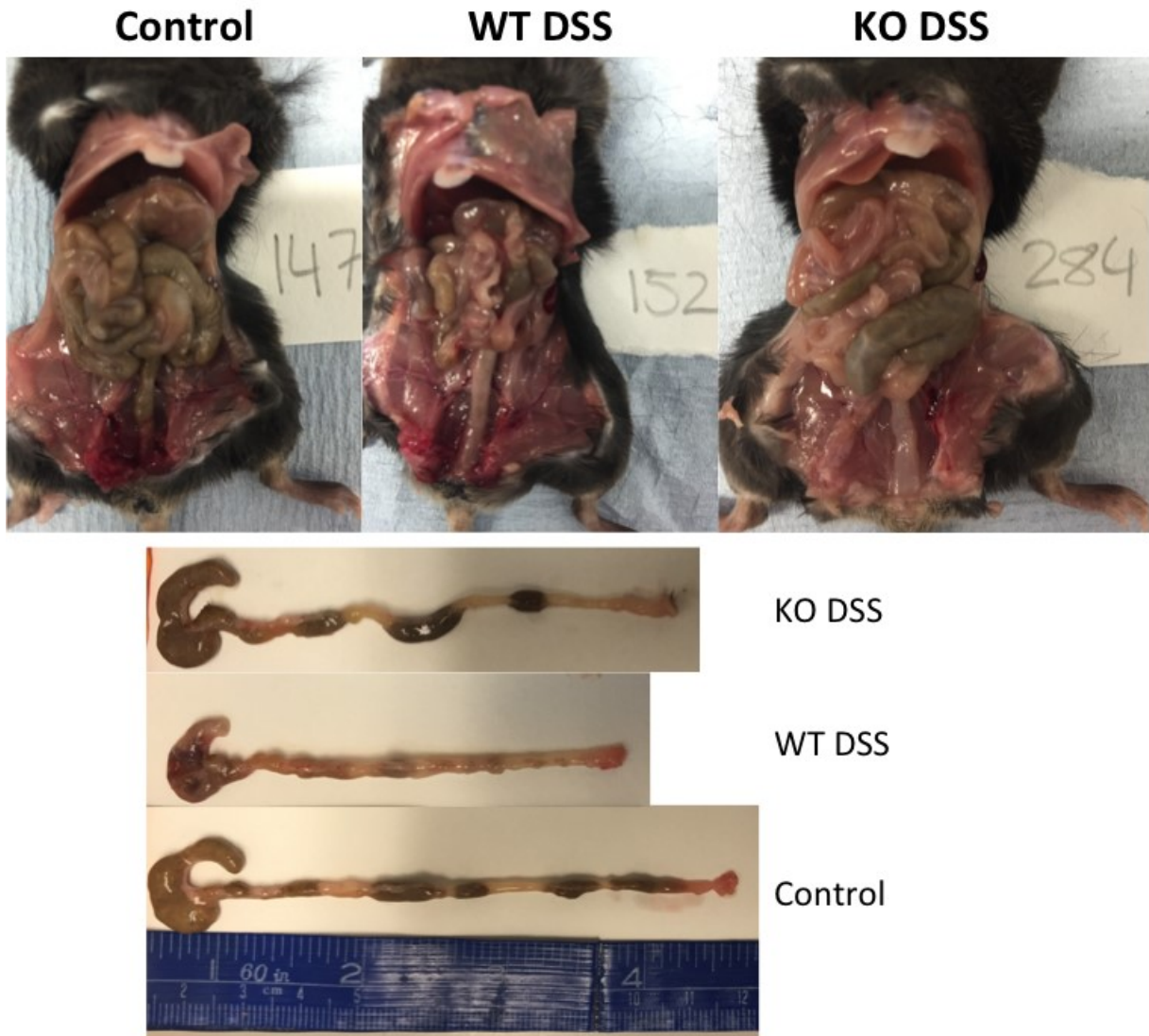


Figure 39. Gut macroscopy and colon length in control and KO mice treated with DSS (WT and *Klrk1*^{-/-}). Note the shortened colon in DSS treated mice, which was not statistically different between both genotypes.

11. Regionalization of the LPLs and IELs along the GIT in mice.

Since the presence or absence of the NKG2D receptor does not significantly influence the immune cell populations in the different GIT segments in mice (except CD4⁺ LPLs in the small intestine), we next sought to investigate how LPLs and IELs are generally distributed along the murine GIT. For this purpose, we pooled all the

mice used in the previous assays (WT and KO) and analysed the main immune cell populations from stomach to colon in both the lamina propria and the intraepithelial compartment.

Within the lamina propria we could see that, although the percentage of CD4⁺ T cells is higher from upper to lower GIT, there are no statistically significant differences among the different organs analysed. However, the proportion of CD8⁺ T cells is statistically significant higher in caecum and colon compared to stomach. On the contrary, myelocytes, recognized with the marker CD11b, were found to be highly abundant in the upper (stomach and small intestine) compared to the lower (caecum and colon) GIT. B cells, known to be CD19⁺, were more represented in the colon and caecum compared to stomach, while CD8⁺CD122⁺ T cells showed the opposite distribution, being those cells more abundant in the stomach compared to both caecum and colon. This double CD8⁺CD122⁺ population consists of cytotoxic T cells expressing the receptor for the IL15. Neither NK1.1⁺ cells nor $\gamma\delta$ T cells showed any differences along the GIT (Fig. 40).

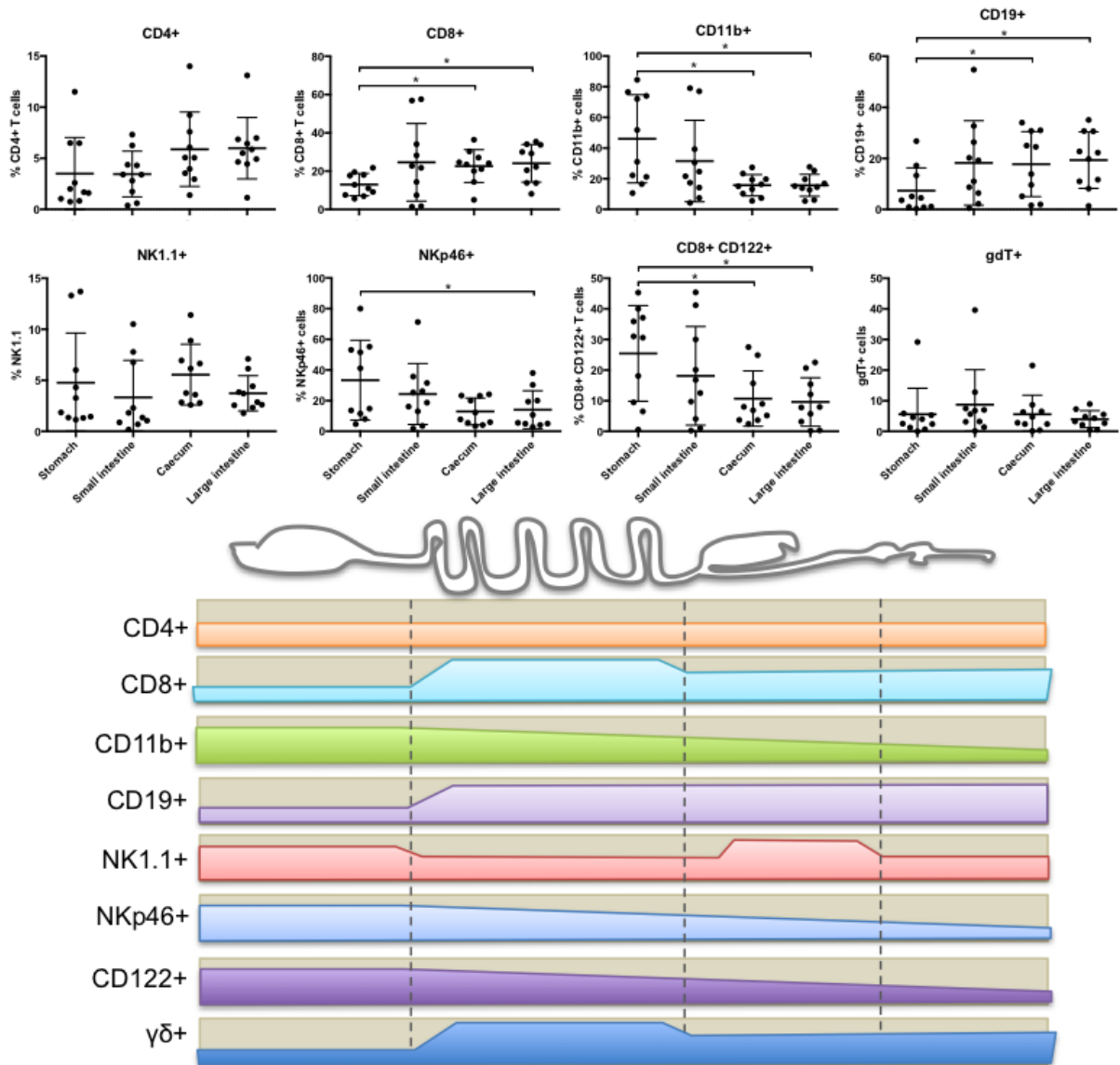


Figure 40. Lamina propria immune cell regionalization along the murine GIT. Upper panel: Scatter plots representing the mean values of percentages of positive cells \pm SD. n=10 (*p<0.05; **p<0.01; * p<0.001; one-way ANOVA and post-hoc Tukey's test). Lower panel: Schematic representation of the immune cells regionalization (relative abundance) along the mouse GIT.**

In the intraepithelial compartment, we found that there were no differences in the percentage of CD4+ T cells along the GIT, although there is a downstream tendency, although not significant from stomach to colon. Unlike, CD8+ T cells showed an increased abundance from upper to lower GIT, resulting significantly more abundant in colon compared to caecum. Similarly, NK1.1 positive cells were also found more

frequently in the colon, compared to small intestine; while B cells were more abundant in the small intestine compared to colon. Neither CD11b+, Nkp46+, CD8+CD122+ nor $\gamma\delta$ T positive cells showed differences along the GIT of mice (Fig 41).

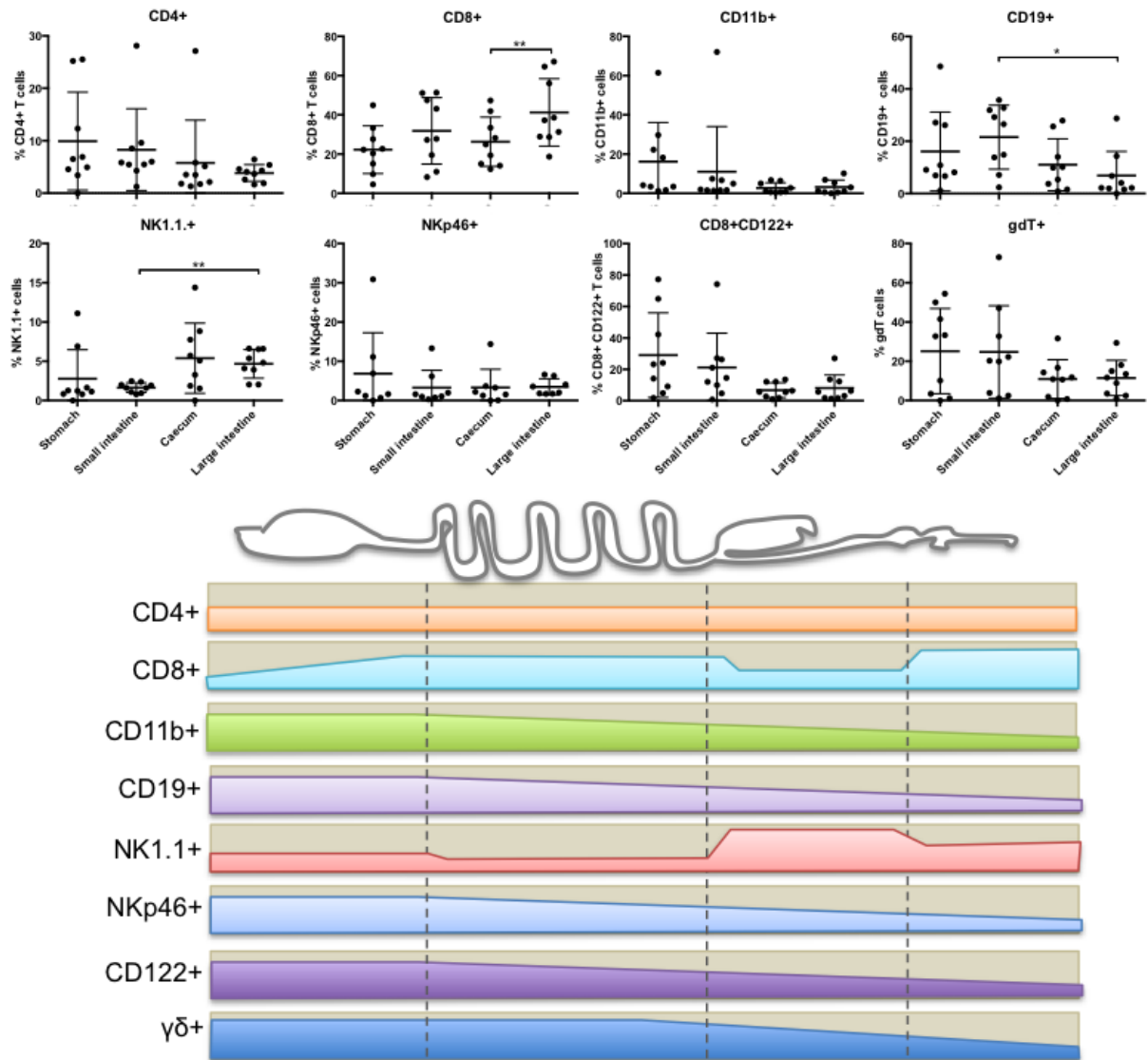


Figure 41. Intraepithelial immune cell regionalization along the murine GIT. Upper panel: Scatter plots represent the mean values of percentages of positive cells \pm SD. n=10 (*p<0.05; **p<0.01; * p<0.001; one-way ANOVA and post-hoc Tukey's test). Lower panel: Schematic representation of the immune cells regionalization (relative abundance) along the mouse GIT.**

12. Absence of the NKG2D receptor does not influence the expression of TLR2, 4 & 5, NKG2D ligands or IL15

We next aimed to investigate whether NKG2DLs, IL15 and TLRs are expressed differently in WT and *Klrk1*^{-/-} mice along the GIT. After analyzing 15-17 mice per group we concluded that the absence of the NKG2D receptor itself is not enough to establish a difference in terms of NKG2DL, IL15 or TLR expression along the GIT (Table 7).

	Relative gene expression to HKG	WT vs. KO	
		KS test	P value
Stomach	rae	0.2353	0.7697
	mult	0.4235	0.1147
	il15	0.2471	0.7155
	tlr2	0.349	0.2862
	tlr4	0.349	0.2862
	tlr5	0.2118	0.8672
Small intestine	rae	0.1581	0.9862
	mult	0.2169	0.8328
	il15	0.2941	0.4739
	tlr2	0.1728	0.9664
	tlr4	0.2831	0.5236
	tlr5	0.3419	0.2902
Caecum	rae	0.2689	0.6354
	mult	0.3487	0.3079
	il15	0.2941	0.4958
	tlr2	0.3294	0.3528
	tlr4	0.2353	0.7697
	tlr5	0.3216	0.3821
Large intestine	rae	0.4392	0.0924
	mult	0.2118	0.8672
	il15	0.3451	0.2987
	tlr2	0.3804	0.1991
	tlr4	0.4471	0.0827
	tlr5	0.3882	0.1809

Table 7. Relative gene expression to housekeeping gene (HKG) (*hprt*) along the mice GIT (stomach, small intestine, caecum and large intestine) measured by qRT-PCR. n=15-17. No differences were appreciated between WT and *Klrk1*^{-/-} mice by non-parametric Kolmogorov-Smirnov test.

13. TLR gene expression present positive correlations with the NKG2D system along the GIT, which can be genotype-dependent.

Afterwards, we studied the correlation between mRNA expression of TLRs and NKG2D system (NKG2D, NKG2DLs, and IL15) along the GIT, and how TLR expression may be differently expressed when the NKG2D receptor is absent. Therefore, we isolated mRNA from stomach, small intestine, caecum and colon from WT and *Klrk1*^{-/-} mice and analyzed gene expression of the main TLRs present in the gut (TLR2, TLR4 and TLR5) as well as the more prominent NKG2D ligand families found in the murine gut (Rae1 and Mult1). Likewise, we also analyzed IL15 gene expression in those samples and checked for a possible correlation with TLRs. After applying a normality test, we found that our samples were not normally distributed. Therefore, we computed for every pair of data the Spearman correlation to obtain a correlation matrix.

These results provided clear evidence of a positive correlation between TLRs and the NKG2D system (Fig. 42). It is interesting to note that in WT mice, we only found in the stomach positive correlations between TLR5 and Rae1 and between TLR5 and IL15. In the small intestine TLR2 is positively correlated with Rae1, Mult1 and *Klrk1*. Similarly, TLR4 is positively correlated with Mult1, *Klrk1* and IL15, but not with Rae1. Moreover, TLR5 was just positively correlated with Rae1. Interestingly, in the caecum we found the same correlations as in the small intestine. Finally, in the large intestine, both TLR2 and TLR4 present a high correlation with *Klrk1* and IL15, and TLR5 was positively correlated with Rae1, *Klrk1* and IL15.

In the case of *Klrk1*^{-/-} mice we found some differences compared to WT mice. In the case of the stomach, all the TLRs present positive correlations with NKG2DLs in some extent. In particular, TLR2 positively correlates with Mult1; TLR4 with Rae1 and Mult1, and TL5 with Rae-1. In the small intestine we found that all the TLRs analyzed positively correlate with Mult1 and IL15. Additionally, TLR5 was also found being positively correlated with Rae1. Interestingly, caecum presented the same positive

correlations as the ones presented in the small intestine (as it was the case for WT mice). Finally, in the large intestine we found that all the three TLRs analyzed had a positive correlation with Rae1, Mult1 and Il15.

In general, our results suggest that TLRs expression is closely linked to NKG2D expression along the GIT. Interestingly, the correlations here presented are location-dependent and in most of the cases subject to change depending on the presence/absence of the NKG2D receptor. Note that while in the stomach from WT mice positive correlations are limited to TLR5, in the absent of NKG2D receptor, these positive correlations are extended to TLR2 and TLR4. In small intestine and caecum (which share the same correlations for both WT and KO mice), correlation between TLR5 and Mult is NKG2D-dependent. Likewise, in colon we found that all TLRs analyzed correlate positively with Mult1 just in *Klrk1*^{-/-} mice. This unequal pattern may be due to differences in the microbiota composition, which drive differences in the type of TLRs present and their abundance along the GIT. (For detailed information about r and p values, see Appendix 6).

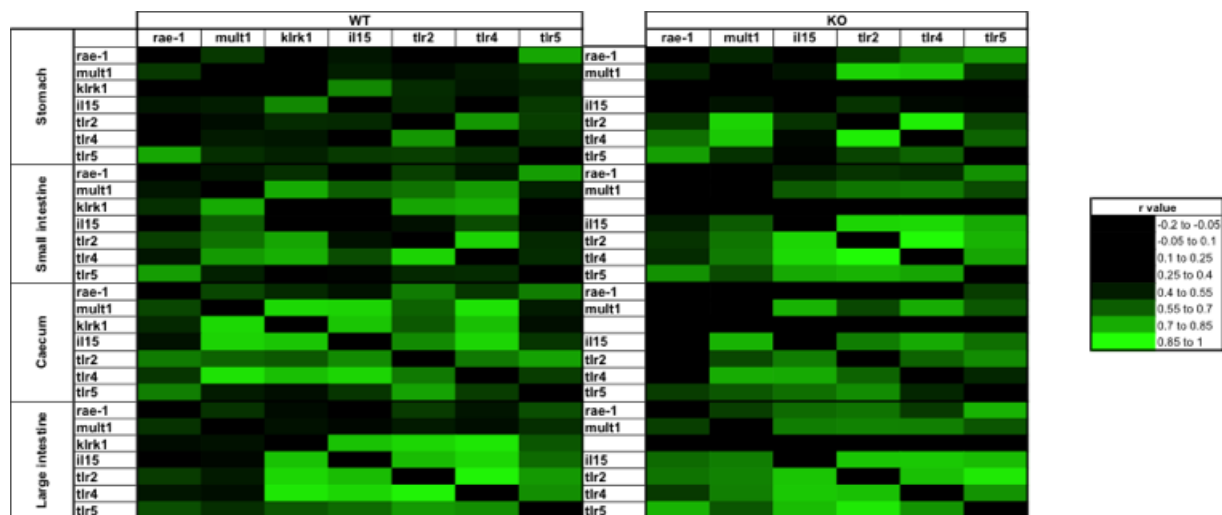


Figure 42. Heat map matrix representing the correlation between TLRs (TLR2, TLR4 and TLR5) and the NKG2D system (*Klrk1* receptor, Rae1 and Mult1 ligands and IL15) in WT and *Klrk1* KO mice.

14. NKG2D receptor deficiency influences gut microbiota composition.

Since we found different correlations of expression levels between determinants of the NKG2D system and TLRs in WT vs. *Klrk1*^{-/-}, we speculated that the microbiota might differ in the mouse genotypes due to the presence/absence of NKG2D receptor. Therefore, we subjected GI biopsies from stomach, small intestine, caecum, and colon, as well as faeces originating from WT (n=11) and *Klrk1*^{-/-} (n=8) mice to comparative 16S rRNA gene profiling. The number of reads generated per sample in each section of the GIT and faeces, and the OTUs per sample can be found in Table 8.

Organ	NKG2D genotype	Reads/sample	OTUs/sample
Stomach	WT	57291 ± 21161	432 ± 102
	KO	59881 ± 26109	403 ± 117
Small intestine	WT	35798 ± 19219	241 ± 73
	KO	40299 ± 23684	224 ± 89
Caecum	WT	43894 ± 18748	678 ± 56
	KO	54493 ± 15927	633 ± 92
Large intestine	WT	46981 ± 20072	558 ± 47
	KO	52763 ± 13264	546 ± 93
Faeces	WT	54043 ± 16772	457 ± 55
	KO	39622 ± 17334	457 ± 54

Table 8. Reads per sample and OTUs along the GIT in WT and *Klrk1*^{-/-} (KO) mice.

Microbial richness, a measure of how many taxa are detectable in the respective sample, showed no difference between entities along the GIT (Fig. 43).

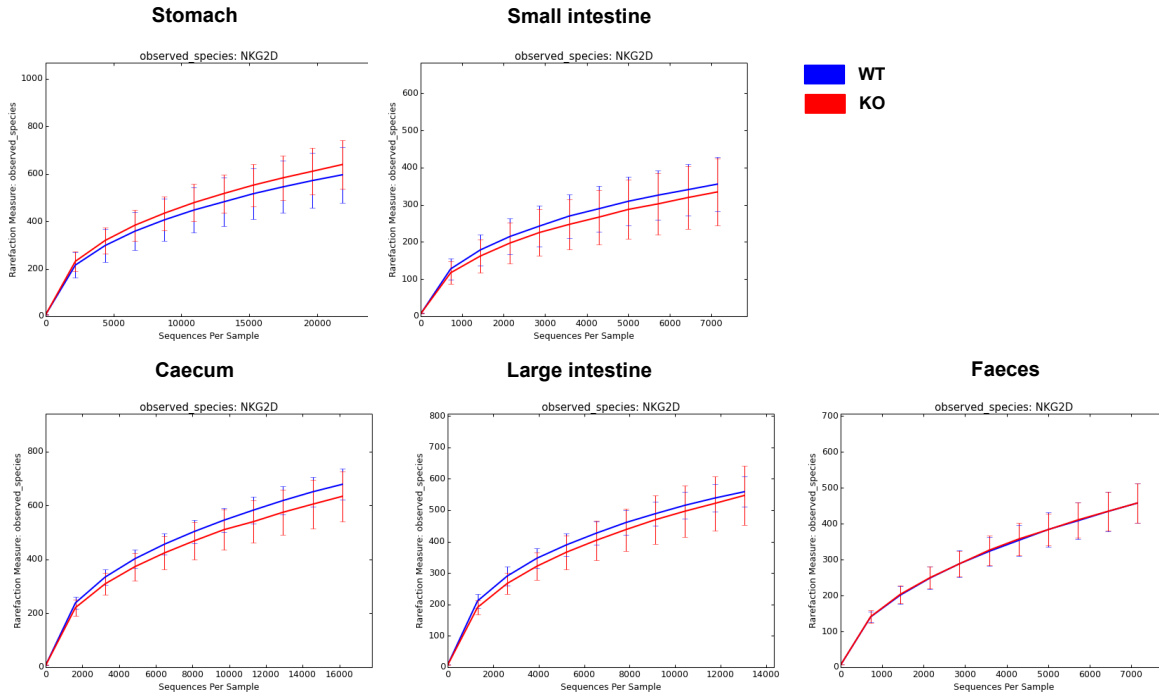


Figure 43. Comparative microbiota analyses of WT and *Klrk1*^{-/-} mice. Microbial richness (i.e. number of identifiable taxa) showed no statistically significant difference between entities in any of the organs along the GIT analyzed.

Although we could see some differences in the relative abundance of some members of the gut microbiota, those differences were not statistically significant between WT and *Klrk1*^{-/-} mice (Fig. 44).

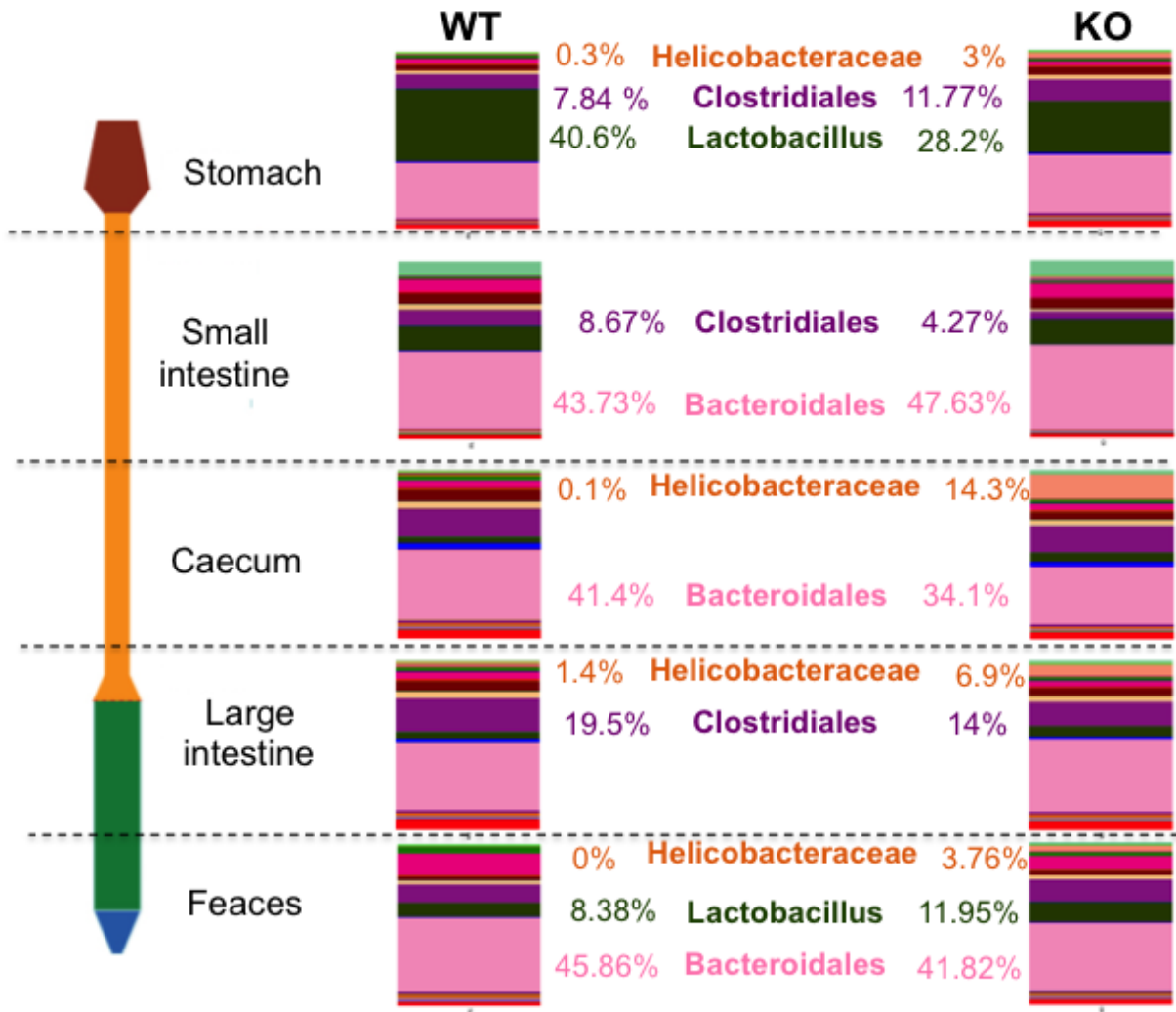


Figure 44. Diagram representing the main differences found between WT and *Klrk1*^{-/-} mice along the GIT and feces in terms of bacteria genera relative abundance. The selected groups belonged to different phylogenetic levels (genus, family, class or order), according to the lowest possible level of identification.

However, since the percentage of certain bacteria was pretty dissimilar, we suspected that there could be some associations with the genotype and that our previous analysis was too stringent to discern between the two groups. Therefore, we used the biomarker discover program LEfSe, to determine differentially abundant OTUs between WT and *Klrk1*^{-/-} mice. Several interesting candidate taxa belonging to the three main phyla presented in the gut (Bacteroidetes, Firmicutes and

Proteobacteria), and also from the phylum Tenericutes were identified to be NKG2D receptor-dependent along the GIT. This means that some species were exclusively found in one group, or presented a statistically significant difference between both genotypes analyzed. In general, members of Firmicutes and Bacteroidetes were found to be associated with WT mice, while members of the Proteobacteria and Tenericutes were related to KO mice. No differences were found in the stomach between both genotypes (Fig. 45 and Table 9). Identified taxa associated with the NKG2D genotype were very low-abundant (the so-called 'rare biosphere') (394), thus biological significance is questionable. However, in previous studies it has been shown that individual bacterial species associated with genotype that presented a relative low abundance had a biological significance (395). Whether the bacterial members associated with the NKG2D genotype identified in our study have a biological role deserve further investigation.

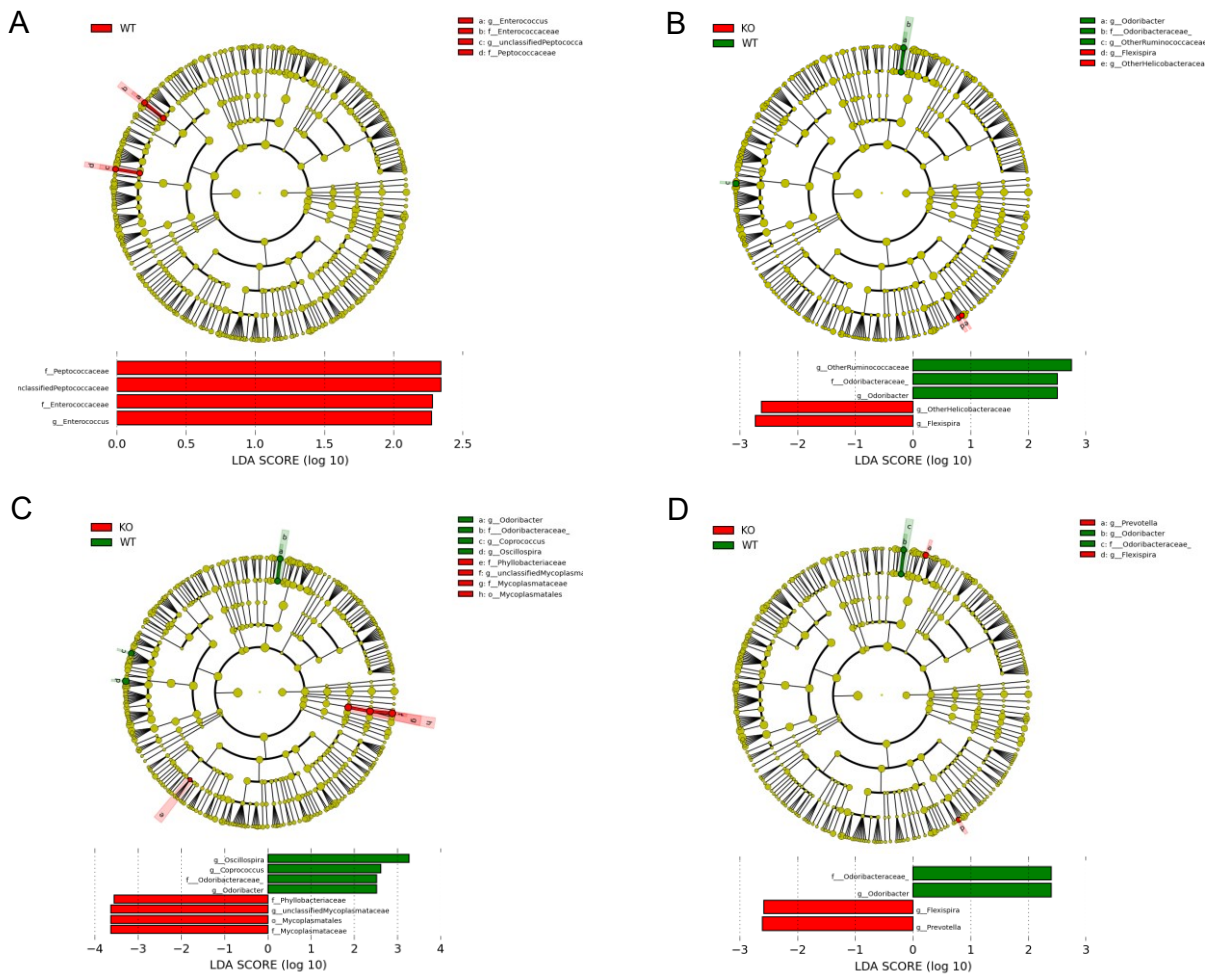


Figure 45. Cladograms representing LEfSe output showing taxonomic representation of statistically differences in microbiota composition between WT and Klrk1^{-/-} mice. LEfSe cladograms and LDA histograms represent the linear discriminant analysis (LDA) score, respectively in (A) small intestine, (B) caecum, (C) large intestine and (D) feces for differentially abundant taxa. Each circle's diameter is proportional to the taxon's abundance in the graph. In every case the LDA score >2. (o_: order; f_: family; g_: genus).

Organ	Discriminant Biomarker	Relative abundance (Mean±SD)	NKG2D genotype	LDA score	p value
Small intestine	g__Enterococcus	0.000725±0.00031	WT	2.275	0.021
	g__unclassifiedPeptococcaceae	0.000632±0.00084	WT	2.345	0.048
Caecum	g__Flexispira	0.000715±0.00096	KO	2.729	0.011
	g__OtherHelicobacteraceae	0.000124±0.00015	KO	2.623	0.033
	g__OtherRuminococcaceae	0.003058±0.00097	WT	2.752	0.039
	g__Odoribacter	0.001542±0.00102	WT	2.511	0.048
Large intestine	g__Odoribacter	0.001584±0.00090	WT	2.523	0.010
	g__Oscillospira	0.010116±0.00324	WT	3.273	0.026
	g__Coprococcus	0.001229±0.00107	WT	2.613	0.026
	g__unclassifiedMycoplasmataceae	0.013885±0.01452	KO	3.627	0.032
	f__Phyllobacteriaceae	0.00000877±0.0000013	KO	3.553	0.032
Feces	g__Odoribacter	0.000949±0.00058	WT	2.406	0.013
	g__Prevotella	0.002175±0.00101	KO	2.605	0.026
	g__Flexispira	0.000262±0.00044	KO	2.587	0.032

Table 9. Table 5. Statistically significant biomarkers across all taxonomic levels (f_:family; g_: genus) with a LDA score >2 and p-value <0.05.

V. Discussion

In the recent years, the gut microbiota has gained prominence because of its influence on host health (1). One important effect of the microbiota is its promotion of immune system maturation (2, 33-35), which begins already *in utero* (233). Disturbances in the gut microbiota may lead into GI disorders (396), such as CeD, IBD or LyG.

The pathogenesis of corpus-dominant LyG is so far unknown, but its responsiveness to antibiotic treatment suggests a bacterial trigger for disease development (83, 84, 397). In this study we subjected human stomach biopsies to comparative microbial community profiling and found that *H. pylori* infection is not the cause of LyG, which is instead characterized by overabundance of *P. acnes*. Moreover, we identified the NKG2D/NKG2DL system and the pro-inflammatory cytokine IL15 significantly induced in LyG, identifying the likely molecular determinants responsible for IEL recruitment, the typical phenotype represented by the disease. When human stomach ECs were challenged with *P. acnes* or the microbial metabolites SCFAs, NKG2DLs were induced, recapitulating the findings in human disease specimens. Interestingly, *H. pylori* omitted induction or even induced the repression of NKG2DLs. These findings have been published in an original article (281).

In our *in vitro* approach using Caco-2 colon ECs, we found that in contrast to gastric ECs, only butyrate and not propionate stimulate the induction of MICA/B ligands, both at the mRNA and protein level. This result may be linked to the fact that butyrate is the main energy source of colonocytes (221, 398). Additionally, differences in the gastric and colon microbiota may play a role in the way that SCFAs are used by GI ECs. Additionally, HCl also induced NKG2DLs on colon ECs, while it did not have any effect on gastric ECs. The expression of NKG2DLs in this case may be stress-related, since HCl is normally found in the stomach, but not in colon.

Immune recognition mediated by the activating receptor NKG2D plays an important role for the elimination of stressed cells. NKG2DLs are expressed at low levels on epithelia under healthy conditions, however their expression is greatly enhanced due to factors causing cell stress like viral infection, heat-shock or neoplastic transformation (257, 276). In CeD, duodenal epithelia challenged with gliadin (i.e. the stressor) overexpress the NKG2DL MICA. In the presence of IL15, cytotoxic CD8⁺ lymphocytes expressing the activating receptor NKG2D are then recruited to the duodenal epithelium leading to destruction of stressed cells via a cytotoxic T-cell response, which subsequently leads to villus atrophy, the hallmark lesion observed in CeD (85, 324). Recently, it has been shown that NKG2DL expression is modulated by the GI microbiota, either by direct microbe-cell interaction (e.g. via adherent *E. coli*) or by microbial products like SCFAs (323, 362). Moreover, manipulation of the microbiota with antibiotics either lead to increased or decreased NKG2DL expression in mice, dependent on the microbial spectra covered by the substance (361).

In this study, we have shown that the NKG2D system is not just induced because of cell stress, but also is constitutively expressed along the GIT. However, expression levels are variable, as shown in the light of different GI disorders. For example, although LyG and LyC share several features, including infiltration of lymphocytes within the epithelium (328), the NKG2D system is only up-regulated in LyG, but not in LyC. These differences may be due to the different microbiota found in the stomach and the colon. However, a microbiota analysis in LyC samples should be performed to extract some conclusions in this regard. Similarly, we found differences within the two IBD entities: CD and UC. In UC we got a similar pattern expression to that found in LyC, with no changes in NKG2D expression and MICB, and a downregulation of MICA and IL15 compared to healthy controls. However, in CD samples obtained from ileum all the NKG2D system players, including NKG2D receptor, MICA and MICB ligands and IL15 were upregulated compared to healthy controls. This outcome could be explained taking into account that CD and UC represent two heterogeneous pathologies, although they share some clinical and pathological features. For example, on the genetic level, they share 110 out of 163 loci, many of which cluster in

pathways relevant to innate and adaptive immune system (399). This fact is reflected in the similarities observed by the specialists between both diseases and also in the difficulties to make a definitive diagnosis (36). However, studies carried out in identical twins have confirmed that the environment has a stronger influence compared to genetic factors, since concordance rate is just around 50% for CD and 10% for UC patients (400). Among the environmental factors, smoking has been related to a better prognosis for UC cases, but not for CD. Additionally, diet, drugs (including antibiotics and nonsteroidal anti-inflammatory drugs), stress and infection have an implication in the pathogenesis of IBD. Although the exact mechanisms involved in the initiation of the disease are unknowns, all of these factors contribute in altering the mucosal barrier integrity, the immune responses and the gut microbiota which in the end trigger an inflammatory response (401). In regard of the immune response triggered, both entities share enhanced immune cell recruitment into the gut characterized by the release of pro-inflammatory cytokines. However, while CD presents a T_{H1} and T_{H17} -mediated process, UC trigger a T_{H2} response. Therefore, therapy for both diseases may be also different (401). These differences in the T cell response triggered in both pathologies might have some relation with the variance we appreciate in regard of NKG2D system activation, since it is known that in humans just certain subsets of $CD4^+$ T cells are able to express the NKG2D receptor (402). Additionally, differences in the gut microbiota found in ileum and colon may also contribute to the distinct NKG2D system outcomes. In fact, within CD, ileal and colonic forms of the disease present distinct microbiome patterns, being those presenting ileal CD richer in *Escherichia*, whereas colonic CD patients presented higher levels of *Faecalibacterium*, Clostridiales and Ruminococcaceae (403). In our study, differences in NKG2D system activation in CD and UC may be location-dependent, considering that our CD samples correspond to ileum and UC samples to colon. It has also been reported in pediatric patients that activation of the NKG2D system differs in patients with active or quiescent IBD (331). Therefore, status of the disease may also be considered when analyzing NKG2D system activation. In the same study, the authors found a similar activation pattern in both CD and UC, which may be due the relative absence of many environmental variables in pediatric

patients. Thus, some environmental factors could have an implication in the different NKG2D system activation seen in our study.

Historically, the stomach has been viewed as a quasi-sterile environment due to its acidity and that only bacteria with specific abilities (e.g. *H. pylori* with its urease production) are able to colonize this habitat. However, it has now become clear that the stomach microbiota is quite diverse and that it contributes also to the development of various gastric pathologies (404-407). Of note *P. acnes*, a classical skin bacterium, has been recently identified as a part of the stomach microbiota (406, 408-410). By use of culture-dependent and -independent techniques, *P. acnes* was found to be a member of the stomach microbiota in healthy individuals, representing more than 20% of microbes in certain cases (410). Interestingly, *P. acnes* was found only in mucosal specimens and not in the gastric fluid, indicating the preferred niche of this bacterium (411). Whether specific pathotypes of *P. acnes* contribute to LyG development or if just the increase of *P. acnes* over a certain level is sufficient to induce NKG2DL overexpression is so far not known and should be a focus for future investigations. Nevertheless, *P. acnes* is able to resist acid-stress and it displays a variety of virulence mechanisms, which could contribute to inflammation, epithelial cell stress and ultimately to NKG2D/NKG2DL activation (178, 187, 412-416).

Interestingly, in HpG, a condition certainly favoring cell-stress of gastric epithelia due to its prominent inflammation, neither NKG2D nor MICA or IL15 were found induced. In contrast, we noted only a slight induction of MICB in human stomach biopsies. Nevertheless, *H. pylori* failed to induce or even repressed the mRNA and extracellular MICA/B protein expression in challenge experiments using gastric EC lines. Importantly, the NKG2D/NKG2DL system together with IL15 are important for tumor-surveillance, necessary for elimination of neoplastic cells (321). The system has been, therefore, investigated as a potent target for cancer immunotherapy in various studies (417-421). From our data it could be speculated that *H. pylori* omits NKG2D/NKG2DL system activation and this might eventually favor stomach cancer development as a long-term sequel of *H. pylori* infection due to an impaired innate

antitumor immunity. The down-regulation of *il15* by *H. pylori* in HpG has also been reported recently (422). Thus, investigating the NKG2D/NKG2DL system in the context of HpG and gastric adenocarcinoma development should be an important research aim in future.

Additionally, we have shown for first time the effect that the depletion of the NKG2D receptor elicits on the host immune system and the gut microbiota. Absence of the NKG2D receptor in mice does not cause significant differences in the immune cell populations tested along the GIT, both in the lamina propria or intraepithelial compartment under physiological or inflammatory conditions. This fact reveals a normal development of immune cells despite the absence of the NKG2D receptor. Only in the case of CD4⁺ T cells found in the small intestine, the frequencies were higher in WT compared to *Klrk1*^{-/-} mice under physiological conditions. This effect has been previously reported in viral infections, where small intestine resulted more sensitive to the infection in different simian immunodeficiency virus models and humans (423, 424). Whether NKG2D depletion is related to viral infection susceptibility is a subject that deserves further investigation.

The GIT represents the largest compartment of the human immune system. In the last years the influence of diet and gut bacteria on host physiology and pathology has been intensively studied (28). Additionally, there are enormous topographical differences in the representation of adaptive and innate immune cells along the GIT. We investigated the distribution of different immune cell populations in the lamina propria and the intraepithelial compartment along the GIT of mice. These basic investigations are important to understand the different representations as well as functionality of the NKG2D system in human and mice. For example, while in humans CD8⁺ T cells are more abundant in the upper (stomach) compared to the lower GIT (390), we have seen in mice that CD8⁺ T cells are found in higher frequencies in the lower GIT compared to the upper GIT, both in the lamina propria and intraepithelial compartments. CD11b represents a cellular antigen that is typically found in leukocytes, including macrophages, monocytes, granulocytes, NK cells and certain

subsets of DCs. It mediates inflammation by regulating leukocyte adhesion and migration. Thus, it has been implicated in several immune processes such as phagocytosis, cell-mediated cytotoxicity, chemotaxis and cellular activation (425). In our study we found that CD11b⁺ cells are more abundant in the upper GIT compared to the lower GIT, which is in accordance with other reports (reviewed by Mowat, A.M. et al (28)). Nevertheless, macrophages are found in higher frequencies in the colon compared to the small intestine (426). Conversely, B cells from the lamina propria were increased in the caecum and colon compared to the stomach. However B cells found in the intraepithelial compartment were more frequent in the small intestine. This fact may be directly related to the production of IgA, which is at the same time depending on the resident microbiota (427).

It has been shown that TLR agonists are able to induce the expression of NKG2DLs in epithelial and immune cells (363, 428). For example, Hamerman, J et al., demonstrated that NK cells and infected macrophages communicate through a Rae1-NKG2D interaction (363). In another study, it was shown that the over-expression of ULBP1 and ULBP2 on mDCs aided NK cell proliferation through an mDC-NK cell interaction in the presence of IL2, reflecting the importance of NKG2DLs in mediating NK cell activation by mDCs (429). TLR-NKG2D interaction has been also reported on IECs. TLR3 agonists were shown to induce the expression of Rae1 on IECs and therefore to interact with CD8 α IELs aided by IL15 derived from TLR3-activated IECs (304). This fact suggests TLR signaling may contribute to the abnormal expression of NKG2DLs, inducing tissue injury through the activation of the NKG2D system. Although *a priori* we were not able to identify differences in the expression of NKG2D ligands, IL15 or TLRs (2, 4 and 5) between WT and *Klrk1*^{-/-} mice; we found several and interesting positive correlations between players of the NKG2D system and TLRs along the GIT that, interestingly were different in WT and *Klrk1*^{-/-} mice and location-dependent. To note, TLR5, which recognize flagellin, presented positive correlations exclusively with Rae1, but not with Mult1 along the GIT in WT mice; whereas in KO it correlated not only with Rae1, but also with Mult1. This finding suggests that Mult1 is susceptible to microbiota changes due the absence of NKG2D

receptor. This is in controversy with a previous study, where it was reported that Rae1 but not Mult1 could be regulated by the gut microbiota (361). Interestingly, it has been recently reported that in mice TLR5 avoided commensal bacteria (mainly belonging to the phylum Firmicutes) to penetrate the mucosal barrier by production of anti-flagellin IgA antibodies, which immobilize bacteria and downregulate production of flagella, preventing the potential harmful motility (430). In our study we found members of the Firmicutes associated with WT genotype, while members of the Proteobacteria were related to KO genotype. Whether TLR5 correlation with Rae1 or Mult1 in WT and KO, respectively is directly associated with the predominance of Firmicutes or Proteobacteria should be addressed in future. To date, just few studies have assessed differences in the pattern of PRRs along the GIT. However, it is known that TLR2 expression is higher in proximal compared to distal colon (431), while TLR4 is expressed at higher levels in colon compared to small intestine (431, 432). Although little is known about the meaning of these differences, they might also be related to gut microbiota composition.

Therefore, we next assessed the microbiota composition along the GIT in WT and *Klrk1*^{-/-} mice and found several very low-abundant taxa associated with the NKG2D genotype. Of note, these taxa were also location-dependent. Members of the Firmicutes and Bacteroidetes were in general associated with the WT genotype, which resembles the results obtained in the human microbiota analysis for healthy stomach corpus biopsies (281). On the contrary, increased relative abundance of taxa belonging to Proteobacteria and Tenericutes were linked with NKG2D receptor ablation. The expansion of phyla Proteobacteria and Tenericutes has been associated with different pathologies, such as colorectal adenomas (433). In the *IL10*^{-/-} mouse, used to model human IBD, it was found that after four weeks of colonization of formerly GF mice with an SPF intestinal microbiota, *IL10*^{-/-} mice present a moderate inflammation that was accompanied by a decrease in diversity and richness of intestinal microbiota. Interestingly, the phyla Proteobacteria and Tenericutes were increased when comparing to one-week colonization; while Bacteroidetes and Firmicutes were depleted over time (434), which resembles

changes observed in human IBD patients. These findings suggest that inflammation induce the loss of diversity in favor of Proteobacteria and Tenericutes. Moreover, it has been also reported that in fecal samples from colonic, but not ileal CD patients, Tenericutes have been found to be significantly elevated (435).

In our study, mice used for microbiota analysis were adults between 8 and 24 weeks. One explanation for the slight differences found between genotypes may be due the cohousing between WT and KO for such a long period, in which coprophagy may have homogenize the gut microbiota and weaken the effects due to genotype differences (436). However, this fact gives us at the same time a strong argument that the findings are actually associated to differences in NKG2D expression. In a similar approach using younger mice (< 8weeks), we could probably target a critical developmental window (437), and therefore it would be possible to discern special features in the microbiota related to NKG2D genotype. The so-called 'rare biosphere', used for low-abundance microbial populations (generally <0.1% of total community relative abundance(438)), has been found to play important ecological roles, serving as reservoirs of genetic and functional diversity (439). However, little is known about the role these species have in the different environments. Understanding the role that low-abundant taxa found to be associated with the NKG2D genotype play in the gut and how they can contribute to health or the development of GI disorders is a topic that should be addressed in future.

VI. Conclusions

Our study identifies the NKG2D/NKG2DL system and the pro-inflammatory cytokine IL15 as likely molecular players in corpus-dominant LyG. Thus similarities between LyG and the paradigm disease of intraepithelial lymphocytosis, CeD, exist also on the molecular level. The identified *P. acnes* increase in LyG possibly contributes to pathogenesis evidenced also by the *in-vitro* cell challenge experiments. Identifying

the causes leading to *P. acnes* overgrowth or which additional factors contribute to NKG2D/NKG2DL and IL15 activation should initiate prospective studies investigating LyG.

Additionally, we have seen that in HpG the NKG2D system is not induced, although the gastric epithelium is for sure under cell stress. Moreover, *in vitro* assays demonstrate that *H. pylori* is not able to induce NKG2DLs or the pro-inflammatory cytokine IL15, which would facilitate the colonization and progression of cellular damage and further ulcers or even gastric cancer. Therefore, studying the mechanism behind this immune evasion would be worth it to understand the role that *H. pylori* plays in gastric cancer and also to find a possible non-antibiotic treatment to prevent the harmful effects of *H. pylori* infection.

In other GI paradigmatic diseases we found a similar picture, with differences between the two entities including in IBD. While in ileal CD samples we detect an upregulation of the NKG2D system, colon UC samples showed no activation. This outcome could be location-dependent, and related to microbiota composition. By *in vitro* culture using colon EC lines, we also saw differences in the effect that SCFAs have in those cells comparing to gastric EC lines. This could mean that ECs may be more sensitive to specific SCFAs

We finally showed in a mouse model lacking the NKG2D receptor, that the NKG2D system influences the shaping of the gut microbiota, as demonstrated by NKG2D system/TLRs correlation and microbiota analysis. We saw that mice absent of the NKG2D receptor provoked slight differences in the microbiota, which resemble that found in dysbiotic diseases, such as IBD.

To sum up, we can conclude that the NKG2D system modulates host- microbial interactions under healthy and GI pathological conditions. NKG2D system was found to be up- or downmodulated depending on the inflammatory GI disease analyzed, probably due to the location within the GI tract and the microbiota composition found

along the GIT. Moreover, dysbiosis found in the several GI pathologies analyzed may be responsible for a different outcome in the NKG2D system expression. Therefore, targeting the NKG2D system could be useful in the treatment of dysbiotic GI diseases.

VII. Bibliography

1. Sommer F, Backhed F. The gut microbiota--masters of host development and physiology. *Nat Rev Microbiol*. 2013;11(4):227-38.
2. Maynard CL, Elson CO, Hatton RD, Weaver CT. Reciprocal interactions of the intestinal microbiota and immune system. *Nature*. 2012;489(7415):231-41.
3. Helander HF, Fandriks L. Surface area of the digestive tract - revisited. *Scand J Gastroenterol*. 2014;49(6):681-9.
4. Turner JR. Intestinal mucosal barrier function in health and disease. *Nat Rev Immunol*. 2009;9(11):799-809.
5. Donaldson GP, Lee SM, Mazmanian SK. Gut biogeography of the bacterial microbiota. *Nat Rev Microbiol*. 2016;14(1):20-32.
6. Eckburg PB, Bik EM, Bernstein CN, Purdom E, Dethlefsen L, Sargent M, et al. Diversity of the human intestinal microbial flora. *Science*. 2005;308(5728):1635-8.
7. Mantis NJ, Rol N, Corthesy B. Secretory IgA's complex roles in immunity and mucosal homeostasis in the gut. *Mucosal immunology*. 2011;4(6):603-11.
8. Petersson J, Schreiber O, Hansson GC, Gendler SJ, Velcich A, Lundberg JO, et al. Importance and regulation of the colonic mucus barrier in a mouse model of colitis. *Am J Physiol Gastrointest Liver Physiol*. 2011;300(2):G327-33.
9. Hatayama H, Iwashita J, Kuwajima A, Abe T. The short chain fatty acid, butyrate, stimulates MUC2 mucin production in the human colon cancer cell line, LS174T. *Biochem Biophys Res Commun*. 2007;356(3):599-603.
10. Johansson MEV, Larsson JMH, Hansson GC. The two mucus layers of colon are organized by the MUC2 mucin, whereas the outer layer is a legislator of host-microbial interactions. *Proceedings of the National Academy of Sciences of the United States of America*. 2011;108(Suppl 1):4659-65.
11. Huang JY, Lee SM, Mazmanian SK. The human commensal *Bacteroides fragilis* binds intestinal mucin. *Anaerobe*. 2011;17(4):137-41.
12. Vaishnava S, Behrendt CL, Ismail AS, Eckmann L, Hooper LV. Paneth cells directly sense gut commensals and maintain homeostasis at the intestinal host-microbial interface. *Proc Natl Acad Sci U S A*. 2008;105(52):20858-63.
13. Peterson DA, McNulty NP, Guruge JL, Gordon JI. IgA response to symbiotic bacteria as a mediator of gut homeostasis. *Cell host & microbe*. 2007;2(5):328-39.
14. Fukuda S, Toh H, Hase K, Oshima K, Nakanishi Y, Yoshimura K, et al. Bifidobacteria can protect from enteropathogenic infection through production of acetate. *Nature*. 2011;469(7331):543-7.
15. Jass JR, Walsh MD. Altered mucin expression in the gastrointestinal tract: a review. *J Cell Mol Med*. 2001;5(3):327-51.
16. Kyo K, Parkes M, Takei Y, Nishimori H, Vyas P, Satsangi J, et al. Association of ulcerative colitis with rare VNTR alleles of the human intestinal mucin gene, MUC3. *Hum Mol Genet*. 1999;8(2):307-11.

17. Newton JL, Jordan N, Oliver L, Strugala V, Pearson J, James OF, et al. *Helicobacter pylori* in vivo causes structural changes in the adherent gastric mucus layer but barrier thickness is not compromised. *Gut*. 1998;43(4):470-5.
18. Byrd JC, Yan P, Sternberg L, Yunker CK, Scheiman JM, Bresalier RS. Aberrant expression of gland-type gastric mucin in the surface epithelium of *Helicobacter pylori*-infected patients. *Gastroenterology*. 1997;113(2):455-64.
19. Byrd JC, Yunker CK, Xu QS, Sternberg LR, Bresalier RS. Inhibition of gastric mucin synthesis by *Helicobacter pylori*. *Gastroenterology*. 2000;118(6):1072-9.
20. Reis CA, David L, Correa P, Carneiro F, de Bolos C, Garcia E, et al. Intestinal metaplasia of human stomach displays distinct patterns of mucin (MUC1, MUC2, MUC5AC, and MUC6) expression. *Cancer Res*. 1999;59(5):1003-7.
21. Lopez-Ferrer A, de Bolos C, Barranco C, Garrido M, Isern J, Carlstedt I, et al. Role of fucosyltransferases in the association between apomucin and Lewis antigen expression in normal and malignant gastric epithelium. *Gut*. 2000;47(3):349-56.
22. Goto Y, Kiyono H. Epithelial barrier: an interface for the cross-communication between gut flora and immune system. *Immunol Rev*. 2012;245(1):147-63.
23. Yu LC, Wang JT, Wei SC, Ni YH. Host-microbial interactions and regulation of intestinal epithelial barrier function: From physiology to pathology. *World J Gastrointest Pathophysiol*. 2012;3(1):27-43.
24. Eckmann L, Jung HC, Schurer-Maly C, Panja A, Morzycka-Wroblewska E, Kagnoff MF. Differential cytokine expression by human intestinal epithelial cell lines: regulated expression of interleukin 8. *Gastroenterology*. 1993;105(6):1689-97.
25. Kuwano Y, Tominaga K, Kawahara T, Sasaki H, Takeo K, Nishida K, et al. Tumor necrosis factor alpha activates transcription of the NADPH oxidase organizer 1 (NOXO1) gene and upregulates superoxide production in colon epithelial cells. *Free Radic Biol Med*. 2008;45(12):1642-52.
26. Kuwano Y, Kawahara T, Yamamoto H, Teshima-Kondo S, Tominaga K, Masuda K, et al. Interferon-gamma activates transcription of NADPH oxidase 1 gene and upregulates production of superoxide anion by human large intestinal epithelial cells. *Am J Physiol Cell Physiol*. 2006;290(2):C433-43.
27. Kawahara T, Kuwano Y, Teshima-Kondo S, Takeya R, Sumimoto H, Kishi K, et al. Role of nicotinamide adenine dinucleotide phosphate oxidase 1 in oxidative burst response to Toll-like receptor 5 signaling in large intestinal epithelial cells. *Journal of immunology*. 2004;172(5):3051-8.
28. Mowat AM, Agace WW. Regional specialization within the intestinal immune system. *Nat Rev Immunol*. 2014;14(10):667-85.
29. Eberl G. Inducible lymphoid tissues in the adult gut: recapitulation of a fetal developmental pathway? *Nat Rev Immunol*. 2005;5(5):413-20.
30. Cebra JJ, Periwal SB, Lee G, Lee F, Shroff KE. Development and maintenance of the gut-associated lymphoid tissue (GALT): the roles of enteric bacteria and viruses. *Dev Immunol*. 1998;6(1-2):13-8.
31. Kelly D, Mulder IE. Microbiome and immunological interactions. *Nutr Rev*. 2012;70 Suppl 1:S18-30.
32. Round JL, Mazmanian SK. The gut microbiota shapes intestinal immune responses during health and disease. *Nat Rev Immunol*. 2009;9(5):313-23.

33. Hooper LV, Littman DR, Macpherson AJ. Interactions between the microbiota and the immune system. *Science*. 2012;336(6086):1268-73.
34. Duerkop BA, Vaishnava S, Hooper LV. Immune responses to the microbiota at the intestinal mucosal surface. *Immunity*. 2009;31(3):368-76.
35. Slack E, Hapfelmeier S, Stecher B, Velykoredko Y, Stoel M, Lawson MA, et al. Innate and adaptive immunity cooperate flexibly to maintain host-microbiota mutualism. *Science*. 2009;325(5940):617-20.
36. Jostins L, Ripke S, Weersma RK, Duerr RH, McGovern DP, Hui KY, et al. Host-microbe interactions have shaped the genetic architecture of inflammatory bowel disease. *Nature*. 2012;491(7422):119-24.
37. Xavier RJ, Podolsky DK. Unravelling the pathogenesis of inflammatory bowel disease. *Nature*. 2007;448(7152):427-34.
38. Lees CW, Barrett JC, Parkes M, Satsangi J. New IBD genetics: common pathways with other diseases. *Gut*. 2011;60(12):1739-53.
39. Manichanh C, Borruel N, Casellas F, Guarner F. The gut microbiota in IBD. *Nat Rev Gastroenterol Hepatol*. 2012;9(10):599-608.
40. Gophna U, Sommerfeld K, Gophna S, Doolittle WF, Veldhuyzen van Zanten SJ. Differences between tissue-associated intestinal microfloras of patients with Crohn's disease and ulcerative colitis. *J Clin Microbiol*. 2006;44(11):4136-41.
41. Walker AW, Sanderson JD, Churcher C, Parkes GC, Hudspith BN, Rayment N, et al. High-throughput clone library analysis of the mucosa-associated microbiota reveals dysbiosis and differences between inflamed and non-inflamed regions of the intestine in inflammatory bowel disease. *BMC microbiology*. 2011;11:7.
42. Gevers D, Kugathasan S, Denson LA, Vazquez-Baeza Y, Van Treuren W, Ren B, et al. The treatment-naive microbiome in new-onset Crohn's disease. *Cell host & microbe*. 2014;15(3):382-92.
43. Petersen C, Round JL. Defining dysbiosis and its influence on host immunity and disease. *Cellular microbiology*. 2014;16(7):1024-33.
44. Kostic AD, Xavier RJ, Gevers D. The microbiome in inflammatory bowel disease: current status and the future ahead. *Gastroenterology*. 2014;146(6):1489-99.
45. Manichanh C, Rigottier-Gois L, Bonnaud E, Gloux K, Pelletier E, Frangeul L, et al. Reduced diversity of faecal microbiota in Crohn's disease revealed by a metagenomic approach. *Gut*. 2006;55(2):205-11.
46. Gisbert JP, Marin AC, Chaparro M. The Risk of Relapse after Anti-TNF Discontinuation in Inflammatory Bowel Disease: Systematic Review and Meta-Analysis. *Am J Gastroenterol*. 2016;111(5):632-47.
47. Green PH, Cellier C. Celiac disease. *The New England journal of medicine*. 2007;357(17):1731-43.
48. Kaukinen K, Partanen J, Maki M, Collin P. HLA-DQ typing in the diagnosis of celiac disease. *Am J Gastroenterol*. 2002;97(3):695-9.
49. Rossi M, Schwartz KB. Editorial: Celiac disease and intestinal bacteria: not only gluten? *J Leukoc Biol*. 2010;87(5):749-51.
50. Verdu EF, Galipeau HJ, Jabri B. Novel players in coeliac disease pathogenesis: role of the gut microbiota. *Nat Rev Gastroenterol Hepatol*. 2015.

51. Collado MC, Calabuig M, Sanz Y. Differences between the fecal microbiota of coeliac infants and healthy controls. *Curr Issues Intest Microbiol.* 2007;8(1):9-14.
52. Collado MC, Donat E, Ribes-Koninckx C, Calabuig M, Sanz Y. Imbalances in faecal and duodenal Bifidobacterium species composition in active and non-active coeliac disease. *BMC microbiology.* 2008;8:232.
53. Collado MC, Donat E, Ribes-Koninckx C, Calabuig M, Sanz Y. Specific duodenal and faecal bacterial groups associated with paediatric coeliac disease. *J Clin Pathol.* 2009;62(3):264-9.
54. Nadal I, Donat E, Ribes-Koninckx C, Calabuig M, Sanz Y. Imbalance in the composition of the duodenal microbiota of children with coeliac disease. *J Med Microbiol.* 2007;56(Pt 12):1669-74.
55. Sanz Y, Sanchez E, Marzotto M, Calabuig M, Torriani S, Dellaglio F. Differences in faecal bacterial communities in coeliac and healthy children as detected by PCR and denaturing gradient gel electrophoresis. *FEMS immunology and medical microbiology.* 2007;51(3):562-8.
56. De Palma G, Nadal I, Medina M, Donat E, Ribes-Koninckx C, Calabuig M, et al. Intestinal dysbiosis and reduced immunoglobulin-coated bacteria associated with coeliac disease in children. *BMC microbiology.* 2010;10:63.
57. Sanchez E, Donat E, Ribes-Koninckx C, Calabuig M, Sanz Y. Intestinal Bacteroides species associated with coeliac disease. *J Clin Pathol.* 2010;63(12):1105-11.
58. Sanchez E, Ribes-Koninckx C, Calabuig M, Sanz Y. Intestinal Staphylococcus spp. and virulent features associated with coeliac disease. *J Clin Pathol.* 2012;65(9):830-4.
59. Sanchez E, Donat E, Ribes-Koninckx C, Fernandez-Murga ML, Sanz Y. Duodenal-mucosal bacteria associated with celiac disease in children. *Appl Environ Microbiol.* 2013;79(18):5472-9.
60. Schippa S, Iebba V, Barbato M, Di Nardo G, Totino V, Checchi MP, et al. A distinctive 'microbial signature' in celiac pediatric patients. *BMC microbiology.* 2010;10:175.
61. Nistal E, Caminero A, Vivas S, Ruiz de Morales JM, Saenz de Miera LE, Rodriguez-Aparicio LB, et al. Differences in faecal bacteria populations and faecal bacteria metabolism in healthy adults and celiac disease patients. *Biochimie.* 2012;94(8):1724-9.
62. Wacklin P, Kaukinen K, Tuovinen E, Collin P, Lindfors K, Partanen J, et al. The duodenal microbiota composition of adult celiac disease patients is associated with the clinical manifestation of the disease. *Inflamm Bowel Dis.* 2013;19(5):934-41.
63. Wacklin P, Laurikka P, Lindfors K, Collin P, Salmi T, Lahdeaho ML, et al. Altered duodenal microbiota composition in celiac disease patients suffering from persistent symptoms on a long-term gluten-free diet. *Am J Gastroenterol.* 2014;109(12):1933-41.
64. Portal-Celhay C, Perez-Perez GI. Immune responses to Helicobacter pylori colonization: mechanisms and clinical outcomes. *Clin Sci (Lond).* 2006;110(3):305-14.

65. Sugimoto M, Yamaoka Y. Virulence factor genotypes of *Helicobacter pylori* affect cure rates of eradication therapy. *Arch Immunol Ther Exp (Warsz)*. 2009;57(1):45-56.
66. Sugano K, Tack J, Kuipers EJ, Graham DY, El-Omar EM, Miura S, et al. Kyoto global consensus report on *Helicobacter pylori* gastritis. *Gut*. 2015;64(9):1353-67.
67. Parsonnet J, Isaacson PG. Bacterial infection and MALT lymphoma. *The New England journal of medicine*. 2004;350(3):213-5.
68. Uemura N, Okamoto S, Yamamoto S, Matsumura N, Yamaguchi S, Yamakido M, et al. *Helicobacter pylori* infection and the development of gastric cancer. *The New England journal of medicine*. 2001;345(11):784-9.
69. Blaser MJ, Atherton JC. *Helicobacter pylori* persistence: biology and disease. *J Clin Invest*. 2004;113(3):321-33.
70. O'Connor A, Gisbert JP, O'Morain C, Ladas S. Treatment of *Helicobacter pylori* Infection 2015. *Helicobacter*. 2015;20 Suppl 1:54-61.
71. McNicholl AG, Gisbert JP. Ensuring the highest eradication rates in *H. pylori*: the case of non-bismuth quadruple concomitant therapy. *Eur J Intern Med*. 2016.
72. Molina-Infante J, Romano M, Fernandez-Bermejo M, Federico A, Gravina AG, Pozzati L, et al. Optimized nonbismuth quadruple therapies cure most patients with *Helicobacter pylori* infection in populations with high rates of antibiotic resistance. *Gastroenterology*. 2013;145(1):121-8 e1.
73. Molina-Infante J, Gisbert JP. Optimizing clarithromycin-containing therapy for *Helicobacter pylori* in the era of antibiotic resistance. *World J Gastroenterol*. 2014;20(30):10338-47.
74. Garza-Gonzalez E, Perez-Perez GI, Maldonado-Garza HJ, Bosques-Padilla FJ. A review of *Helicobacter pylori* diagnosis, treatment, and methods to detect eradication. *World J Gastroenterol*. 2014;20(6):1438-49.
75. Malfertheiner P, Selgrad M, Bornschein J. *Helicobacter pylori*: clinical management. *Curr Opin Gastroenterol*. 2012;28(6):608-14.
76. Wang ZH, Gao QY, Fang JY. Meta-analysis of the efficacy and safety of Lactobacillus-containing and Bifidobacterium-containing probiotic compound preparation in *Helicobacter pylori* eradication therapy. *J Clin Gastroenterol*. 2013;47(1):25-32.
77. Ahmad K, Fatemeh F, Mehri N, Maryam S. Probiotics for the treatment of pediatric *Helicobacter pylori* infection: a randomized double blind clinical trial. *Iran J Pediatr*. 2013;23(1):79-84.
78. Vakiani E, Yantiss RK. Lymphocytic Gastritis: Clinicopathologic Features, Etiologic Associations, and Pathogenesis. *Pathology Case Reviews*. 2008;13(5):167-71.
79. Lynch DA, Sobala GM, Dixon MF, Gledhill A, Jackson P, Crabtree JE, et al. Lymphocytic gastritis and associated small bowel disease: a diffuse lymphocytic gastroenteropathy? *J Clin Pathol*. 1995;48(10):939-45.
80. Oberhuber G, Bodingbauer M, Mosberger I, Stolte M, Vogelsang H. High proportion of granzyme B-positive (activated) intraepithelial and lamina propria lymphocytes in lymphocytic gastritis. *Am J Surg Pathol*. 1998;22(4):450-8.
81. Wu TT, Hamilton SR. Lymphocytic gastritis: association with etiology and topology. *Am J Surg Pathol*. 1999;23(2):153-8.

82. Nielsen JA, Roberts CA, Lager DJ, Putcha RV, Jain R, Lewin M. Lymphocytic Gastritis is not Associated with active *Helicobacter pylori* Infection. *Helicobacter*. 2014.
83. Muller H, Volkholz H, Stolte M. Healing of lymphocytic gastritis by eradication of *Helicobacter pylori*. *Digestion*. 2001;63(1):14-9.
84. Hayat M, Arora DS, Dixon MF, Clark B, O'Mahony S. Effects of *Helicobacter pylori* eradication on the natural history of lymphocytic gastritis. *Gut*. 1999;45(4):495-8.
85. Meresse B, Chen Z, Ciszewski C, Tretiakova M, Bhagat G, Krausz TN, et al. Coordinated induction by IL15 of a TCR-independent NKG2D signaling pathway converts CTL into lymphokine-activated killer cells in celiac disease. *Immunity*. 2004;21(3):357-66.
86. D'Argenio V, Salvatore F. The role of the gut microbiome in the healthy adult status. *Clin Chim Acta*. 2015;451(Pt A):97-102.
87. Sender R, Fuchs S, Milo R. Are We Really Vastly Outnumbered? Revisiting the Ratio of Bacterial to Host Cells in Humans. *Cell*. 2016;164(3):337-40.
88. Ley RE, Peterson DA, Gordon JI. Ecological and evolutionary forces shaping microbial diversity in the human intestine. *Cell*. 2006;124(4):837-48.
89. Turnbaugh PJ, Ley RE, Mahowald MA, Magrini V, Mardis ER, Gordon JI. An obesity-associated gut microbiome with increased capacity for energy harvest. *Nature*. 2006;444(7122):1027-31.
90. Schippa S, Conte MP. Dysbiotic events in gut microbiota: impact on human health. *Nutrients*. 2014;6(12):5786-805.
91. Qin J, Li R, Raes J, Arumugam M, Burgdorf KS, Manichanh C, et al. A human gut microbial gene catalogue established by metagenomic sequencing. *Nature*. 2010;464(7285):59-65.
92. Frank DN, St Amand AL, Feldman RA, Boedeker EC, Harpaz N, Pace NR. Molecular-phylogenetic characterization of microbial community imbalances in human inflammatory bowel diseases. *Proc Natl Acad Sci U S A*. 2007;104(34):13780-5.
93. Ley RE, Turnbaugh PJ, Klein S, Gordon JI. Microbial ecology: human gut microbes associated with obesity. *Nature*. 2006;444(7122):1022-3.
94. Spor A, Koren O, Ley R. Unravelling the effects of the environment and host genotype on the gut microbiome. *Nat Rev Microbiol*. 2011;9(4):279-90.
95. Martin HM, Campbell BJ, Hart CA, Mpofu C, Nayar M, Singh R, et al. Enhanced *Escherichia coli* adherence and invasion in Crohn's disease and colon cancer. *Gastroenterology*. 2004;127(1):80-93.
96. Eckburg PB, Relman DA. The role of microbes in Crohn's disease. *Clin Infect Dis*. 2007;44(2):256-62.
97. Ley RE, Backhed F, Turnbaugh P, Lozupone CA, Knight RD, Gordon JI. Obesity alters gut microbial ecology. *Proc Natl Acad Sci U S A*. 2005;102(31):11070-5.
98. De Filippo C, Cavalieri D, Di Paola M, Ramazzotti M, Poullet JB, Massart S, et al. Impact of diet in shaping gut microbiota revealed by a comparative study in children from Europe and rural Africa. *Proc Natl Acad Sci U S A*. 2010;107(33):14691-6.

99. Marcos A, Nova E, Montero A. Changes in the immune system are conditioned by nutrition. *Eur J Clin Nutr.* 2003;57 Suppl 1:S66-9.
100. Kau AL, Ahern PP, Griffin NW, Goodman AL, Gordon JI. Human nutrition, the gut microbiome and the immune system. *Nature.* 2011;474(7351):327-36.
101. Gordon JI, Dewey KG, Mills DA, Medzhitov RM. The human gut microbiota and undernutrition. *Sci Transl Med.* 2012;4(137):137ps12.
102. Kabat AM, Srinivasan N, Maloy KJ. Modulation of immune development and function by intestinal microbiota. *Trends in immunology.* 2014;35(11):507-17.
103. Arumugam M, Raes J, Pelletier E, Le Paslier D, Yamada T, Mende DR, et al. Enterotypes of the human gut microbiome. *Nature.* 2011;473(7346):174-80.
104. Belkaid Y, Hand TW. Role of the microbiota in immunity and inflammation. *Cell.* 2014;157(1):121-41.
105. Sekirov I, Russell SL, Antunes LC, Finlay BB. Gut microbiota in health and disease. *Physiological reviews.* 2010;90(3):859-904.
106. Clemente JC, Ursell LK, Parfrey LW, Knight R. The impact of the gut microbiota on human health: an integrative view. *Cell.* 2012;148(6):1258-70.
107. DuPont AW, DuPont HL. The intestinal microbiota and chronic disorders of the gut. *Nat Rev Gastroenterol Hepatol.* 2011;8(9):523-31.
108. Xu X, Xu P, Ma C, Tang J, Zhang X. Gut microbiota, host health, and polysaccharides. *Biotechnol Adv.* 2013;31(2):318-37.
109. Salonen A, de Vos WM. Impact of diet on human intestinal microbiota and health. *Annu Rev Food Sci Technol.* 2014;5:239-62.
110. Keeney KM, Finlay BB. Enteric pathogen exploitation of the microbiota-generated nutrient environment of the gut. *Current opinion in microbiology.* 2011;14(1):92-8.
111. LeBlanc JG, Milani C, de Giori GS, Sesma F, van Sinderen D, Ventura M. Bacteria as vitamin suppliers to their host: a gut microbiota perspective. *Current opinion in biotechnology.* 2013;24(2):160-8.
112. Fraune S, Bosch TC. Why bacteria matter in animal development and evolution. *Bioessays.* 2010;32(7):571-80.
113. Tlaskalova-Hogenova H, Stepankova R, Kozakova H, Hudcovic T, Vannucci L, Tuckova L, et al. The role of gut microbiota (commensal bacteria) and the mucosal barrier in the pathogenesis of inflammatory and autoimmune diseases and cancer: contribution of germ-free and gnotobiotic animal models of human diseases. *Cell Mol Immunol.* 2011;8(2):110-20.
114. Perez-Lopez A, Behnsen J, Nuccio SP, Raffatellu M. Mucosal immunity to pathogenic intestinal bacteria. *Nat Rev Immunol.* 2016;16(3):135-48.
115. Rigottier-Gois L. Dysbiosis in inflammatory bowel diseases: the oxygen hypothesis. *The ISME journal.* 2013;7(7):1256-61.
116. Tamboli CP, Neut C, Desreumaux P, Colombel JF. Dysbiosis in inflammatory bowel disease. *Gut.* 2004;53(1):1-4.
117. Sobhani I, Tap J, Roudot-Thoraval F, Roperch JP, Letulle S, Langella P, et al. Microbial dysbiosis in colorectal cancer (CRC) patients. *PLoS One.* 2011;6(1):e16393.
118. Sears CL, Garrett WS. Microbes, microbiota, and colon cancer. *Cell host & microbe.* 2014;15(3):317-28.

119. Wu N, Yang X, Zhang R, Li J, Xiao X, Hu Y, et al. Dysbiosis signature of fecal microbiota in colorectal cancer patients. *Microb Ecol.* 2013;66(2):462-70.
120. Irrazabal T, Belcheva A, Girardin SE, Martin A, Philpott DJ. The multifaceted role of the intestinal microbiota in colon cancer. *Mol Cell.* 2014;54(2):309-20.
121. Marchesi JR, Dutilh BE, Hall N, Peters WH, Roelofs R, Boleij A, et al. Towards the human colorectal cancer microbiome. *PLoS One.* 2011;6(5):e20447.
122. Williams BL, Hornig M, Buie T, Bauman ML, Cho Paik M, Wick I, et al. Impaired carbohydrate digestion and transport and mucosal dysbiosis in the intestines of children with autism and gastrointestinal disturbances. *PLoS One.* 2011;6(9):e24585.
123. Henao-Mejia J, Elinav E, Jin C, Hao L, Mehal WZ, Strowig T, et al. Inflammasome-mediated dysbiosis regulates progression of NAFLD and obesity. *Nature.* 2012;482(7384):179-85.
124. Elinav E, Nowarski R, Thaiss CA, Hu B, Jin C, Flavell RA. Inflammation-induced cancer: crosstalk between tumours, immune cells and microorganisms. *Nat Rev Cancer.* 2013;13(11):759-71.
125. Xuan C, Shamonki JM, Chung A, Dinome ML, Chung M, Sieling PA, et al. Microbial dysbiosis is associated with human breast cancer. *PLoS One.* 2014;9(1):e83744.
126. Sheflin AM, Whitney AK, Weir TL. Cancer-promoting effects of microbial dysbiosis. *Curr Oncol Rep.* 2014;16(10):406.
127. Schwabe RF, Jobin C. The microbiome and cancer. *Nat Rev Cancer.* 2013;13(11):800-12.
128. Guarner F, Bourdet-Sicard R, Brandtzaeg P, Gill HS, McGuirk P, van Eden W, et al. Mechanisms of disease: the hygiene hypothesis revisited. *Nat Clin Pract Gastroenterol Hepatol.* 2006;3(5):275-84.
129. Martin R, Nauta AJ, Ben Amor K, Knippels LM, Knol J, Garssen J. Early life: gut microbiota and immune development in infancy. *Beneficial microbes.* 2010;1(4):367-82.
130. Decker E, Engelmann G, Findeisen A, Gerner P, Laass M, Ney D, et al. Cesarean delivery is associated with celiac disease but not inflammatory bowel disease in children. *Pediatrics.* 2010;125(6):e1433-40.
131. Marild K, Stephansson O, Montgomery S, Murray JA, Ludvigsson JF. Pregnancy outcome and risk of celiac disease in offspring: a nationwide case-control study. *Gastroenterology.* 2012;142(1):39-45 e3.
132. Algert CS, McElduff A, Morris JM, Roberts CL. Perinatal risk factors for early onset of Type 1 diabetes in a 2000-2005 birth cohort. *Diabet Med.* 2009;26(12):1193-7.
133. Bonifacio E, Warncke K, Winkler C, Wallner M, Ziegler AG. Cesarean section and interferon-induced helicase gene polymorphisms combine to increase childhood type 1 diabetes risk. *Diabetes.* 2011;60(12):3300-6.
134. Kero J, Gissler M, Gronlund MM, Kero P, Koskinen P, Hemminki E, et al. Mode of delivery and asthma -- is there a connection? *Pediatric research.* 2002;52(1):6-11.

135. Roudit C, Scholtens S, de Jongste JC, Wijga AH, Gerritsen J, Postma DS, et al. Asthma at 8 years of age in children born by caesarean section. *Thorax*. 2009;64(2):107-13.
136. Rautava S, Kalliomaki M, Isolauri E. New therapeutic strategy for combating the increasing burden of allergic disease: Probiotics-A Nutrition, Allergy, Mucosal Immunology and Intestinal Microbiota (NAMI) Research Group report. *The Journal of allergy and clinical immunology*. 2005;116(1):31-7.
137. Giongo A, Gano KA, Crabb DB, Mukherjee N, Novelo LL, Casella G, et al. Toward defining the autoimmune microbiome for type 1 diabetes. *The ISME journal*. 2011;5(1):82-91.
138. Russell SL, Gold MJ, Hartmann M, Willing BP, Thorson L, Wlodarska M, et al. Early life antibiotic-driven changes in microbiota enhance susceptibility to allergic asthma. *EMBO reports*. 2012;13(5):440-7.
139. Artis D. Epithelial-cell recognition of commensal bacteria and maintenance of immune homeostasis in the gut. *Nat Rev Immunol*. 2008;8(6):411-20.
140. Medzhitov R. Recognition of microorganisms and activation of the immune response. *Nature*. 2007;449(7164):819-26.
141. Chow J, Mazmanian SK. A pathobiont of the microbiota balances host colonization and intestinal inflammation. *Cell host & microbe*. 2010;7(4):265-76.
142. Mazmanian SK, Round JL, Kasper DL. A microbial symbiosis factor prevents intestinal inflammatory disease. *Nature*. 2008;453(7195):620-5.
143. Flores BM, Fennell CL, Kuller L, Bronsdon MA, Morton WR, Stamm WE. Experimental infection of pig-tailed macaques (*Macaca nemestrina*) with *Campylobacter cinaedi* and *Campylobacter fennelliae*. *Infect Immun*. 1990;58(12):3947-53.
144. Fox JG, Chien CC, Dewhirst FE, Paster BJ, Shen Z, Melito PL, et al. *Helicobacter canadensis* sp. nov. isolated from humans with diarrhea as an example of an emerging pathogen. *J Clin Microbiol*. 2000;38(7):2546-9.
145. Amieva MR, El-Omar EM. Host-bacterial interactions in *Helicobacter pylori* infection. *Gastroenterology*. 2008;134(1):306-23.
146. Konno M, Yokota S, Suga T, Takahashi M, Sato K, Fujii N. Predominance of mother-to-child transmission of *Helicobacter pylori* infection detected by random amplified polymorphic DNA fingerprinting analysis in Japanese families. *Pediatr Infect Dis J*. 2008;27(11):999-1003.
147. Kusters JG, van Vliet AH, Kuipers EJ. Pathogenesis of *Helicobacter pylori* infection. *Clin Microbiol Rev*. 2006;19(3):449-90.
148. Chen Y, Blaser MJ. *Helicobacter pylori* colonization is inversely associated with childhood asthma. *J Infect Dis*. 2008;198(4):553-60.
149. Cover TL, Blaser MJ. *Helicobacter pylori* in health and disease. *Gastroenterology*. 2009;136(6):1863-73.
150. Cho I, Blaser MJ. The human microbiome: at the interface of health and disease. *Nature reviews Genetics*. 2012;13(4):260-70.
151. Cussac V, Ferrero RL, Labigne A. Expression of *Helicobacter pylori* urease genes in *Escherichia coli* grown under nitrogen-limiting conditions. *J Bacteriol*. 1992;174(8):2466-73.

152. Eaton KA, Brooks CL, Morgan DR, Krakowka S. Essential role of urease in pathogenesis of gastritis induced by *Helicobacter pylori* in gnotobiotic piglets. *Infect Immun.* 1991;59(7):2470-5.
153. Labigne A, Cussac V, Courcoux P. Shuttle cloning and nucleotide sequences of *Helicobacter pylori* genes responsible for urease activity. *J Bacteriol.* 1991;173(6):1920-31.
154. Perez-Perez GI, Olivares AZ, Cover TL, Blaser MJ. Characteristics of *Helicobacter pylori* variants selected for urease deficiency. *Infect Immun.* 1992;60(9):3658-63.
155. Leying H, Suerbaum S, Geis G, Haas R. Cloning and genetic characterization of a *Helicobacter pylori* flagellin gene. *Mol Microbiol.* 1992;6(19):2863-74.
156. Cover TL, Blanke SR. *Helicobacter pylori* VacA, a paradigm for toxin multifunctionality. *Nat Rev Microbiol.* 2005;3(4):320-32.
157. Gebert B, Fischer W, Weiss E, Hoffmann R, Haas R. *Helicobacter pylori* vacuolating cytotoxin inhibits T lymphocyte activation. *Science.* 2003;301(5636):1099-102.
158. Torres VJ, VanCompernelle SE, Sundrud MS, Unutmaz D, Cover TL. *Helicobacter pylori* vacuolating cytotoxin inhibits activation-induced proliferation of human T and B lymphocyte subsets. *Journal of immunology.* 2007;179(8):5433-40.
159. Malfertheiner P, Link A, Selgrad M. *Helicobacter pylori*: perspectives and time trends. *Nat Rev Gastroenterol Hepatol.* 2014;11(10):628-38.
160. Odenbreit S, Puls J, Sedlmaier B, Gerland E, Fischer W, Haas R. Translocation of *Helicobacter pylori* CagA into gastric epithelial cells by type IV secretion. *Science.* 2000;287(5457):1497-500.
161. Jones KR, Whitmire JM, Merrell DS. A Tale of Two Toxins: *Helicobacter Pylori* CagA and VacA Modulate Host Pathways that Impact Disease. *Front Microbiol.* 2010;1:115.
162. Amieva MR, Vogelmann R, Covacci A, Tompkins LS, Nelson WJ, Falkow S. Disruption of the epithelial apical-junctional complex by *Helicobacter pylori* CagA. *Science.* 2003;300(5624):1430-4.
163. Bagnoli F, Buti L, Tompkins L, Covacci A, Amieva MR. *Helicobacter pylori* CagA induces a transition from polarized to invasive phenotypes in MDCK cells. *Proc Natl Acad Sci U S A.* 2005;102(45):16339-44.
164. Murata-Kamiya N, Kurashima Y, Teishikata Y, Yamahashi Y, Saito Y, Higashi H, et al. *Helicobacter pylori* CagA interacts with E-cadherin and deregulates the beta-catenin signal that promotes intestinal transdifferentiation in gastric epithelial cells. *Oncogene.* 2007;26(32):4617-26.
165. Oliveira MJ, Costa AM, Costa AC, Ferreira RM, Sampaio P, Machado JC, et al. CagA associates with c-Met, E-cadherin, and p120-catenin in a multiproteic complex that suppresses *Helicobacter pylori*-induced cell-invasive phenotype. *J Infect Dis.* 2009;200(5):745-55.
166. Zeaiter Z, Huynh HQ, Kanyo R, Stein M. CagA of *Helicobacter pylori* alters the expression and cellular distribution of host proteins involved in cell signaling. *FEMS Microbiol Lett.* 2008;288(2):227-34.
167. Mimuro H, Suzuki T, Tanaka J, Asahi M, Haas R, Sasakawa C. Grb2 is a key mediator of *Helicobacter pylori* CagA protein activities. *Mol Cell.* 2002;10(4):745-55.

168. Chang YJ, Wu MS, Lin JT, Pestell RG, Blaser MJ, Chen CC. Mechanisms for *Helicobacter pylori* CagA-induced cyclin D1 expression that affect cell cycle. *Cellular microbiology*. 2006;8(11):1740-52.
169. Lee IO, Kim JH, Choi YJ, Pillinger MH, Kim SY, Blaser MJ, et al. *Helicobacter pylori* CagA phosphorylation status determines the gp130-activated SHP2/ERK and JAK/STAT signal transduction pathways in gastric epithelial cells. *The Journal of biological chemistry*. 2010;285(21):16042-50.
170. Brandt S, Kwok T, Hartig R, Konig W, Backert S. NF-kappaB activation and potentiation of proinflammatory responses by the *Helicobacter pylori* CagA protein. *Proc Natl Acad Sci U S A*. 2005;102(26):9300-5.
171. Saadat I, Higashi H, Obuse C, Umeda M, Murata-Kamiya N, Saito Y, et al. *Helicobacter pylori* CagA targets PAR1/MARK kinase to disrupt epithelial cell polarity. *Nature*. 2007;447(7142):330-3.
172. Umeda M, Murata-Kamiya N, Saito Y, Ohba Y, Takahashi M, Hatakeyama M. *Helicobacter pylori* CagA causes mitotic impairment and induces chromosomal instability. *The Journal of biological chemistry*. 2009;284(33):22166-72.
173. Blaser MJ. The role of *Helicobacter pylori* in gastritis and its progression to peptic ulcer disease. *Alimentary pharmacology & therapeutics*. 1995;9 Suppl 1:27-30.
174. Hatakeyama M, Brzozowski T. Pathogenesis of *Helicobacter pylori* infection. *Helicobacter*. 2006;11 Suppl 1:14-20.
175. Grice EA, Segre JA. The skin microbiome. *Nat Rev Microbiol*. 2011;9(4):244-53.
176. Dessinioti C, Katsambas AD. The role of *Propionibacterium acnes* in acne pathogenesis: facts and controversies. *Clin Dermatol*. 2010;28(1):2-7.
177. Funke G, von Graevenitz A, Clarridge JE, 3rd, Bernard KA. Clinical microbiology of coryneform bacteria. *Clin Microbiol Rev*. 1997;10(1):125-59.
178. Delgado S, Suarez A, Mayo B. Identification, typing and characterisation of *Propionibacterium* strains from healthy mucosa of the human stomach. *International journal of food microbiology*. 2011;149(1):65-72.
179. Perry A, Lambert P. *Propionibacterium acnes*: infection beyond the skin. *Expert Rev Anti Infect Ther*. 2011;9(12):1149-56.
180. Harada K, Furubo S, Ozaki S, Hiramatsu K, Sudo Y, Nakanuma Y. Increased expression of WAF1 in intrahepatic bile ducts in primary biliary cirrhosis relates to apoptosis. *J Hepatol*. 2001;34(4):500-6.
181. Cohen RJ, Shannon BA, McNeal JE, Shannon T, Garrett KL. *Propionibacterium acnes* associated with inflammation in radical prostatectomy specimens: a possible link to cancer evolution? *J Urol*. 2005;173(6):1969-74.
182. Fassi Fehri L, Mak TN, Laube B, Brinkmann V, Ogilvie LA, Mollenkopf H, et al. Prevalence of *Propionibacterium acnes* in diseased prostates and its inflammatory and transforming activity on prostate epithelial cells. *International Journal of Medical Microbiology*. 2011;301(1):69-78.
183. Eishi Y, Suga M, Ishige I, Kobayashi D, Yamada T, Takemura T, et al. Quantitative analysis of mycobacterial and propionibacterial DNA in lymph nodes of Japanese and European patients with sarcoidosis. *J Clin Microbiol*. 2002;40(1):198-204.

184. Graham GM, Farrar MD, Cruse-Sawyer JE, Holland KT, Ingham E. Proinflammatory cytokine production by human keratinocytes stimulated with *Propionibacterium acnes* and *P. acnes* GroEL. *Br J Dermatol*. 2004;150(3):421-8.
185. Kim J, Ochoa MT, Krutzik SR, Takeuchi O, Uematsu S, Legaspi AJ, et al. Activation of toll-like receptor 2 in acne triggers inflammatory cytokine responses. *Journal of immunology*. 2002;169(3):1535-41.
186. Lomholt HB, Kilian M. Population genetic analysis of *Propionibacterium acnes* identifies a subpopulation and epidemic clones associated with acne. *PLoS One*. 2010;5(8):e12277.
187. Brzuszkiewicz E, Weiner J, Wollherr A, Thurmer A, Hupeden J, Lomholt HB, et al. Comparative genomics and transcriptomics of *Propionibacterium acnes*. *PloS one*. 2011;6(6):e21581.
188. Bowe WP, Logan AC. Acne vulgaris, probiotics and the gut-brain-skin axis - back to the future? *Gut Pathog*. 2011;3(1):1.
189. Montalban-Arques A, De Schryver P, Bossier P, Gorkiewicz G, Mulero V, Gatlin DM, 3rd, et al. Selective Manipulation of the Gut Microbiota Improves Immune Status in Vertebrates. *Frontiers in immunology*. 2015;6:512.
190. Tan J, McKenzie C, Potamitis M, Thorburn AN, Mackay CR, Macia L. The role of short-chain fatty acids in health and disease. *Advances in immunology*. 2014;121:91-119.
191. Tazoe H, Otomo Y, Kaji I, Tanaka R, Karaki SI, Kuwahara A. Roles of short-chain fatty acids receptors, GPR41 and GPR43 on colonic functions. *Journal of physiology and pharmacology : an official journal of the Polish Physiological Society*. 2008;59 Suppl 2:251-62.
192. Lupton JR. Microbial degradation products influence colon cancer risk: the butyrate controversy. *J Nutr*. 2004;134(2):479-82.
193. Topping DL, Clifton PM. Short-chain fatty acids and human colonic function: roles of resistant starch and nonstarch polysaccharides. *Physiological reviews*. 2001;81(3):1031-64.
194. Wong JM, de Souza R, Kendall CW, Emam A, Jenkins DJ. Colonic health: fermentation and short chain fatty acids. *J Clin Gastroenterol*. 2006;40(3):235-43.
195. Cook SI, Sellin JH. Review article: short chain fatty acids in health and disease. *Alimentary pharmacology & therapeutics*. 1998;12(6):499-507.
196. Mahowald MA, Rey FE, Seedorf H, Turnbaugh PJ, Fulton RS, Wollam A, et al. Characterizing a model human gut microbiota composed of members of its two dominant bacterial phyla. *Proc Natl Acad Sci U S A*. 2009;106(14):5859-64.
197. Halestrap AP, Wilson MC. The monocarboxylate transporter family--role and regulation. *IUBMB Life*. 2012;64(2):109-19.
198. Chang PV, Hao L, Offermanns S, Medzhitov R. The microbial metabolite butyrate regulates intestinal macrophage function via histone deacetylase inhibition. *Proc Natl Acad Sci U S A*. 2014;111(6):2247-52.
199. Waldecker M, Kautenburger T, Daumann H, Busch C, Schrenk D. Inhibition of histone-deacetylase activity by short-chain fatty acids and some polyphenol metabolites formed in the colon. *J Nutr Biochem*. 2008;19(9):587-93.
200. Le Poul E, Loison C, Struyf S, Springael JY, Lannoy V, Decobecq ME, et al. Functional characterization of human receptors for short chain fatty acids and their

role in polymorphonuclear cell activation. *The Journal of biological chemistry*. 2003;278(28):25481-9.

201. Tazoe H, Otomo Y, Karaki S, Kato I, Fukami Y, Terasaki M, et al. Expression of short-chain fatty acid receptor GPR41 in the human colon. *Biomed Res*. 2009;30(3):149-56.

202. Brown AJ, Goldsworthy SM, Barnes AA, Eilert MM, Tcheang L, Daniels D, et al. The Orphan G protein-coupled receptors GPR41 and GPR43 are activated by propionate and other short chain carboxylic acids. *The Journal of biological chemistry*. 2003;278(13):11312-9.

203. Louis P, Hold GL, Flint HJ. The gut microbiota, bacterial metabolites and colorectal cancer. *Nat Rev Microbiol*. 2014;12(10):661-72.

204. Feingold KR, Moser A, Shigenaga JK, Grunfeld C. Inflammation stimulates niacin receptor (GPR109A/HCA2) expression in adipose tissue and macrophages. *Journal of lipid research*. 2014;55(12):2501-8.

205. Sellin JH. The pathophysiology of diarrhea. *Clin Transplant*. 2001;15 Suppl 4:2-10.

206. Rabassa AA, Rogers AI. The role of short-chain fatty acid metabolism in colonic disorders. *Am J Gastroenterol*. 1992;87(4):419-23.

207. Canani RB, Costanzo MD, Leone L, Pedata M, Meli R, Calignano A. Potential beneficial effects of butyrate in intestinal and extraintestinal diseases. *World J Gastroenterol*. 2011;17(12):1519-28.

208. Mathewson ND, Jenq R, Mathew AV, Koenigsnecht M, Hanash A, Toubai T, et al. Gut microbiome-derived metabolites modulate intestinal epithelial cell damage and mitigate graft-versus-host disease. *Nat Immunol*. 2016;17(5):505-13.

209. Cummings JH, Macfarlane GT. The control and consequences of bacterial fermentation in the human colon. *J Appl Bacteriol*. 1991;70(6):443-59.

210. Millard AL, Mertes PM, Ittelet D, Villard F, Jeannesson P, Bernard J. Butyrate affects differentiation, maturation and function of human monocyte-derived dendritic cells and macrophages. *Clin Exp Immunol*. 2002;130(2):245-55.

211. Hossain Z, Konishi M, Hosokawa M, Takahashi K. Effect of polyunsaturated fatty acid-enriched phosphatidylcholine and phosphatidylserine on butyrate-induced growth inhibition, differentiation and apoptosis in Caco-2 cells. *Cell Biochem Funct*. 2006;24(2):159-65.

212. Roy CC, Kien CL, Bouthillier L, Levy E. Short-chain fatty acids: ready for prime time? *Nutr Clin Pract*. 2006;21(4):351-66.

213. Brestoff JR, Artis D. Commensal bacteria at the interface of host metabolism and the immune system. *Nat Immunol*. 2013;14(7):676-84.

214. Shapiro H, Thaiss CA, Levy M, Elinav E. The cross talk between microbiota and the immune system: metabolites take center stage. *Curr Opin Immunol*. 2014;30:54-62.

215. Kim CH, Park J, Kim M. Gut microbiota-derived short-chain Fatty acids, T cells, and inflammation. *Immune network*. 2014;14(6):277-88.

216. Macia L, Thorburn AN, Binge LC, Marino E, Rogers KE, Maslowski KM, et al. Microbial influences on epithelial integrity and immune function as a basis for inflammatory diseases. *Immunol Rev*. 2012;245(1):164-76.

217. Meijer K, de Vos P, Priebe MG. Butyrate and other short-chain fatty acids as modulators of immunity: what relevance for health? *Current opinion in clinical nutrition and metabolic care*. 2010;13(6):715-21.
218. Saemann MD, Bohmig GA, Osterreicher CH, Burtscher H, Parolini O, Diakos C, et al. Anti-inflammatory effects of sodium butyrate on human monocytes: potent inhibition of IL-12 and up-regulation of IL-10 production. *FASEB J*. 2000;14(15):2380-2.
219. Vinolo MAR, Ferguson GJ, Kulkarni S, Damoulakis G, Anderson K, Bohlooly-Y M, et al. SCFAs Induce Mouse Neutrophil Chemotaxis through the GPR43 Receptor. *PLoS ONE*. 2011;6(6):e21205.
220. Maslowski KM, Vieira AT, Ng A, Kranich J, Sierro F, Yu D, et al. Regulation of inflammatory responses by gut microbiota and chemoattractant receptor GPR43. *Nature*. 2009;461(7268):1282-6.
221. Donohoe DR, Garge N, Zhang X, Sun W, O'Connell TM, Bunger MK, et al. The microbiome and butyrate regulate energy metabolism and autophagy in the mammalian colon. *Cell Metab*. 2011;13(5):517-26.
222. Arpaia N, Campbell C, Fan X, Dikiy S, van der Veeken J, deRoos P, et al. Metabolites produced by commensal bacteria promote peripheral regulatory T-cell generation. *Nature*. 2013;504(7480):451-5.
223. Smith PM, Howitt MR, Panikov N, Michaud M, Gallini CA, Bohlooly YM, et al. The microbial metabolites, short-chain fatty acids, regulate colonic Treg cell homeostasis. *Science*. 2013;341(6145):569-73.
224. Ren H, Musch MW, Kojima K, Boone D, Ma A, Chang EB. Short-chain fatty acids induce intestinal epithelial heat shock protein 25 expression in rats and IEC 18 cells. *Gastroenterology*. 2001;121(3):631-9.
225. Alva-Murillo N, Ochoa-Zarzosa A, Lopez-Meza JE. Short chain fatty acids (propionic and hexanoic) decrease *Staphylococcus aureus* internalization into bovine mammary epithelial cells and modulate antimicrobial peptide expression. *Veterinary microbiology*. 2012;155(2-4):324-31.
226. Dewulf EM, Cani PD, Neyrinck AM, Possemiers S, Van Holle A, Muccioli GG, et al. Inulin-type fructans with prebiotic properties counteract GPR43 overexpression and PPARgamma-related adipogenesis in the white adipose tissue of high-fat diet-fed mice. *J Nutr Biochem*. 2011;22(8):712-22.
227. Hong YH, Nishimura Y, Hishikawa D, Tsuzuki H, Miyahara H, Gotoh C, et al. Acetate and propionate short chain fatty acids stimulate adipogenesis via GPCR43. *Endocrinology*. 2005;146(12):5092-9.
228. Peng L, He Z, Chen W, Holzman IR, Lin J. Effects of butyrate on intestinal barrier function in a Caco-2 cell monolayer model of intestinal barrier. *Pediatric research*. 2007;61(1):37-41.
229. Burger-van Paassen N, Vincent A, Puiman PJ, van der Sluis M, Bouma J, Boehm G, et al. The regulation of intestinal mucin MUC2 expression by short-chain fatty acids: implications for epithelial protection. *The Biochemical journal*. 2009;420(2):211-9.
230. Smits LP, Bouter KE, de Vos WM, Borody TJ, Nieuwdorp M. Therapeutic potential of fecal microbiota transplantation. *Gastroenterology*. 2013;145(5):946-53.

231. Shanahan F. The gut microbiota-a clinical perspective on lessons learned. *Nat Rev Gastroenterol Hepatol.* 2012;9(10):609-14.
232. Mold JE, Michaelsson J, Burt TD, Muench MO, Beckerman KP, Busch MP, et al. Maternal alloantigens promote the development of tolerogenic fetal regulatory T cells in utero. *Science.* 2008;322(5907):1562-5.
233. Rautava S, Luoto R, Salminen S, Isolauri E. Microbial contact during pregnancy, intestinal colonization and human disease. *Nat Rev Gastroenterol Hepatol.* 2012;9(10):565-76.
234. Onderdonk AB, Delaney ML, DuBois AM, Allred EN, Leviton A, Extremely Low Gestational Age Newborns Study I. Detection of bacteria in placental tissues obtained from extremely low gestational age neonates. *Am J Obstet Gynecol.* 2008;198(1):110 e1-7.
235. Satokari R, Gronroos T, Laitinen K, Salminen S, Isolauri E. Bifidobacterium and Lactobacillus DNA in the human placenta. *Lett Appl Microbiol.* 2009;48(1):8-12.
236. Steel JH, Malatos S, Kennea N, Edwards AD, Miles L, Duggan P, et al. Bacteria and inflammatory cells in fetal membranes do not always cause preterm labor. *Pediatric research.* 2005;57(3):404-11.
237. Mshvildadze M, Neu J, Shuster J, Theriaque D, Li N, Mai V. Intestinal microbial ecology in premature infants assessed with non-culture-based techniques. *J Pediatr.* 2010;156(1):20-5.
238. Roduit C, Wohlgensinger J, Frei R, Bitter S, Bieli C, Loeliger S, et al. Prenatal animal contact and gene expression of innate immunity receptors at birth are associated with atopic dermatitis. *The Journal of allergy and clinical immunology.* 2011;127(1):179-85, 85 e1.
239. Gomez de Agüero M, Ganai-Vonarburg SC, Fuhrer T, Rupp S, Uchimura Y, Li H, et al. The maternal microbiota drives early postnatal innate immune development. *Science.* 2016;351(6279):1296-302.
240. Dominguez-Bello MG, Costello EK, Contreras M, Magris M, Hidalgo G, Fierer N, et al. Delivery mode shapes the acquisition and structure of the initial microbiota across multiple body habitats in newborns. *Proc Natl Acad Sci U S A.* 2010;107(26):11971-5.
241. Bager P, Wohlfahrt J, Westergaard T. Caesarean delivery and risk of atopy and allergic disease: meta-analyses. *Clin Exp Allergy.* 2008;38(4):634-42.
242. Harmsen HJ, Wildeboer-Veloo AC, Raangs GC, Wagendorp AA, Klijn N, Bindels JG, et al. Analysis of intestinal flora development in breast-fed and formula-fed infants by using molecular identification and detection methods. *Journal of pediatric gastroenterology and nutrition.* 2000;30(1):61-7.
243. Penders J, Thijs C, Vink C, Stelma FF, Snijders B, Kummeling I, et al. Factors influencing the composition of the intestinal microbiota in early infancy. *Pediatrics.* 2006;118(2):511-21.
244. Cherrier M, Ohnmacht C, Cording S, Eberl G. Development and function of intestinal innate lymphoid cells. *Curr Opin Immunol.* 2012;24(3):277-83.
245. Ismail AS, Severson KM, Vaishnava S, Behrendt CL, Yu X, Benjamin JL, et al. Gammadelta intraepithelial lymphocytes are essential mediators of host-microbial homeostasis at the intestinal mucosal surface. *Proc Natl Acad Sci U S A.* 2011;108(21):8743-8.

246. Round JL, Lee SM, Li J, Tran G, Jabri B, Chatila TA, et al. The Toll-like receptor 2 pathway establishes colonization by a commensal of the human microbiota. *Science*. 2011;332(6032):974-7.
247. Takeda K, Akira S. Toll-like receptors in innate immunity. *Int Immunol*. 2005;17(1):1-14.
248. Akira S, Takeda K, Kaisho T. Toll-like receptors: critical proteins linking innate and acquired immunity. *Nat Immunol*. 2001;2(8):675-80.
249. Abreu MT, Vora P, Faure E, Thomas LS, Arnold ET, Arditi M. Decreased expression of Toll-like receptor-4 and MD-2 correlates with intestinal epithelial cell protection against dysregulated proinflammatory gene expression in response to bacterial lipopolysaccharide. *Journal of immunology*. 2001;167(3):1609-16.
250. Cario E, Podolsky DK. Intestinal epithelial TOLLerance versus inTOLLerance of commensals. *Mol Immunol*. 2005;42(8):887-93.
251. Gewirtz AT, Simon PO, Jr., Schmitt CK, Taylor LJ, Hagedorn CH, O'Brien AD, et al. *Salmonella typhimurium* translocates flagellin across intestinal epithelia, inducing a proinflammatory response. *J Clin Invest*. 2001;107(1):99-109.
252. Vijay-Kumar M, Aitken JD, Kumar A, Neish AS, Uematsu S, Akira S, et al. Toll-like receptor 5-deficient mice have dysregulated intestinal gene expression and nonspecific resistance to *Salmonella*-induced typhoid-like disease. *Infect Immun*. 2008;76(3):1276-81.
253. Smith KD, Andersen-Nissen E, Hayashi F, Strobe K, Bergman MA, Barrett SL, et al. Toll-like receptor 5 recognizes a conserved site on flagellin required for protofilament formation and bacterial motility. *Nat Immunol*. 2003;4(12):1247-53.
254. Andersen-Nissen E, Smith KD, Strobe KL, Barrett SL, Cookson BT, Logan SM, et al. Evasion of Toll-like receptor 5 by flagellated bacteria. *Proc Natl Acad Sci U S A*. 2005;102(26):9247-52.
255. Gewirtz AT, Yu Y, Krishna US, Israel DA, Lyons SL, Peek RM, Jr. *Helicobacter pylori* flagellin evades toll-like receptor 5-mediated innate immunity. *J Infect Dis*. 2004;189(10):1914-20.
256. Otte JM, Cario E, Podolsky DK. Mechanisms of cross hyporesponsiveness to Toll-like receptor bacterial ligands in intestinal epithelial cells. *Gastroenterology*. 2004;126(4):1054-70.
257. Raulet DH. Roles of the NKG2D immunoreceptor and its ligands. *Nat Rev Immunol*. 2003;3(10):781-90.
258. Garrity D, Call ME, Feng J, Wucherpfennig KW. The activating NKG2D receptor assembles in the membrane with two signaling dimers into a hexameric structure. *Proc Natl Acad Sci U S A*. 2005;102(21):7641-6.
259. Wu J, Song Y, Bakker AB, Bauer S, Spies T, Lanier LL, et al. An activating immunoreceptor complex formed by NKG2D and DAP10. *Science*. 1999;285(5428):730-2.
260. Upshaw JL, Arneson LN, Schoon RA, Dick CJ, Billadeau DD, Leibson PJ. NKG2D-mediated signaling requires a DAP10-bound Grb2-Vav1 intermediate and phosphatidylinositol-3-kinase in human natural killer cells. *Nat Immunol*. 2006;7(5):524-32.
261. Raulet DH, Gasser S, Gowen BG, Deng W, Jung H. Regulation of ligands for the NKG2D activating receptor. *Annual review of immunology*. 2013;31:413-41.

262. Sutherland CL, Chalupny NJ, Schooley K, VandenBos T, Kubin M, Cosman D. UL16-binding proteins, novel MHC class I-related proteins, bind to NKG2D and activate multiple signaling pathways in primary NK cells. *Journal of immunology*. 2002;168(2):671-9.
263. Champsaur M, Lanier LL. Effect of NKG2D ligand expression on host immune responses. *Immunol Rev*. 2010;235(1):267-85.
264. Eagle RA, Trowsdale J. Promiscuity and the single receptor: NKG2D. *Nat Rev Immunol*. 2007;7(9):737-44.
265. Gasser S, Orsulic S, Brown EJ, Raulet DH. The DNA damage pathway regulates innate immune system ligands of the NKG2D receptor. *Nature*. 2005;436(7054):1186-90.
266. Yamamoto K, Fujiyama Y, Andoh A, Bamba T, Okabe H. Oxidative stress increases MICA and MICB gene expression in the human colon carcinoma cell line (CaCo-2). *Biochim Biophys Acta*. 2001;1526(1):10-2.
267. Peraldi MN, Berrou J, Dulphy N, Seidowsky A, Haas P, Boissel N, et al. Oxidative stress mediates a reduced expression of the activating receptor NKG2D in NK cells from end-stage renal disease patients. *Journal of immunology*. 2009;182(3):1696-705.
268. Yamada N, Yamanegi K, Ohyama H, Hata M, Nakasho K, Futani H, et al. Hypoxia downregulates the expression of cell surface MICA without increasing soluble MICA in osteosarcoma cells in a HIF-1alpha-dependent manner. *Int J Oncol*. 2012;41(6):2005-12.
269. Smith HR, Heusel JW, Mehta IK, Kim S, Dorner BG, Naidenko OV, et al. Recognition of a virus-encoded ligand by a natural killer cell activation receptor. *Proc Natl Acad Sci U S A*. 2002;99(13):8826-31.
270. Zou Y, Bresnahan W, Taylor RT, Stastny P. Effect of human cytomegalovirus on expression of MHC class I-related chains A. *Journal of immunology*. 2005;174(5):3098-104.
271. Chalupny NJ, Rein-Weston A, Dosch S, Cosman D. Down-regulation of the NKG2D ligand MICA by the human cytomegalovirus glycoprotein UL142. *Biochem Biophys Res Commun*. 2006;346(1):175-81.
272. Groh V, Wu J, Yee C, Spies T. Tumour-derived soluble MIC ligands impair expression of NKG2D and T-cell activation. *Nature*. 2002;419(6908):734-8.
273. Smyth MJ, Swann J, Cretney E, Zerafa N, Yokoyama WM, Hayakawa Y. NKG2D function protects the host from tumor initiation. *J Exp Med*. 2005;202(5):583-8.
274. Vetter CS, Lieb W, Brocker EB, Becker JC. Loss of nonclassical MHC molecules MIC-A/B expression during progression of uveal melanoma. *British journal of cancer*. 2004;91(8):1495-9.
275. Gleimer M, Parham P. Stress management: MHC class I and class I-like molecules as reporters of cellular stress. *Immunity*. 2003;19(4):469-77.
276. Groh V, Bahram S, Bauer S, Herman A, Beauchamp M, Spies T. Cell stress-regulated human major histocompatibility complex class I gene expressed in gastrointestinal epithelium. *Proc Natl Acad Sci U S A*. 1996;93(22):12445-50.

277. Chalupny NJ, Sutherland CL, Lawrence WA, Rein-Weston A, Cosman D. ULBP4 is a novel ligand for human NKG2D. *Biochem Biophys Res Commun.* 2003;305(1):129-35.
278. Pagliari D, Cianci R, Frosali S, Landolfi R, Cammarota G, Newton EE, et al. The role of IL-15 in gastrointestinal diseases: a bridge between innate and adaptive immune response. *Cytokine Growth Factor Rev.* 2013;24(5):455-66.
279. Liu Z, Geboes K, Colpaert S, D'Haens GR, Rutgeerts P, Ceuppens JL. IL-15 is highly expressed in inflammatory bowel disease and regulates local T cell-dependent cytokine production. *Journal of immunology.* 2000;164(7):3608-15.
280. Vainer B, Nielsen OH, Hendel J, Horn T, Kirman I. Colonic expression and synthesis of interleukin 13 and interleukin 15 in inflammatory bowel disease. *Cytokine.* 2000;12(10):1531-6.
281. Montalban-Arques A, Wurm P, Trajanoski S, Schauer S, Kienesberger S, Halwachs B, et al. Propionibacterium acnes overabundance and NKG2D system activation in corpus-dominant lymphocytic gastritis. *J Pathol.* In press.
282. Dubois S, Mariner J, Waldmann TA, Tagaya Y. IL-15Ralpha recycles and presents IL-15 in trans to neighboring cells. *Immunity.* 2002;17(5):537-47.
283. Kobayashi H, Dubois S, Sato N, Sabzevari H, Sakai Y, Waldmann TA, et al. Role of trans-cellular IL-15 presentation in the activation of NK cell-mediated killing, which leads to enhanced tumor immunosurveillance. *Blood.* 2005;105(2):721-7.
284. Motegi A, Kinoshita M, Inatsu A, Habu Y, Saitoh D, Seki S. IL-15-induced CD8+CD122+ T cells increase antibacterial and anti-tumor immune responses: implications for immune function in aged mice. *J Leukoc Biol.* 2008;84(4):1047-56.
285. Hiromatsu T, Yajima T, Matsuguchi T, Nishimura H, Wajjwalku W, Arai T, et al. Overexpression of interleukin-15 protects against Escherichia coli-induced shock accompanied by inhibition of tumor necrosis factor-alpha-induced apoptosis. *J Infect Dis.* 2003;187(9):1442-51.
286. Kennedy MK, Glaccum M, Brown SN, Butz EA, Viney JL, Embers M, et al. Reversible defects in natural killer and memory CD8 T cell lineages in interleukin 15-deficient mice. *J Exp Med.* 2000;191(5):771-80.
287. Maeurer MJ, Trinder P, Hommel G, Walter W, Freitag K, Atkins D, et al. Interleukin-7 or interleukin-15 enhances survival of Mycobacterium tuberculosis-infected mice. *Infect Immun.* 2000;68(5):2962-70.
288. Reinecker HC, MacDermott RP, Mirau S, Dignass A, Podolsky DK. Intestinal epithelial cells both express and respond to interleukin 15. *Gastroenterology.* 1996;111(6):1706-13.
289. Ebert EC. Interleukin 15 is a potent stimulant of intraepithelial lymphocytes. *Gastroenterology.* 1998;115(6):1439-45.
290. Cheroutre H, Lambomez F, Mucida D. The light and dark sides of intestinal intraepithelial lymphocytes. *Nat Rev Immunol.* 2011;11(7):445-56.
291. Sheridan BS, Lefrancois L. Intraepithelial lymphocytes: to serve and protect. *Curr Gastroenterol Rep.* 2010;12(6):513-21.
292. Hayday A, Theodoridis E, Ramsburg E, Shires J. Intraepithelial lymphocytes: exploring the Third Way in immunology. *Nat Immunol.* 2001;2(11):997-1003.
293. Ebert EC. Human intestinal intraepithelial lymphocytes have potent chemotactic activity. *Gastroenterology.* 1995;109(4):1154-9.

294. Shires J, Theodoridis E, Hayday AC. Biological insights into TCRgammadelta+ and TCRalpha+ intraepithelial lymphocytes provided by serial analysis of gene expression (SAGE). *Immunity*. 2001;15(3):419-34.
295. Offit PA, Svoboda YM. Rotavirus-specific cytotoxic T lymphocyte response of mice after oral inoculation with candidate rotavirus vaccine strains RRV or WC3. *J Infect Dis*. 1989;160(5):783-8.
296. Tang F, Chen Z, Ciszewski C, Setty M, Solus J, Tretiakova M, et al. Cytosolic PLA2 is required for CTL-mediated immunopathology of celiac disease via NKG2D and IL-15. *J Exp Med*. 2009;206(3):707-19.
297. Chardes T, Buzoni-Gatel D, Lepage A, Bernard F, Bout D. *Toxoplasma gondii* oral infection induces specific cytotoxic CD8 alpha/beta+ Thy-1+ gut intraepithelial lymphocytes, lytic for parasite-infected enterocytes. *Journal of immunology*. 1994;153(10):4596-603.
298. Muller S, Buhler-Jungo M, Mueller C. Intestinal intraepithelial lymphocytes exert potent protective cytotoxic activity during an acute virus infection. *Journal of immunology*. 2000;164(4):1986-94.
299. Ebert EC, Roberts AI. Lymphokine-activated killing by human intestinal lymphocytes. *Cell Immunol*. 1993;146(1):107-16.
300. Guy-Grand D, Malassis-Seris M, Briottet C, Vassalli P. Cytotoxic differentiation of mouse gut thymodependent and independent intraepithelial T lymphocytes is induced locally. Correlation between functional assays, presence of perforin and granzyme transcripts, and cytoplasmic granules. *J Exp Med*. 1991;173(6):1549-52.
301. Shibahara T, Wilcox JN, Couse T, Madara JL. Characterization of epithelial chemoattractants for human intestinal intraepithelial lymphocytes. *Gastroenterology*. 2001;120(1):60-70.
302. Montalban-Arques A, Gorkiewicz G, Mulero V, Galindo-Villegas J. Cytokine Intervention: A Double Edged Sword in the NKG2D System Regulation. *Immunome Research*. 2014.
303. Yamagata T, Mathis D, Benoist C. Self-reactivity in thymic double-positive cells commits cells to a CD8 alpha lineage with characteristics of innate immune cells. *Nat Immunol*. 2004;5(6):597-605.
304. Zhou R, Wei H, Sun R, Zhang J, Tian Z. NKG2D recognition mediates Toll-like receptor 3 signaling-induced breakdown of epithelial homeostasis in the small intestines of mice. *Proc Natl Acad Sci U S A*. 2007;104(18):7512-5.
305. Poussier P, Ning T, Banerjee D, Julius M. A unique subset of self-specific intrainestinal T cells maintains gut integrity. *J Exp Med*. 2002;195(11):1491-7.
306. Kuhl AA, Pawlowski NN, Grollich K, Loddenkemper C, Zeitz M, Hoffmann JC. Aggravation of intestinal inflammation by depletion/deficiency of gammadelta T cells in different types of IBD animal models. *J Leukoc Biol*. 2007;81(1):168-75.
307. Roberts SJ, Ng BY, Filler RB, Lewis J, Glusac EJ, Hayday AC, et al. Characterizing tumor-promoting T cells in chemically induced cutaneous carcinogenesis. *Proc Natl Acad Sci U S A*. 2007;104(16):6770-5.
308. Komano H, Fujiura Y, Kawaguchi M, Matsumoto S, Hashimoto Y, Obana S, et al. Homeostatic regulation of intestinal epithelia by intraepithelial gamma delta T cells. *Proc Natl Acad Sci U S A*. 1995;92(13):6147-51.

309. Guy-Grand D, DiSanto JP, Henchoz P, Malassis-Seris M, Vassalli P. Small bowel enteropathy: role of intraepithelial lymphocytes and of cytokines (IL-12, IFN-gamma, TNF) in the induction of epithelial cell death and renewal. *Eur J Immunol.* 1998;28(2):730-44.
310. Boismenu R, Havran WL. Modulation of epithelial cell growth by intraepithelial gamma delta T cells. *Science.* 1994;266(5188):1253-5.
311. Bhagat G, Naiyer AJ, Shah JG, Harper J, Jabri B, Wang TC, et al. Small intestinal CD8+TCRgammadelta+NKG2A+ intraepithelial lymphocytes have attributes of regulatory cells in patients with celiac disease. *J Clin Invest.* 2008;118(1):281-93.
312. Giacomelli R, Parzanese I, Frieri G, Passacantando A, Pizzuto F, Pimpo T, et al. Increase of circulating gamma/delta T lymphocytes in the peripheral blood of patients affected by active inflammatory bowel disease. *Clin Exp Immunol.* 1994;98(1):83-8.
313. Kanazawa H, Ishiguro Y, Munakata A, Morita T. Multiple accumulation of Vdelta2+ gammadelta T-cell clonotypes in intestinal mucosa from patients with Crohn's disease. *Dig Dis Sci.* 2001;46(2):410-6.
314. Young MM, Deschamps C, Trastek VF, Allen MS, Miller DL, Schleck CD, et al. Esophageal reconstruction for benign disease: early morbidity, mortality, and functional results. *Ann Thorac Surg.* 2000;70(5):1651-5.
315. Mention JJ, Ben Ahmed M, Begue B, Barbe U, Verkarre V, Asnafi V, et al. Interleukin 15: a key to disrupted intraepithelial lymphocyte homeostasis and lymphomagenesis in celiac disease. *Gastroenterology.* 2003;125(3):730-45.
316. Jabri B, de Serre NP, Cellier C, Evans K, Gache C, Carvalho C, et al. Selective expansion of intraepithelial lymphocytes expressing the HLA-E-specific natural killer receptor CD94 in celiac disease. *Gastroenterology.* 2000;118(5):867-79.
317. Jarvinen TT, Kaukinen K, Laurila K, Kyronpalo S, Rasmussen M, Maki M, et al. Intraepithelial Lymphocytes in Celiac Disease. *Am J Gastroenterol.* 2003;98(6):1332-7.
318. Galazka G, Jurewicz A, Orłowski W, Stasiolek M, Brosnan CF, Raine CS, et al. EAE tolerance induction with Hsp70-peptide complexes depends on H60 and NKG2D activity. *Journal of immunology.* 2007;179(7):4503-12.
319. Borchers MT, Harris NL, Wesselkamper SC, Vitucci M, Cosman D. NKG2D ligands are expressed on stressed human airway epithelial cells. *Am J Physiol Lung Cell Mol Physiol.* 2006;291(2):L222-31.
320. Diefenbach A, Jensen ER, Jamieson AM, Raulet DH. Rae1 and H60 ligands of the NKG2D receptor stimulate tumour immunity. *Nature.* 2001;413(6852):165-71.
321. Guerra N, Tan YX, Joncker NT, Choy A, Gallardo F, Xiong N, et al. NKG2D-deficient mice are defective in tumor surveillance in models of spontaneous malignancy. *Immunity.* 2008;28(4):571-80.
322. Vilarinho S, Ogasawara K, Nishimura S, Lanier LL, Baron JL. Blockade of NKG2D on NKT cells prevents hepatitis and the acute immune response to hepatitis B virus. *Proc Natl Acad Sci U S A.* 2007;104(46):18187-92.
323. Tieng V, Le Bouguéne C, du Merle L, Bertheau P, Desreumaux P, Janin A, et al. Binding of Escherichia coli adhesin AfaE to CD55 triggers cell-surface expression of the MHC class I-related molecule MICA. *Proceedings of the National Academy of Sciences.* 2002;99(5):2977-82.

324. Hue S, Mention JJ, Monteiro RC, Zhang S, Cellier C, Schmitz J, et al. A direct role for NKG2D/MICA interaction in villous atrophy during celiac disease. *Immunity*. 2004;21(3):367-77.
325. Molinero LL, Fuertes MB, Girart MV, Fainboim L, Rabinovich GA, Costas MA, et al. NF-kappa B regulates expression of the MHC class I-related chain A gene in activated T lymphocytes. *Journal of immunology*. 2004;173(9):5583-90.
326. Cerboni C, Zingoni A, Cippitelli M, Piccoli M, Frati L, Santoni A. Antigen-activated human T lymphocytes express cell-surface NKG2D ligands via an ATM/ATR-dependent mechanism and become susceptible to autologous NK-cell lysis. *Blood*. 2007;110(2):606-15.
327. Eagle RA, Jafferji I, Barrow AD. Beyond Stressed Self: Evidence for NKG2D Ligand Expression on Healthy Cells. *Curr Immunol Rev*. 2009;5(1):22-34.
328. Fernandez-Messina L, Reyburn HT, Vales-Gomez M. Human NKG2D-ligands: cell biology strategies to ensure immune recognition. *Frontiers in immunology*. 2012;3:299.
329. Diefenbach A, Jamieson AM, Liu SD, Shastri N, Raulet DH. Ligands for the murine NKG2D receptor: expression by tumor cells and activation of NK cells and macrophages. *Nat Immunol*. 2000;1(2):119-26.
330. Watson NF, Ramage JM, Madjd Z, Spendlove I, Ellis IO, Scholefield JH, et al. Immunosurveillance is active in colorectal cancer as downregulation but not complete loss of MHC class I expression correlates with a poor prognosis. *Int J Cancer*. 2006;118(1):6-10.
331. La Scaleia R, Stoppacciaro A, Oliva S, Morrone S, Di Nardo G, Santoni A, et al. NKG2D/Ligand dysregulation and functional alteration of innate immunity cell populations in pediatric IBD. *Inflamm Bowel Dis*. 2012;18(10):1910-22.
332. Nikitina-Zake L, Rajalingham R, Rumba I, Sanjeevi CB. Killer cell immunoglobulin-like receptor genes in Latvian patients with type 1 diabetes mellitus and healthy controls. *Ann N Y Acad Sci*. 2004;1037:161-9.
333. Groh V, Bruhl A, El-Gabalawy H, Nelson JL, Spies T. Stimulation of T cell autoreactivity by anomalous expression of NKG2D and its MIC ligands in rheumatoid arthritis. *Proc Natl Acad Sci U S A*. 2003;100(16):9452-7.
334. Groh V, Smythe K, Dai Z, Spies T. Fas-ligand-mediated paracrine T cell regulation by the receptor NKG2D in tumor immunity. *Nat Immunol*. 2006;7(7):755-62.
335. Fernandez-Morera JL, Rodriguez-Rodero S, Lahoz C, Tunon A, Astudillo A, Garcia-Suarez O, et al. Soluble MHC class I chain-related protein B serum levels correlate with disease activity in relapsing-remitting multiple sclerosis. *Hum Immunol*. 2008;69(4-5):235-40.
336. Fernandez-Morera JL, Rodriguez-Rodero S, Tunon A, Martinez-Borra J, Vidal-Castineira JR, Lopez-Vazquez A, et al. Genetic influence of the nonclassical major histocompatibility complex class I molecule MICB in multiple sclerosis susceptibility. *Tissue Antigens*. 2008;72(1):54-9.
337. Guerra N, Pestal K, Juarez T, Beck J, Tkach K, Wang L, et al. A selective role of NKG2D in inflammatory and autoimmune diseases. *Clinical immunology*. 2013;149(3):432-9.

338. Soriani A, Zingoni A, Cerboni C, Iannitto ML, Ricciardi MR, Di Gialleonardo V, et al. ATM-ATR-dependent up-regulation of DNAM-1 and NKG2D ligands on multiple myeloma cells by therapeutic agents results in enhanced NK-cell susceptibility and is associated with a senescent phenotype. *Blood*. 2009;113(15):3503-11.
339. Venkataraman GM, Suci D, Groh V, Boss JM, Spies T. Promoter region architecture and transcriptional regulation of the genes for the MHC class I-related chain A and B ligands of NKG2D. *Journal of immunology*. 2007;178(2):961-9.
340. Garrido C, Brunet M, Didelot C, Zermati Y, Schmitt E, Kroemer G. Heat shock proteins 27 and 70: anti-apoptotic proteins with tumorigenic properties. *Cell Cycle*. 2006;5(22):2592-601.
341. Nomura M, Zou Z, Joh T, Takihara Y, Matsuda Y, Shimada K. Genomic structures and characterization of Rae1 family members encoding GPI-anchored cell surface proteins and expressed predominantly in embryonic mouse brain. *J Biochem*. 1996;120(5):987-95.
342. Gourzi P, Leonova T, Papavasiliou FN. A role for activation-induced cytidine deaminase in the host response against a transforming retrovirus. *Immunity*. 2006;24(6):779-86.
343. Ogasawara K, Benjamin J, Takaki R, Phillips JH, Lanier LL. Function of NKG2D in natural killer cell-mediated rejection of mouse bone marrow grafts. *Nat Immunol*. 2005;6(9):938-45.
344. Poggi A, Prevosto C, Massaro AM, Negrini S, Urbani S, Pierri I, et al. Interaction between human NK cells and bone marrow stromal cells induces NK cell triggering: role of NKp30 and NKG2D receptors. *Journal of immunology*. 2005;175(10):6352-60.
345. Mincheva-Nilsson L, Nagaeva O, Chen T, Stendahl U, Antsiferova J, Mogren I, et al. Placenta-derived soluble MHC class I chain-related molecules down-regulate NKG2D receptor on peripheral blood mononuclear cells during human pregnancy: a possible novel immune escape mechanism for fetal survival. *Journal of immunology*. 2006;176(6):3585-92.
346. Poggi A, Venturino C, Catellani S, Clavio M, Miglino M, Gobbi M, et al. Vdelta1 T lymphocytes from B-CLL patients recognize ULBP3 expressed on leukemic B cells and up-regulated by trans-retinoic acid. *Cancer Res*. 2004;64(24):9172-9.
347. Dinarello CA. Proinflammatory cytokines. *Chest*. 2000;118(2):503-8.
348. Dhanji S, Teh HS. IL-2-activated CD8+CD44high cells express both adaptive and innate immune system receptors and demonstrate specificity for syngeneic tumor cells. *Journal of immunology*. 2003;171(7):3442-50.
349. Verneris MR, Karimi M, Baker J, Jayaswal A, Negrin RS. Role of NKG2D signaling in the cytotoxicity of activated and expanded CD8+ T cells. *Blood*. 2004;103(8):3065-72.
350. Dann SM, Wang HC, Gambarin KJ, Actor JK, Robinson P, Lewis DE, et al. Interleukin-15 activates human natural killer cells to clear the intestinal protozoan cryptosporidium. *J Infect Dis*. 2005;192(7):1294-302.
351. Maasho K, Opoku-Anane J, Marusina AI, Coligan JE, Borrego F. NKG2D is a costimulatory receptor for human naive CD8+ T cells. *Journal of immunology*. 2005;174(8):4480-4.

352. Burgess SJ, Marusina AI, Pathmanathan I, Borrego F, Coligan JE. IL-21 down-regulates NKG2D/DAP10 expression on human NK and CD8+ T cells. *Journal of immunology*. 2006;176(3):1490-7.
353. Parrish-Novak J, Dillon SR, Nelson A, Hammond A, Sprecher C, Gross JA, et al. Interleukin 21 and its receptor are involved in NK cell expansion and regulation of lymphocyte function. *Nature*. 2000;408(6808):57-63.
354. Castriconi R, Cantoni C, Della Chiesa M, Vitale M, Marcenaro E, Conte R, et al. Transforming growth factor beta 1 inhibits expression of NKp30 and NKG2D receptors: consequences for the NK-mediated killing of dendritic cells. *Proc Natl Acad Sci U S A*. 2003;100(7):4120-5.
355. Schwinn N, Vokhminova D, Sucker A, Textor S, Striegel S, Moll I, et al. Interferon-gamma down-regulates NKG2D ligand expression and impairs the NKG2D-mediated cytotoxicity of MHC class I-deficient melanoma by natural killer cells. *Int J Cancer*. 2009;124(7):1594-604.
356. Yadav D, Ngolab J, Lim RS, Krishnamurthy S, Bui JD. Cutting edge: down-regulation of MHC class I-related chain A on tumor cells by IFN-gamma-induced microRNA. *Journal of immunology*. 2009;182(1):39-43.
357. Jinushi M, Takehara T, Kanto T, Tatsumi T, Groh V, Spies T, et al. Critical role of MHC class I-related chain A and B expression on IFN-alpha-stimulated dendritic cells in NK cell activation: impairment in chronic hepatitis C virus infection. *Journal of immunology*. 2003;170(3):1249-56.
358. Zhang C, Niu J, Zhang J, Wang Y, Zhou Z, Zhang J, et al. Opposing effects of interferon-alpha and interferon-gamma on the expression of major histocompatibility complex class I chain-related A in tumors. *Cancer Sci*. 2008;99(6):1279-86.
359. Allez M, Tieng V, Nakazawa A, Treton X, Pacault V, Dulphy N, et al. CD4+NKG2D+ T cells in Crohn's disease mediate inflammatory and cytotoxic responses through MICA interactions. *Gastroenterology*. 2007;132(7):2346-58.
360. Sasaki T, Hiwatashi N, Yamazaki H, Noguchi M, Toyota T. The role of interferon gamma in the pathogenesis of Crohn's disease. *Gastroenterol Jpn*. 1992;27(1):29-36.
361. Hansen CH, Holm TL, Krych L, Andresen L, Nielsen DS, Rune I, et al. Gut microbiota regulates NKG2D ligand expression on intestinal epithelial cells. *Eur J Immunol*. 2012;43(2):447-57.
362. Andresen L, Hansen KA, Jensen H, Pedersen SF, Stougaard P, Hansen HR, et al. Propionic acid secreted from propionibacteria induces NKG2D ligand expression on human-activated T lymphocytes and cancer cells. *Journal of immunology*. 2009;183(2):897-906.
363. Hamerman JA, Ogasawara K, Lanier LL. Cutting edge: Toll-like receptor signaling in macrophages induces ligands for the NKG2D receptor. *Journal of immunology*. 2004;172(4):2001-5.
364. Flajnik MF, Kasahara M. Comparative genomics of the MHC: glimpses into the evolution of the adaptive immune system. *Immunity*. 2001;15(3):351-62.
365. Flajnik MF, Kasahara M. Origin and evolution of the adaptive immune system: genetic events and selective pressures. *Nature reviews Genetics*. 2010;11(1):47-59.

366. Kasahara M, Suzuki T, Pasquier LD. On the origins of the adaptive immune system: novel insights from invertebrates and cold-blooded vertebrates. *Trends in immunology*. 2004;25(2):105-11.
367. Kondo M, Maruoka T, Otsuka N, Kasamatsu J, Fugo K, Hanzawa N, et al. Comparative genomic analysis of mammalian NKG2D ligand family genes provides insights into their origin and evolution. *Immunogenetics*. 2010;62(7):441-50.
368. Wong ES, Sanderson CE, Deakin JE, Whittington CM, Papenfuss AT, Belov K. Identification of natural killer cell receptor clusters in the platypus genome reveals an expansion of C-type lectin genes. *Immunogenetics*. 2009;61(8):565-79.
369. Cutler AF, Havstad S, Ma CK, Blaser MJ, Perez-Perez GI, Schubert TT. Accuracy of invasive and noninvasive tests to diagnose *Helicobacter pylori* infection. *Gastroenterology*. 1995;109(1):136-41.
370. Schneider S, Carra G, Sahin U, Hoy B, Rieder G, Wessler S. Complex cellular responses of *Helicobacter pylori*-colonized gastric adenocarcinoma cells. *Infect Immun*. 2011;79(6):2362-71.
371. Kienesberger S, Cox LM, Livanos A, Zhang XS, Chung J, Perez-Perez GI, et al. Gastric *Helicobacter pylori* Infection Affects Local and Distant Microbial Populations and Host Responses. *Cell Rep*. 2016;14(6):1395-407.
372. Lee A, O'Rourke J, De Ungria MC, Robertson B, Daskalopoulos G, Dixon MF. A standardized mouse model of *Helicobacter pylori* infection: introducing the Sydney strain. *Gastroenterology*. 1997;112(4):1386-97.
373. Thompson LJ, Danon SJ, Wilson JE, O'Rourke JL, Salama NR, Falkow S, et al. Chronic *Helicobacter pylori* infection with Sydney strain 1 and a newly identified mouse-adapted strain (Sydney strain 2000) in C57BL/6 and BALB/c mice. *Infect Immun*. 2004;72(8):4668-79.
374. Woodcock DM, Crowther PJ, Doherty J, Jefferson S, DeCruz E, Noyer-Weidner M, et al. Quantitative evaluation of *Escherichia coli* host strains for tolerance to cytosine methylation in plasmid and phage recombinants. *Nucleic acids research*. 1989;17(9):3469-78.
375. Iraporda C, Errea A, Romanin DE, Cayet D, Pereyra E, Pignataro O, et al. Lactate and short chain fatty acids produced by microbial fermentation downregulate proinflammatory responses in intestinal epithelial cells and myeloid cells. *Immunobiology*. 2015;220(10):1161-9.
376. Pfaffl MW. A new mathematical model for relative quantification in real-time RT-PCR. *Nucleic acids research*. 2001;29(9):e45.
377. Clayton A, Tabi Z. Exosomes and the MICA-NKG2D system in cancer. *Blood Cells Mol Dis*. 2005;34(3):206-13.
378. Liu Z, DeSantis TZ, Andersen GL, Knight R. Accurate taxonomy assignments from 16S rRNA sequences produced by highly parallel pyrosequencers. *Nucleic acids research*. 2008;36(18):e120.
379. Gorkiewicz G, Thallinger GG, Trajanoski S, Lackner S, Stocker G, Hinterleitner T, et al. Alterations in the colonic microbiota in response to osmotic diarrhea. *PLoS One*. 2013;8(2):e55817.
380. Schloss PD, Gevers D, Westcott SL. Reducing the effects of PCR amplification and sequencing artifacts on 16S rRNA-based studies. *PLoS One*. 2011;6(12):e27310.

381. Quince C, Lanzen A, Curtis TP, Davenport RJ, Hall N, Head IM, et al. Accurate determination of microbial diversity from 454 pyrosequencing data. *Nature methods*. 2009;6(9):639-41.
382. Huse SM, Welch DM, Morrison HG, Sogin ML. Ironing out the wrinkles in the rare biosphere through improved OTU clustering. *Environmental Microbiology*. 2010;12(7):1889-98.
383. Edgar RC, Haas BJ, Clemente JC, Quince C, Knight R. UCHIME improves sensitivity and speed of chimera detection. *Bioinformatics*. 2011;27(16):2194-200.
384. Wang Q, Garrity GM, Tiedje JM, Cole JR. Naive Bayesian classifier for rapid assignment of rRNA sequences into the new bacterial taxonomy. *Applied and environmental microbiology*. 2007;73(16):5261-7.
385. Quast C, Pruesse E, Yilmaz P, Gerken J, Schweer T, Yarza P, et al. The SILVA ribosomal RNA gene database project: improved data processing and web-based tools. *Nucleic acids research*. 2013;41(Database issue):D590-6.
386. Pruesse E, Quast C, Knittel K, Fuchs BM, Ludwig W, Peplies J, et al. SILVA: a comprehensive online resource for quality checked and aligned ribosomal RNA sequence data compatible with ARB. *Nucleic acids research*. 2007;35(21):7188-96.
387. Caporaso JG, Kuczynski J, Stombaugh J, Bittinger K, Bushman FD, Costello EK, et al. QIIME allows analysis of high-throughput community sequencing data. *Nature methods*. 2010;7(5):335-6.
388. Edgar RC. Search and clustering orders of magnitude faster than BLAST. *Bioinformatics*. 2010;26(19):2460-1.
389. Segata N, Izard J, Waldron L, Gevers D, Miropolsky L, Garrett WS, et al. Metagenomic biomarker discovery and explanation. *Genome Biol*. 2011;12(6):R60.
390. Tauschmann M, Prietl B, Treiber G, Gorkiewicz G, Kump P, Hogenauer C, et al. Distribution of CD4(pos) -, CD8(pos) - and regulatory T cells in the upper and lower gastrointestinal tract in healthy young subjects. *PLoS One*. 2013;8(11):e80362.
391. Allegretti YL, Bondar C, Guzman L, Cueto Rua E, Chopita N, Fuertes M, et al. Broad MICA/B expression in the small bowel mucosa: a link between cellular stress and celiac disease. *PLoS One*. 2013;8(9):e73658.
392. Gamet L, Daviaud D, Denis-Pouxviel C, Remesy C, Murat JC. Effects of short-chain fatty acids on growth and differentiation of the human colon-cancer cell line HT29. *International journal of cancer Journal international du cancer*. 1992;52(2):286-9.
393. Engelmann GL, Staecker JL, Richardson AG. Effect of sodium butyrate on primary cultures of adult rat hepatocytes. *In Vitro Cell Dev Biol*. 1987;23(2):86-92.
394. Lynch MD, Neufeld JD. Ecology and exploration of the rare biosphere. *Nat Rev Microbiol*. 2015;13(4):217-29.
395. Staubach F, Kunzel S, Baines AC, Yee A, McGee BM, Backhed F, et al. Expression of the blood-group-related glycosyltransferase B4galnt2 influences the intestinal microbiota in mice. *The ISME journal*. 2012;6(7):1345-55.
396. Kamada N, Seo SU, Chen GY, Nunez G. Role of the gut microbiota in immunity and inflammatory disease. *Nat Rev Immunol*. 2013;13(5):321-35.
397. Madisch A, Miehke S, Neuber F, Morgner A, Kuhlisch E, Rappel S, et al. Healing of lymphocytic gastritis after *Helicobacter pylori* eradication therapy--a

- randomized, double-blind, placebo-controlled multicentre trial. *Alimentary pharmacology & therapeutics*. 2006;23(4):473-9.
398. Hamer HM, Jonkers D, Venema K, Vanhoutvin S, Troost FJ, Brummer RJ. Review article: the role of butyrate on colonic function. *Alimentary pharmacology & therapeutics*. 2008;27(2):104-19.
399. Ellinghaus D, Bethune J, Petersen BS, Franke A. The genetics of Crohn's disease and ulcerative colitis--status quo and beyond. *Scand J Gastroenterol*. 2015;50(1):13-23.
400. Halfvarson J, Bodin L, Tysk C, Lindberg E, Järnerot G. Inflammatory bowel disease in a Swedish twin cohort: a long-term follow-up of concordance and clinical characteristics. *Gastroenterology*. 2003;124(7):1767-73.
401. Sartor RB. Mechanisms of disease: pathogenesis of Crohn's disease and ulcerative colitis. *Nat Clin Pract Gastroenterol Hepatol*. 2006;3(7):390-407.
402. Pariente B, Mocan I, Camus M, Dutertre CA, Ettersperger J, Cattan P, et al. Activation of the receptor NKG2D leads to production of Th17 cytokines in CD4+ T cells of patients with Crohn's disease. *Gastroenterology*. 2011;141(1):217-26, 26 e1-2.
403. Naftali T, Reshef L, Kovacs A, Porat R, Amir I, Konikoff FM, et al. Distinct Microbiotas are Associated with Ileum-Restricted and Colon-Involving Crohn's Disease. *Inflamm Bowel Dis*. 2016;22(2):293-302.
404. Bik EM, Eckburg PB, Gill SR, Nelson KE, Purdom EA, Francois F, et al. Molecular analysis of the bacterial microbiota in the human stomach. *Proc Natl Acad Sci U S A*. 2006;103(3):732-7.
405. Maldonado-Contreras A, Goldfarb KC, Godoy-Vitorino F, Karaoz U, Contreras M, Blaser MJ, et al. Structure of the human gastric bacterial community in relation to *Helicobacter pylori* status. *The ISME journal*. 2011;5(4):574-9.
406. Yang I, Nell S, Suerbaum S. Survival in hostile territory: the microbiota of the stomach. *FEMS microbiology reviews*. 2013;37(5):736-61.
407. Lofgren JL, Whary MT, Ge Z, Muthupalani S, Taylor NS, Mobley M, et al. Lack of commensal flora in *Helicobacter pylori*-infected INS-GAS mice reduces gastritis and delays intraepithelial neoplasia. *Gastroenterology*. 2011;140(1):210-20.
408. Monstein HJ, Tiveljung A, Kraft CH, Borch K, Jonasson J. Profiling of bacterial flora in gastric biopsies from patients with *Helicobacter pylori*-associated gastritis and histologically normal control individuals by temperature gradient gel electrophoresis and 16S rDNA sequence analysis. *J Med Microbiol*. 2000;49(9):817-22.
409. Zilberstein B, Quintanilha AG, Santos MA, Pajecki D, Moura EG, Alves PR, et al. Digestive tract microbiota in healthy volunteers. *Clinics (Sao Paulo)*. 2007;62(1):47-54.
410. Delgado S, Cabrera-Rubio R, Mira A, Suárez A, Mayo B. Microbiological survey of the human gastric ecosystem using culturing and pyrosequencing methods. *Microbial ecology*. 2013;65(3):763-72.
411. von Rosenvinge EC, Song Y, White JR, Maddox C, Blanchard T, Fricke WF. Immune status, antibiotic medication and pH are associated with changes in the stomach fluid microbiota. *The ISME journal*. 2013;7(7):1354-66.

412. Lodes MJ, Secrist H, Benson DR, Jen S, Shanebeck KD, Guderian J, et al. Variable expression of immunoreactive surface proteins of *Propionibacterium acnes*. *Microbiology*. 2006;152(Pt 12):3667-81.
413. Holland C, Mak TN, Zimny-Arndt U, Schmid M, Meyer TF, Jungblut PR, et al. Proteomic identification of secreted proteins of *Propionibacterium acnes*. *BMC microbiology*. 2010;10:230.
414. Mak TN, Fischer N, Laube B, Brinkmann V, Metruccio MM, Sfanos KS, et al. *Propionibacterium acnes* host cell tropism contributes to vimentin-mediated invasion and induction of inflammation. *Cellular microbiology*. 2012;14(11):1720-33.
415. Nakatsuji T, Tang DC, Zhang L, Gallo RL, Huang CM. *Propionibacterium acnes* CAMP factor and host acid sphingomyelinase contribute to bacterial virulence: potential targets for inflammatory acne treatment. *PLoS One*. 2011;6(4):e14797.
416. Tomida S, Nguyen L, Chiu BH, Liu J, Sodergren E, Weinstock GM, et al. Pan-genome and comparative genome analyses of *propionibacterium acnes* reveal its genomic diversity in the healthy and diseased human skin microbiome. *mBio*. 2013;4(3):e00003-13.
417. Coudert JD, Held W. The role of the NKG2D receptor for tumor immunity. *Seminars in cancer biology*. 2006;16(5):333-43.
418. Nausch N, Cerwenka A. NKG2D ligands in tumor immunity. *Oncogene*. 2008;27(45):5944-58.
419. Lopez-Soto A, Huergo-Zapico L, Acebes-Huerta A, Villa-Alvarez M, Gonzalez S. NKG2D signaling in cancer immunosurveillance. *Int J Cancer*. 2015;136(8):1741-50.
420. El-Gazzar A, Groh V, Spies T. Immunobiology and conflicting roles of the human NKG2D lymphocyte receptor and its ligands in cancer. *Journal of immunology*. 2013;191(4):1509-15.
421. Waldmann TA. The biology of interleukin-2 and interleukin-15: implications for cancer therapy and vaccine design. *Nat Rev Immunol*. 2006;6(8):595-601.
422. Luzzza F, Parrello T, Monteleone G, Sebkova L, Imeneo M, La Vecchia A, et al. Changes in the mucosal expression of interleukin 15 in *Helicobacter pylori*-associated gastritis. *FEMS immunology and medical microbiology*. 1999;24(2):233-8.
423. Cassol E, Malfeld S, Mahasha P, Bond R, Slavik T, Seebregts C, et al. Impaired CD4+ T-cell restoration in the small versus large intestine of HIV-1-positive South Africans receiving combination antiretroviral therapy. *J Infect Dis*. 2013;208(7):1113-22.
424. Fukazawa Y, Miyake A, Ibuki K, Inaba K, Saito N, Motohara M, et al. Small intestine CD4+ T cells are profoundly depleted during acute simian-human immunodeficiency virus infection, regardless of viral pathogenicity. *J Virol*. 2008;82(12):6039-44.
425. Solovjov DA, Pluskota E, Plow EF. Distinct roles for the alpha and beta subunits in the functions of integrin alphaMbeta2. *The Journal of biological chemistry*. 2005;280(2):1336-45.
426. Denning TL, Norris BA, Medina-Contreras O, Manicassamy S, Geem D, Madan R, et al. Functional specializations of intestinal dendritic cell and macrophage subsets that control Th17 and regulatory T cell responses are dependent on the T

- cell/APC ratio, source of mouse strain, and regional localization. *Journal of immunology*. 2011;187(2):733-47.
427. Brandtzaeg P, Johansen FE. Mucosal B cells: phenotypic characteristics, transcriptional regulation, and homing properties. *Immunol Rev*. 2005;206:32-63.
428. Eissmann P, Evans JH, Mehrabi M, Rose EL, Nedvetzki S, Davis DM. Multiple mechanisms downstream of TLR-4 stimulation allow expression of NKG2D ligands to facilitate macrophage/NK cell crosstalk. *Journal of immunology*. 2010;184(12):6901-9.
429. Ebihara T, Masuda H, Akazawa T, Shingai M, Kikuta H, Ariga T, et al. Induction of NKG2D ligands on human dendritic cells by TLR ligand stimulation and RNA virus infection. *Int Immunol*. 2007;19(10):1145-55.
430. Cullender TC, Chassaing B, Janzon A, Kumar K, Muller CE, Werner JJ, et al. Innate and adaptive immunity interact to quench microbiome flagellar motility in the gut. *Cell host & microbe*. 2013;14(5):571-81.
431. Wang Y, Devkota S, Musch MW, Jabri B, Nagler C, Antonopoulos DA, et al. Regional mucosa-associated microbiota determine physiological expression of TLR2 and TLR4 in murine colon. *PLoS One*. 2010;5(10):e13607.
432. Ortega-Cava CF, Ishihara S, Rumi MA, Kawashima K, Ishimura N, Kazumori H, et al. Strategic compartmentalization of Toll-like receptor 4 in the mouse gut. *Journal of immunology*. 2003;170(8):3977-85.
433. Lu Y, Chen J, Zheng J, Hu G, Wang J, Huang C, et al. Mucosal adherent bacterial dysbiosis in patients with colorectal adenomas. *Scientific reports*. 2016;6:26337.
434. Maharshak N, Packey CD, Ellermann M, Manick S, Siddle JP, Huh EY, et al. Altered enteric microbiota ecology in interleukin 10-deficient mice during development and progression of intestinal inflammation. *Gut Microbes*. 2013;4(4):316-24.
435. Willing BP, Dicksved J, Halfvarson J, Andersson AF, Lucio M, Zheng Z, et al. A pyrosequencing study in twins shows that gastrointestinal microbial profiles vary with inflammatory bowel disease phenotypes. *Gastroenterology*. 2010;139(6):1844-54 e1.
436. Elinav E, Strowig T, Kau AL, Henao-Mejia J, Thaiss CA, Booth CJ, et al. NLRP6 inflammasome regulates colonic microbial ecology and risk for colitis. *Cell*. 2011;145(5):745-57.
437. Cox LM, Yamanishi S, Sohn J, Alekseyenko AV, Leung JM, Cho I, et al. Altering the intestinal microbiota during a critical developmental window has lasting metabolic consequences. *Cell*. 2014;158(4):705-21.
438. Pedros-Alio C. The rare bacterial biosphere. *Ann Rev Mar Sci*. 2012;4:449-66.
439. Elshahed MS, Youssef NH, Spain AM, Sheik C, Najjar FZ, Sukharnikov LO, et al. Novelty and uniqueness patterns of rare members of the soil biosphere. *Appl Environ Microbiol*. 2008;74(17):5422-8.

VIII. Appendix

Appendix 1. Human samples used in this study

Organ	Entity	Sample ID	Gene expression	Microbiota analysis	Histology	P. acnes qPCR	Comment	Organ	Entity	Sample ID	Gene expression	Microbiota analysis	Histology	P. acnes qPCR	Comment			
Stomach	HC	22318/13	x					Duodenum	CeD	H7988/13	x							
		22887/13	x				x			H7987/13	x							
		H84234/12	x							surgical specimen also containing muscle & fat	52910/12	x					Marsh IIIa, >50 IELs/100 enterocytes	
		H15721/11	x		x					same patient 15721&23/11	80732/12	x					Marsh IIIa, >30 IELs/100 enterocytes	
		H18543/11	x							Duodenum&Antrum available, H/E not seen	73374/12	x					Marsh IIIa, >40 IELs/100 enterocytes	
		H1601/11	x		x					Antrum available, H/E not seen	78375/12	x					Marsh IIIa, >40 IELs/100 enterocytes	
		H15723/11	x							same patient 15721&23/11	22760/12	x					Marsh IIIb, 80-100 IELs/100 enterocytes	
		15676/11		x	x					gg, Antrumgastritis	77511/12	x					Marsh IIIb, 100 IELs/100 enterocytes	
		15674/11		x	x					gg, Antrumgastritis	15436/12	x					Marsh IIIc, >55 IELs/100 enterocytes	
		15770/11		x	x					gg, Antrumgastritis	1558/12	x					Marsh IIIa	
		15993/11		x	x						1559/12	x					Marsh IIIa	
		16269/11		x	x						15808/12	x					Marsh IIIa, >50 IELs/100 enterocytes	
		15689/11		x	x						2608/13	x					Marsh IIIb, >80 IELs/100 enterocytes	
		79466/09	x								6555/13	x					Marsh IIIa, >50 IELs/100 enterocytes	
		25120/13	x							x	16892/13	x					Marsh I, 45 IELs/100 enterocytes (potential celiac)	
		25144/13	x								69120/12	x					Marsh IIIa, >40 IELs/100 enterocytes	
		17337/13	x			x					26021/13	x						
		80342/11		x		x					28622/13	x						H. pylori associated active duodenitis
		86250/11				x					27359/13	x						H. pylori ++ Stomach
		17340/13								x	91356/12	x						
		39969/14								x	86881/14	x						
		4296/14								x	21299/15	x						
		86174/13								x	22179/15	x						
		105825/11								x	23769/15	x						
		62074/09	x		x	x					23813/15	x						
		73013/09	x		x	x					24262/15	x						
		79466/09	x		x	x					27474/15	x						
		31947/10	x		x	x					27452/15	x						
		47954/06	x		x						63525/13	x						
		22037/07	x		x						60050/11	x						
		58616/07	x		x						79679/12	x						
		107112/07	x		x					x	14083/12	x						
		108824/07	x		x						72711/13	x						
		110530/07	x		x						44327/12	x						
		130255/09	x		x					x	30269/13	x						
		70755/10	x		x					x	63075/13	x						
		48572/10	x		x						87125/14	x						
		26421/08				x					87092/14	x						
		5224/12	x								26731/15	x						
		5227/12	x								16709/14	x						
		50073/12	x								10828/14	x						
		90074/12	x								81571/02	x						
		14350/12	x								91340/12	x						
		44886/12	x								84485/14	x						
		58274/12	x								84149/14	x						
		81744/12	x								84147/14	x						
		76610/12	x								83764/14	x						
		26026/13	x								83398/14	x						
		42036/09								x	83397/14	x						
		H118335/11	x								83239/14	x						
		H91358/12	x			x					82918/14	x						
		H6461/13	x								82917/14	x						
		H6463/13	x								17634/14	x						
		H16013/11	x								40184/14	x						
		H15764/11	x								40185/14	x						
		H15858/11	x								26177/15	x						
		15687/11								x	96570/11	x						
		15737/11			x						107095/10	x						
		15984/11			x						5877/14	x						
		15999/11			x						74747/14	x						
		16065/11			x						72220/13	x						
		20688/13	x			x					7164/13	x						
		26357/13	x								45902/14	x						
		27496/13	x			x				x	87116/14	x						
		27799/13	x			x					83866/14	x						
		27361/13	x								51816/14	x						
		26023/13				x				x	114633/09	x						
		85917/11				x					45166/14	x						
		73775/11				x					54811/14	x						
		15762/11								x	57950/14	x						
		105428/11								x	17311/14	x						
		82931/13								x	32228/14	x						
		85548/13								x	25122/14	x						
		86892/14								x								
		22278/13	x															
		22316/13	x															
		22453/13	x															
		22645/13	x															
		22685/13	x															
		23056/13	x															
		91367/12	x															
		27494/13	x															
		25864/13	x															
		25118/13	x															
		25142/13	x															
		17338/13	x															
		17335/13	x															
		42034/09	x															
		105802/09	x															
		5222/12	x															
		5229/12	x															
		50071/12	x															
		14348/12	x															
		80274/12	x															

CeD: Celiac disease; CD: Crohn's disease; HC: healthy controls; HP: *H. pylori*; HpG: *H. pylori*-gastritis; LyC: Lymphocytic colitis; LyG: Lymphocytic gastritis; UC: Ulcerative colitis.

Appendix 2. Mice used in this study

Animal no.	Age at Death	Sex	NKG2D	Feces	Histology				RNA				Microbiota				Immunophenotyping	DSS experiment
					Stomach	SB	Caecum	LB	Stomach	SB	Caecum	LB	Stomach	SB	Caecum	LB		
31.1	24	M	KO	x	x	x	x	x					x	x	x	x		
488	17	F	KO	x	x	x	x	x					x	x	x	x		
459	17	M	WT	x	x	x	x	x					x	x	x	x		
492	19	M	WT	x	x	x	x	x					x	x	x	x		
494	19	M	WT	x	x	x	x	x					x	x	x	x		
433	21	M	WT	x	x	x	x	x					x	x	x	x		
434	21	M	KO	x	x	x	x	x					x	x	x	x		
435	21	M	WT	x	x	x	x	x					x	x	x	x		
436	21	M	WT	x	x	x	x	x					x	x	x	x		
437	21	M	KO	x	x	x	x	x					x	x	x	x		
438	21	M	WT	x	x	x	x	x					x	x	x	x		
431	10	M	KO	x	x	x	x	x					x	x	x	x		
429	10	M	WT	x	x	x	x	x					x	x	x	x		
40.3	16	F	KO	x	x	x	x	x					x	x	x	x		
40.4	10	F	WT	x	x	x	x	x					x	x	x	x		
407	13	M	KO	x	x	x	x	x					x	x	x	x		
403	13	M	WT	x	x	x	x	x					x	x	x	x		
399	11	F	KO	x	x	x	x	x					x	x	x	x		
395	11	F	WT	x	x	x	x	x					x	x	x	x		
365	15	M	WT	x	x	x	x	x	x	x	x		x	x	x	x		
363	15	M	WT	x	x	x	x	x	x	x	x	x	x	x	x	x		
362	15	M	KO	x	x	x	x	x	x	x	x	x	x	x	x	x		
353	15	F	KO	x	x	x	x	x	x	x	x	x	x	x	x	x		
351	14	F	WT	x	x	x	x	x	x	x	x	x	x	x	x	x		
350	14	F	WT	x	x	x	x	x	x				x	x	x	x		
347	14	M	KO	x	x	x	x	x	x	x	x	x	x	x	x	x		
346	14	M	WT	x	x	x	x	x	x	x	x	x	x	x	x	x		
343	14	F	WT	x	x	x	x	x	x	x	x	x	x	x	x	x		
340	14	F	KO	x	x	x	x	x	x	x	x	x	x	x	x	x		
338	12	F	WT	x	x	x	x	x	x	x	x	x	x	x	x	x		
337	12	F	KO	x	x	x	x	x	x	x	x	x	x	x	x	x		
336	12	F	KO	x	x	x	x	x	x	x	x	x	x	x	x	x		
45.1	11	F	WT	x	x	x	x	x	x	x	x	x	x	x	x	x		
45.2	11	F	KO	x	x	x	x	x	x	x	x	x	x	x	x	x		
45.4	8	F	KO	x	x	x	x	x		x	x	x	x	x	x	x		
45.5	8	F	WT	x	x	x	x	x	x	x	x	x	x	x	x	x		
45.6	8	F	KO	x	x	x	x	x	x	x	x	x	x	x	x	x		
41.2	20	M	KO	x													x	
428	21	M	WT	x													x	
245	14	F	KO	x				x					x				x	x
239	11	F	KO														x	
238	11	F	KO	x				x					x				x	x
196	7	F	WT														x	
195	7	F	WT	x				x					x				x	x
256	15	F	WT														x	
303	20	F	WT														x	
273	16	F	WT														x	
284	17	F	KO														x	
282	17	F	WT														x	
254	14	F	KO	x													x	

Appendix 3 Primers used in this study

A. Human primers

Gene symbol	GenBank accession no.	Gene name	Primers	Sequence (5' to 3')
<i>ACTB</i>	NM_001101	<i>Beta actin</i>	F	CGTGCTGCTGACCGAGG
			R	ACAGCCTGGATAGCAACGTAC
<i>KLRK1*</i>	NM_007360.3	<i>Killer cell lectin-like receptor subfamily K, member 1</i>	F	TCTAGATCAGGAAGTGGAGACA
			R	TCTTGATTCTTGTGGATAAAAGCCT
<i>MICA</i>	NM_000247	<i>MHC class I polypeptide-related sequence A</i>	F	AGCCGCTGAGAGGGTGG
			R	GAAGATGCCAGCCAGAAGCA
<i>MICB</i>	NM_005931	<i>MHC class I polypeptide-related sequence B</i>	F	CACCTGCTACATGGAACACAGC
			R	ACATGGAATGTCTGCCAATGATC
<i>ULBP1</i>	NM_025218	<i>UL16 binding protein 1</i>	F	TGGTTCAGGTCTGGACTTAGG
			R	GCTTCTGCACCTGCTGTCT
<i>ULBP2</i>	NM_025217	<i>UL16 binding protein 2</i>	F	GGGATGACGGTGTATGCATA
			R	CAAGATCCTTCTGTGCCTCC
<i>ULBP3</i>	NM_024518	<i>UL16 binding protein 3</i>	F	CATGTCTGGGCAAATGAATG
			R	CCGTACCTGCTATTGACTG
<i>RAET1E</i>	NM_001243325.1	<i>Retinoic acid early transcript 1E</i>	F	CTGGCTCAGGGAATTCTTAGG
			R	CTAGAAGAAGACCAGTGG ATATC
<i>IL15</i>	NM_000585.4	<i>Interleukin-15 isoform 1 preproprotein</i>	F	CATGTCTTCATTTTGGGCTGT
			R	GGGTGAACATCACTTTCCGT

B. Mice primers

qPCR method	Gene symbol	GenBank accession no.	Gene name	Primers	Sequence (5' to 3')
Sybr Green	<i>Hprt</i>	NM_013556.2	hypoxanthine guanine phosphoribosyl transferase	F	TCAGTCAACGGGGGACATAAA
				R	GGGGCTGTACTGCTTAACCAG
	<i>Ulp1</i>	NM_029975.2	UL16 binding protein 1	F	CAATGTCTCTGTCTCGGAA
				R	CTGAACACGTCTCAGGCACT
	<i>Rae-1</i>	NM_175112.5	ribonucleic acid export 1	F	CCACATTTACAAGTCACCATGATT
				R	GATAACCCCTGATTCATCATTAGC
TaqMan	<i>Hprt</i>	NM_013556.2	hypoxanthine guanine phosphoribosyl transferase		Mm00446968_m1
	<i>Il6</i>	NM_031168.2	interleukin 6		Mm00446190_m1
	<i>Il15</i>	NM_001254747.1	interleukin 15		Mm00434210_m1
	<i>Klrk1</i>	NM_024518	killer cell lectin-like receptor subfamily K, member 1		Mm00473603_m1
	<i>Tlr2</i>	NM_011905.3	toll-like receptor 2		Mm01213946_g1
	<i>Tlr4</i>	NM_021297.3	toll-like receptor 4		Mm00445273_m1
	<i>Tlr5</i>	NM_016928.3	toll-like receptor 5		Mm00546288_s1

Appendix 4 DSS mice experiment data compilation

	Treatment	Cage number	Mo use	Age (w)	SEX	Label	Weight (g)																Gut length (cm)	Colon weight (with no content) (g)	Colon weigh (with content)t (g)	Colon weight (with no content) (mg)			
							Day 0	Day 1	% BW	Day 2	%BW	Day 3	%BW	Day 4	%BW	Day 5	%BW	Day 6	%BW	Day 7	%BW	Day 8					%BW		
1	DSS 1	78209	245	22	F	WT	26.3	26.4	100.4	25.6	97.3	25.2	95.8	25.3	96.2	25.3	96.2	24.5	93.2	24.3	92.4	24.6	93.5	12.4	-	-	-		
2			238	18.57	F	KO	22.2	21.7	97.7	21.3	95.9	21.2	95.5	20.4	91.9	21.2	95.5	20.4	91.9	20.2	91.0	19.6	88.3	9.4	0.62	620	620		
3			195	15.14	F	WT	22	22.2	100.9	21.5	97.7	21.4	97.3	21.9	99.5	21.9	99.5	21	95.5	21	95.5	21	95.5	21	95.5	10.4	0.6	600	600
4			69.3	10.86	F	KO	21.4	21	98.1	20.9	97.7	21	98.1	21.2	99.1	20.2	94.4	18.5	86.4	17.7	82.7	17.1	79.9	9.9	0.53	530	530		
5			52.3	23.29	F	WT	21.8	21.5	98.6	21.8	100.0	21.7	99.5	21.9	100.5	21.8	100.0	20.7	95.0	20.5	94.0	20.3	93.1	8.9	0.62	620	620		
6			235	20.71	F	WT	21.3	21.4	100.5	21.5	100.9	21.4	100.5	21.1	99.1	20.8	97.7	20.1	94.4	19.8	93.0	19.3	90.6	9	-	-	-	-	
7	DSS 2	78573	160	13	F	KO	20	20.4	102.0	20.4	102.0	21	105.0	20.3	101.5	19.1	95.5	19	95.0	18.8	94.0	19.1	95.5	9.6	0.51	510	510		
8			161	13	F	WT	20.9	21	100.5	21.4	102.4	21.4	102.4	21.6	103.3	21	100.5	20.8	99.5	20.3	97.1	21	100.5	10.6	0.61	610	610		
9			163	13	F	WT	21.6	21.5	99.5	21.7	100.5	21.3	98.6	21.4	99.1	21	97.2	21	97.2	20.9	96.8	21	97.2	11	0.6	600	600		
10			208	16.29	F	KO	21	21	100.0	20.7	98.6	20.7	98.6	20.4	97.1	20.4	97.1	19.9	94.8	19.4	92.4	19.4	92.4	9.3	0.57	570	570		
11			233	20.71	F	WT	24.9	24.6	98.8	24.7	99.2	24.9	100.0	24.8	99.6	24.4	98.0	24.4	98.0	24.3	97.6	24.9	100.0	12.6	0.8	800	800		
12			61.3	18.14	F	KO	21.3	21.5	100.9	22.1	103.8	21.9	102.8	21.5	100.9	21.3	100.0	20.6	96.7	19.9	93.4	20.1	94.4	10.9	0.57	570	570		
13	Control 1	78479	61.5	16.43	F	WT	26.2	24.5	93.5	24.7	94.3	24.5	93.5	25.1	95.8	25	95.4	24.9	95.0	24.9	95.0	25.6	97.7	11.8	0.8	800	800		
14			63.2	12.57	F	WT	20.5	20.2	98.5	20.1	98.0	19.8	96.6	20.3	99.0	20.4	99.5	20.1	98.0	20.2	98.5	20.8	101.5	12.8	0.79	790	790		
15			67.3	12.71	F	WT	20.6	20	97.1	20	97.1	19.9	96.6	20.7	100.5	20.8	101.0	20.7	100.5	20.3	98.5	20.3	98.5	12.7	0.66	660	660		
16	Control 2	77566	256	23.14	F	WT	21.7	22.7	104.6	23.1	106.5	23.6	108.8	22	101.4	22.2	102.3	22.3	102.8	22.5	103.7	22.8	105.1	12.3	0.57	570	570		
17			303	27.29	F	WT	26.8	25.7	95.9	26.1	97.4	26.3	98.1	25.1	93.7	25.6	95.5	25.6	95.5	25.9	96.6	25.5	95.1	12.3	0.64	640	640		
18			273	23.71	F	WT	26	25.4	97.7	24.7	95.0	25	96.2	24.2	93.1	24.1	92.7	24.4	93.8	24.6	94.6	25.1	96.5	13.7	0.75	750	750		
19			282	25.14	F	WT	24.1	22.9	95.0	23.5	97.5	24.5	101.7	23.4	97.1	22.9	95.0	22.8	94.6	23.3	96.7	24.4	101.2	13.5	0.78	780	780		
20	DSS 3	79247	149	13.29	M	WT	28.6	28.6	100.0	29.6	103.5	29.3	102.4	28.8	100.7	28	97.9	26.8	93.7	26.4	92.3	25.7	89.9	9.6	0.8	800	800		
21			150	13.29	M	WT	28.7	28.2	98.3	28.8	100.3	28.4	99.0	27.7	96.5	27.2	94.8	26.5	92.3	27.4	95.5	26.8	93.4	10.3	0.68	680	680		
22			151	13.29	M	WT	28.3	27.9	98.6	28.5	100.7	27.3	96.5	27.2	96.1	27.4	96.8	26.5	93.6	26.4	93.3	26	91.9	10.4	0.72	720	720		
23			152	13.29	M	WT	28.8	28.5	99.0	29.7	103.1	28.9	100.3	28.4	98.6	27.7	96.2	26.4	91.7	25.3	87.8	23.5	81.6	9	0.54	540	540		
24			153	13.29	M	WT	28	27.7	98.9	28.8	102.9	28.1	100.4	27.9	99.6	27.5	98.2	26.5	94.6	26.3	93.9	25.2	90.0	9.8	0.66	660	660		
25			DSS 3'	284	25.14	F	KO	25.6	23.3	91.0	25.5	99.6	25.1	98.0	24.6	96.1	24.5	95.7	24.1	94.1	24.7	96.5	24.1	94.1	10	0.98	980	980	
26	DSS 4	79249	134	11.14	M	KO	27.3	27.9	102.2	27.4	100.4	27.2	99.6	27.4	100.4	27.3	100.0	27.4	100.4	26.7	97.8	26.2	96.0	10.4	0.7	700	700		
27	136	11.14	M	KO	25.5	26.5	103.9	25.7	100.8	25.3	99.2	26	102.0	27.5	107.8	26.1	102.4	25.5	100.0	25.6	100.4	10.1	0.86	860	860				
28	Control 3	79246	144	13.29	M	WT	24.8	25.2	101.6	26.1	105.2	25.9	104.4	25.8	104.0	25.4	102.4	25.5	102.8	25.8	104.0	25.6	103.2	11.3	1.05	1050	1050		
29			145	13.29	M	WT	25.6	25.7	100.4	26.6	103.9	26.1	102.0	26	101.6	25.9	101.2	26.2	102.3	26	101.6	25.6	100.0	10.3	0.54	540	540		
30			146	13.29	M	WT	27.4	27.5	100.4	28.5	104.0	27.8	101.5	27.7	101.1	27.9	101.8	27.9	101.8	28.2	102.9	27.7	101.1	10.8	0.76	760	760		
31			147	13.29	M	WT	26.3	26	98.9	27.2	103.4	26.7	101.5	26.6	101.1	26.2	99.6	26.2	99.6	26.5	100.8	26.4	100.4	11.8	0.95	950	950		
32			148	13.29	M	WT	25.5	26	102.0	26.4	103.5	25.6	100.4	25.9	101.6	25.7	100.8	26	102.0	26.4	103.5	25.9	101.6	12	1.01	1010	1010		
33	DSS 5	78210	240	20.71	M	WT	31.3	32.3	103.2	31.4	100.3	31.3	100.0	31.9	101.9	31.2	99.7	30.2	96.5	29	92.7	28.8	92.0	8.5	0.71	710	710		
34			241	20.71	M	WT	31.9	32.8	102.8	31.8	99.7	31.6	99.1	32.3	101.3	31.4	98.4	30.6	95.9	29.3	91.8	28.4	89.0	10	0.67	670	670		
35			243	20.71	M	WT	30.7	31.3	102.0	30.6	99.7	30.1	98.0	30.9	100.7	30.5	99.3	30.1	98.0	29.3	95.4	29.7	96.7	10.5	0.84	840	840		
36			244	20.71	M	WT	32.3	33.1	102.5	32.4	100.3	31.8	98.5	32.5	100.6	31.4	97.2	30.7	95.0	29.4	91.0	29	89.8	10.2	0.63	630	630		

Colon weight (with content) (mg)	Colon mass (no content)	Colon mass (content) (mg/cm)	% of total BW (no content)	% of total BW (w/content)	Water intake								Tissue collected				Group Comments	Individual comments	
					Day1	Day2	Day3	Day4	Day5	Day6	Day7	Day8	Bleeding (Y/N)	FC (Y/N)	RNA (Y/N)	Feces (Y/N)			
		-												N	N	Y	Y	Loose Stools (Day 1)	Much fat. Loose pellet
	65.96		0.032											N	Y	Y	Y	Loose Stools (Day 2)	
	57.69		0.029											N	Y	Y	Y	Loose Stools (Day 3)	
	53.54		0.031		25ml	20ml	20ml	25ml	20ml	20ml	20ml	20ml		Y	Y	Y	Y	238 a little bit of blood in anus day 5	
	69.66		0.031											N	N	Y	Y	Less activity in general (Rec. day1,2)	Good pellets
														N	N	Y	Y		No fecal pellet
	53.13		0.027											N	Y	Y	Y	Loose Stools (Day 2)	Small mouse
	57.55		0.029											N	Y	Y	Y	Less activity in general (Rec. Day 1)	Diarrhea
	54.55		0.029		20ml	20ml	20ml	20ml	20ml	25ml	25ml	25ml		N	Y	Y	Y		
	61.29		0.029											N	N	Y	Y		Feaces taken from the upper colon (diarrhea)
	63.49		0.032											N	N	Y	Y		
	52.29		0.028											N	N	Y	Y		
	67.80		0.031											N	Y	Y	Y		
	61.72		0.038		15ml	10ml	10ml	10ml	10ml	10ml	10ml	10ml		N	N	Y	Y		
	51.97		0.033											N	N	Y	Y		
	46.34		0.025											N	N	Y	Y		Fat
	52.03		0.025		15ml	10ml	20ml	15ml	20ml	20ml	20ml	25ml		N	N	Y	Y		Fat
	54.74		0.030											N	Y	Y	Y		
	57.78		0.032											N	N	Y	Y		
800		83.33		0.031										N	N	Y	Y		
680		66.02		0.025										N	Y	Y	Y		
720		69.23		0.028	20ml	25ml	20ml	20ml	15ml	20ml	10ml	15ml		N	N	Y	Y	All presen diarrhea	
540		60.00		0.023										N	Y	Y	Y		
660		67.35		0.026										N	N	Y	Y		
980		98.00		0.041	0ml	5ml	5ml	5ml	5ml	5ml	5ml	5ml		N	Y	Y	Y		No diarrhea. Loose pellets
730	67.31	70.19	0.027	0.028	10ml	10ml	5ml	5ml	10ml	10ml	5ml	10ml		N	Y	Y	Y		Diarrhea. Almost no fecal sample
1160	85.15	114.85	0.034	0.045										N	Y	Y	Y		
1050		92.92		0.041										N	Y	Y	Y		
750	52.43	72.82	0.021	0.029										N	Y	Y	Y		
980	70.37	90.74	0.027	0.035	15ml	25ml	25ml	20ml	15ml	15ml	25ml	25ml		N	N	Y	Y		
950		80.51		0.036										N	N	Y	Y		
1010		84.17		0.039										N	N	Y	Y		
850	83.53	100.00	0.025	0.030										N	Y	Y	Y		
690	67.00	69.00	0.024	0.024	20ml	25ml	15ml	20ml	20ml	20ml	10ml	10ml		N	N	Y	Y	All presen diarrhea	
950	80.00	90.48	0.028	0.032										N	N	Y	Y		
740	61.76	72.55	0.022	0.026										N	N	Y	Y		

Appendix 5. Flow cytometry Ab cocktails used in mice experiments.

Immunophenotyping

Ex	Em	<u>Mix 1</u>	ebio	Dilution
		Fluorophore	STAIN no.	
		BUV395	CD8	400
		BV421	gdT	400
		GFP/488	Nkp46	100
		BV605	NKG2D	100
		PE-CF594	NK1.1	400
		APC	CD122	100
		BV650	CD19	400
		AF 700	CD45	400
		BV711	CD4	1600
		PreCp-Cy5.5	Cd11b	150.00
		BU737	CD3	100.00
		Pe-Cy7	CD27	400

DSS experiment

Ex	Em	<u>Mix 1 Stim</u>	BD buffer	Dilution
		Fluorophore	STAIN no.	
		BUV395	CD8	400
		BV421	gdT	400
		GFP/488	NK1.1	400
		PE	IFNg	100
		BV605	NKG2D	100
		PE-CF594	CD3	800
		APC	Rae-1	100
		BV650	CD19	400
		AF 700	CD45	400
		BV711	CD4	1600.00
		PreCp-Cy5.5	CD11b	150.00
		Pe-Cy7	Cd107a	50
		APC-Cy7	Ly6G	100
		BV785	F4/80	40

Appendix 6. Spearman r-values and p values corresponding to TLRs and NKG2D system correlation analysis

WT								
Organ	r value	rae-1	mult1	klrk1	il15	tlr2	tlr4	tlr5
Stomach	rae-1		0.4926471*	0.1544118	0.372549	0.2426471	0.1397059	0.7867647***
	mult1			0.2794118	0.4019608	0.3382353	0.3946078	0.4632353
	klrk1				0.7132353***	0.4509804	0.377451	0.4191177
	il15					0.4411765	0.2303922	0.495098*
	tlr2						0.752451***	0.5122549*
	tlr4							0.4656863
	tlr5							
Small intestine	rae-1		0.3764706	0.4647059	0.07352942	0.5147059*	0.3764706	0.7647059***
	mult1			0.7970588***	0.6029412**	0.6588236***	0.7558824***	0.4147059
	klrk1				0.3	0.7852941***	0.8058823***	0.2558824
	il15					0.3529412	0.5529412**	0.3088235
	tlr2						0.8882353***	0.4411765
	tlr4							0.4529412
	tlr5							
Caecum	rae-1		0.5384616*	0.4417583	0.3582418	0.6791209***	0.4857143	0.6879121***
	mult1			0.8989011***	0.8901099	0.6131868*	0.9208791***	0.3978022
	klrk1				0.8593407***	0.5868132*	0.8461539***	0.345055
	il15					0.7186813***	0.8945055***	0.4857143
	tlr2						0.6747253**	0.7758242***
	tlr4							0.5076923
	tlr5							
Large intestine	rae-1		0.475	0.3321429	0.1821429	0.5035715	0.3714286	0.5607143*
	mult1			0.3571429	0.3142857	0.3928571	0.3392857	0.4642857
	klrk1				0.85***	0.8964286***	0.9321429***	0.5821428*
	il15					0.8357143***	0.8964286***	0.6357143**
	tlr2						0.9607143***	0.7535715***
	tlr4							0.7285714***
	tlr5							

Organ	P value	rae-1	mult1	klrk1	il15	tlr2	tlr4	tlr5
Stomach	rae-1		0.04654085	0.5529729	0.1415001	0.3466611	0.5920006	0.00030955
	mult1			0.2764576	0.1108908	0.1842396	0.1180389	0.06298281
	klrk1				0.00182227	0.07100575	0.1360244	0.09542226
	il15					0.07795361	0.3722216	0.04534029
	tlr2						0.00076074	0.03756755
	tlr4							0.06146933
	tlr5							
Small intestine	rae-1		0.151389	0.0717733	0.7881594	0.04362624	0.151389	0.00087402
	mult1			0.00037861	0.01529366	0.00679001	0.00107431	0.1116177
	klrk1				0.2582911	0.0005212	0.0002941	0.3375778
	il15					0.1802562	0.02854007	0.2439701
	tlr2						1.239E-05	0.08892978
	tlr4							0.08001138
	tlr5							
Caecum	rae-1		0.04996487	0.1158252	0.2089813	0.00938772	0.0809279	0.00823858
	mult1			3.4585E-05	5.1851E-05	0.02237049	1.0609E-05	0.1602026
	klrk1				0.00017335	0.03026095	0.00026897	0.2271973
	il15					0.00504014	4.2526E-05	0.0809279
	tlr2						0.01000561	0.00169171
	tlr4							0.0666882
	tlr5							
Large intestine	rae-1		0.07586304	0.2263833	0.5150466	0.05816482	0.1735245	0.03222256
	mult1			0.1916739	0.2535717	0.1485468	0.2160692	0.08344136
	klrk1				0.00012617	1.7602E-05	1.9185E-06	0.02522563
	il15					0.00020467	1.7602E-05	0.01278407
	tlr2						1.237E-07	0.00173723
	tlr4							0.00286777
	tlr5							

KO							
Organ	r value	rae-1	mult1	il15	tlr2	tlr4	tlr5
Stomach	rae-1		0.4321429	0.08928572	0.4821429	0.65**	0.7678571***
	mult1			0.3642857	0.8892857***	0.8642857***	0.4714286
	il15				0.4785714	0.3178572	0.3071429
	tlr2					0.95***	0.5321429*
	tlr4						0.6178572**
	tlr5						
Small intestine	rae-1		0.2011037	0.4044118	0.4803922	0.4534314	0.7352941***
	mult1			0.593501**	0.6670755***	0.6768855***	0.5493563*
	il15				0.8946078***	0.9019608***	0.7916667***
	tlr2					0.9779412***	0.8161765***
	tlr4						0.7843137***
	tlr5						
Caecum	rae-1		-0.2340914	-0.0689869	0.2481445	-0.3139394	0.6000337**
	mult1			0.6848579***	0.1395168	0.4551874	0.04652654
	il15				0.6241251***	0.7006781***	0.4530162
	tlr2					0.5465408*	0.6765912***
	tlr4						0.2480457
	tlr5						
Large intestine	rae-1		0.5122549*	0.6372549***	0.6617647***	0.5*	0.8161765***
	mult1			0.6862745***	0.6985294***	0.6911765***	0.5784314*
	il15				0.8578432***	0.8627451***	0.8357843***
	tlr2					0.8480392***	0.9387255***
	tlr4						0.7401961***
	tlr5						

Organ	P value	rae-1	mult1	il15	tlr2	tlr4	tlr5
Stomach	rae-1		0.1094347	0.753172	0.07110984	0.01046324	0.0012718
	mult1			0.1824485	2.506E-05	7.4048E-05	0.07834041
	il15				0.07346883	0.2479526	0.2649934
	tlr2					4.0644E-07	0.04375223
	tlr4						0.01622311
	tlr5						
Small intestine	rae-1		0.4359029	0.1085707	0.05293692	0.06933911	0.00113476
	mult1			0.01354293	0.00431868	0.00362996	0.0241265
	il15				4.0645E-06	2.6027E-06	0.0002688
	tlr2					4.4226E-10	0.00012531
	tlr4						0.0003318
	tlr5						
Caecum	rae-1		0.3658243	0.7924832	0.3368891	0.219773	0.01088391
	mult1			0.00241851	0.5933067	0.06636052	0.8592595
	il15				0.00741117	0.00173079	0.06783124
	tlr2					0.02320226	0.0028582
	tlr4						0.3370878
	tlr5						
Large intestine	rae-1		0.03756755	0.00714437	0.00477665	0.04300429	0.00012531
	mult1			0.00308639	0.00244478	0.00281528	0.01675375
	il15				2.5803E-05	2.0779E-05	6.2729E-05
	tlr2					3.8926E-05	1.4764E-07
	tlr4						0.0010153
	tlr5						

Appendix 7. Protocol for gut IELs and LPLs isolation

- 1- Checklist:
 - a. Prepare solutions and medium (see below) and place at 37C. Only the enzymes must be thawed few minutes before using them.
 - b. Bucket of ice
 - c. Tray with aluminum foil (until the time to process one mouse is >25-30' use a deep polystyrene li, fill it with ice, and then cover with foil)
 - d. PBS 1x
 - e. Tools (1 big tweezers, 1 small, 1 regular scissors, 1 curved blunt scissors, blunt needle and 20ml syringe to wash)
 - f. Eppendorfs
 - g. Percoll at rt (early in the morning)
- 2- Harvest ear punch for re-genotyping. Open the mouse to expose the abdomen, take at first spleen and mesenteric lymph nodes if needed. Dissection procedure in Room 614
- 3- Cut out the LB.
- 4- Clean the LB, keep a piece of faeces on ice. Take a picture and weigh the LB (minus caecum).
- 5- Using a scalpel take a 1mm section of the proximal, distal and mid-LB for histo – place in 10% formalin.
- 6- Take time to carefully remove ALL connective tissue from the remaining LB.
- 7- Cut LB longitudinally, place on a piece on a dry piece of tissue and push down to remove the mucus. Return to dissection board and wet with PBS. Cut LB into small pieces (<1 cm), store in ice in PBS.
 - a. Note: Do not wipe with tissue (it reduced the IELs yield)
- 8- If RNA is needed: collect tissue in RNA later (1x ~2 mm along the length for each SB or LB collected into the same eppendorf/tissue)
- 9- When all mice are done, place the intestines into falcons containing 50ml of warm (37°C) PBS/10% FCS+EDTA 5mM. From now on, all steps must be performed in the 37C room.
 - Ana's modification: Prepare HBSS ($V_T=50$ ml) supplemented with 1mMEDTA (25ul), 1mM DTT (50ul) and 2% FBS (1ml). Add 10ml to each sample.
- 10- Incubate for the first wash ~20mins 37°C at 200 rpm (#7 on shaker in 6th floor warm room.
 - Ana's modification: Incubate for 30min 37°C, 200 rpm (shaker, speed 6).

- 11- Retain the supernatant on ice (IELs) at least once more (subsequent washes can be 10-15mins) until the liquid is basically clear. Usually control mice take longer to go clear.
 - Ana's modification: Second wash for 15-20min. Only recover IELs from those samples that are still cloudy. Discard the supernatant if clear. IMPORTANT: Right after collecting the IELs, centrifuge them at 1500rpm for 10min, resuspend with PBS or RPMI (5%FBS) and place them on ice.
- 12- During incubation time, clean working area and tools and discard mouse carcasses into CBS freezer
- 13- Discard the supernatant, add 50ml of PBS and invert the tube multiple times.
- 14- Discard the supernatant and add pre-warmed RPMI containing FCS (10%), 15mM HEPES, collagenase VIII 100U/ml and DNase 50U/ml. 15ml is sufficient for LB
OPTIONAL: Remove sections of LB from tube and chop up smaller
Prepare media with enzymes in 15ml then transfer tissue into it.
 - Ana's modification:
 - o For stomach: Chop the tissue into 1mm pieces to facilitate the digestion.
V_T digestion buffer= 20ml. Use 0.5mg/ml Collagenase IV (1aliquot, 100ul (100ug/ml) and 200ul/ml DNase I (4ul). Use 5ml/sample.
- 15- Incubate 45-50 min at 37°C at 200 rpm, work on the bench from now on.
 - Ana's modification: Check the samples after 30min of digestion (s.intestine is digested quite fast). For the stomach the digestion takes about 60min.
- 16- Finish the digestion by vortexing and using a 20ml syringe.
- 17- Filter the suspension on a 100µm nylon filter to remove tissue debris. Use a 2ml syringe to gently massage the last of the tissue through the filter. Wash through with 3% BSA/PBS supplemented with 5mM EDTA to inhibit collagenase activity.
- 18- Centrifuge 800 g for 10 min
- 19- Discard the supernatant
 - Ana's modification: Discard the supernatant with a Pasteur pipette.
- 20- Ensure that percoll has been brought to room temperature and a p100 solution has been prepared as described below. Resuspend the cells in 4 ml of 40% percoll and layer on top of 4 ml 80%, in a 15 ml falcon.
- 21- Centrifuge at 600 g 20°C for 20 min (Acc 5, Dec 3)
- 22- Remove the upper layer all the way down to just above the ring using a Pasteur pipette. Using a clean Pasteur remove the layer plus most of the percoll underneath but leave a little percoll in the tube. Wash twice with 50ml PBS FCS 2%
 - Ana's modification: Wash once with 25 ml and discard the supernatant with a Pasteur pipette.

- 23- Resuspend in 500ul volume. Count.
- 24- Average yield ~2M/Sb/mouse same for LB
- 25- Flow data to be collected in “flow cytometry/LPL for APC”

Note 1 : Percoll should be prepared the same day of experiment and kept at RT
Prepare isotonic solution before diluting 80% and 40%.
Isotonic percoll (p100): 90% Percoll+ 10% PBS 10X

Note 2 :

Collagenase IV –aliquots 100ug/ml
Collagenase VIII Sigma, C-2139 (stored -20C 6th floor- aliquots 5000U (small bowel) and 1500U for Large bowel)
DNase Sigma, DN-25 (stored -20C 6th floor)
Percoll VWR, 17-0891-019 (+4 5th floor)

Note 3:

Samples for RNA must be kept in RNA later at +4 for 1-2 days, and then transferred at -80 (4th floor) until extraction. To extract RNA, follow Qiagen’s kit protocol (booklet in the box). For the retrotranscription into cDNA, refer to “models of disease/Gut/RNA-CDNA” Excel file, and use the “template” tab to prepare the cDNA. Record in the same file every RNA extraction and retrotranscription (“samples” tab, plus one tab/date for cDNA mix prep).
Every time cDNA is used for quantitative PCR, record plate scheme and data in “gene expression/rtPCR/UPL-Roche” (1 folder/experiment).

Updated AM-A 06/08/15

